Θανάσης Κουτσολέλος

Βιολογική Ανόργανη Χημεία

Πανεπιστήμιο Κρήτης
Τμήμα Χημείας
Εργαστήριο Βιοανόργανης Χημείας

Θανάσης Κουτσολέλος

Βιολογική Ανόργανη Χημεία

Πανεπιστήμιο Κρήτης
Τμήμα Χημείας
Εργαστήριο Βιοανόργανης Χημείας

Inorganic elements of interest in biology and medicine

Na	**Mg**												
K	**Ca**			**V**	**Cr**	**Mn**	**Fe**	**Co**	**Ni**	**Cu**	**Zn**		
		Y			**Mo**	**Tc**				**Ag**	**Cd**		
					W				**Pt**	**Au**	**Hg**		

Yellow: naturally occurring metals
Blue: metals introduced as drugs and diagnostic probes

Periodic Table of the bio-elements:

H																	
Li												B	C	N	O	F	
Na	Mg												Si	P	S	Cl	
K	Ca			V		Mn	Fe	Co	Ni	Cu	Zn			As	Se	Br	
					Mo	Tc							Sn	Sb		I	
	Ba	Gd			W				Pt	Au				Bi			

elements building up bio-mass,

additional essential elements,

essential for some groups of organisms,

medicinally important elements.

Significance of biologically important elements (selection)

- **Na^+ and K^+:** Most important „free“ intra- and extracellular cations. Regulation of the osmotic pressure, membrane potentials, enzyme activity, signalling.
- **Mg^{2+}:** Chlorophyll; anaerobic energy metabolism (ATP → ATP).
- **Ca^{2+}:** Signalling, muscle contraction, enzyme regulation. Main inorganic part of the endoskeletons (bones, teeth, enamel: hydroxyapatite; $Ca_5(PO_4)_3(OH)$). Exoskeletons of mussels, shells, corals, sea urchins etc: aragonite or calcite; $CaCO_3$).
- **$V^{IV/V}$, $Mo^{IV/VI}$, $W^{IV/VI}$, $Mn^{II/III/IV}$, $Fe^{II/III}$, $Ni^{I/II/III}$, $Cu^{I/II}$:** active centres in electron-transport (redox) enzymes, oxygenases, dismutases.
- **Fe and Cu:** Transport of oxygen. Fe^{III}: Iron-storage proteins (ferritins).
- **Fe^{II} + Fe^{III} in magnetite (Fe_3O_4):** orientation of magnetobacteria, pigeons, bees in Earth’s magnetic field.
- **Co:** Synthases and isomerases (cobalamines, e.g. vitamin-B_{12}); methylation of inorganics.
- **Zn^{2+}:** In the active centre of hydrolases, carboanhydrase, alcohol dehydrogenase, synthases; genetic transciption (zinc fingers), stabilisation of tertiary and quartary structures of proteins; repair enzymes.
- **Si^{IV} (“silicate“)**: Involved in the built-up of bones. In the form of SiO_2/silica-gels as support in monocotyledonous plants (like grass) and the shells of diatoms.
- **P^{V} (phosphate):** Constituent in hydroxi- and fluorapatite ($Ca_5(PO_4)_3(OH/F)$); energy metabolism (ATP), NADPH, activation of organic substrate; phospholipids in cell membranes; phosphate esters (DNA, RNA,...).
- **Se^{-II}:** Selenocystein in special enzymes (e.g. glutathionperoxidase) **F^-:** Fluorapatite ($Ca_5(PO_4)_3F$) in dental enamel
- **Cl^-:** Along with hydrogencarbonate the most important free anion. **I:** Constituent of thyroid hormones (such as thyroxine).

Medicinal relevant elements (selection)

- **Li^{+}:** Treatment of bipolar disorder (maniac depression) and hypertension.
- **Gd^{3+}:** Contrast agent in magnetic resonance tomography of soft tissues.
- **$BaSO_4$:** Contrast agent for X-ray tomography. Sun protection.
- **^{99m}Tc** (a metastable γ-emitter; $t_{1/2} = 6$ h): Radio diagnostics (bone cancer, infarct risk, ...)
- **Pt^{II}:** Chemotherapy (e.g. with cisplatin cis-$[Pt(NH_3)_2Cl_2]$) of cancer (ovaria, testes)
- **Au^{I}:** Therapy of rheumatic arthritis.
- **Sb^{III}:** Treatment of inflammatory skin pimples like acne.
- **Bi^{III}:** Treatment of gastritis.

Biological ligands for metal ions: 1) proteins by aminoacids

Summarizing, the role of proteins are numerous:

- -Act as multidentate chelate ligand (via amino acid side chains)
- -Provide spatial fixation
- -Serve as a medium with defined dielectrical properties
- -With Mg^{2+}, Fe^{2+}, and Co^{2+}, proteins form complexes thermodinamically stable but kinetically labile. **Activation energy is too small that exchange reaction is frequent**. In fact nature warrants kinetic stabilization by using another class of ligands: **macrocyclic chelate ligands.**

Biological ligands for metal ions: 2) tetradentate macrocycles

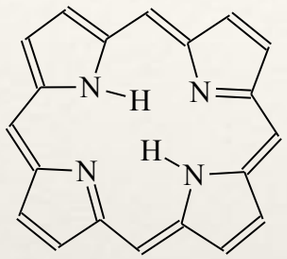

porphyrin

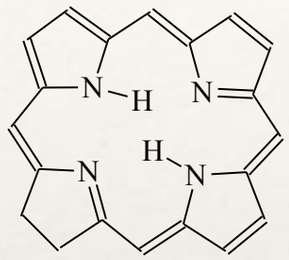

chlorin
(2,3 dihydroporphyrin)

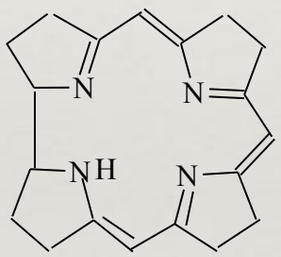

corrin

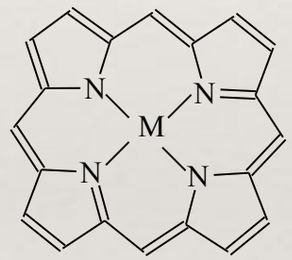

metalloporphyrin complex

- Ring is planar (sp^2 hybridation)
- Tetrapyrrol macrocycles are able to bind labile metal ions
- Tetrapyrrol macrocycles are selective with regard to size of metal ion
- They are the “pigments of life” with intense absorption bands in the visible region.
- Two axial positions remain available: e.g. heme group

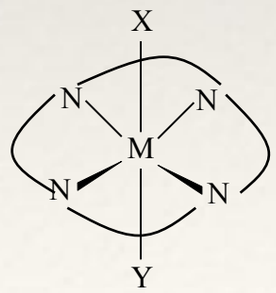

Biological ligands for metal ions: 2) multidentate macrocycles

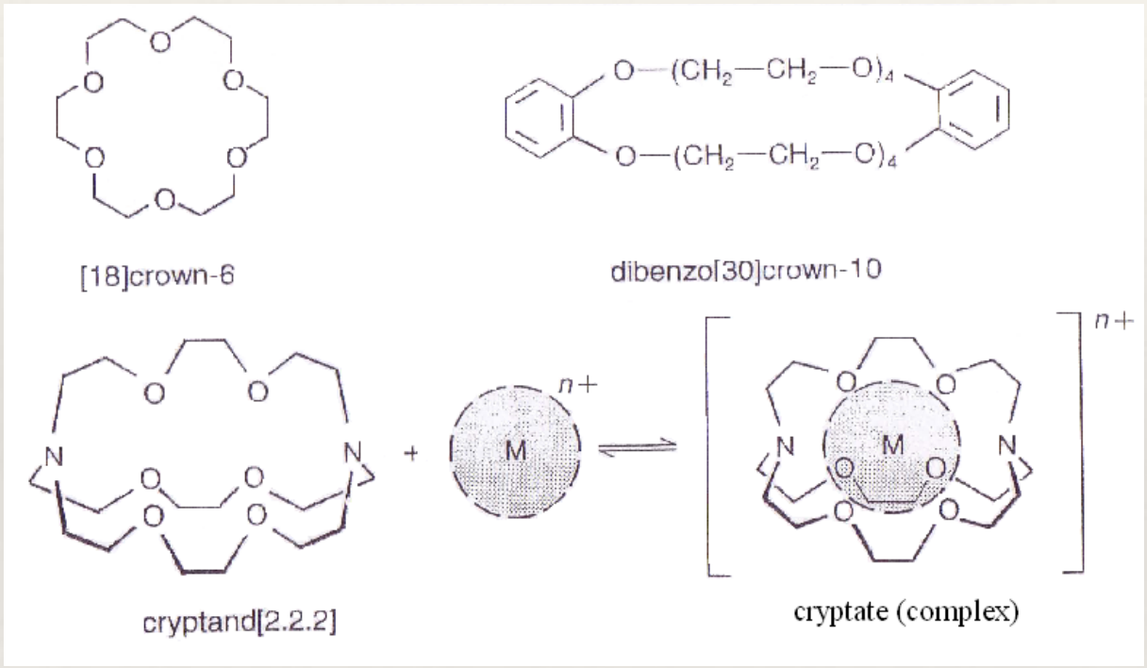

- good for coordination of Na^+, K^+, Mg^{2+}, Ca^{2+}
- Multiple heteroatoms are strategically positioned for bonding metal ions
- ring size is tailored to fit metal ionic radius
- Dissociation is possible but very unlikely
- Inner cavity is polar, outside is lipophile. So these complexes can be transported through biological membranes.

Biological ligands for metal ions: 3) nucleobases

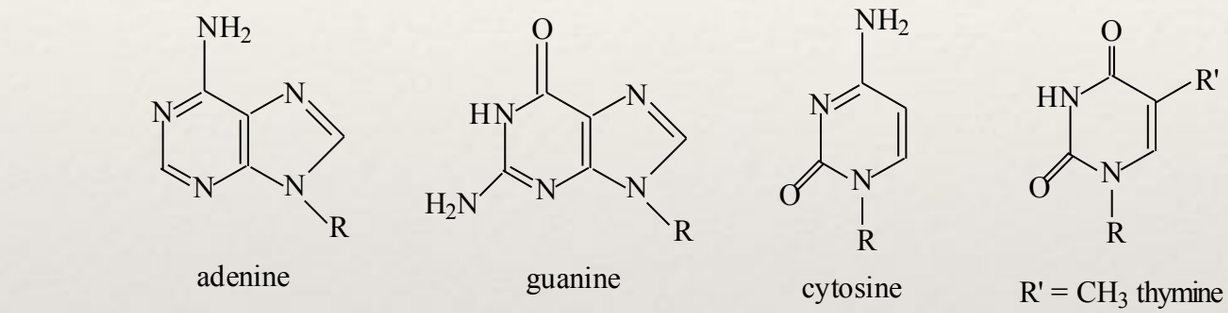

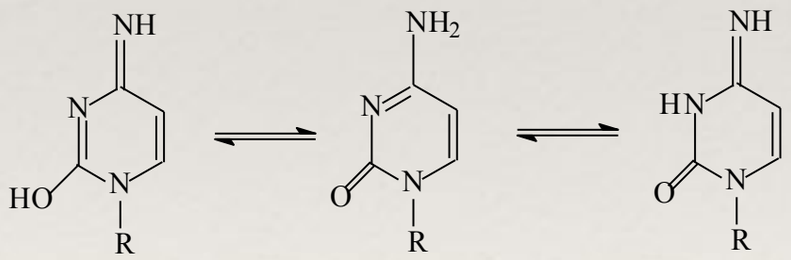

Nucleobases can exist in different tautomeric forms and can be mono or multidentate ligands.
Positively charged metal ions in the nucleus can affect the normal hydrogen-bond interactions that are the basis of base pairing in DNA.
This can be exploited for the development of chemotherapic drugs

Thermodynamic aspects: 1) hard-soft concept

Metals (acids)	Ligands (bases)
Hard H^+ Mn^{2+} Cr^{3+} Ca^{2+} Na^+ Al^{3+} Co^{3+} K^+ Fe^{3+} Mg^{2+}	**Hard** H_2O CO_3^{2-} NH_3 OH^- NO_3^- RNH_2 $CH_3CO_2^-$ ROH PO_4^{3-} RO^- Cl^-
Borderline Fe^{2+} Ni^{2+} Zn^{2+} Co^{2+} Cu^{2+}	**Borderline** NO^{2-} SO_3^{2-} Br- Imidazole
Soft Cu+ Pt2+ Pt4+ Au+ Hg2+ Cd2+ Pb2+	**Soft** R2S RS- R3P RSH RNC CN- SCN- CO

Hard metal is small and not easily polarized.
Fe^{3+} is harder than Fe^{2+}.
Soft metal is large and easily polarizable.

The general rule is that hard metals bind preferentially hard bases and soft acids to soft bases.

Hard-soft concept: metallothionins

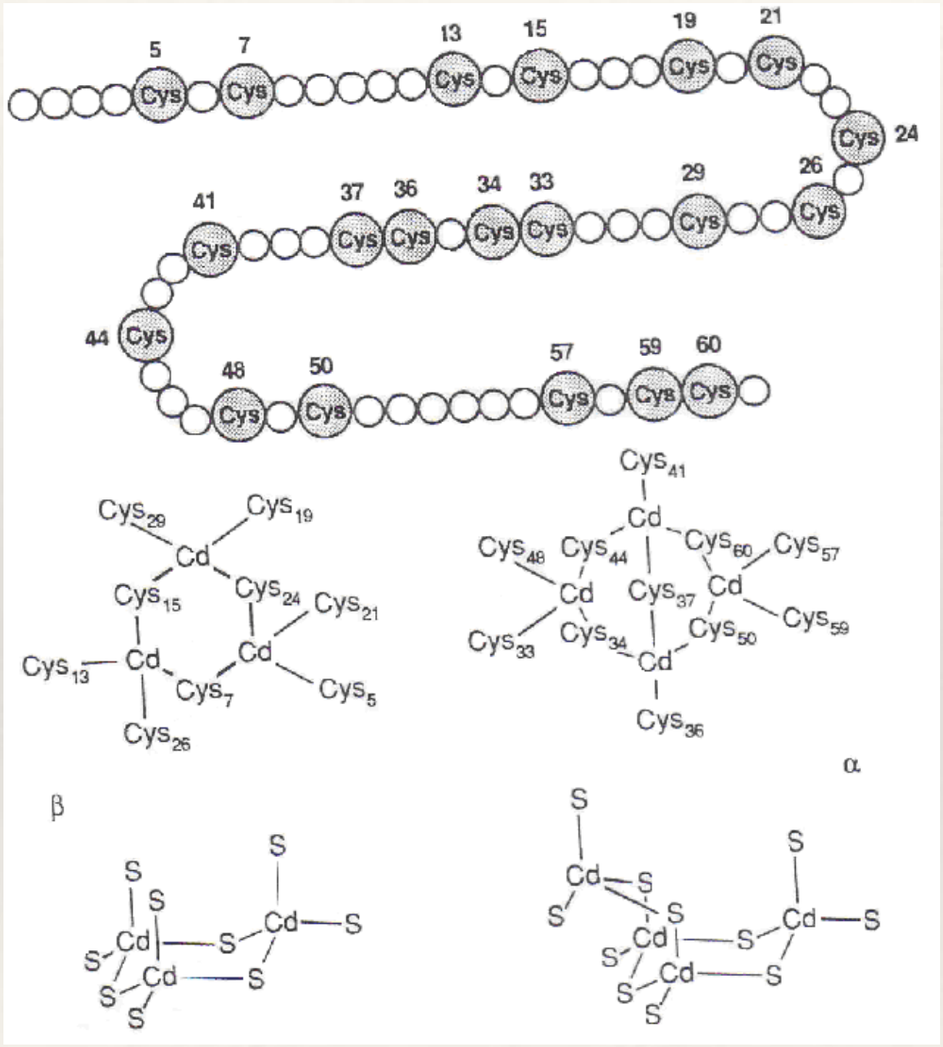

- 30-35% of aminoacid are cysteins with soft –SH groups
- repetitive distribution of Cys-X-Cys etc…
- coordination of soft heavy metal ions such as Cd^{2+}, Hg^{2+}, Pb^{2+}, Zn^{2+}.
- biological function of metallothioneins is to protect cells from toxic heavy metals

Thermodynamic aspects: 2) chelate effect

$$[Co(H_2O)_6]^{3+} + EDTA^{4-} \rightleftharpoons [Co(EDTA)]^{-} + 6H_2O$$

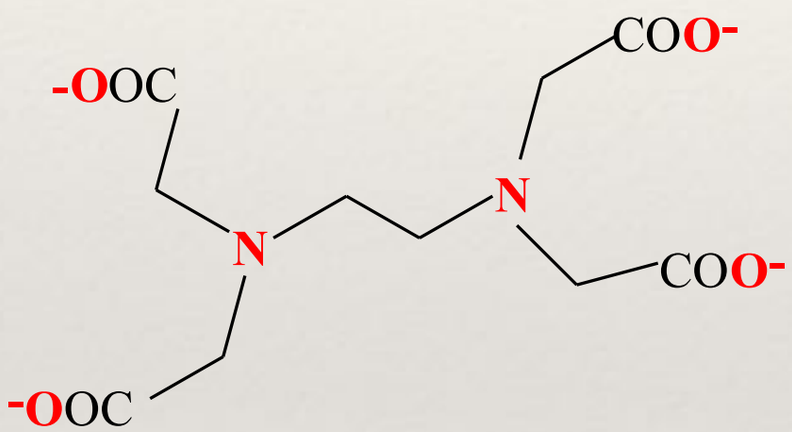

EDTA

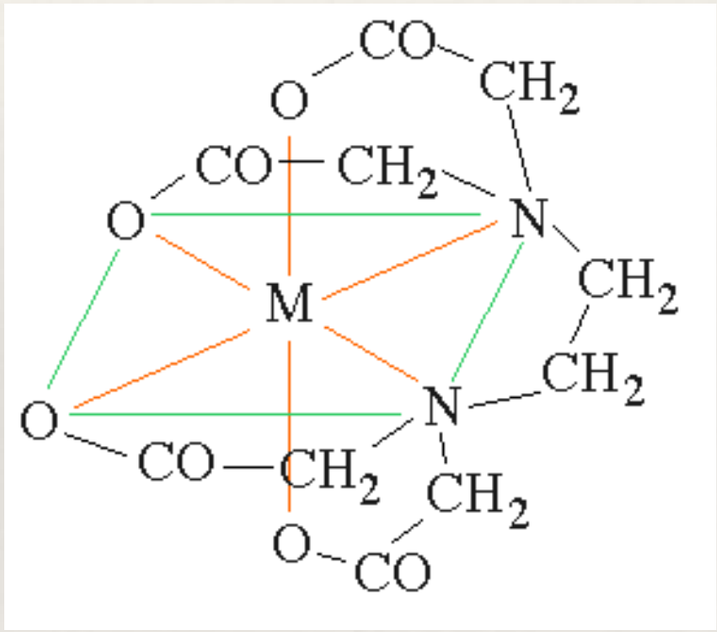

- DG° = DH° - TDS°
- DG° = - RT lnK
- Metal chelate complexes are very stable, because there is a favourable **entropic factor** accompanying the release of non chelating ligands

Example of chelates

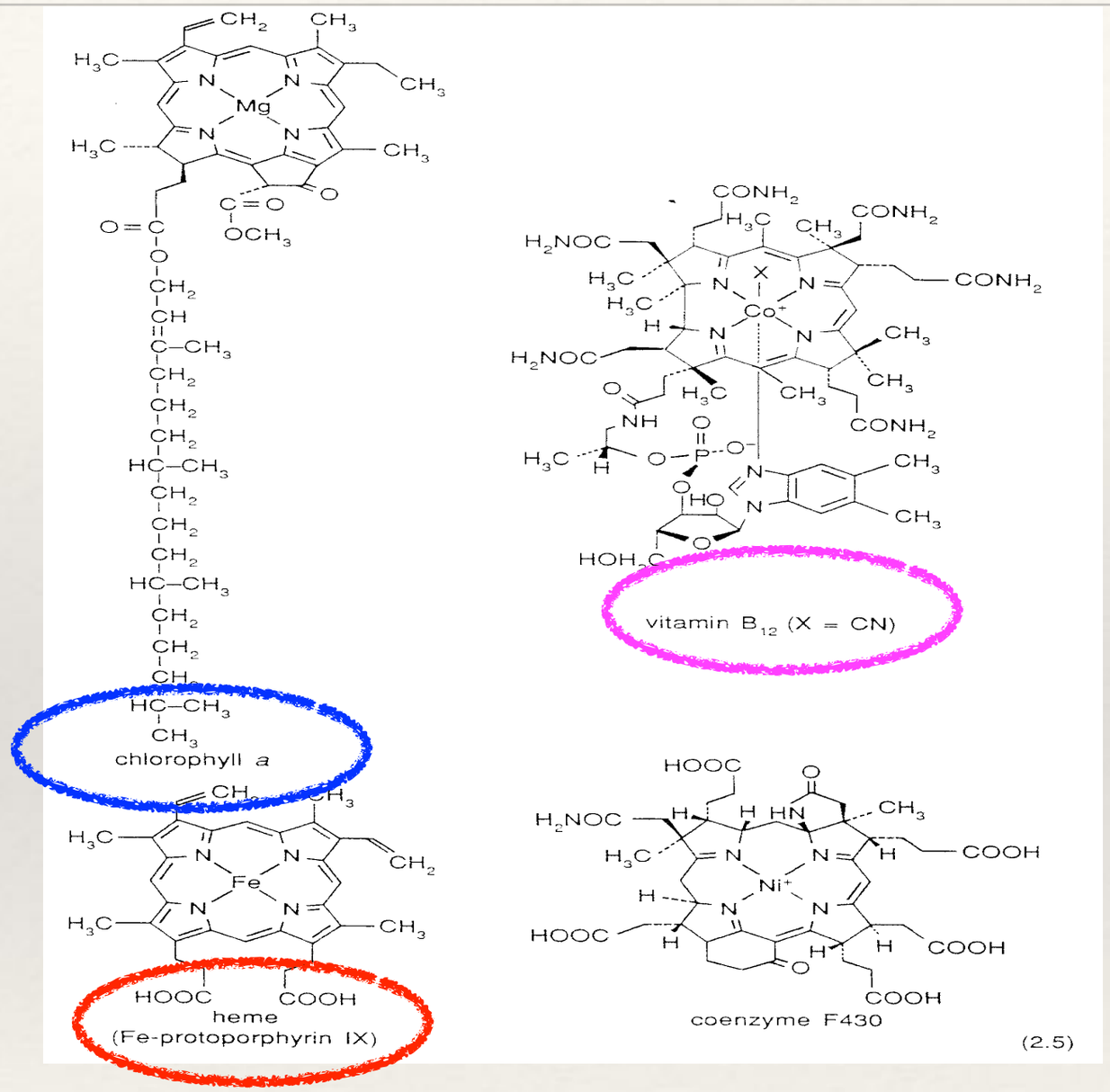

Thermodynamic aspects: 3) pKa values of coordinated ligands

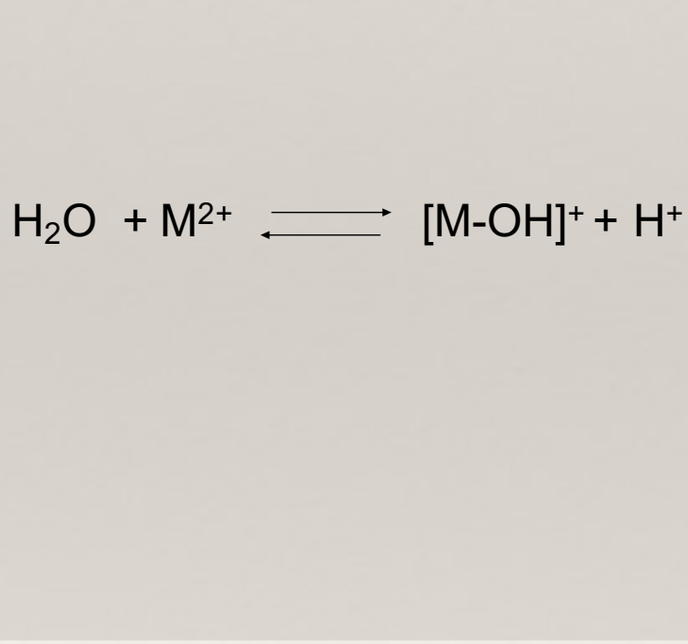

Metal ion	water pK_a
none	14.0
Ca^{2+}	13.4
Mn^{2+}	11.1
Cu^{2+}	10.7
Zn^{2+}	**10.0**

When coordinated to Zn^{2+}, water is 10.000 times more acid than when it is free!!!!

Zinc enzymes: the example of carbonic anhydrase

Deprotonation of the aquo-complex is the well-known **reaction that precedes every metal hydroxide precipitation**

$$[Zn(OH_2)_6]^{2+} \rightleftharpoons [Zn(OH_2)_5OH]^{+} + H^{+} \qquad pK_a = 10$$

in an enzymatic system, deprotonation of a coordinated water to form an hydroxo ligand is a fundamental step of many hydrolytic mechanisms. The pK_a value drops to 7!!!

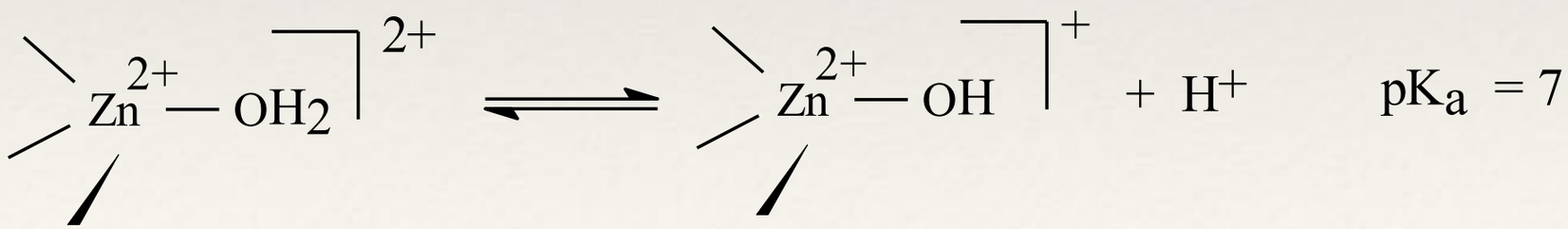

The role of zinc in carbonic anhydrase

- zinc has a d^{10} configuration (non redox)
- it has strong Lewis acidic properties
- it prefers low coordination numbers
- it bears very distorted geometries
- it binds water in a very labile way.

Carbonic anhydrase accelerates the following reaction of a factor of 10^7

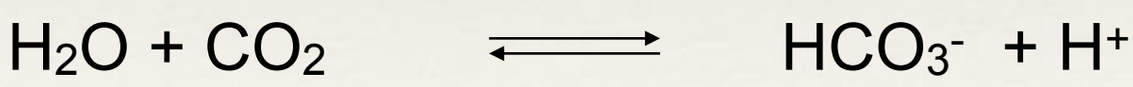

Carbonic anhydrase: mechanism

- Zinc is coordinated to three histidine residues. The fourth position is occupied by H2O.
- Geometry is distorted tetrahedral
- Deprotonation of water molecule is essential for the nucleophilic attack to CO2.
- His64 has an important role in the polarization of the O-H bond and in the formation of Zn-hydroxide species

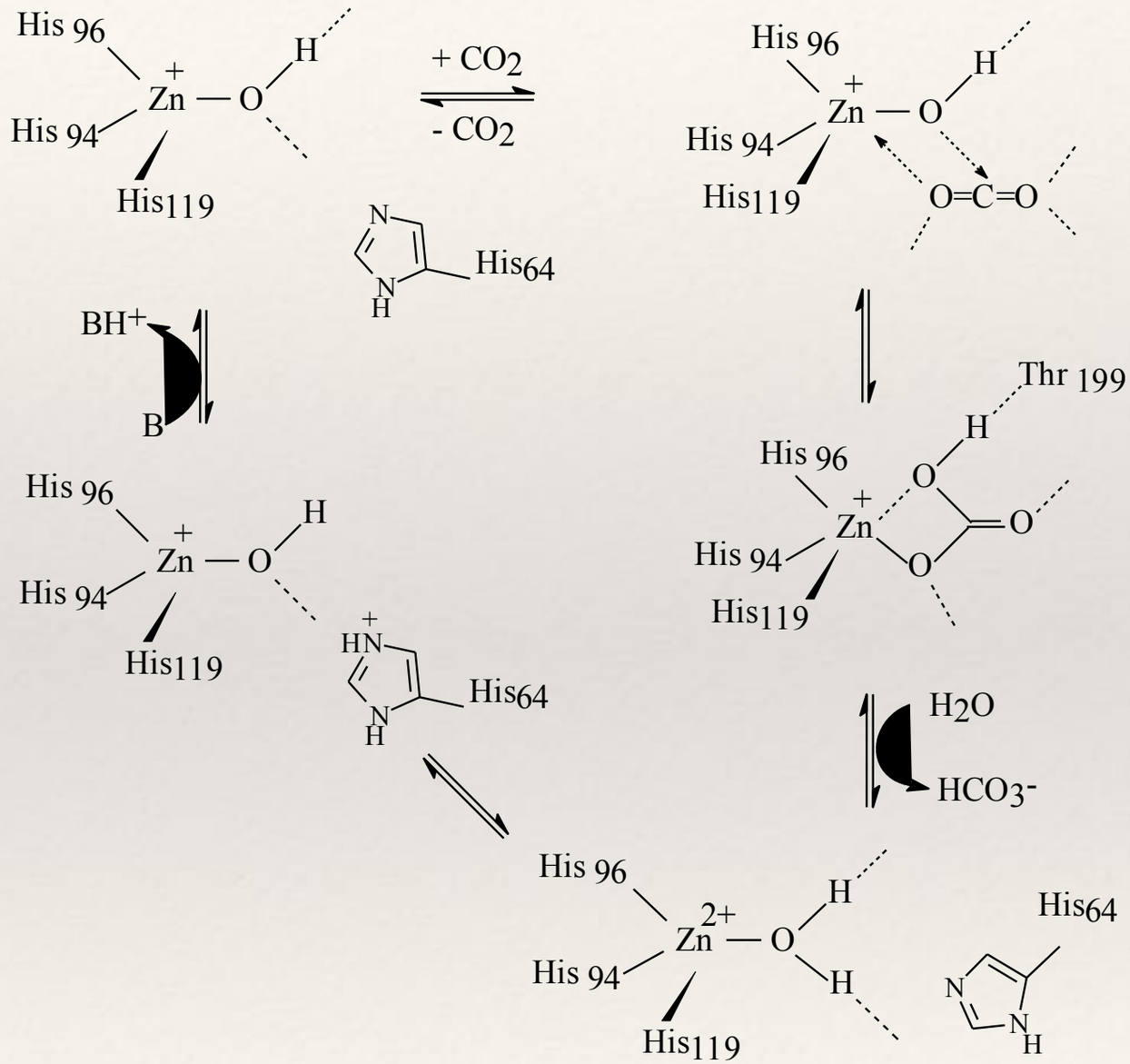

Thermodynamic aspects: 4) tuning of redox potentials

Compound name	$E_{1/2}$, V (Cu^{2+}/Cu^{+})
$Cu(O\text{-}sal)_2en$	-1.21
$Cu(Me\text{-}sal)_2$	-0.90
$Cu(Et\text{-}sal)_2$	-0.86
$Cu(S\text{-}sal)_2en$	-0.83
$Cu(i\text{-}Pr\text{-}sal)_2$	-0.74
$Cu(t\text{-}Bu\text{-}sal)_2$	-0.66

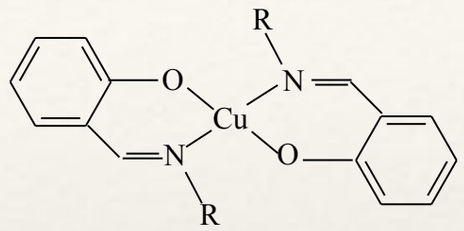

$Cu(R\text{-}sal)_2$

Cu^{2+} is typically square-planar.
Cu^{+} prefers tetrahedral four-coordinate geometries.

High redox potentials are achieved by the proteins containing copper through distortion of the coordination geometry

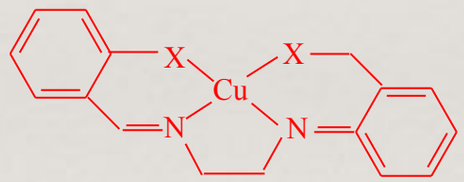

$Cu(X\text{-}sal)_2en$
X = O or S

Cu^{+} is softer than Cu^{2+}

High redox potentials are achieved by the proteins containing copper through the use of soft donor ligands.

Thermodynamic aspects: 5) biopolymer effects

Biopolymer affects the thermodynamic stability of a metal center, since it can control, through its three dimensional structure,-Stereochemistry

- Ligands available for coordination
- Local hydrophilicity and hydrophobicity
- Steric blockage of coordination sites
- Hydrogen bonding formation

These considerations are very important in order to understand how metals function in biology

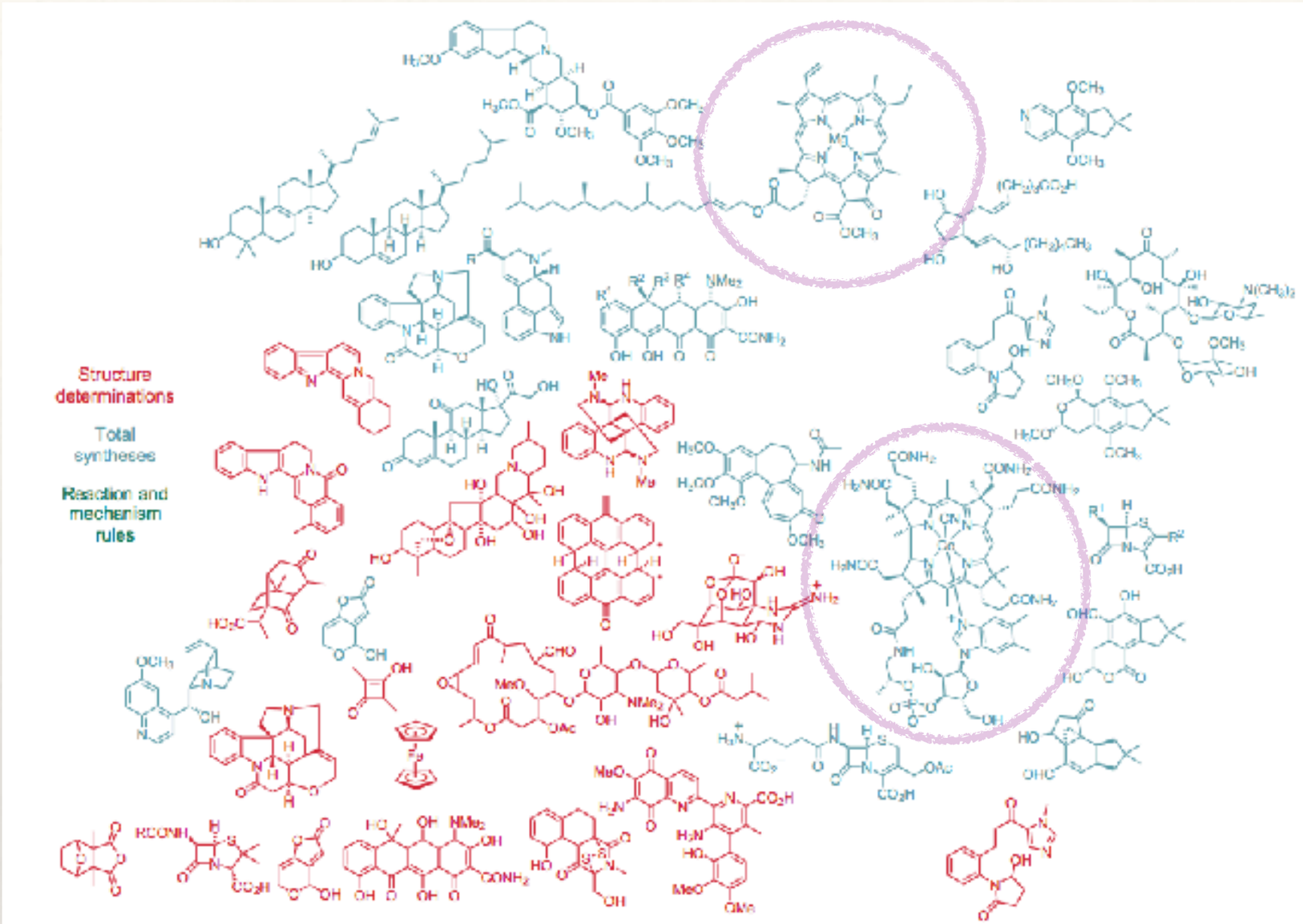
Structure determinations
Total syntheses
Reaction and mechanism rules
Woodward Nobel
Hoffmann–Fukui Nobel
Ultraviolet rules
Octant rule
Woodward–Hoffmann rules
Death
1940
1945
1950
1955
1960
1965
1970
1975
1980
1985
An alternative world
Woodward Nobel for structure determination and mechanistic analysis
Woodward shares Nobel for sandwich compounds
Woodward Nobel for organic synthesis
Woodward shares Nobel for Woodward–Hoffmann rules

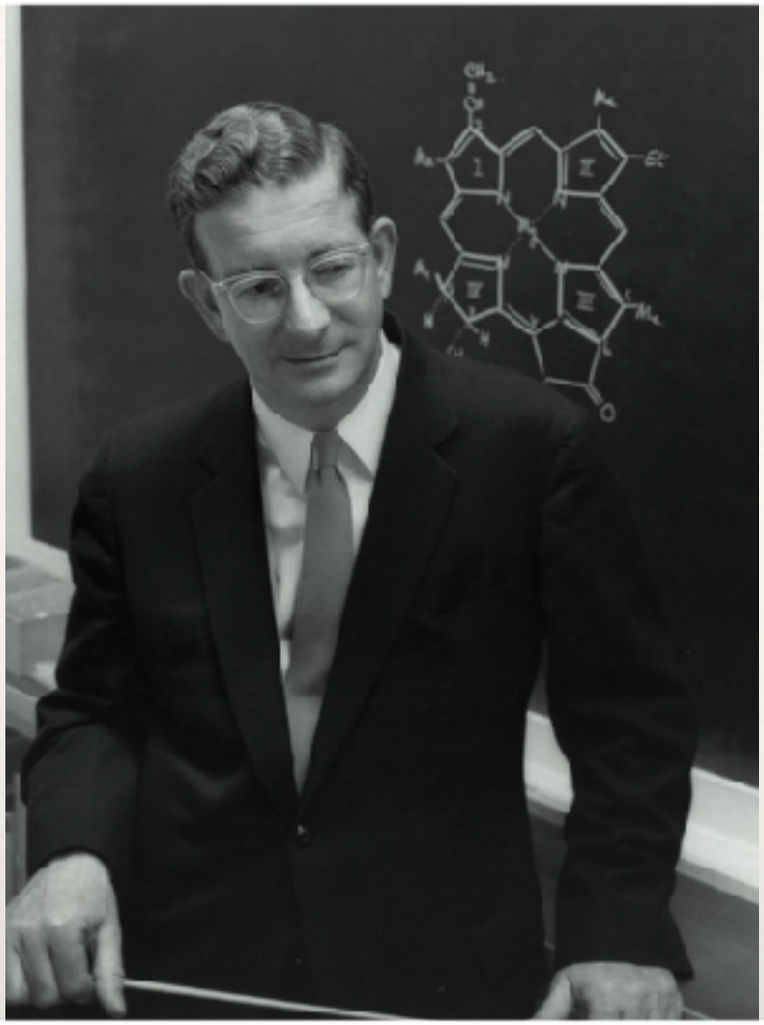

to Prof. R. B. Woodward

"for his outstanding achievements in the art of organic synthesis".

The Nobel Prize in Chemistry 1965

http://www.bioinfo.org.cn/book/biochemistry/chapt18/sim9.htm

for the determination of
the three-dimensional structure
of a photosynthetic reaction center.

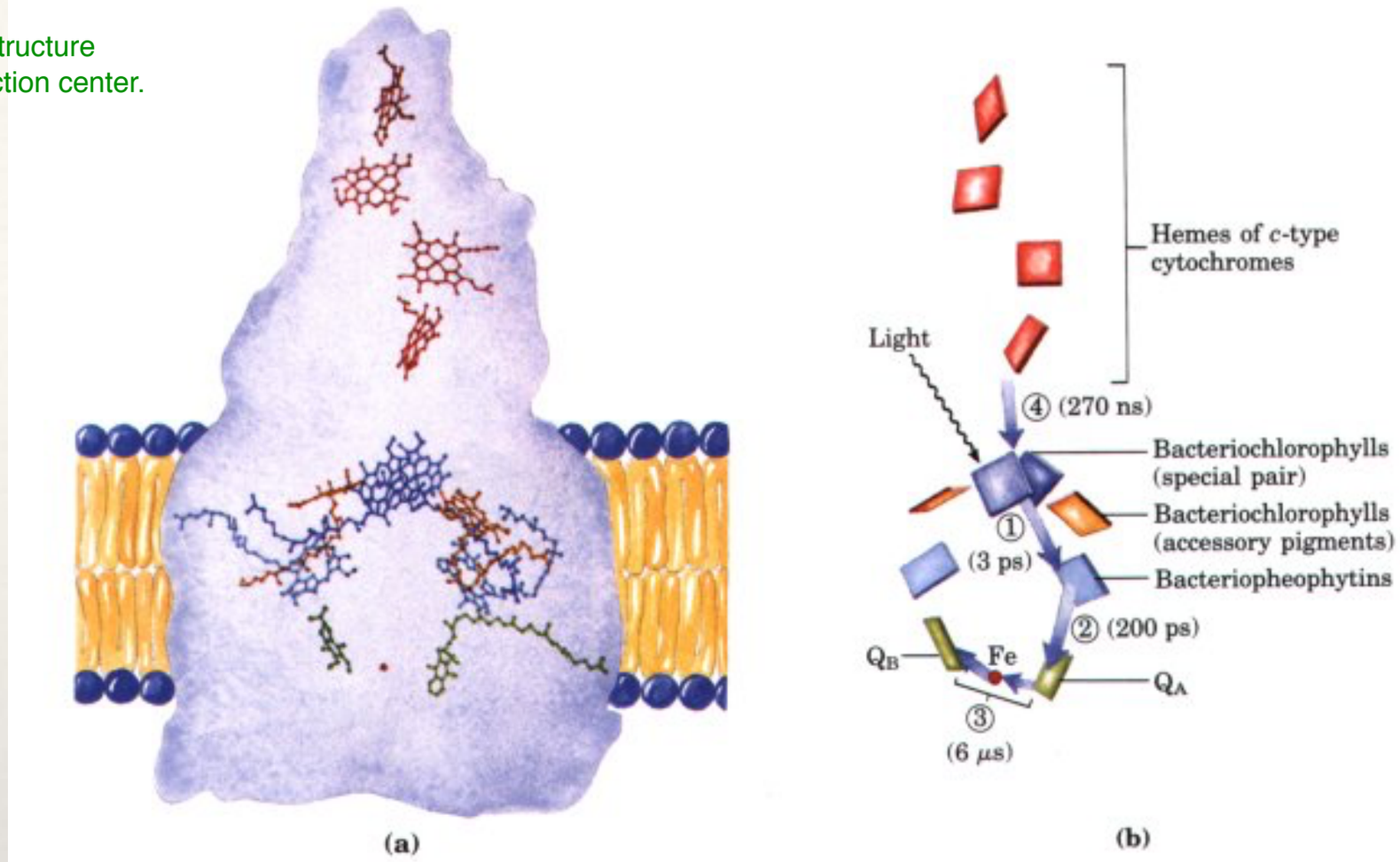

to Prof. ***J. Deisenhofer****, Texas, USA ,* ***R. Huber, H. Michel****, Max-Planck-Institut*

The Nobel Prize in Chemistry 1988



http://www.bioinfo.org.cn/book/biochemistry/chapt18/sim9.htm

for his contributions to the theory of electron transfer reactions in chemical systems

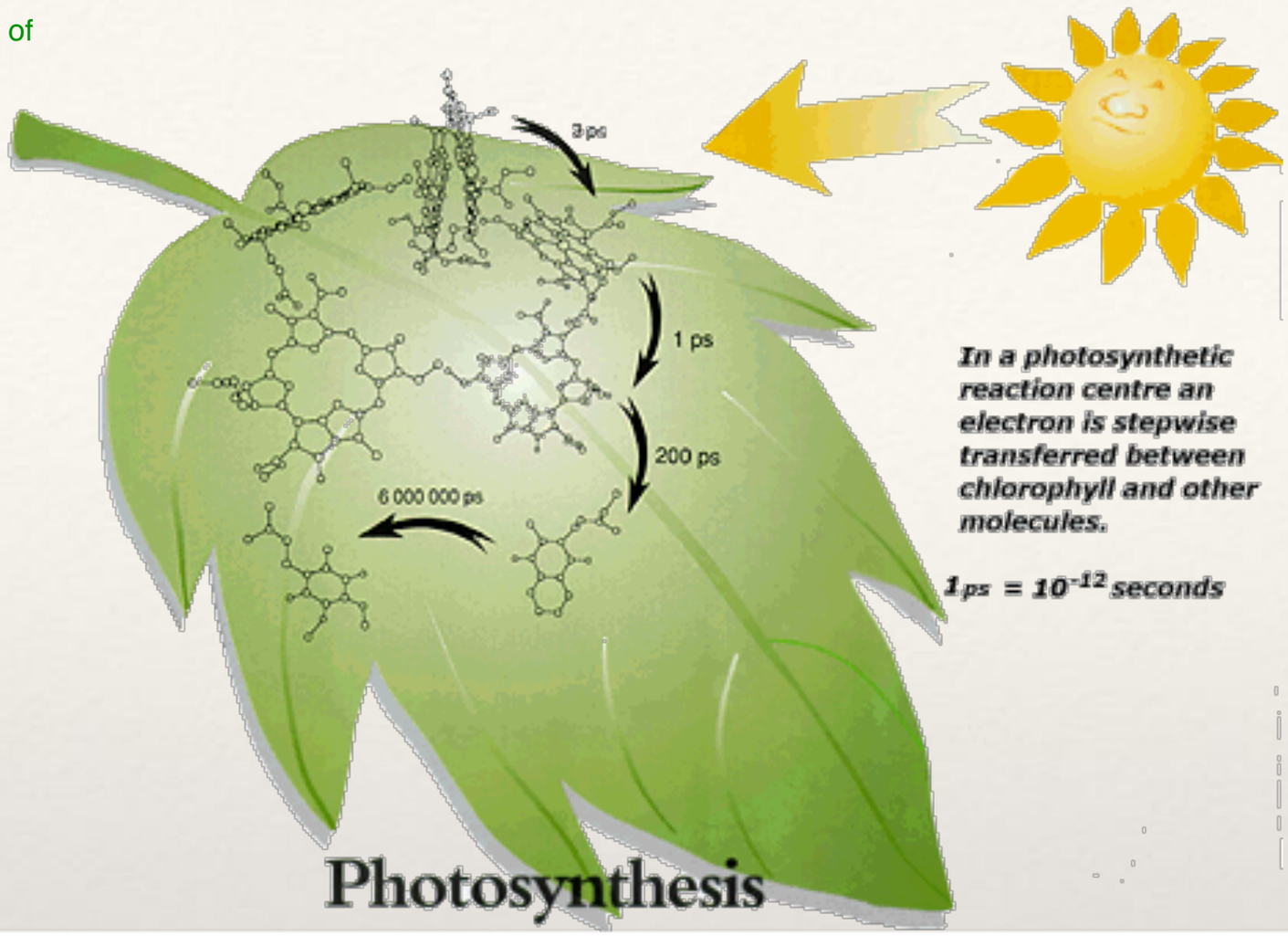

to Prof. ***Rudolph A. Marcus****, California Institute of Technology, Pasadena, California, USA*

The Nobel Prize in Chemistry 1992

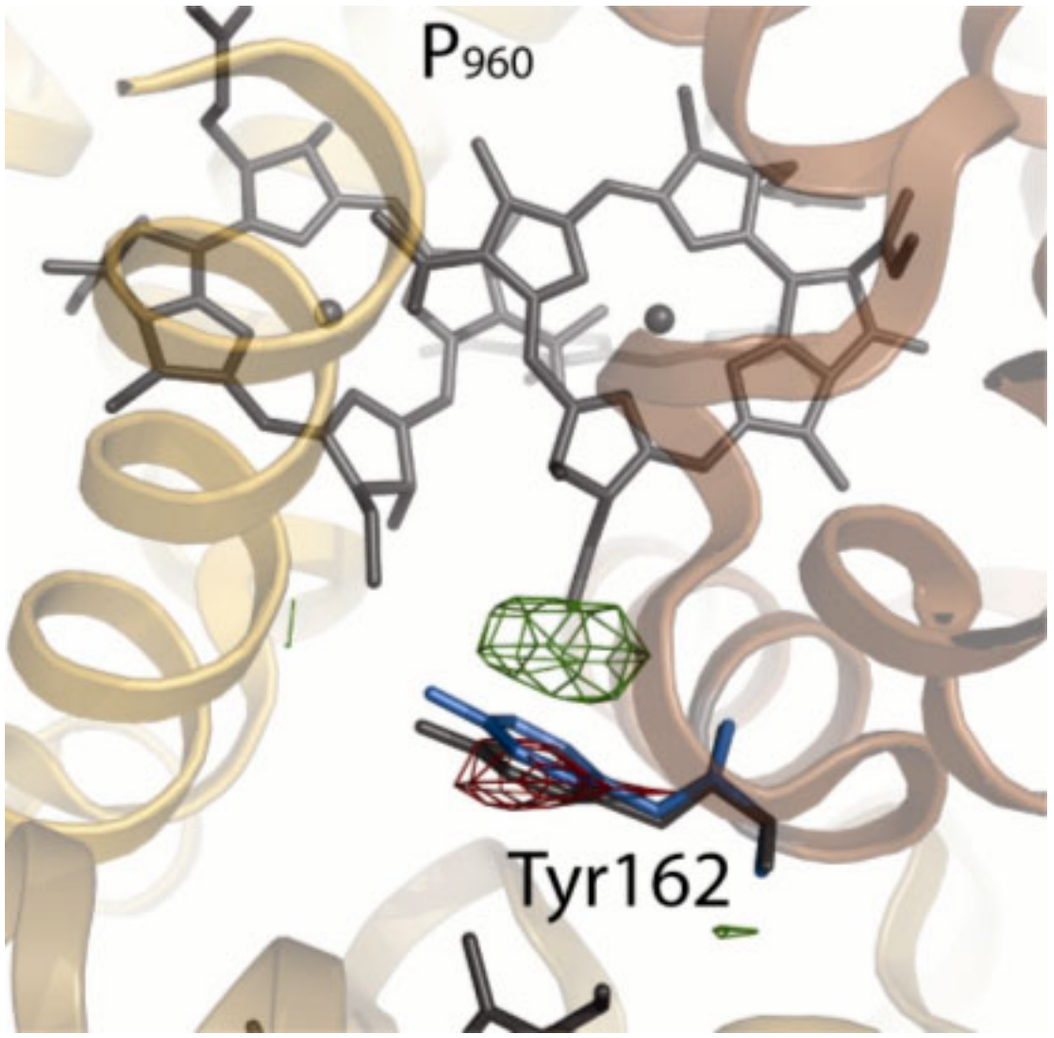
P960
Tyr162

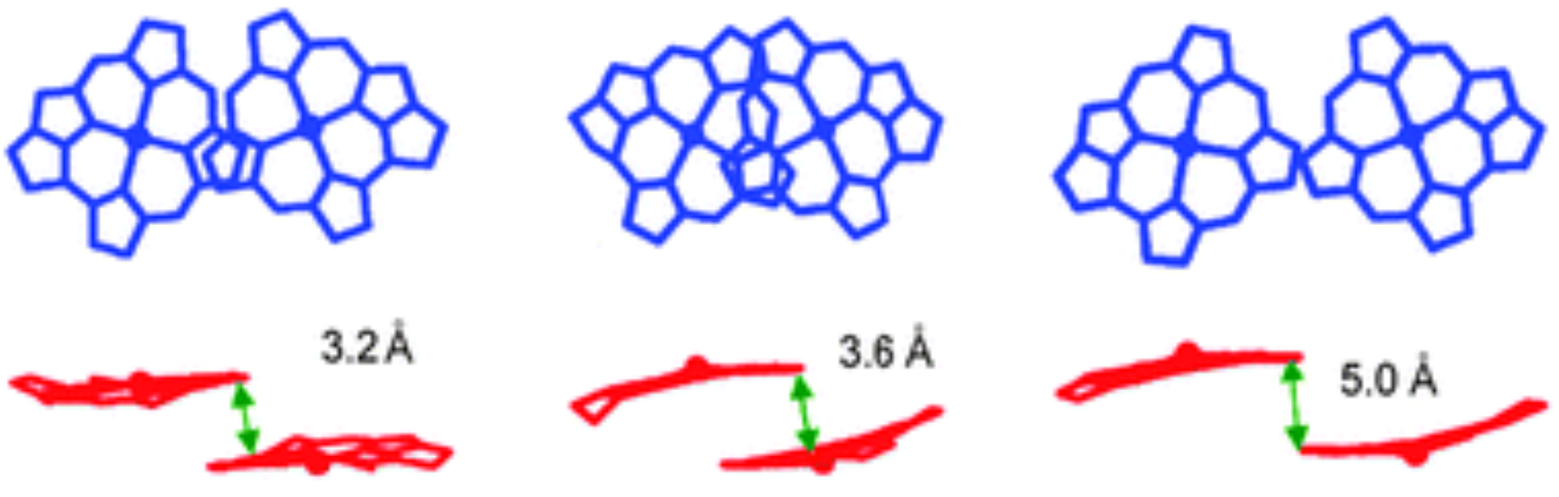
3.2Å
3.6 Å
5.0 Å

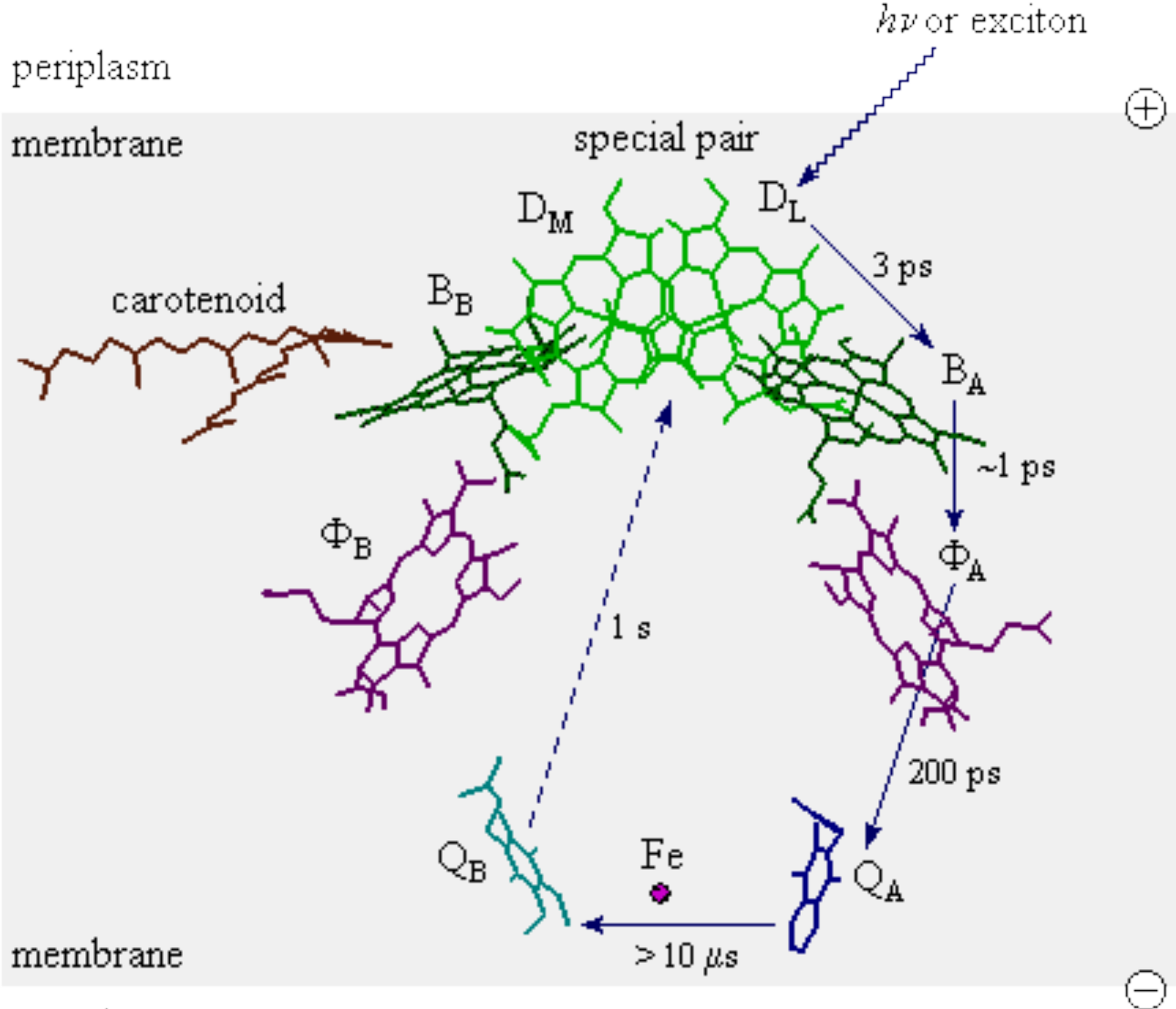
periplasm
membrane
hν or exciton
special pair
D_M
D_L
carotenoid
B_B
3 ps
B_A
~1 ps
Φ_B
Φ_A
1 s
200 ps
Q_B
Fe
Q_A
membrane
> 10 μs
cytoplasm

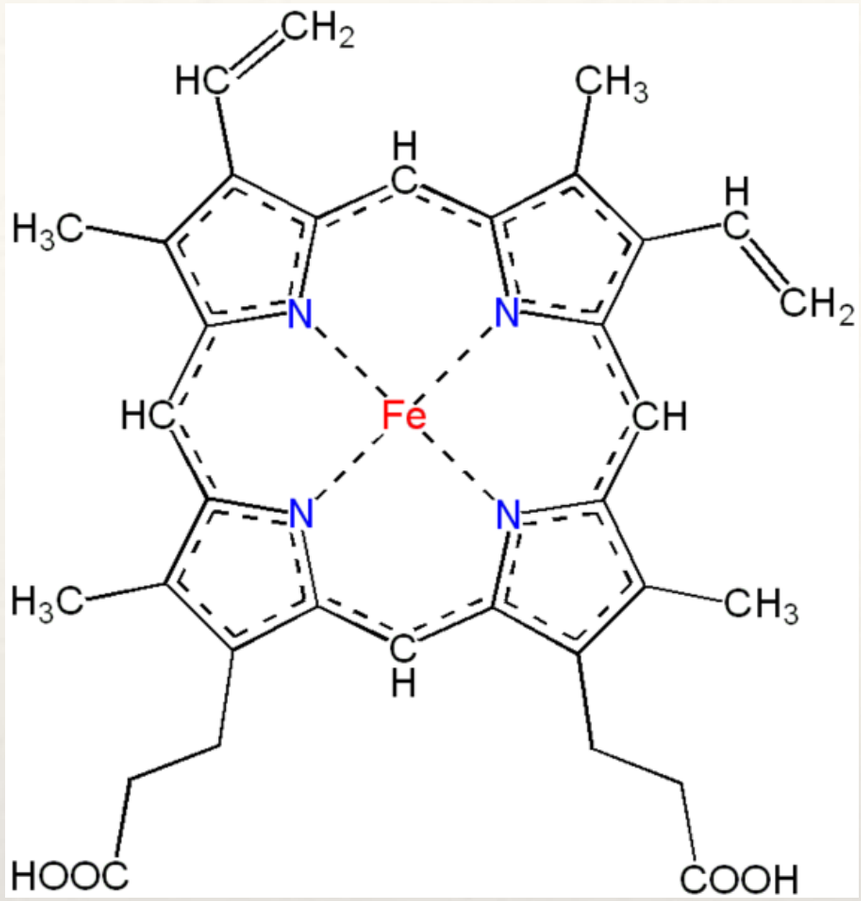

The heme group

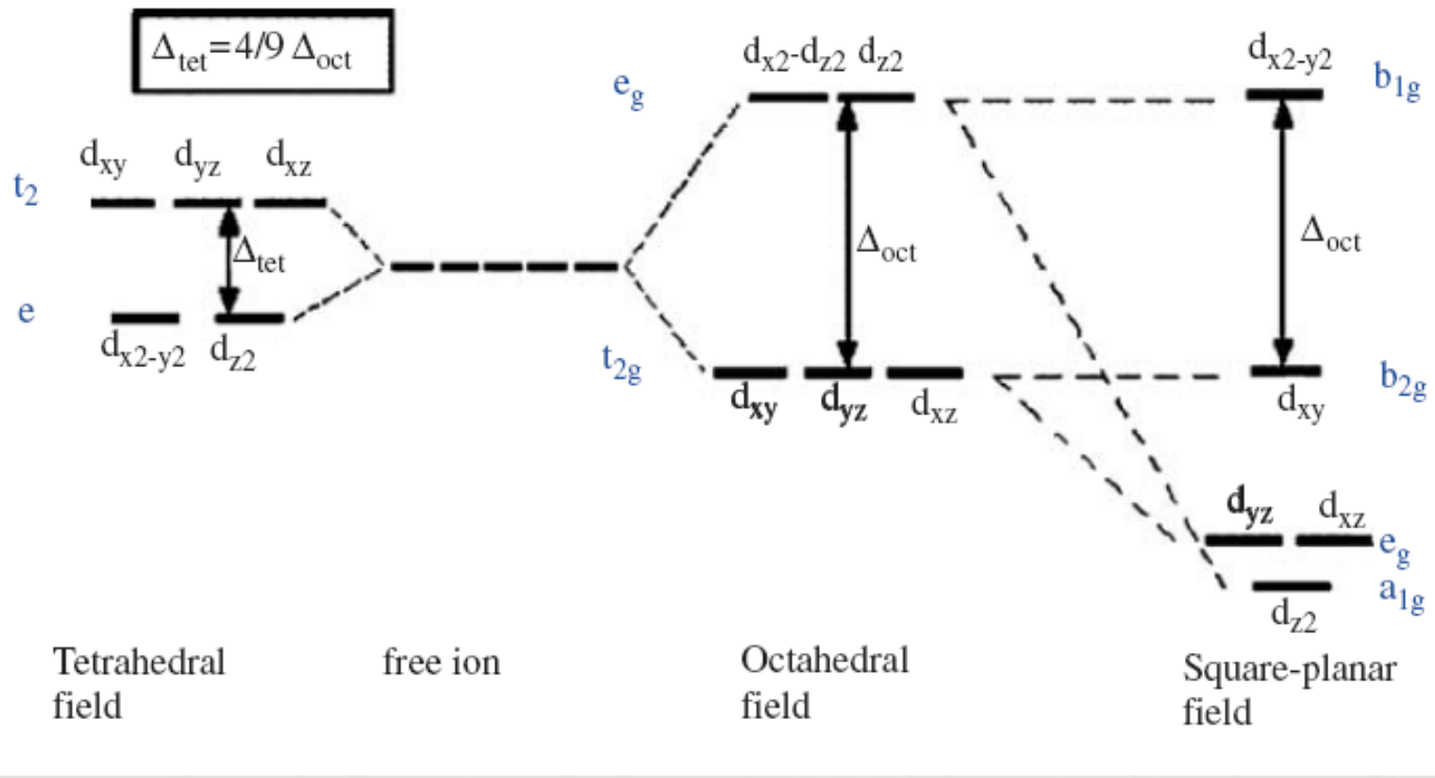

Iron

Crystal field d-orbital splitting diagrams for common iron geometries

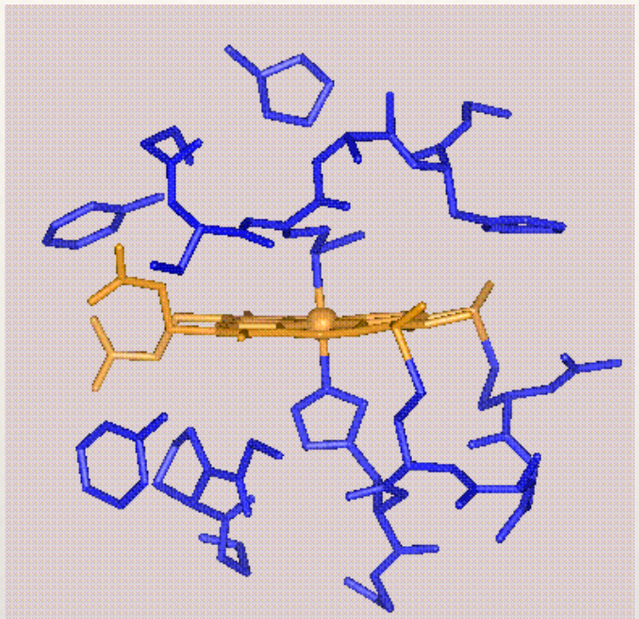

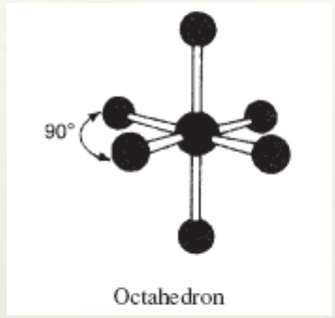

Heme iron may be present in one of three oxidation states:

Fe^{II}	($d6$)	ferrous
Fe^{III}	($d5$)	ferric
Fe^{IV}	($d4$)	ferryl

Electronic state of iron in heme

With four equatorial nitrogen ligands from the porphyrin and two axial ligands from the protein, heme iron has an octahedral ligand geometry

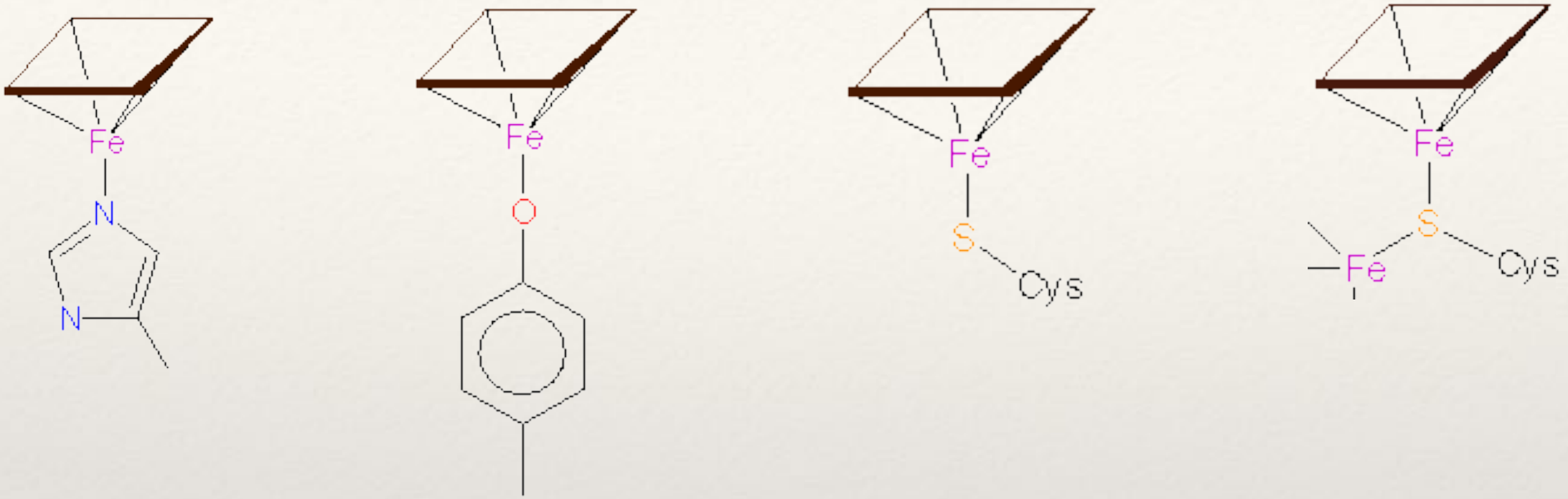

Pentavalent iron geometry

With four equatorial nitrogen ligands from the porphyrin and two axial ligands from the protein, heme iron has an octahedral ligand geometry

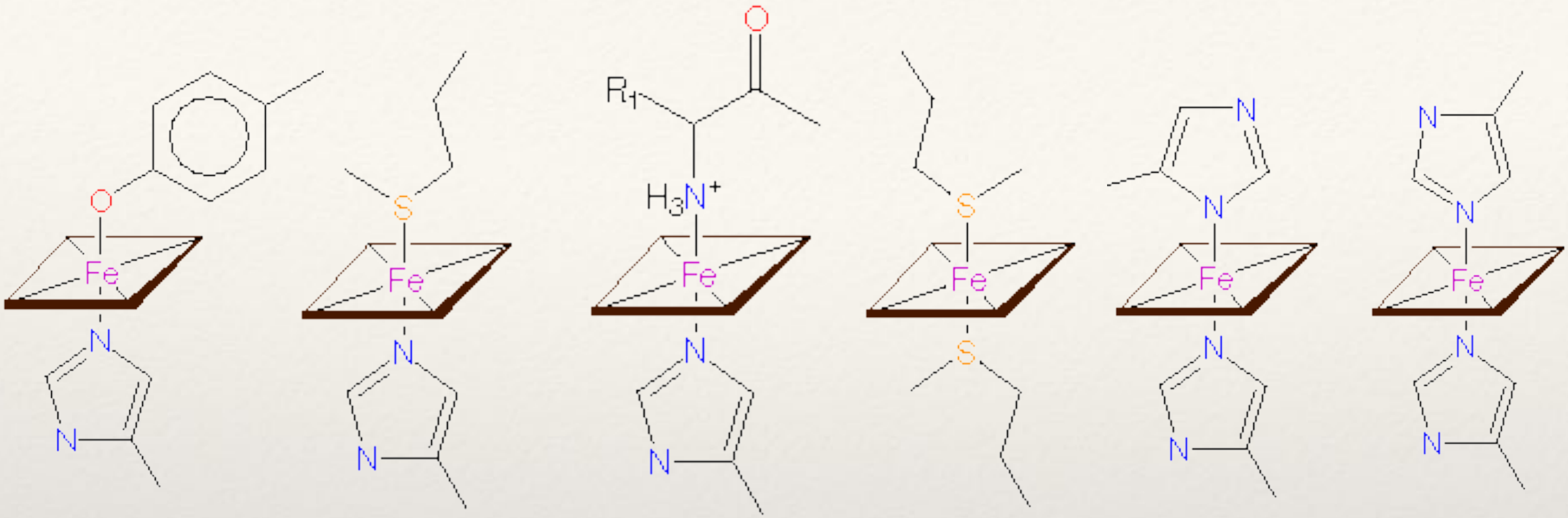

Hexavalent iron geometry

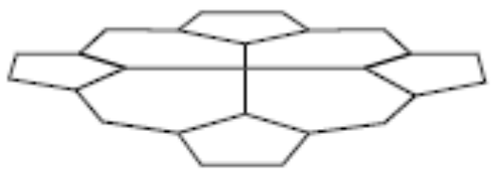

sad (B_{2u}), 65 cm^{-1}

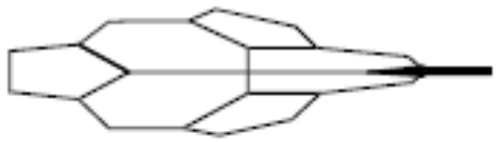

ruf (B_{1u}), 88 cm^{-1}

dom (A_{2u}), 135 cm^{-1}

wav (*x*) [$E_{g(x)}$], 176 cm^{-1}

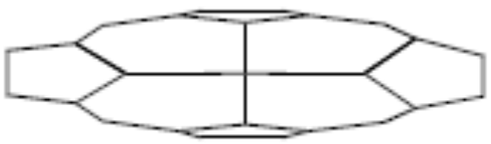

wav (*y*) [$E_{g(y)}$], 176 cm^{-1}

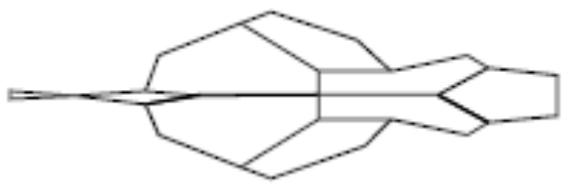

pro (A_{1u}), 335 cm^{-1}

Symmetric normal-coordinate deformations of hemes.

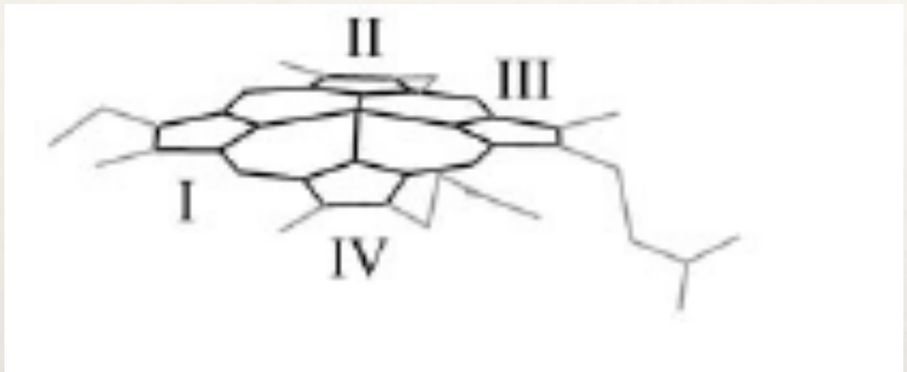

Porphyrin conformation in different proteins

tetrapyrrole biosynthetic pathways

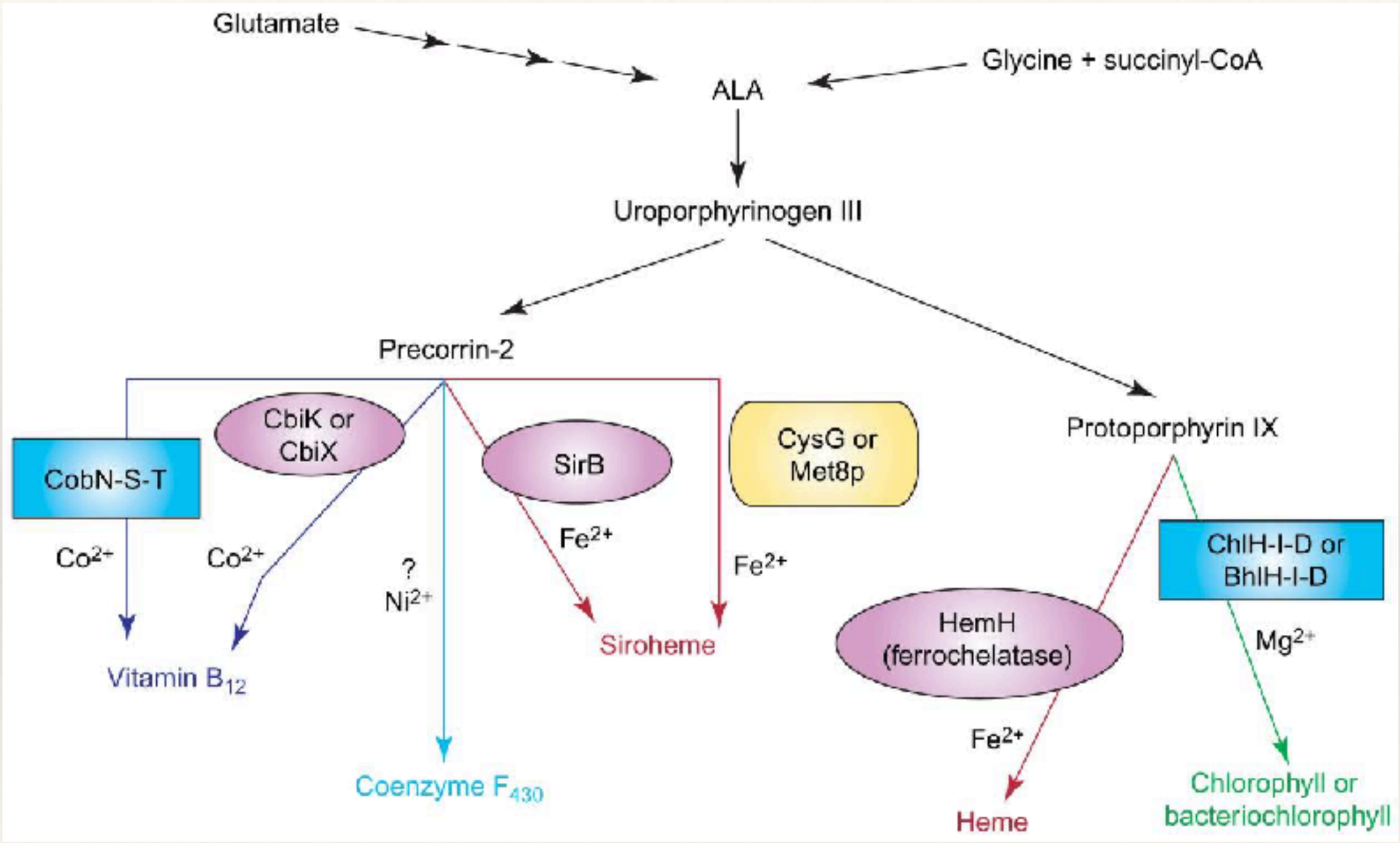

The relationship between tetrapyrrole biosynthetic pathways. Uroporphyrinogen III is the tetrapyrrole that is common to all tetrapyrrole biosynthetic pathways. 5-Aminolevulinate (ALA), a precursor of uroporphyrinogen III, derives from glycine and succinyl-CoA (in eukaryotes other than plants and the α subgroup of the photosynthetic purple bacteria) or glutamate (in plants and most bacteria). Class I, II and III chelatases are shown in blue, purple and yellow, respectively.

Trends Biochem Sci. 2006 Mar;31(3):135-42. Epub 2006 Feb 15.

Porphyrin- and metal ion-binding sites in ferrochelatase.

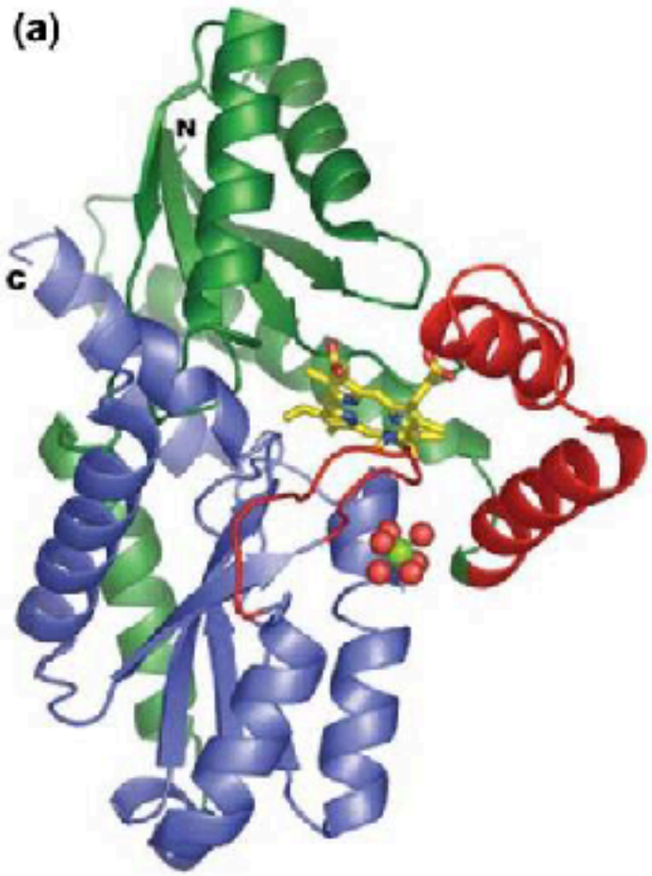

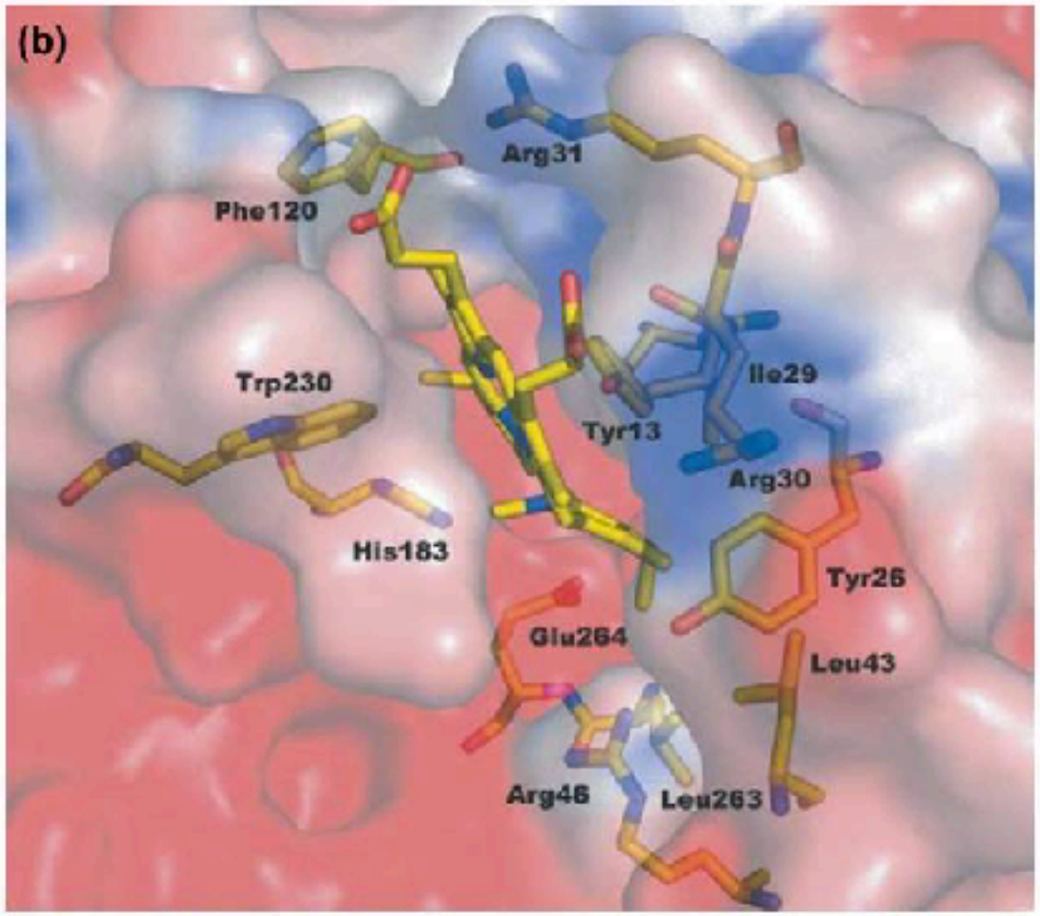

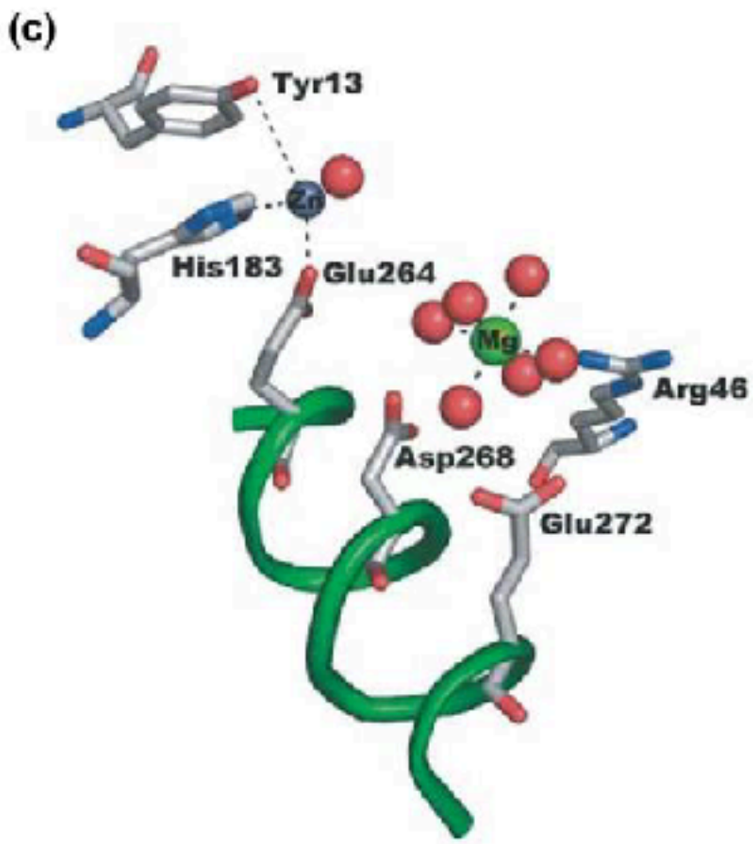

Trends Biochem Sci. 2006 Mar;31(3):135-42. Epub 2006 Feb 15.

- Porphyrin- and metal ion-binding sites in ferrochelatase. (a) Structure of B. subtilis ferrochelatase in complex with the transition-state inhibitor N-methylmesoporphyrin (N-MeMP). The structure is composed of two Rossmann-type domains (green and blue), in which a central four-stranded β sheet is flanked by α helices. A cleft defined by structural elements (red) from both domains accommodates the porphyrin- and metal-binding sites. The inhibitor N-MeMP is shown in the cleft (carbon atoms, yellow; oxygen, red; nitrogen, blue). On binding to the enzyme, porphyrin is distorted and the protein undergoes a conformational transition, during which the cleft is widened. This process is typical of an 'induced-fit' mechanism of catalysis. A fully hydrated Mg^{2+} ion is always located ~8 Å from the nitrogen atom of the distorted ring A of the porphyrin (Mg^{2+}, green sphere; water, red spheres). (b) Interaction of N-MeMP with amino acids in the substrate-binding cleft of B. subtilis ferrochelatase. The side chains of the residues that contribute directly to the stabilization of porphyrin binding are shown in stick representation. Arg30 and Arg31 are on the surface of the molecule and contribute to neutralization of the negative charge of the propionic acid side chains of the porphyrin. Tyr13, Ile29, His183, Trp230 and Glu264 stabilize the position of the macrocycle in the cleft. The hydroxyl group of Tyr13 is directed towards the center of the ring and coordinates a metal ion in a complex of ferrochelatase with Cu^{2+} inserted into N-MeMP. Tyr26 and Leu43 constitute part of the switch region, which triggers the conformational transition in the enzyme on porphyrin binding. (c) Two metal-binding sites in B. subtilis ferrochelatase. The two sites are shown with a Zn^{2+} ion (gray sphere) and a fully hydrated Mg^{2+} ion (green sphere). The distance between the metal ions is ~7 Å. His183 and Glu264 are among the few residues that are invariant in all protoporphyrin IX ferrochelatases. The side chains of residues Glu272, Asp268 and Glu264 are aligned along a π helix (green) in a line connecting the two metal sites. Only a π helix can provide such an alignment of side chains. The π helix differs from the α helix in that it has 4.1 residues per turn and is stabilized by hydrogen bonds between residues i and i+5 (an α helix has 3.6 residues per turn and hydrogen bonds between residues i and i+4).

Trends Biochem Sci. 2006 Mar;31(3):135-42. Epub 2006 Feb 15.

Porphyrin- and metal ion-binding sites in ferrochelatase.

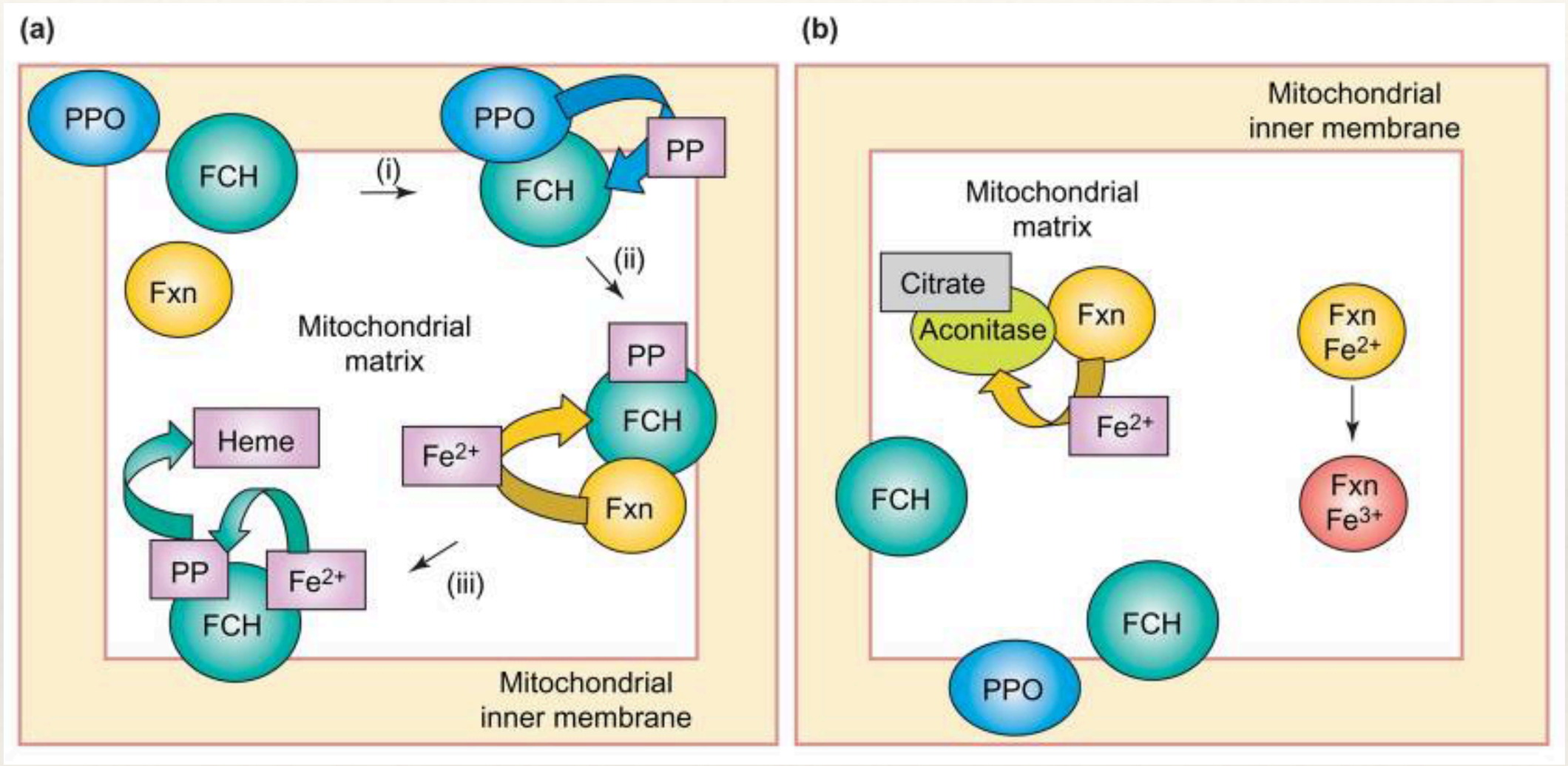

Proposed model of modulation of ferrochelatase–frataxin interactions by protoporphyrin. **(a)** **Protoporphyrinogen oxidase (PPO)** makes protoporphyrin (PP) available to ferrochelatase (FCH) via a transient interaction (i). Frataxin (Fxn) then delivers Fe2+ to ferrochelatase (ii), which promotes its insertion into protoporphyrin to yield heme (iii). **(b)** **In the absence of protoporphyrin**, frataxin might donate Fe2+ to other proteins (e.g. aconitase) [42] or could incorporate surplus iron in a stable ferrihydrite mineral

Trends Biochem Sci. 2006 Mar;31(3):135-42. Epub 2006 Feb 15.

Mechanism of porphyrin metallation by ferrochelatase

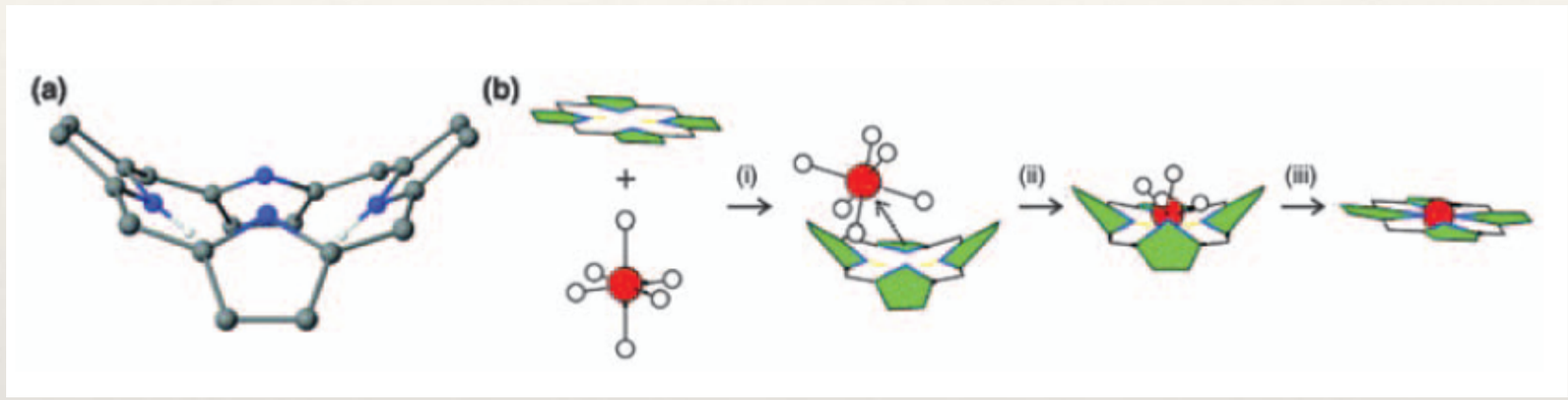

(a) Out-of-plane saddle structure in which two pyrrole rings with unprotonated nitrogens (blue spheres) point upwards, while the other two, protonated (blue and white spheres) point downwards. (b) Steps in the mechanism for incorporation of the metal ion (red) into the porphyrin (pyrrole rings in green)

Porphyrins throughout the Chemistry Curriculum

- Porphyrins are ubiquitous compounds with many useful chemical, physical, and biological properties. This presentation will provide examples of the use of porphyrins in teaching chemistry in a variety of courses

General Chemistry

- Spectroscopy is introduced by giving students a colored sample. The students are then are asked to obtain a visible spectra of the compound. The students are divided into groups of four and they discuss what needs to be done. After they determine what is a spectra, they start to think about what equipment is needed. After they discover a spectrometer is required, they must determine how to put a sample in the spectrometer. The samples given include transition metal compounds, organic dyes, and of course porphyrin.

Porphyrins throughout the Chemistry Curriculum

Organic Chemistry

- The fabrication of porphyrins involve reactions taught as part of an organic chemistry course. One of the reactions is electrophilic aromatic substitution. This reaction is demonstrated by treating either an aldehyde or acid chloride with the aromatic heterocycle, pyrrole. Simple aryl porphyrins are synthesized by treating an aryl aldehyde with pyrrole in refluxing proprionic acid commonly called the Alder-Longo method.

Porphyrins throughout the Chemistry Curriculum

Inorganic Chemistry

- Porphyrins are naturally occurring macrocycles found in animal and plant tissue. Several synthetic porphyrins are readily prepared. They are fairly rigid are macrocyclics that are excellent ligands that can coordinate a wide variety of metals and even some nonmetals. Porphyrins are able to complex with metals in a variety of oxidation states. In the laboratory portion of the course, students prepare and characterize manganese porphyrins coordination compounds to multiple oxidation states.

- Synthetic porphyrins and metalloporphyrins are highly symmetrical compounds. These provide excellent examples for instruction in the assignment of point groups. Often changes in symmetry upon metallation of a porphyrin will manifest itself in the change in the UV-visible spectra. Porphyrin compounds of iron are commonly known as heme. Heme is ubiquitous in many metalloproteins and provide an excellent example of the importance of inorganic compounds that are biologically active.

Porphyrins throughout the Chemistry Curriculum

Analytical Chemistry

- The purification of porphyrinato-manganse-ethiol was developed by analytical chemistry courses. The compound can be separated from any porphyriato-manganese nitride starting material using column chromatography by elution with acetone. The product can be eluted with methanol. Alumina was found to decompose the product but silica gel was found to be useful.
- Future Analytical classes will work on a band broadening problem. Elemental analysis have been high in sulfur. Sulfur elutes with the product but it may be possible to remove the excess via sublimation.
- They are also used to discuss fluorescence spectroscopy and electrochemistry.

Porphyrins throughout the Chemistry Curriculum

Biochemistry

- Iron porphyrins commonly known as heme are prosthetic groups for a wide variety of metalloproteins. These metalloproteins are used to transport and store oxygen, activate oxygen for use in detoxification and biosynthesis, and participate in electron transport processes. At UoC, the biological importance of heme based metalloproteins are part of bioinorganic chemistry course. This course is required of chemistry majors and minors.
- The heme containing metalloenzymes, catalase and horseradish peroxidase, are readily available for study. These enzymes are commonly used to explore enzyme kinetics and the effects of condition on activity.

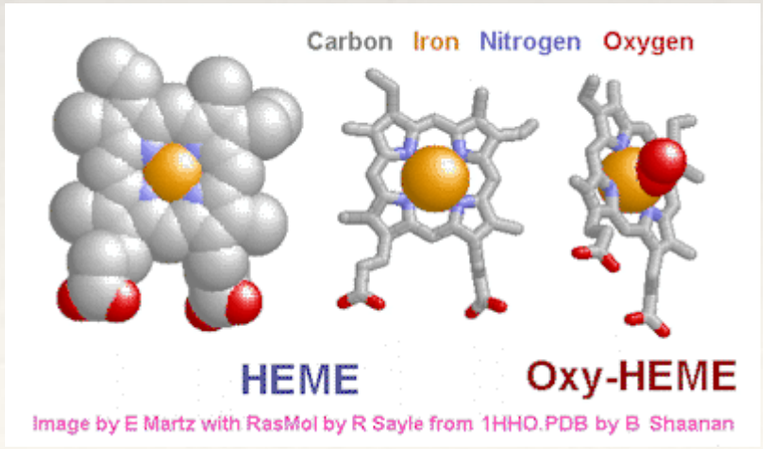

Natural porphyrin rings

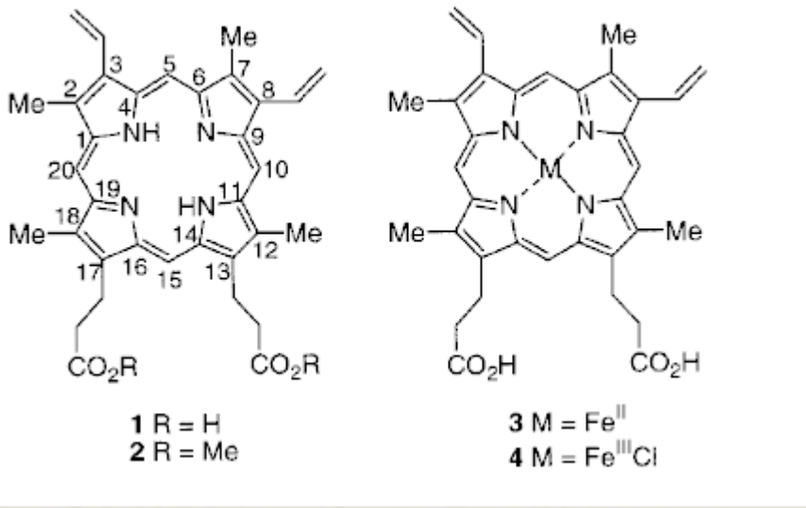

1 R = H
2 R = Me

3 M = Fe^{II}
4 M = $Fe^{III}Cl$

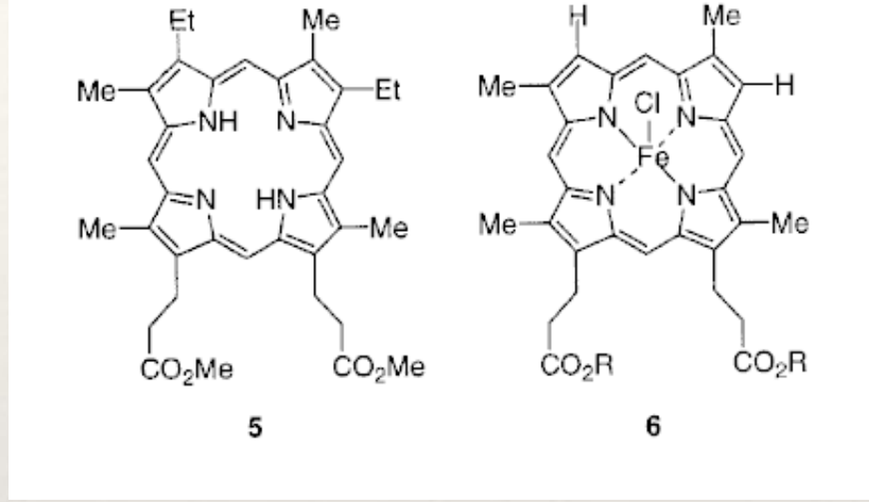

5

6

1. Protoporphyrin IX

3. Περιέχεται στη αιμογλοβίνη και μυογλοβίνη (μεταφέρει O_2 και CO_2. Ο Fe έχει αξονικό υποκαταστάτη –N υπόλειμα αμινοξέος. Οξειδώνεται δύσκολα E_o *($Fe^{III}P/Fe^{II}P$) =0.82 V*

5. mesoporphyrin IX

6. Deuterohemin

Natural porphyrin rings

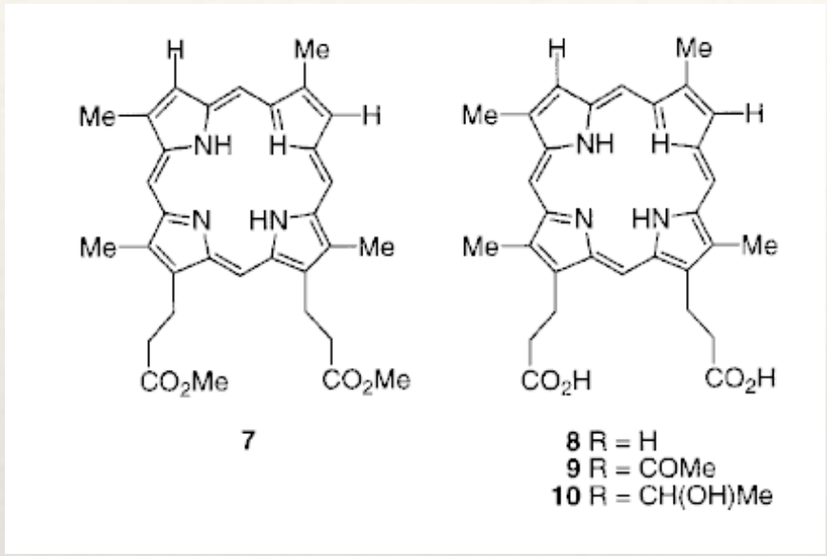

8. Duteroporphyrin IX (η πρώτη απομονωμένη πορφυρίνη στη βραβευμένη με Nobel σύνθεση αιμίνης του Fischer)

10. Hematoporphyrin IX (πρώτη απομονωμένη πορφυρίνη από το αίμα 1867)

Χρησιμοποιείται με το εμπορικό όνομα photofrin για την PDT

Synthesis of tetra phenyl porphyrin

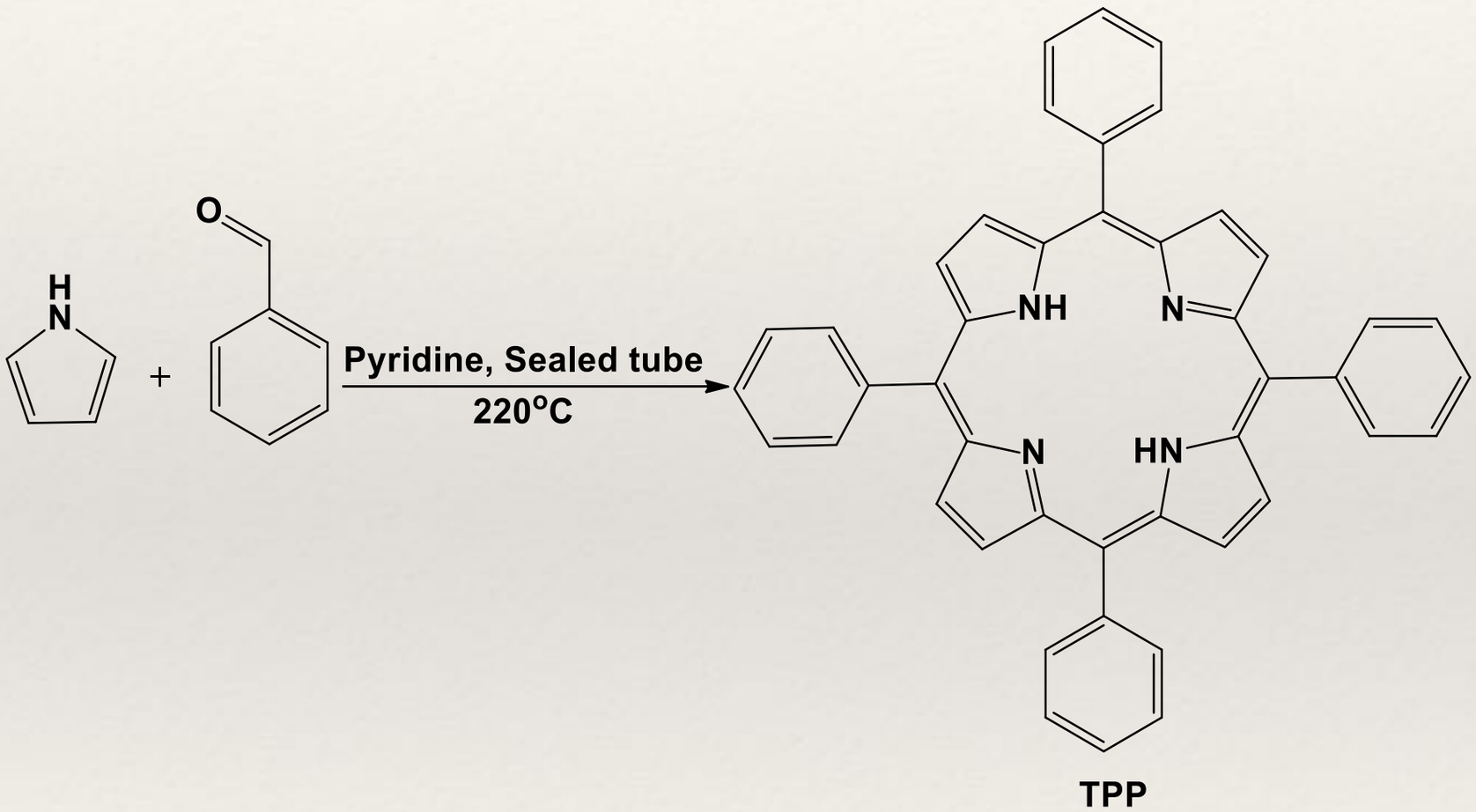

TPP

Mechanism for the Synthesis of tetra phenyl porphyrin

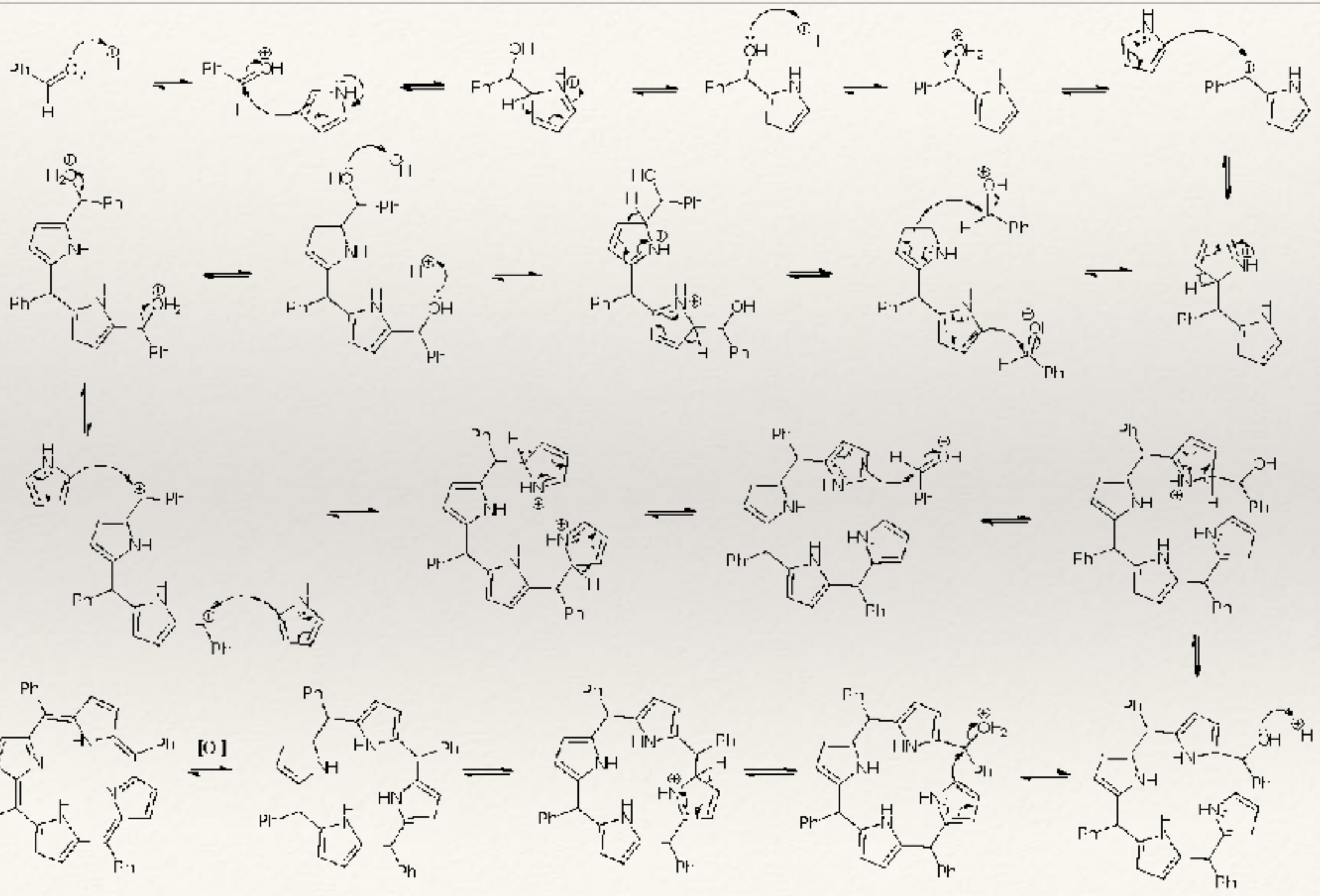

Synthesis of unsymmetrical porphyrin

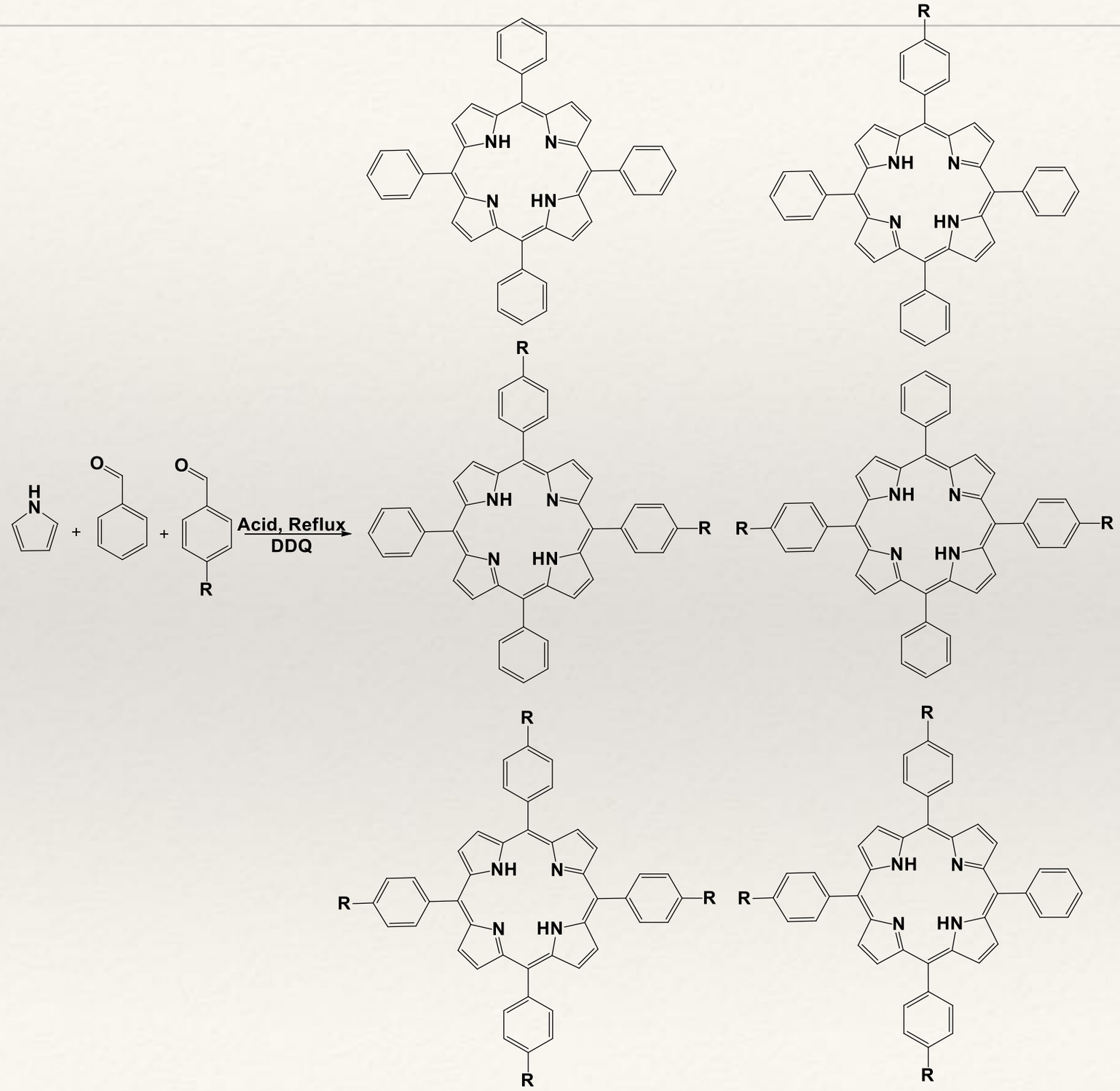

Another approach for the Synthesis of unsymmetrical porphyrin

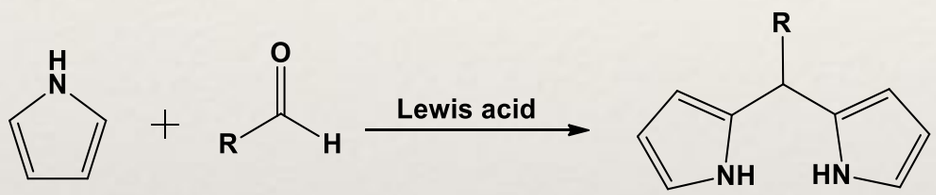

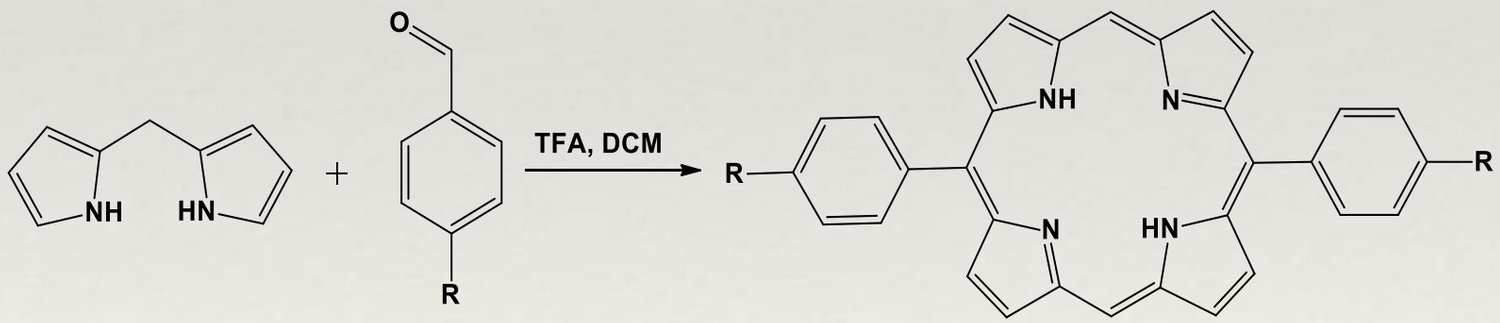

Various unsymmetrical porphyrins

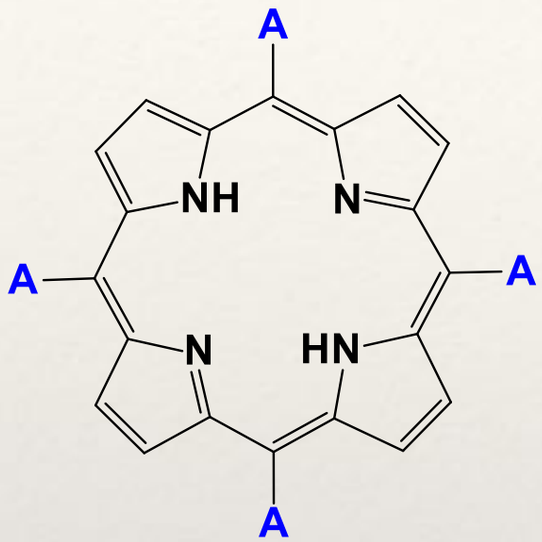

A_4-Porphyrin

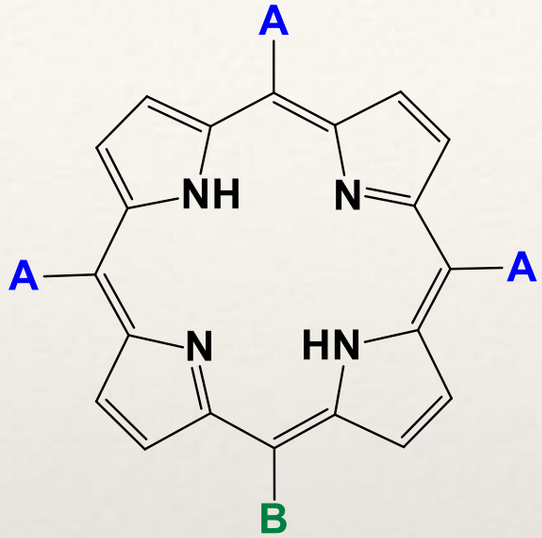

A_3B-Porphyrin

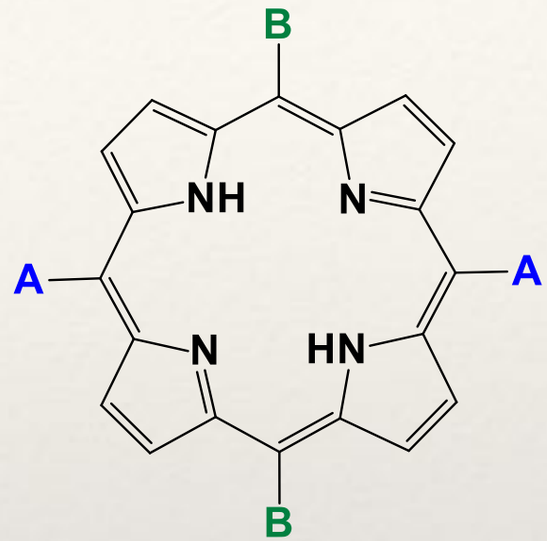

A_2B_2-Porphyrin

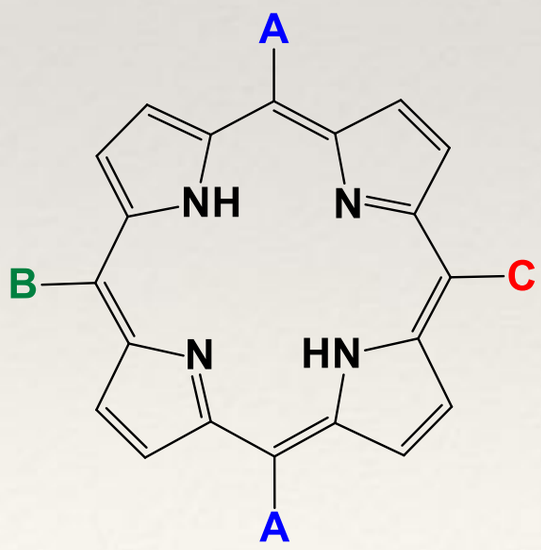

A_2BC-Porphyrin

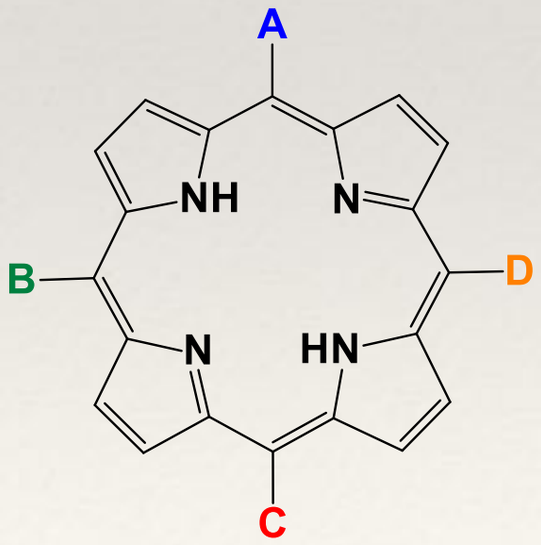

ABCD-Porphyrin

Synthetic metalloporphyrin rings

1: M(p)

A

B

C

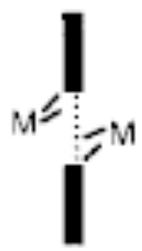

L

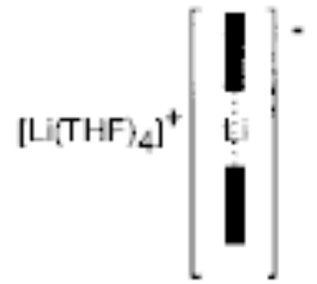

L'

L''

G

Z–Z = OAc

K

Electronic Properties

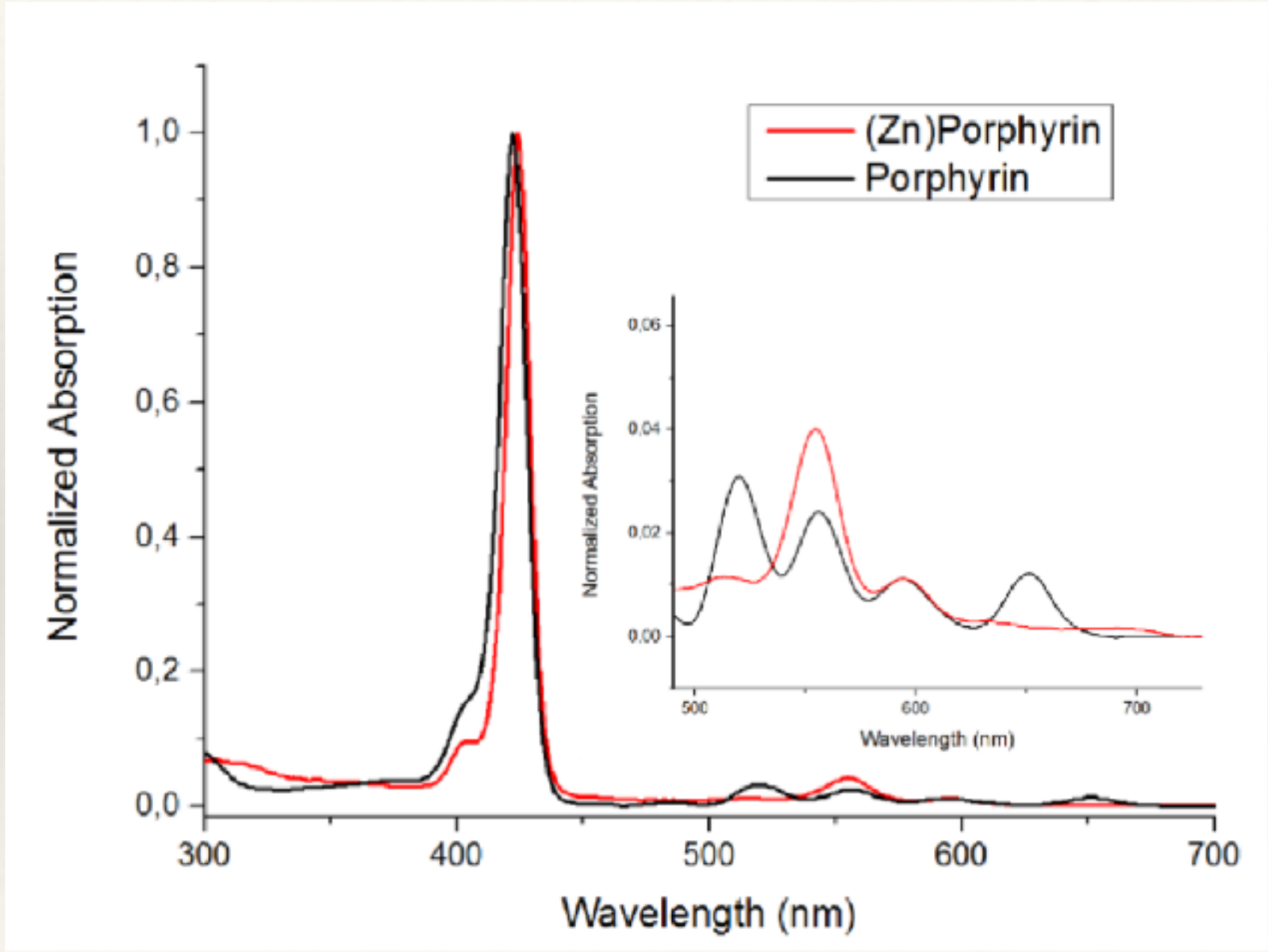

The UV-Vis absorption spectra of a free base porphyrin (black line) and a zinc metallated porphyrin (red line).

Electronic Properties

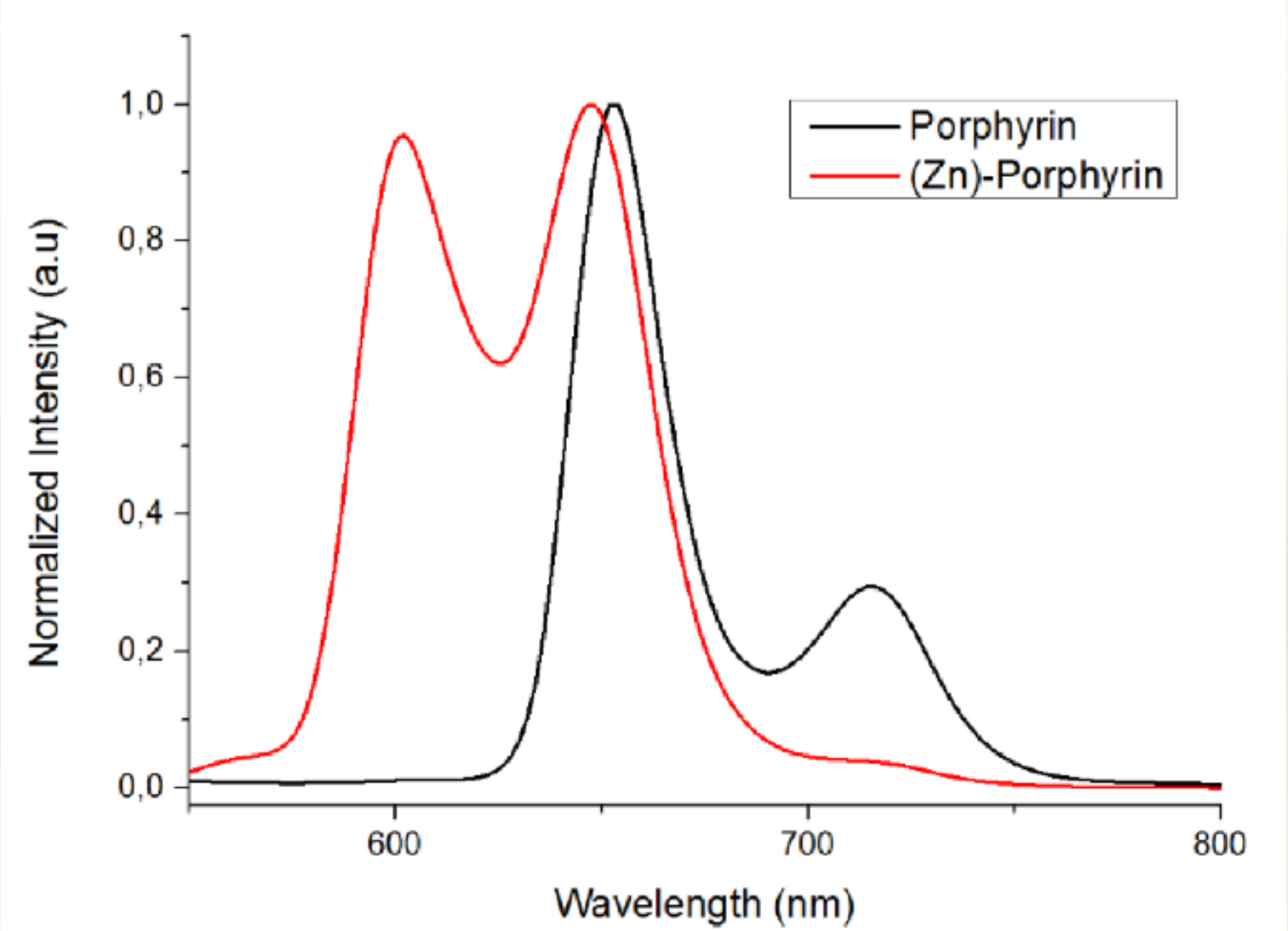

Typical fluorescence spectra of a free base porphyrin (black line) and a zinc metallated porphyrin (red line).

Electronic Properties

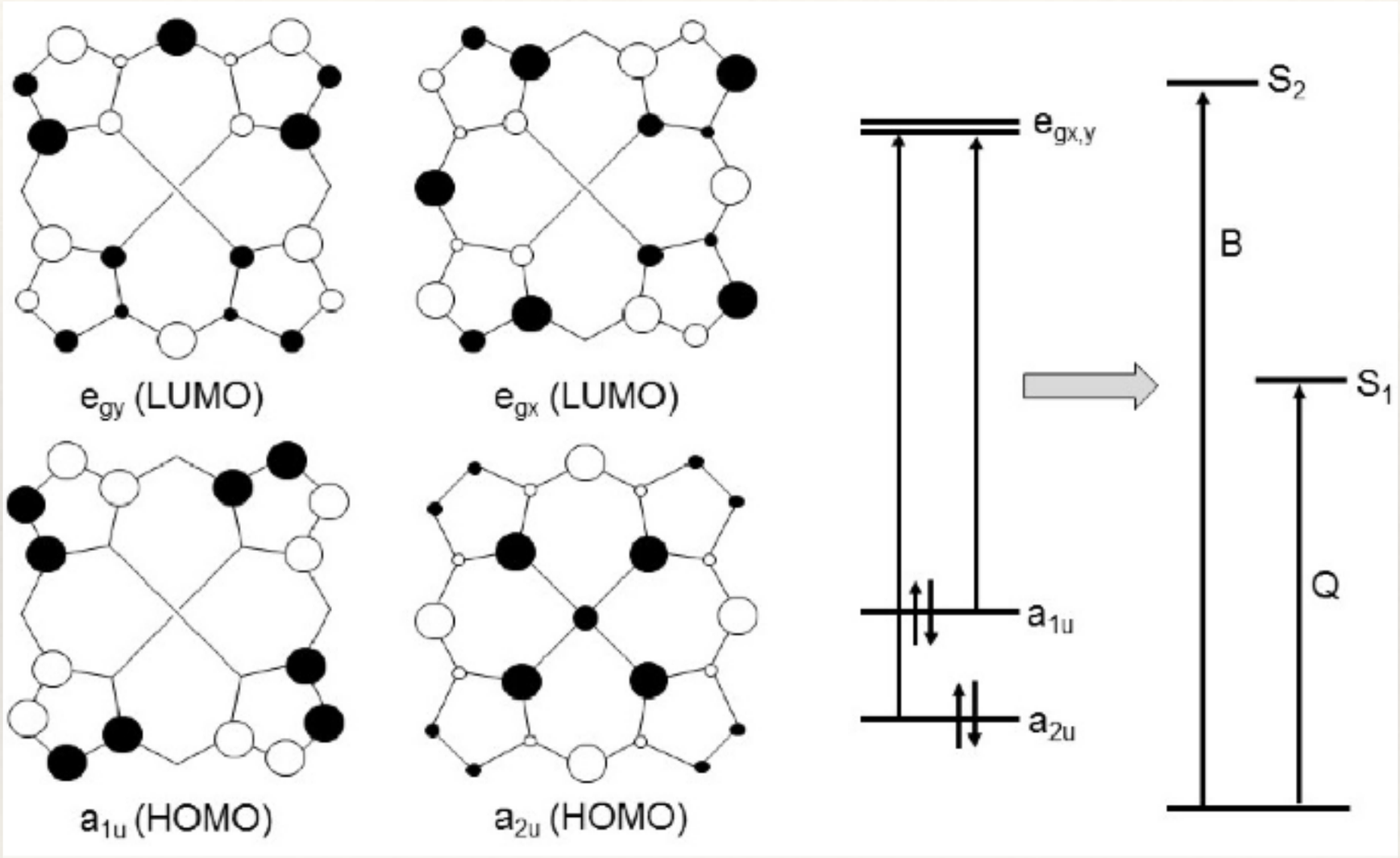

M.Gouterman, *J.Phys.Chem.,* 1959, 30, 1139

Their absorption features derive from single electron transitions between the two highest occupied (HOMO, HOMO-1) π-orbitals and the two lowest unoccupied (LUMO and LUMO+1) π*-orbitals.

Electronic Properties

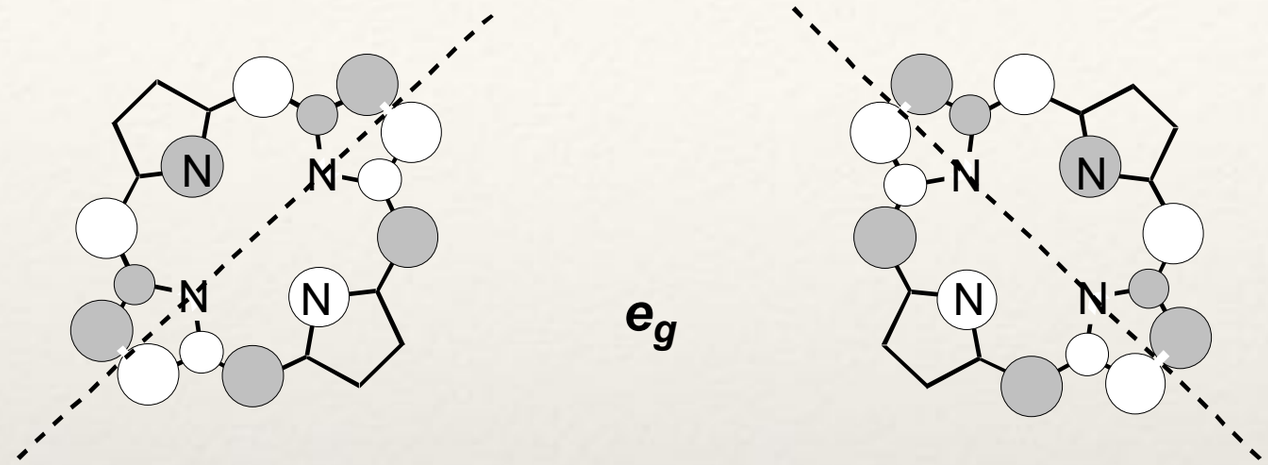

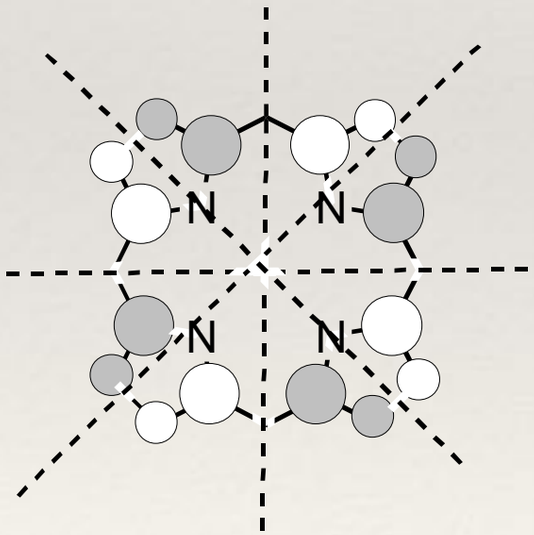

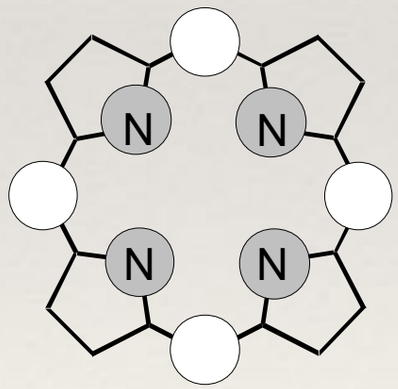

M.Gouterman, *J.Phys.Chem.,* 1959, 30, 1139

Their absorption features derive from single electron transitions between the two highest occupied (HOMO, HOMO-1) π-orbitals and the two lowest unoccupied (LUMO and LUMO+1) π*-orbitals.

Electronic Properties

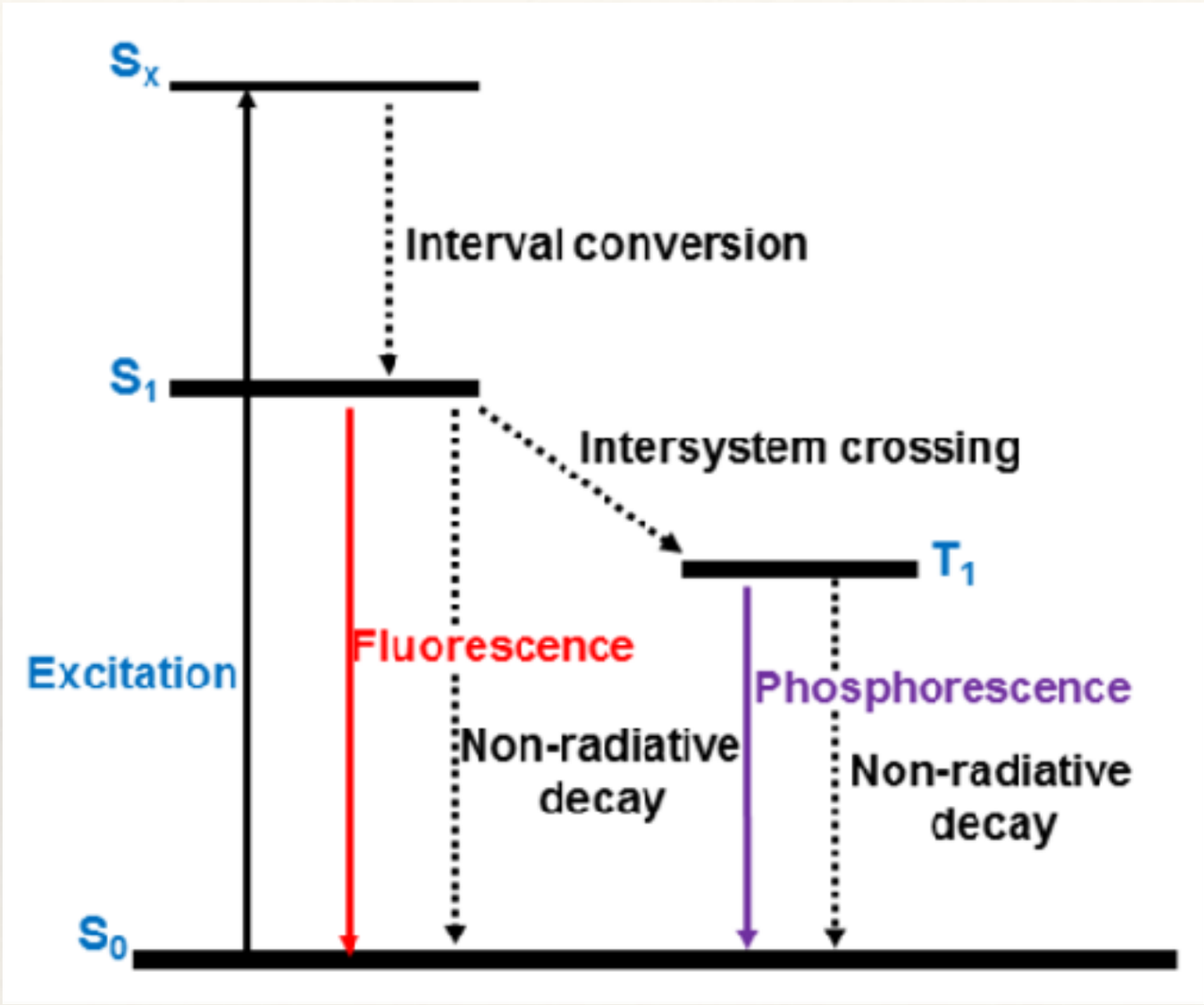

Jablonski diagram illustrating the singlet and triplet states formed of a photon excited porphyrin moiety. Solid lines represent the radiation processes while dashed lines radiationless processes.

L-M Στερεοηλεκτρονιακή επίδραση στη ταινία Soret

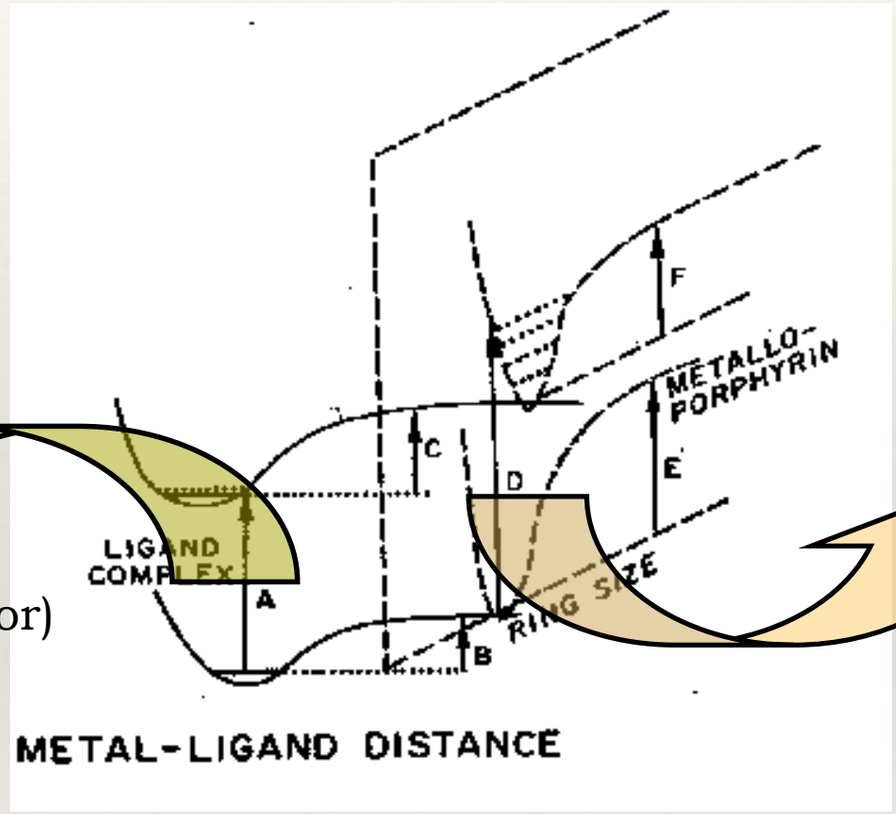

A:ενέργεια μετάβασης LM(Por)

D:ενέργεια μετάβασης (Por)M

Ο συνδυασμός των ενεργειακών διαφορών D , A οδηγεί στη στερεοηλεκτρονική μετατόπιση (red shift) που παρατηρείται στο σχηματισμό της (Por)ML από (Por)M

Electronic Properties

A $Zn^{II}(TPP)$ *"normal"*

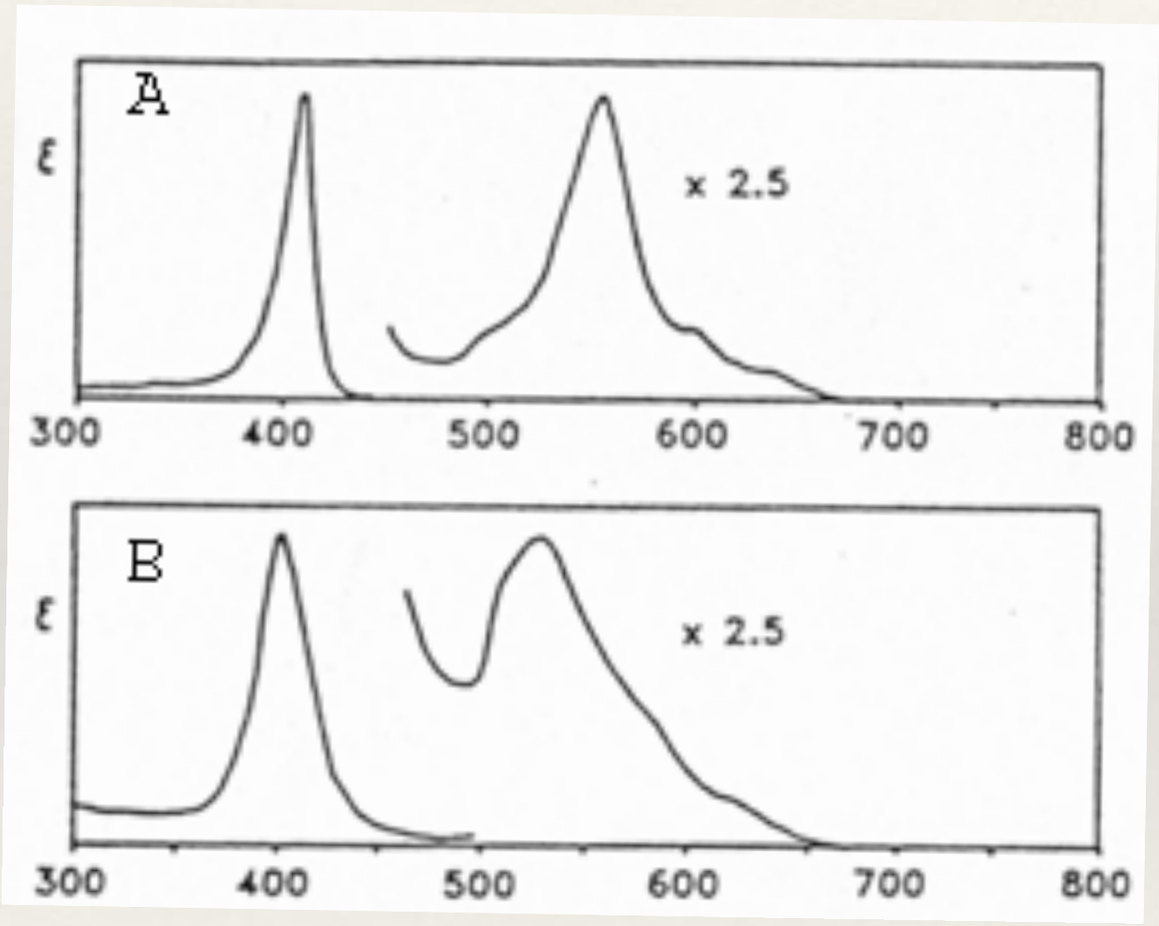

B. $Ni^{II}(TPP)$, "hyspo"

C $Pb^{II}(TPP)$ *"p–hyper"*

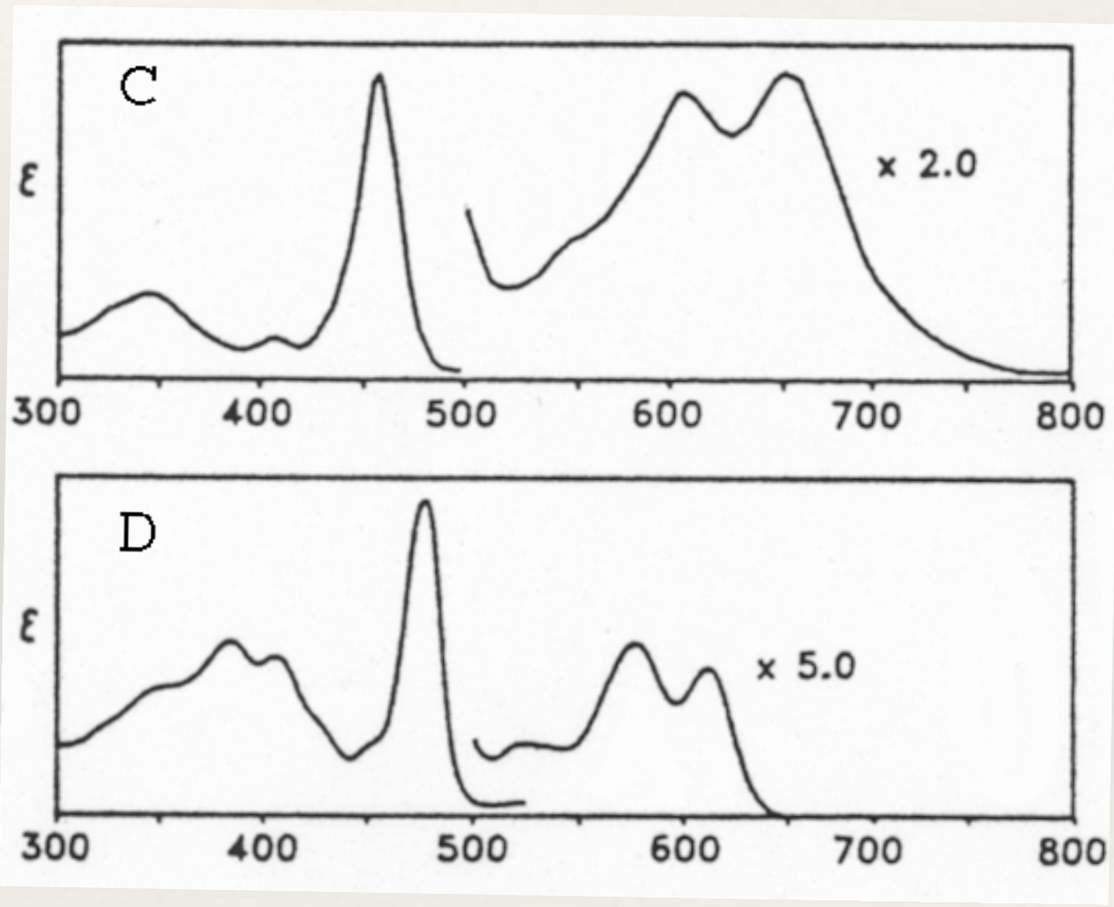

D. $Mn^{III}(TPP)NO_3$, "d-hyper"

K. S. Suslick, New J. Chem. ***1992****, 16, 633*

1. Normal (Por)M (D_{4h})

M: ομάδες 1 έως 5
οξειδωτικές καταστάσεις +1 έως +5 Ηλεκτρονιακή διαμόρφωση d^o ή d^{10}

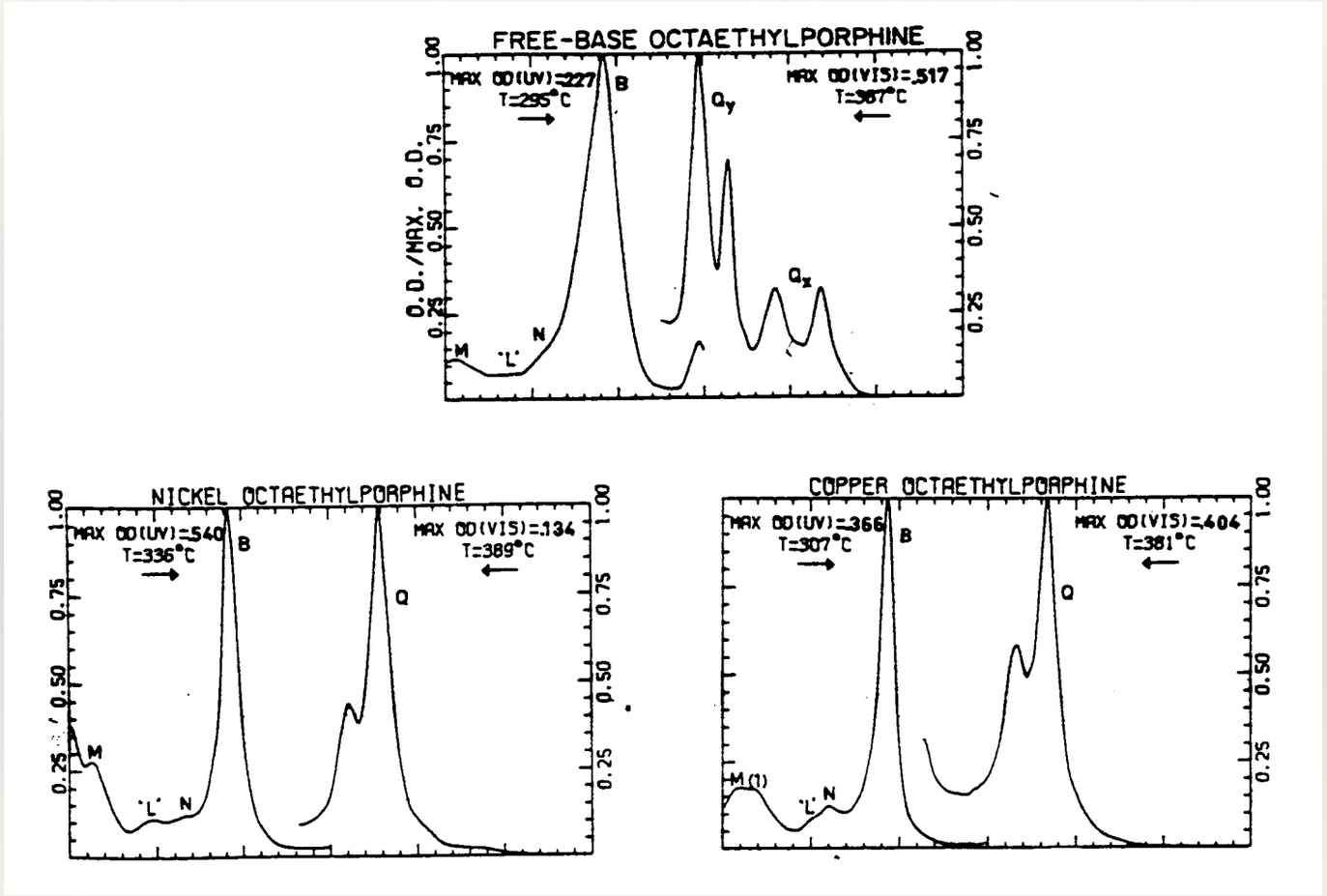

Χαρακτηριστικά

Μία έντονη **B**-ταινία απορρόφησης. Μία ή δύο Q-ταινίες
(ενεργειακή διαφορά ~1250 cm^{-1})

1. Normal (Por)M (D_{4h})

H_2P: 4 ταινίες απορρόφησης μεταξύ 450-700 nm (D_{2h})

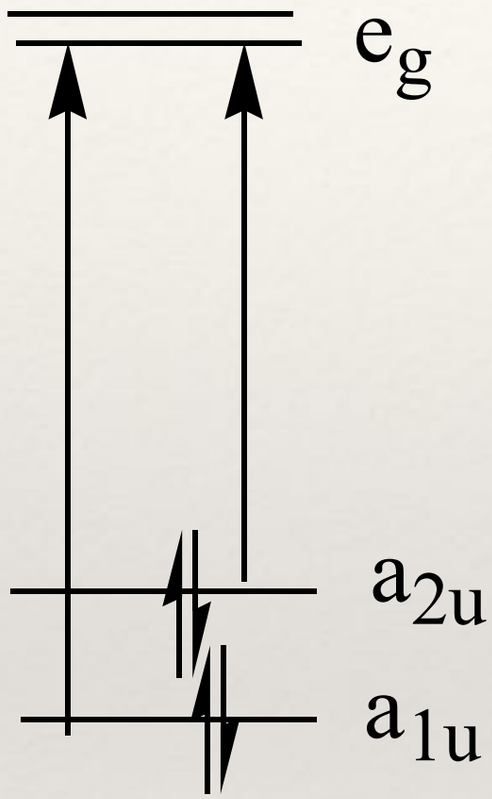

LUMO: e_g

HOMO: a_{1u} , a_{2u}

- **Q μετάβαση:** τα δίπολα μετάβασης αλληλοαναιρούνται (ασθενής απορρόφηση)
- **B μετάβαση:** γραμμικός συνδυασμός των διπόλων μετάβασης (ισχυρή απορρόφηση)
- ***Χημικές Μετατοπίσεις:*** οφείλεται στην αλληλεπίδραση του μετάλλου μ ε τα a_{2u} ,e_g τροχιακά

(Τα a_{1u} έχουν κομβικά σημεία στα πυρρολικά Ν και δεν επηρεάζονται απο το Μέταλλο

2. Hypso (Por)M

M: Ηλεκτρονιακή διαμόρφωση d^6 εως d^9 (κατειλημμένα e_g ($d\pi$) τροχιακά, Pt^{II}, Pd^{II}, Ni^{II})

Χαρακτηριστικά

Υψιχρωμική μετατόπιση της Q ταινίας (λ< 570 nm)
(μίξη των e_g LUMO της πορφυρίνης με τα κατειλημμένα e_g ($d\pi$) που οδηγεί στην αύξηση της ενέργειας των LUMO. Η ενεργειακή διαφορά LUMO - e_g αυξάνει με αύξηση των d ηλεκτρονίων οδηγώντας σε μείωση της μίξης των τροχιακών)

2. Hypso (Por)M

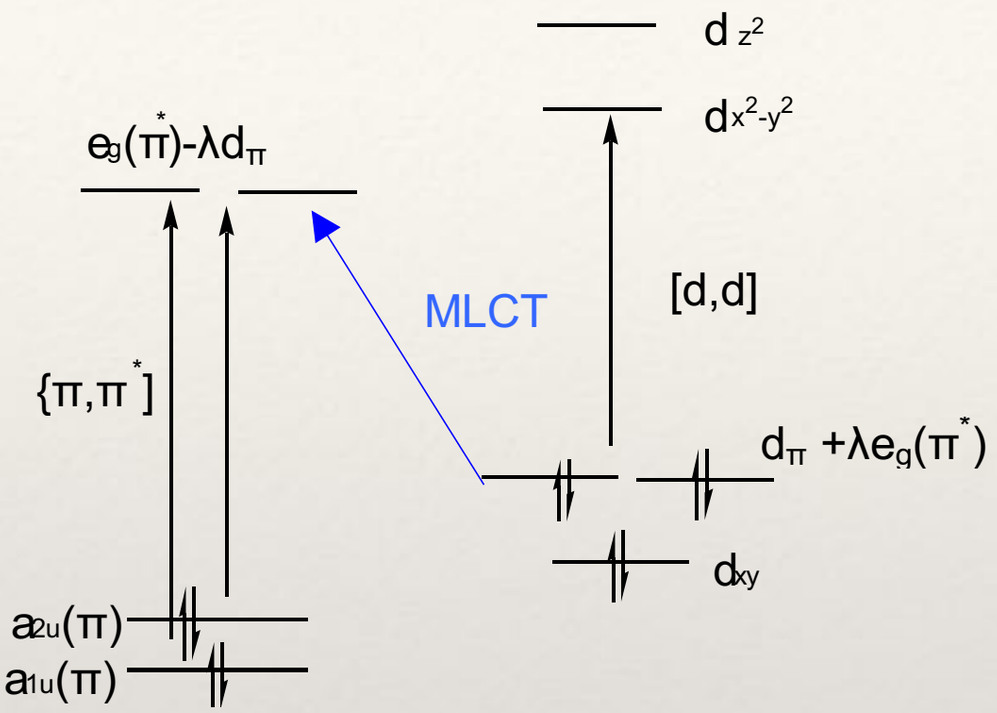

Παράδειγμα: d⁶

Το οπτικό φάσμα εξηγείται ποιοτικά βάσει των παρακάτω παραγόντων

1.Ενεργειακή διαφορά **Δ** μεταξύ των κατειλημμένων $(d_{xy})^2$ $(d_\pi)^4$ και των κενών $(d_z)^2$, $(d_{x^2-y^2})^2$

2.Την ενέργεια για **C.T.** Μεταβάσεις από τον Μέταλλο στο δακτύλιο

3. Οπισθοσύνδεση , λ(*back bonding)* [Μίξη των κατειλημμένων $e_g(d_\pi)$ και κενών $e_g(\pi^*)$ που προκαλεί αύξηση της ενέργειας των $e_g(\pi^*)$ προκαλώντας βαθυχρωμία)

Co^{II} ® Ni^{II} ® Cu^{II} τα φάσματα έχουν μικρότερη μετατόπιση σε μικρότερα μήκη κύματος blue-shifted.

3. Hyper Por(M)

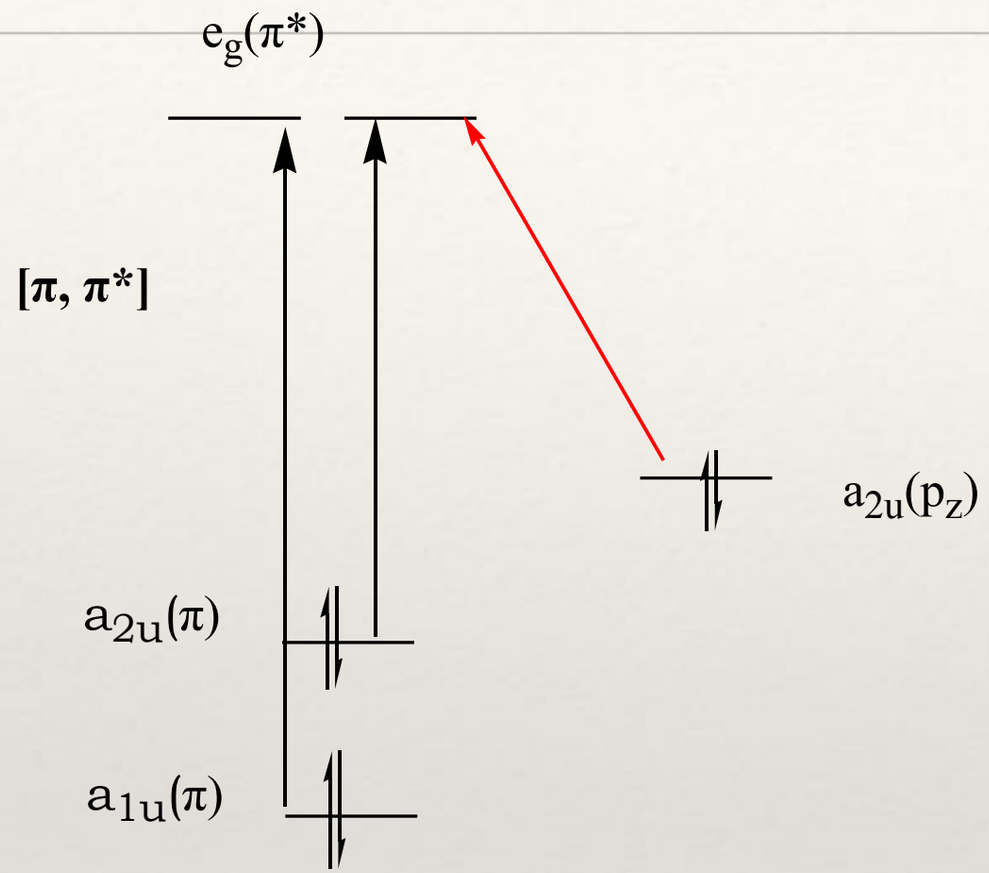

Χαρακτηριστικά

Περισσότερες ταινίες απορρόφησης σε σχέση με normal και hypso

3a.p-type hyper.

M: Sn^{II}, Pb^{II}, As^{II}, Sb^{II}, Bi^{II}

Οι επιπλέον ταινίες οφείλονται σε MLCT.

np_z (metal)®$e_g(\pi^*)$

3. Hyper Por(M)

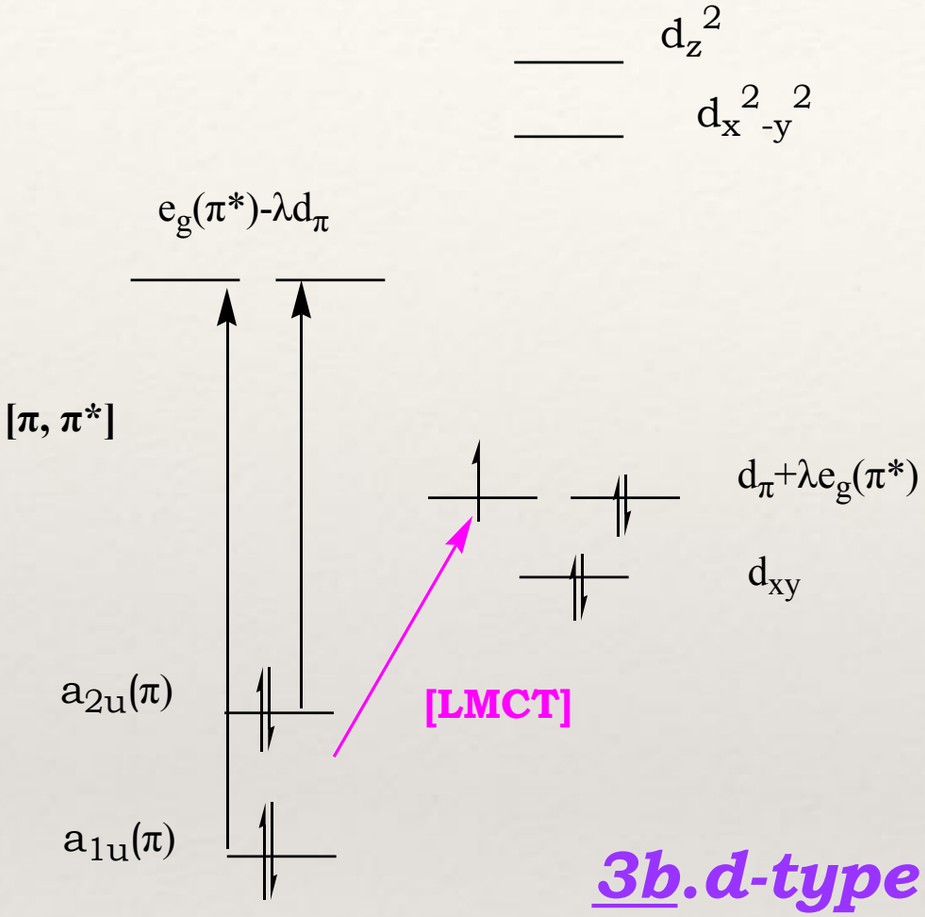

3b.d-type hyper.

M: Fe^{III}, Mn^{III}, Mo^{V}, (d^1 έως d^6 με κενά $e_g(d_\pi)$ τροχιακά)
Οι επιπλέον ταινίες οφείλονται σε LMCT
(οδηγεί σε αλλαγή στην οξειδωτική κατάσταση του μετάλλου Η μίξη των τροχιακών είναι πιο έντονη όταν τα LUMO της πορφυρίνης είναι κοντά ενεργειακά με τα τροχιακά του Μετάλλου).

Applications

- Bioinspired transformations

Supramolecular self assembling

Applications

chloroplast structure

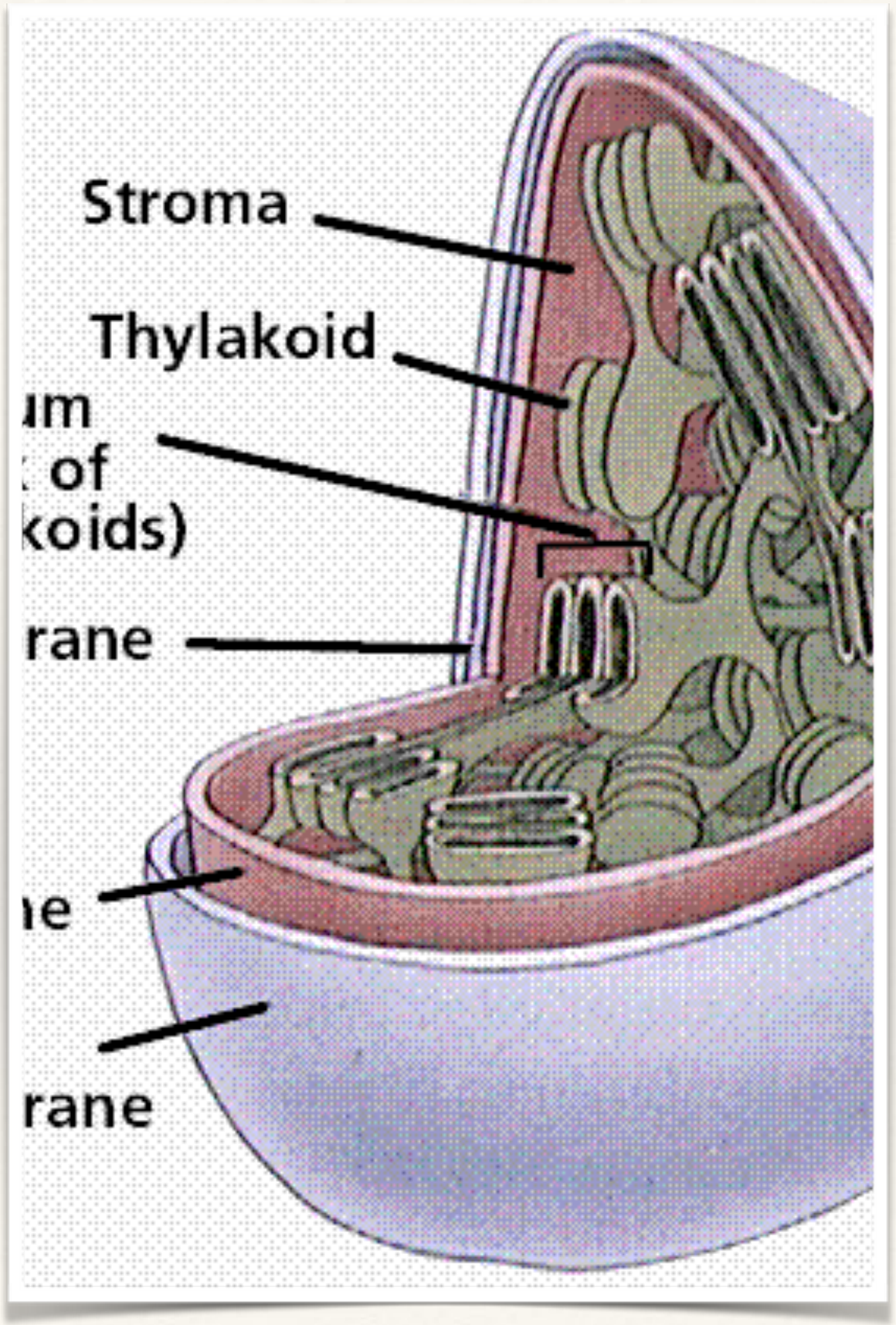

Supramolecular self assembling

Applications

Coloured scanning electron micrograph (SEM) of a section through a plant cell, showing a fractured chloroplast (green).

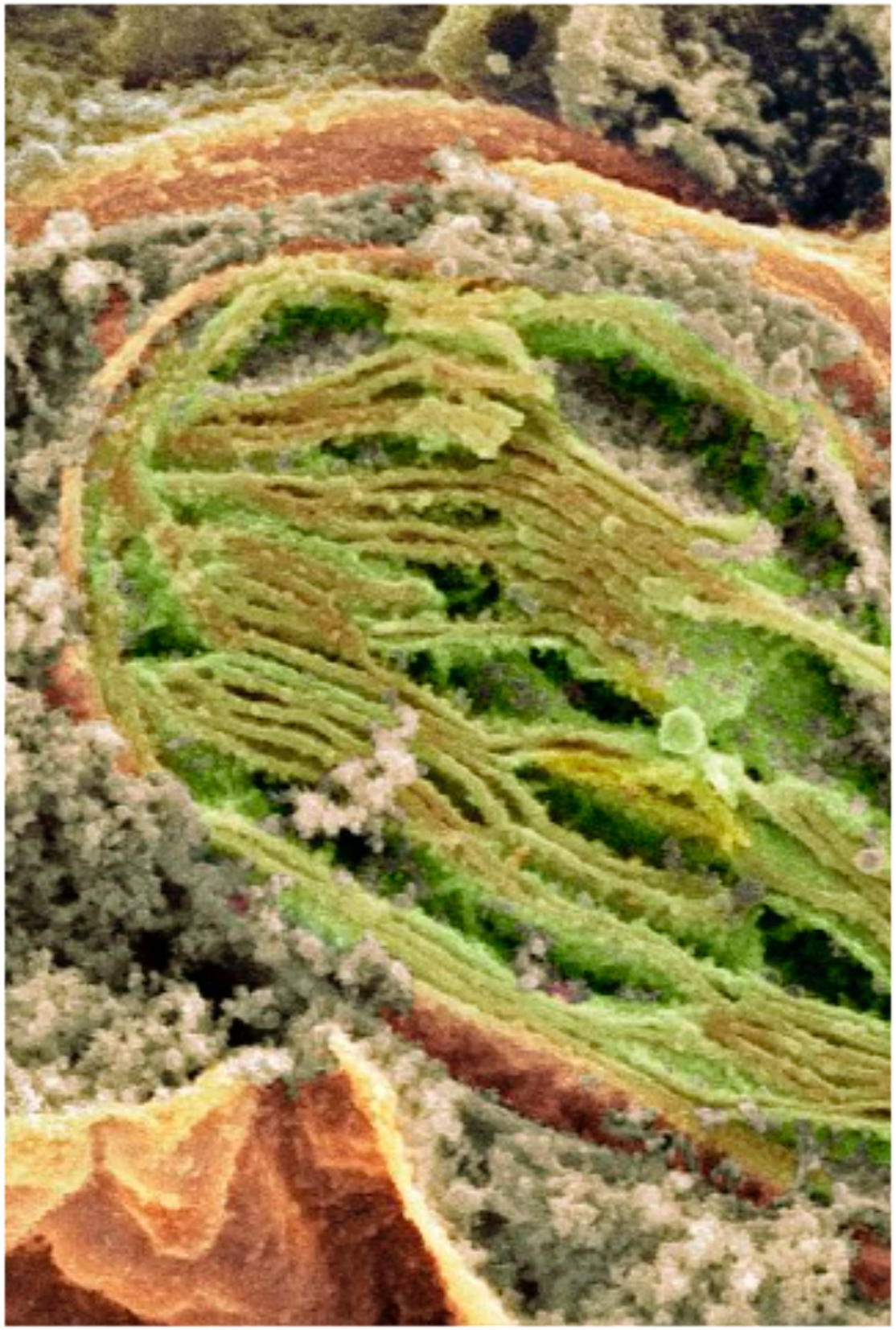

http://www2.estrellamountain.edu/faculty/farabee/BIOBK/biobookps.html

Supramolecular self assembling

Applications

Structure of the chlorosome
From cryo-EM observation of the same chlorosome from different projection angles (tilt series) it became evident that the lamellar system cannot be planar but must be curved (Psencik et al. 2004).
The curved lamellar layers (green) inside the chlorosome consist of BChl aggregates.

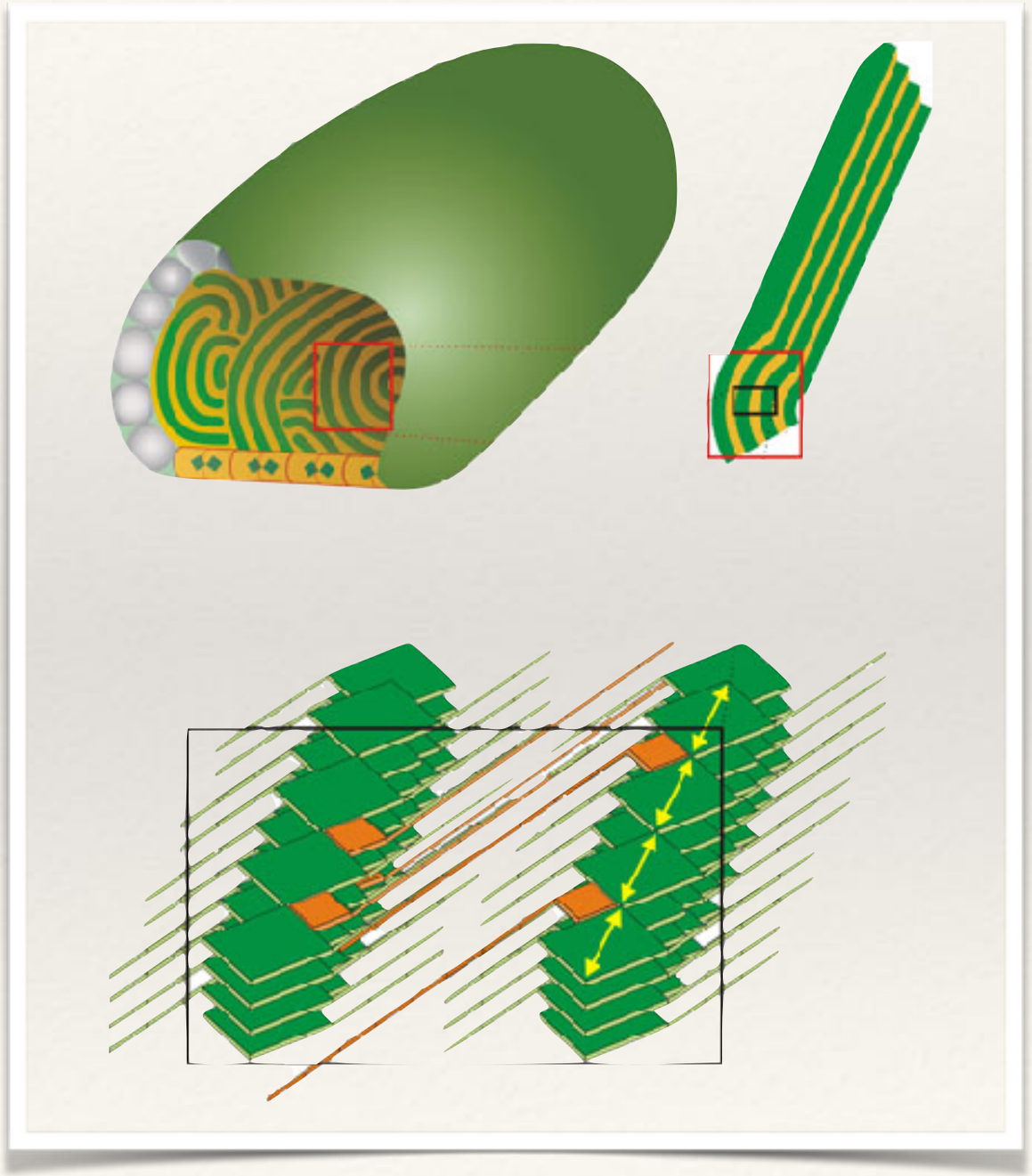

http://kchf-45.karlov.mff.cuni.cz/~jakub/chlorosome.htm

Supramolecular self assembling

Applications

Coloured scanning electron micrograph (SEM) of a section through a plant cell, showing a fractured chloroplast (green).

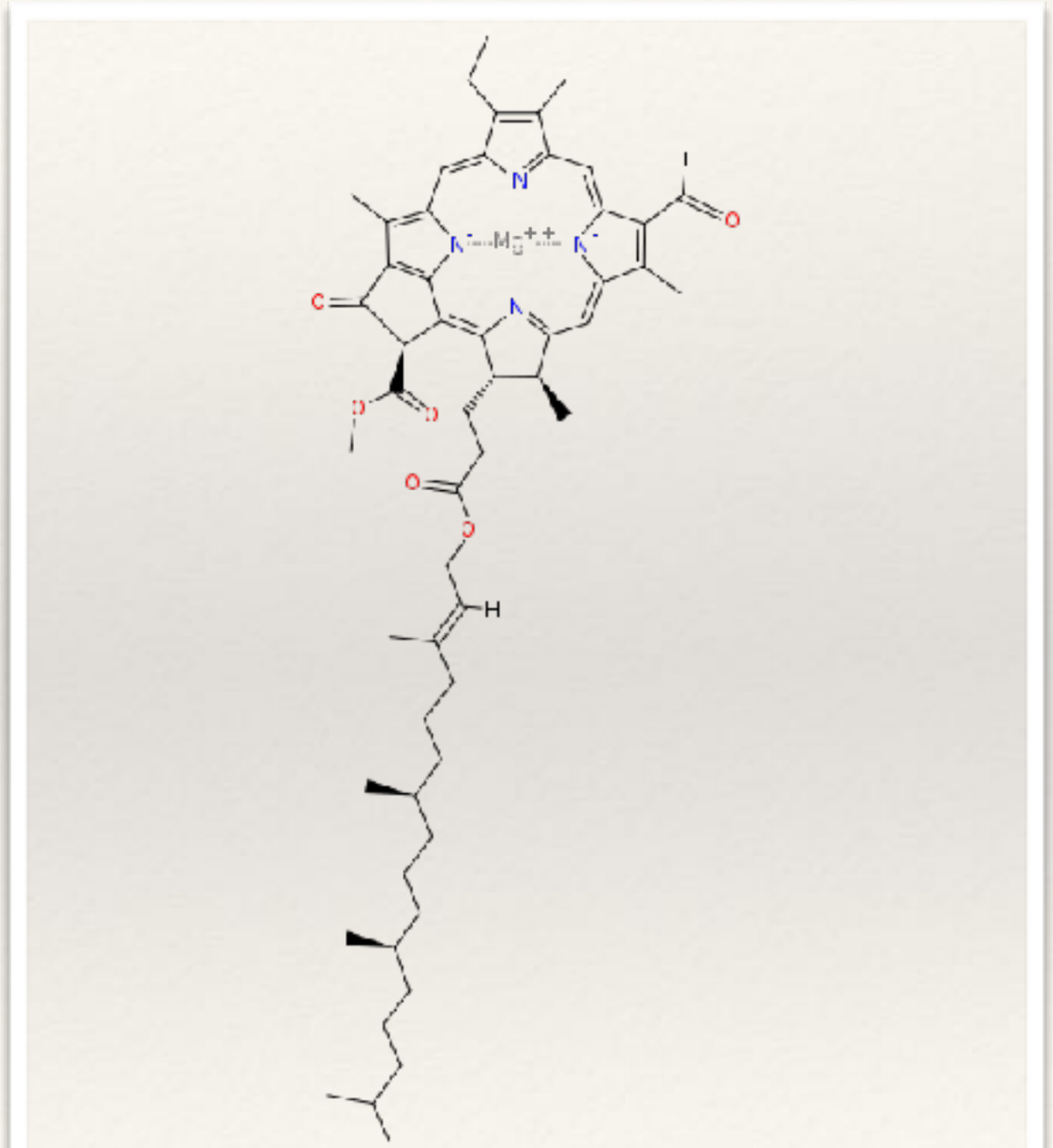

http://www2.estrellamountain.edu/faculty/farabee/BIOBK/biobookps.html

Supramolecular self assembling

Applications

Self assembling in Hybrid Por FF

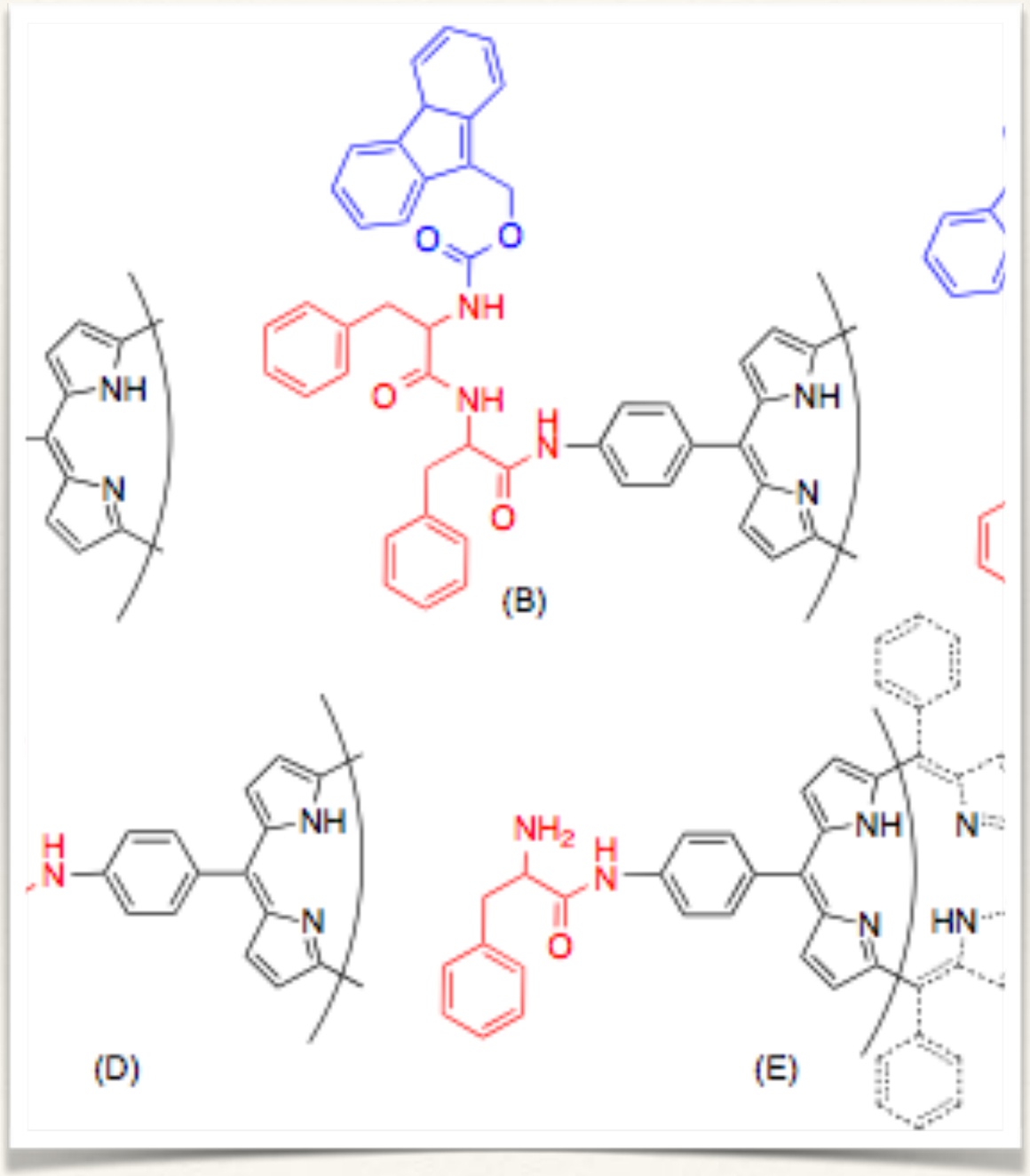

Chemistry, a European Journal, 77, 7213-7219, **2011**

Supramolecular self assembling

Applications

$1.65 \cdot 10^{-6}$ mol
Fmoc-FF-TPP

600µL
Dichloromethane

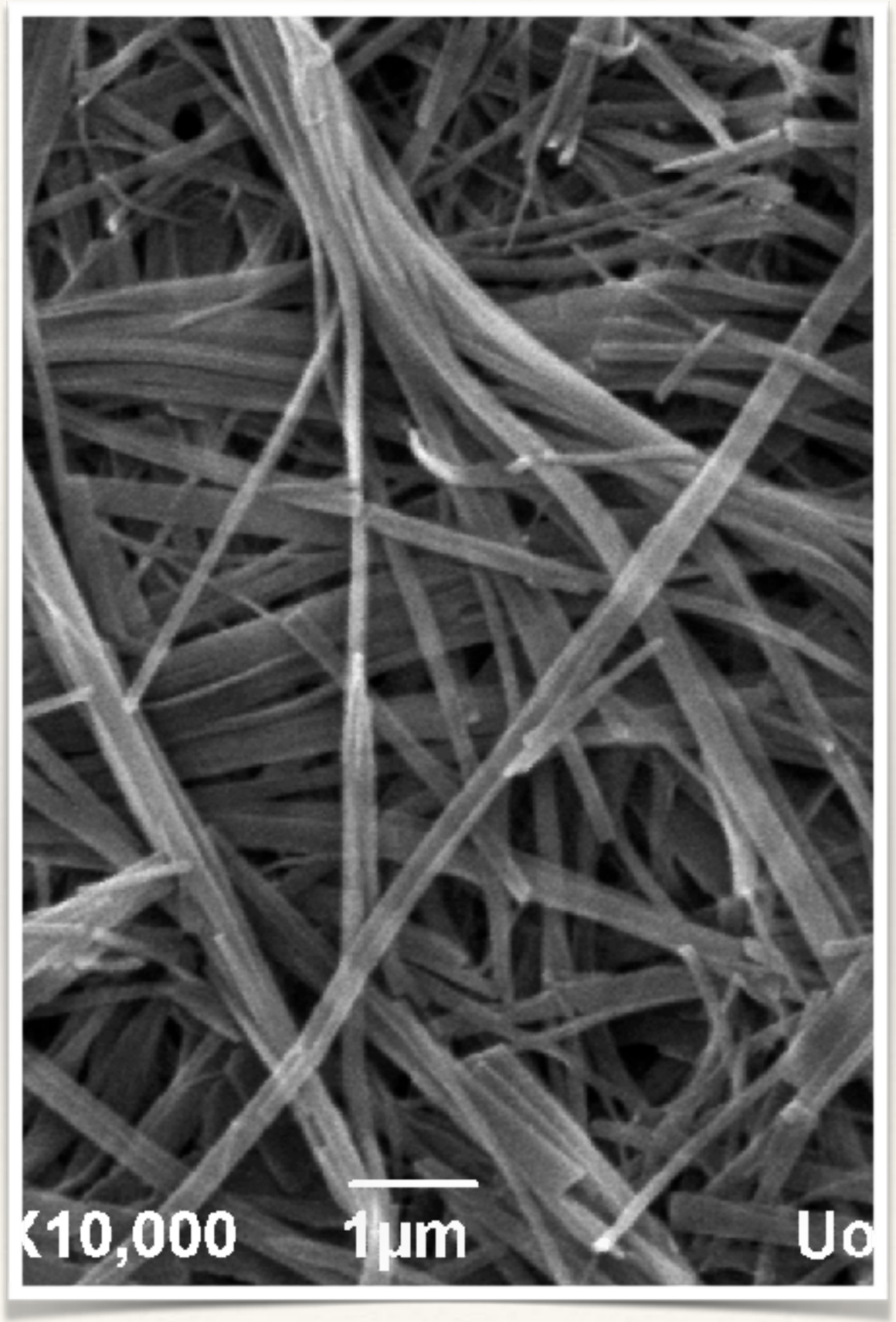

Supramolecular self assembling

Applications

$1.6 \cdot 10^{-6}$ mol
Fmoc-FF-TPP

300µL
HFIP

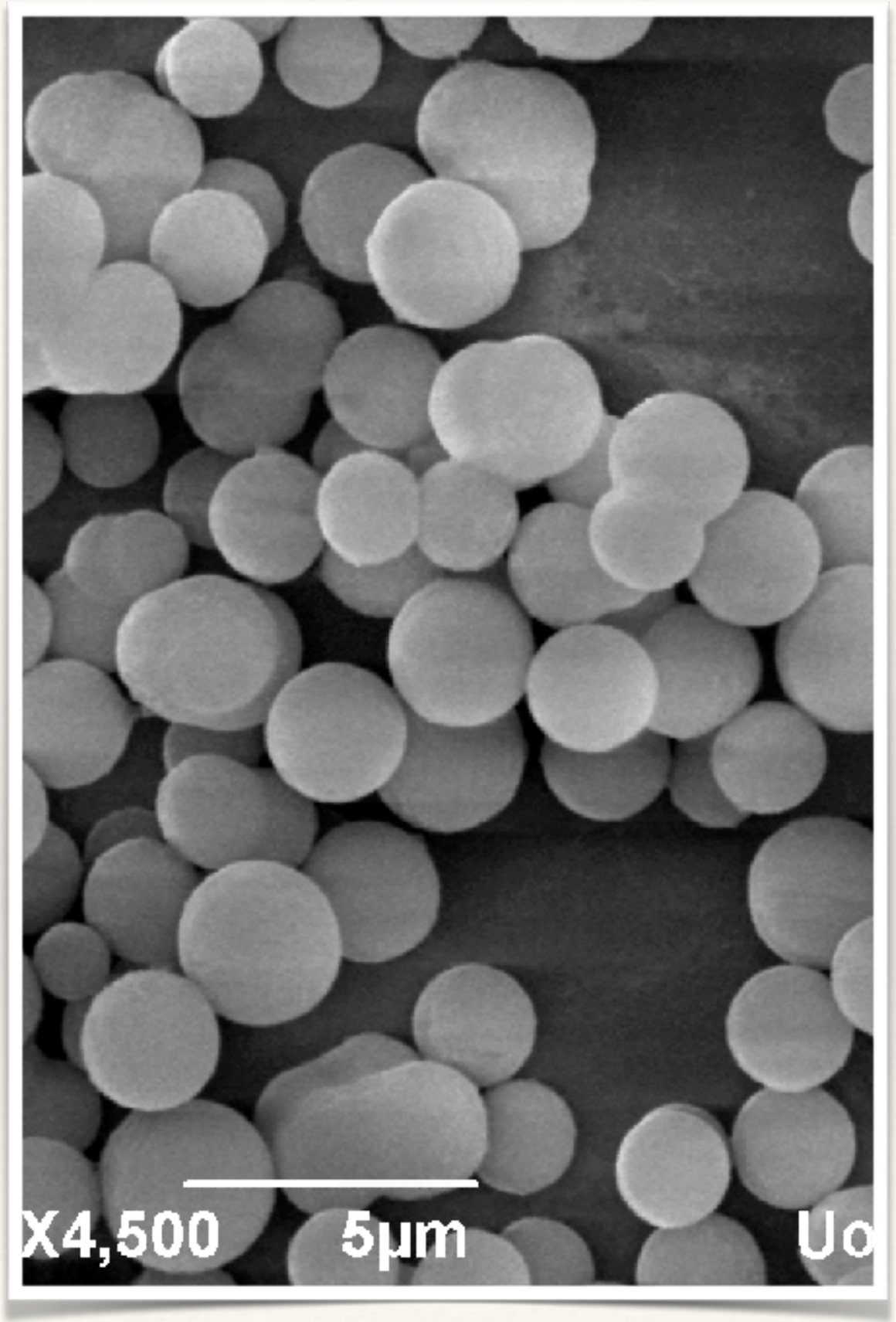

Supramolecular self assembling

Applications

X-ray structure of Por – FF-Fmoc

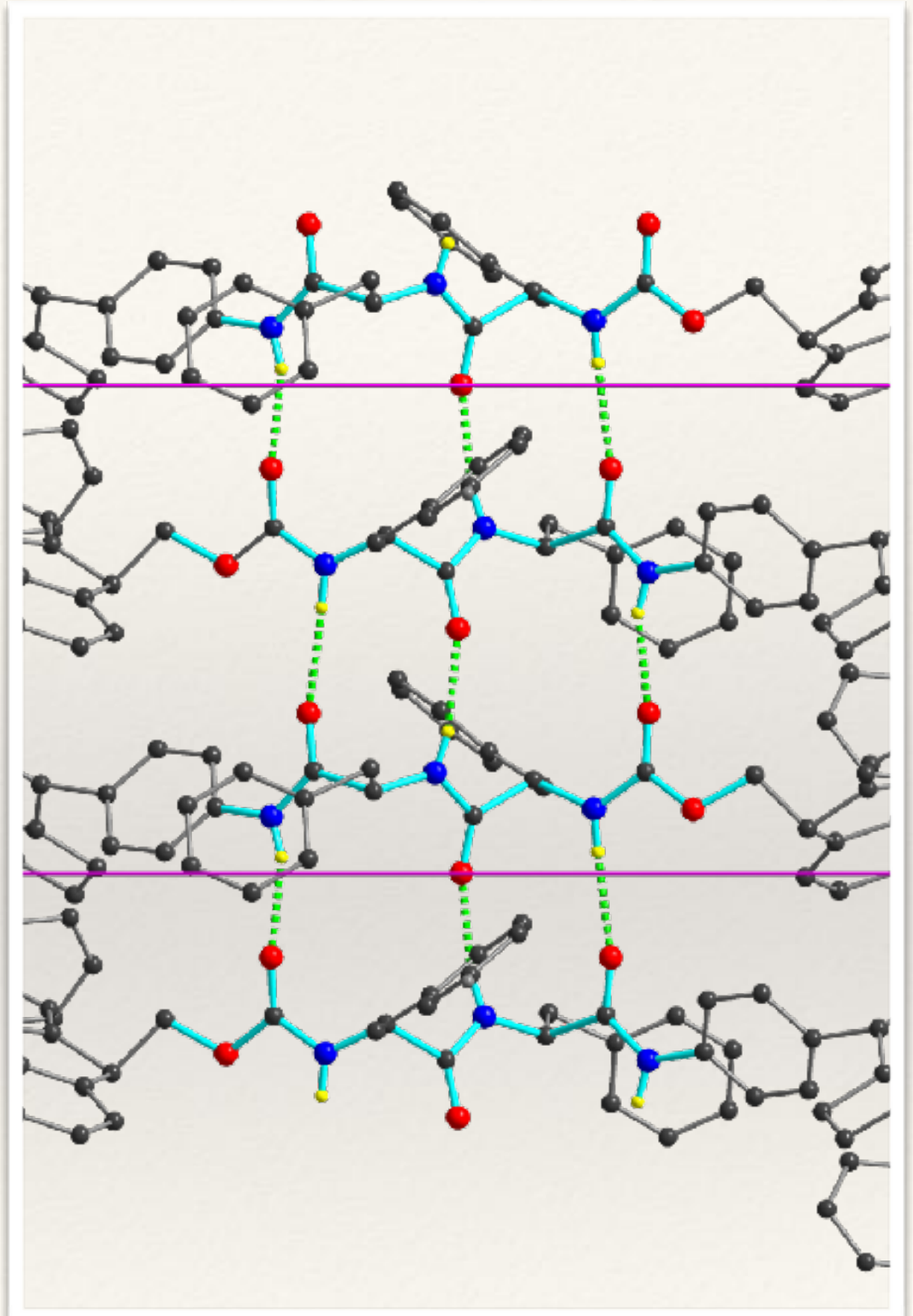

Supramolecular self assembling

Applications

Addition of electrolyte to supramolecular assemblies on TiO_2

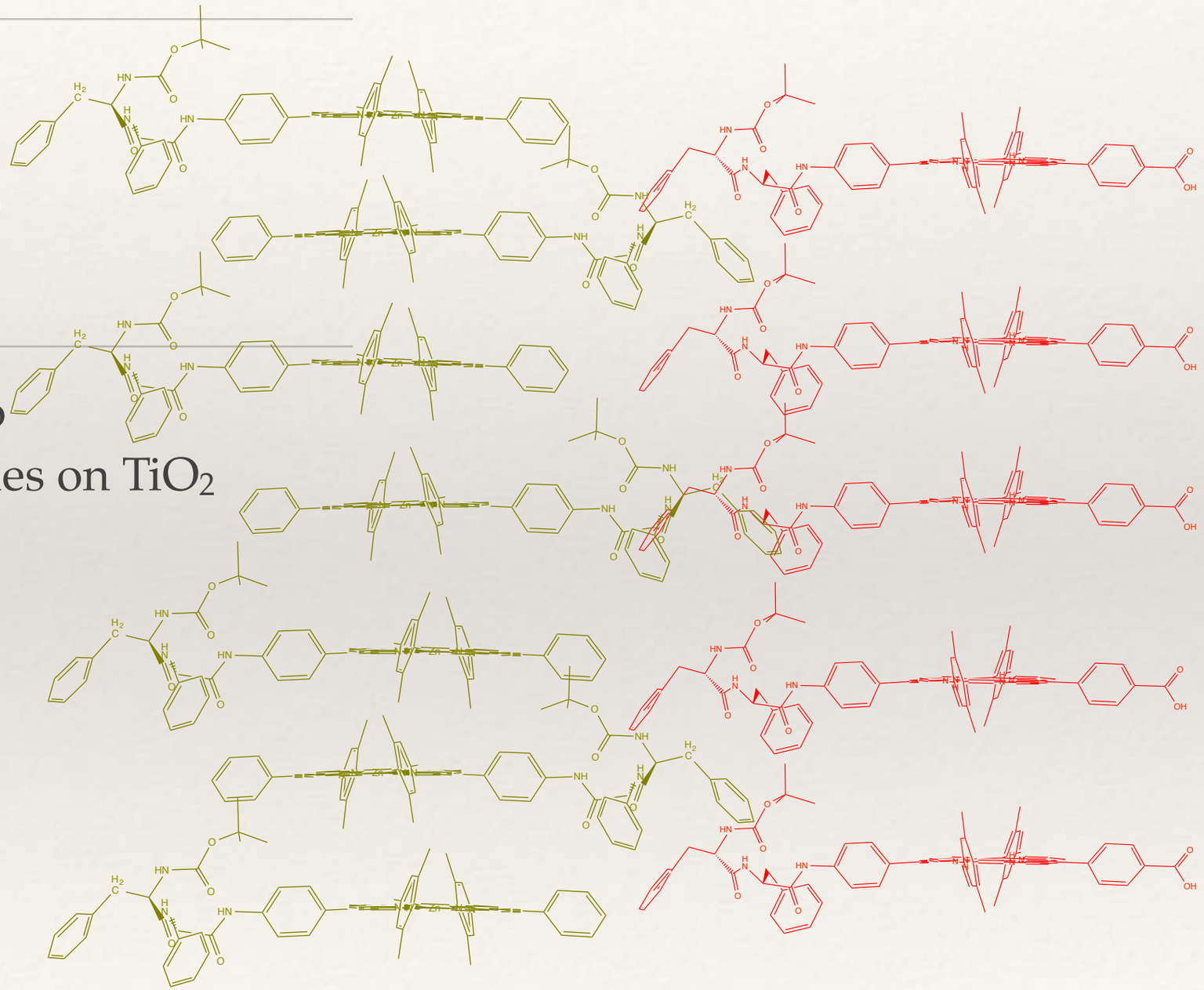

TiO_2

Hydrogen production

Applications

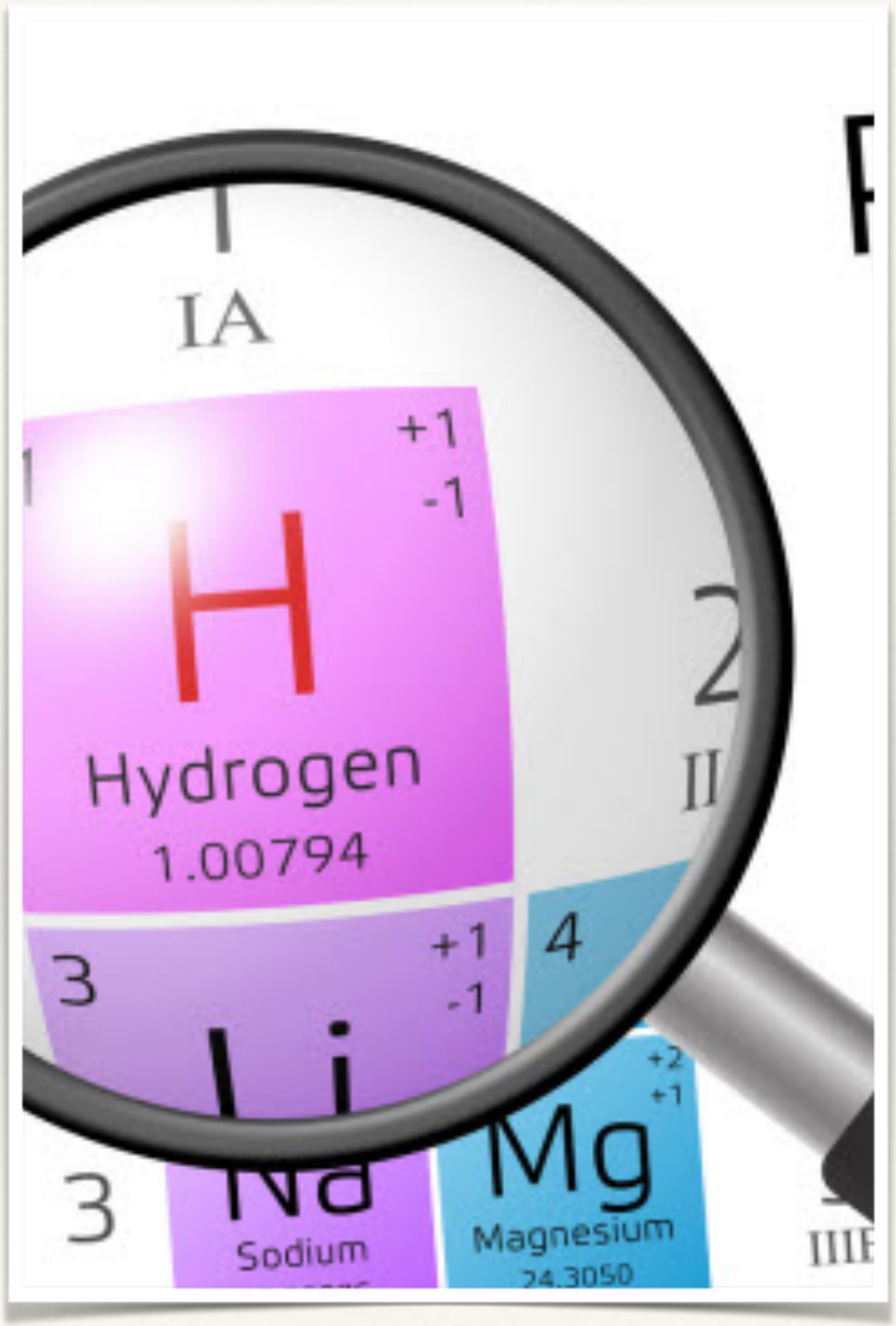

Reimagining Hydrogen: A Small Molecule With Large-Scale Ideas

Berkeley Lab researchers pursue low-cost, efficient technologies for hydrogen generation

By Lawrence Berkeley National Laboratory | October 10, 2017

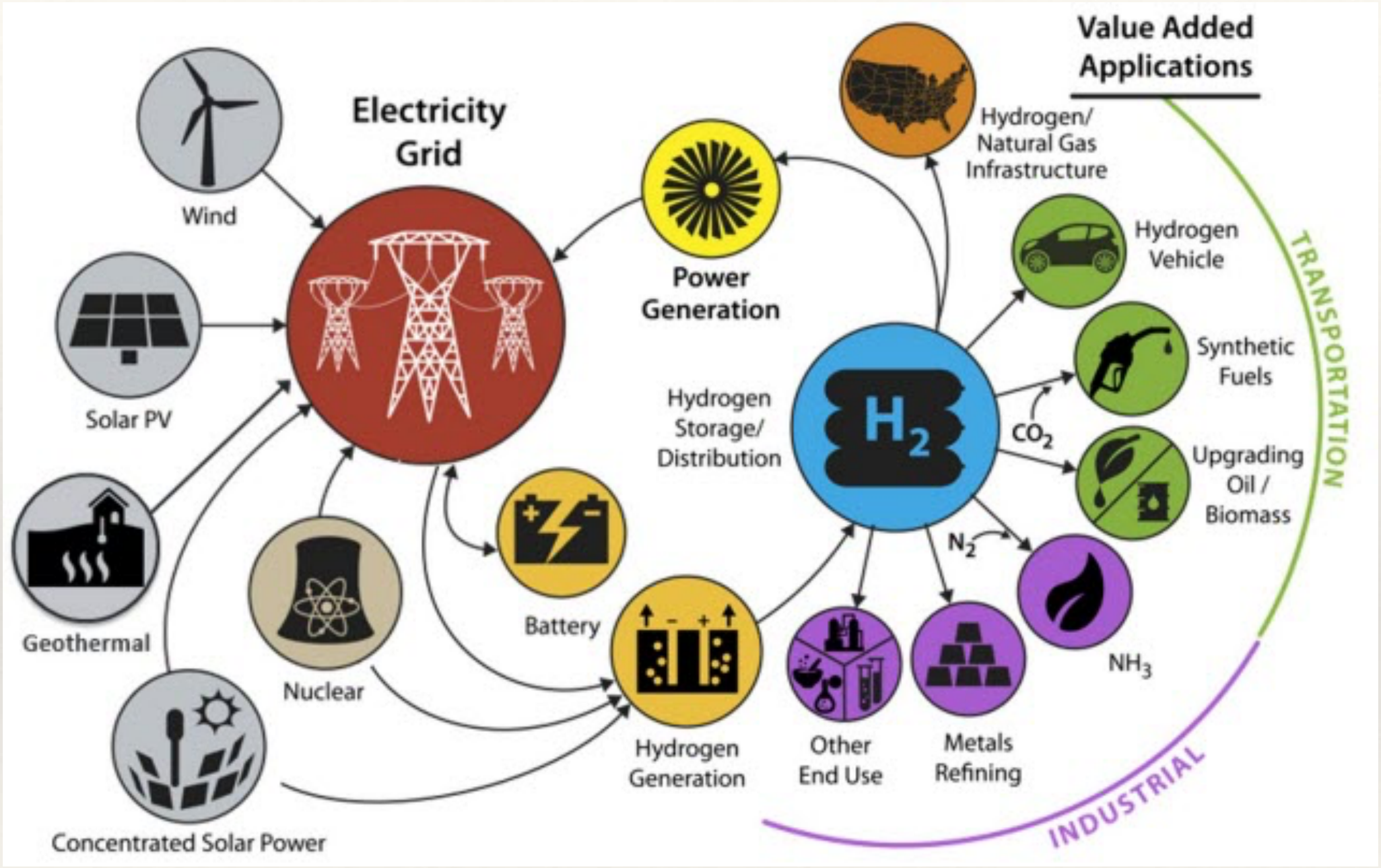

ILLUSTRATION COURTESY OF LAWRENCE BERKELEY NATIONAL LABORATORY

Applications

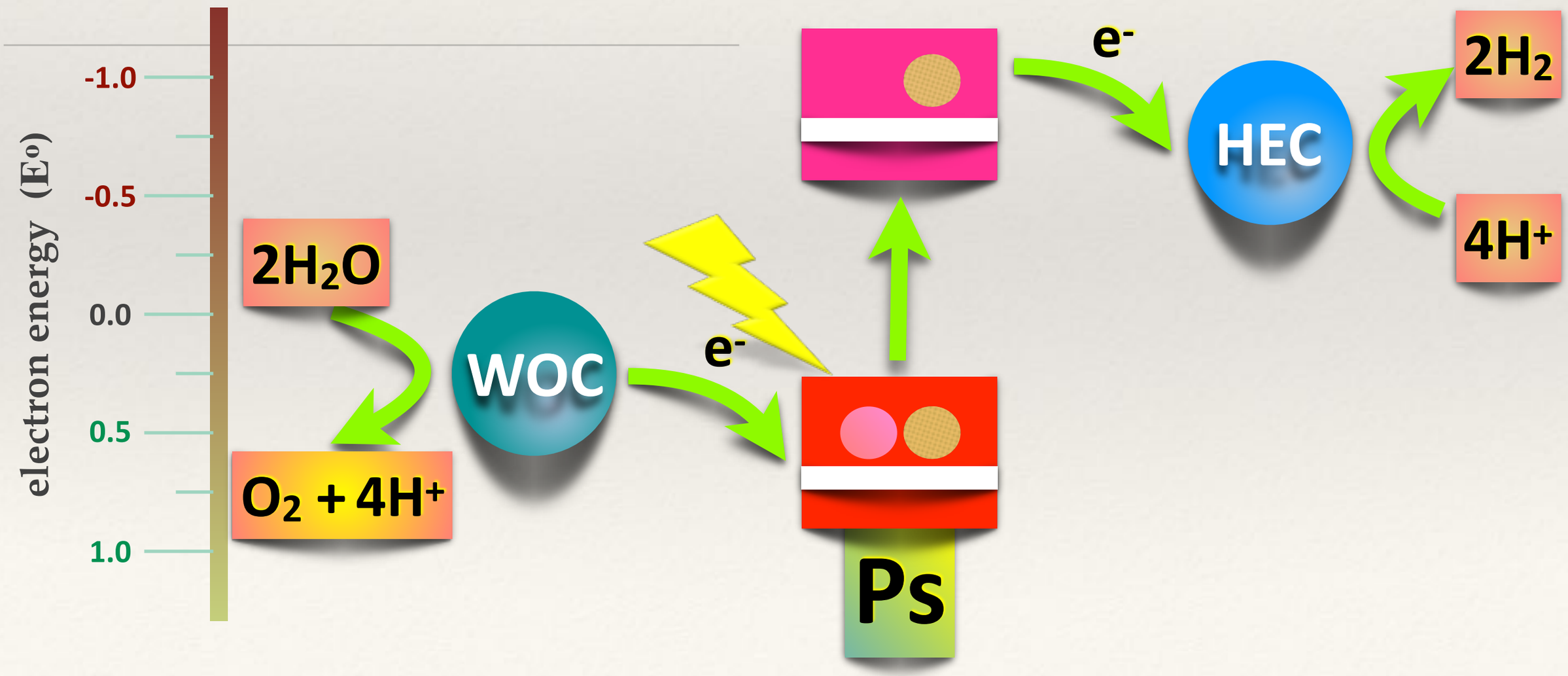

Applications

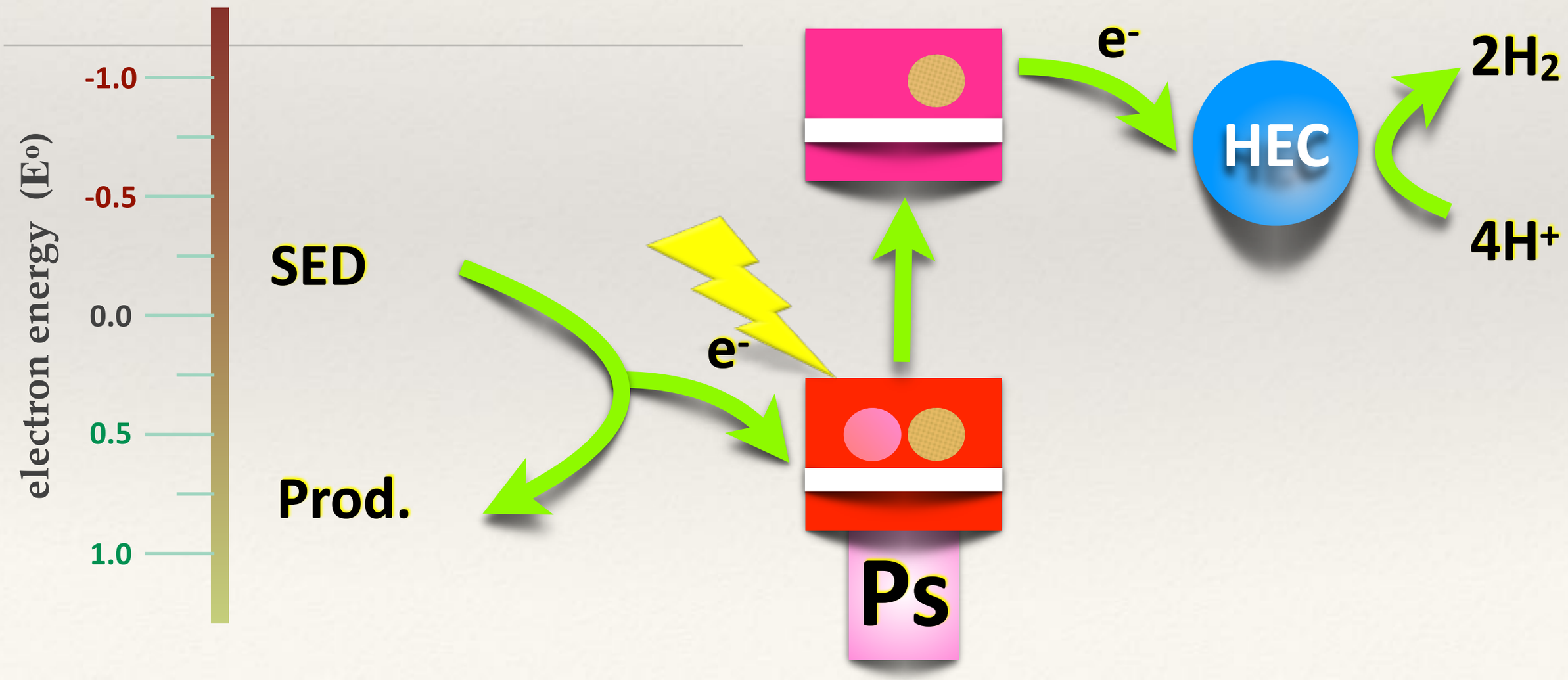

Hydrogen production

Applications

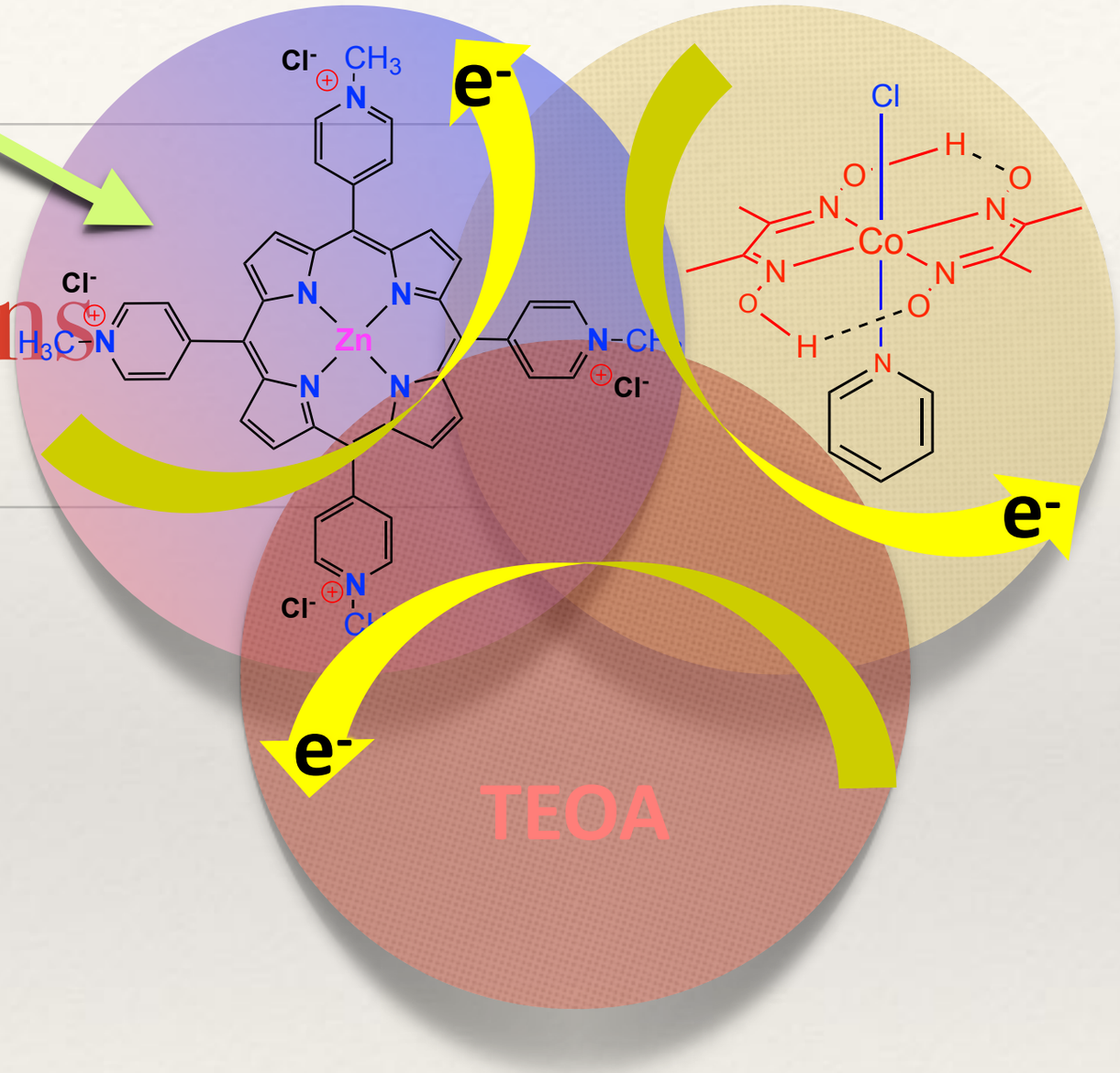

Porphyrin:

- Water Soluble
- Easy Preparation
- Low Cost

Cobaloxime:

- Noble metal free catalyst
- Low Cost
- Facile Synthesis
- High activity in H_2 production

Chem. Commun., 50, 521-523, **2014**

Hydrogen production

Applications

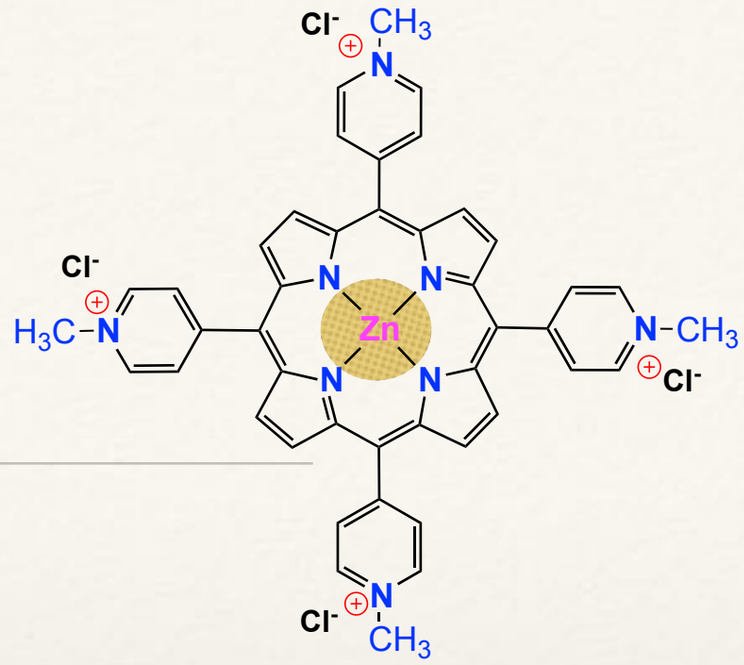

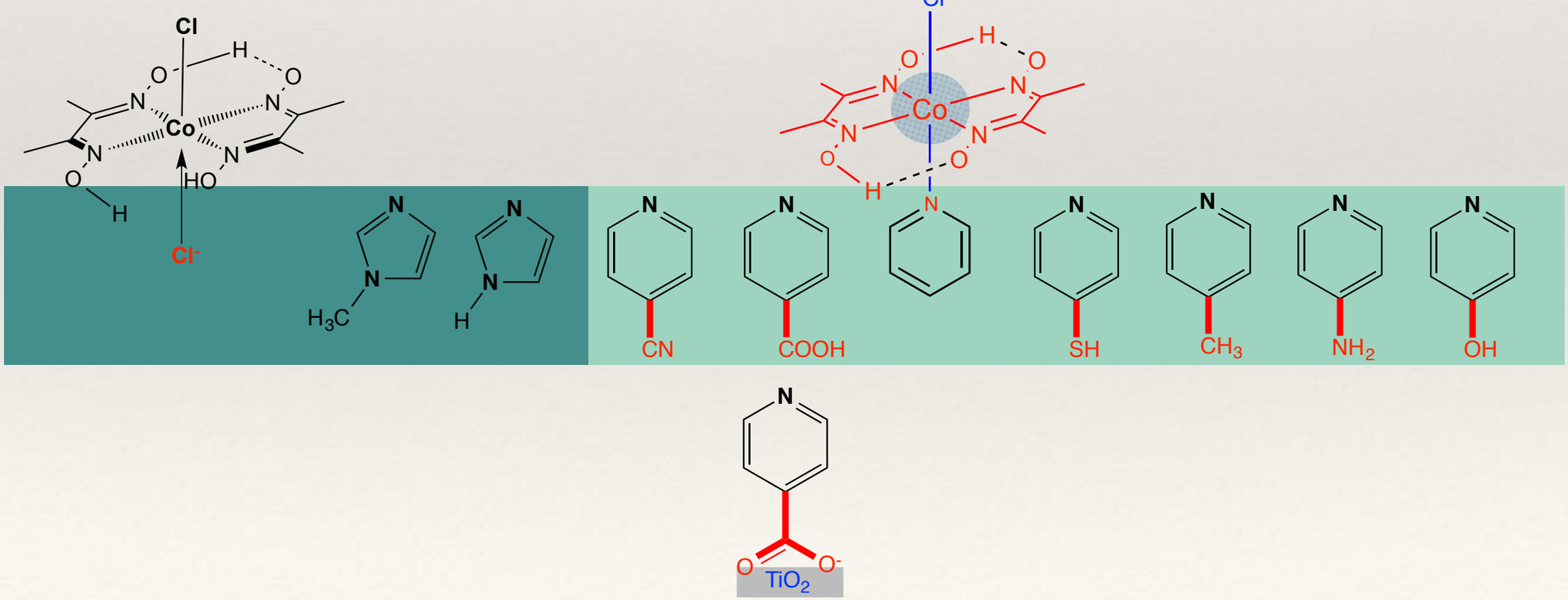

Hydrogen production

Applications

Catalyst	pKa	ν Co-Naxial	ν Co-Cl	Co(III)/Co(II)	Co(II)/Co(I)	TON
1	1.90	435	428	–0.98	–1.50	77
2	4.18	441	428	–1.11	–1.55	40 (223)
3	5.22	455	420	–1.10	–1.53	320
4^2	5.30	480	419	–1.091	–1.59	425
5	6.02	483	418	–1.15	–1.54	443
6^3	9.17	515	416	–1.08	–1.61	-
7^2	11.0	507	409	–1.17	–1.55	-
8	6.90	495	413	–1.26	–1.58	565
9	7.40	503	412	–1.31	–1.57	1135
10	-		414	–1.29	–1.52	190

Applications

Key points for an efficient dssc

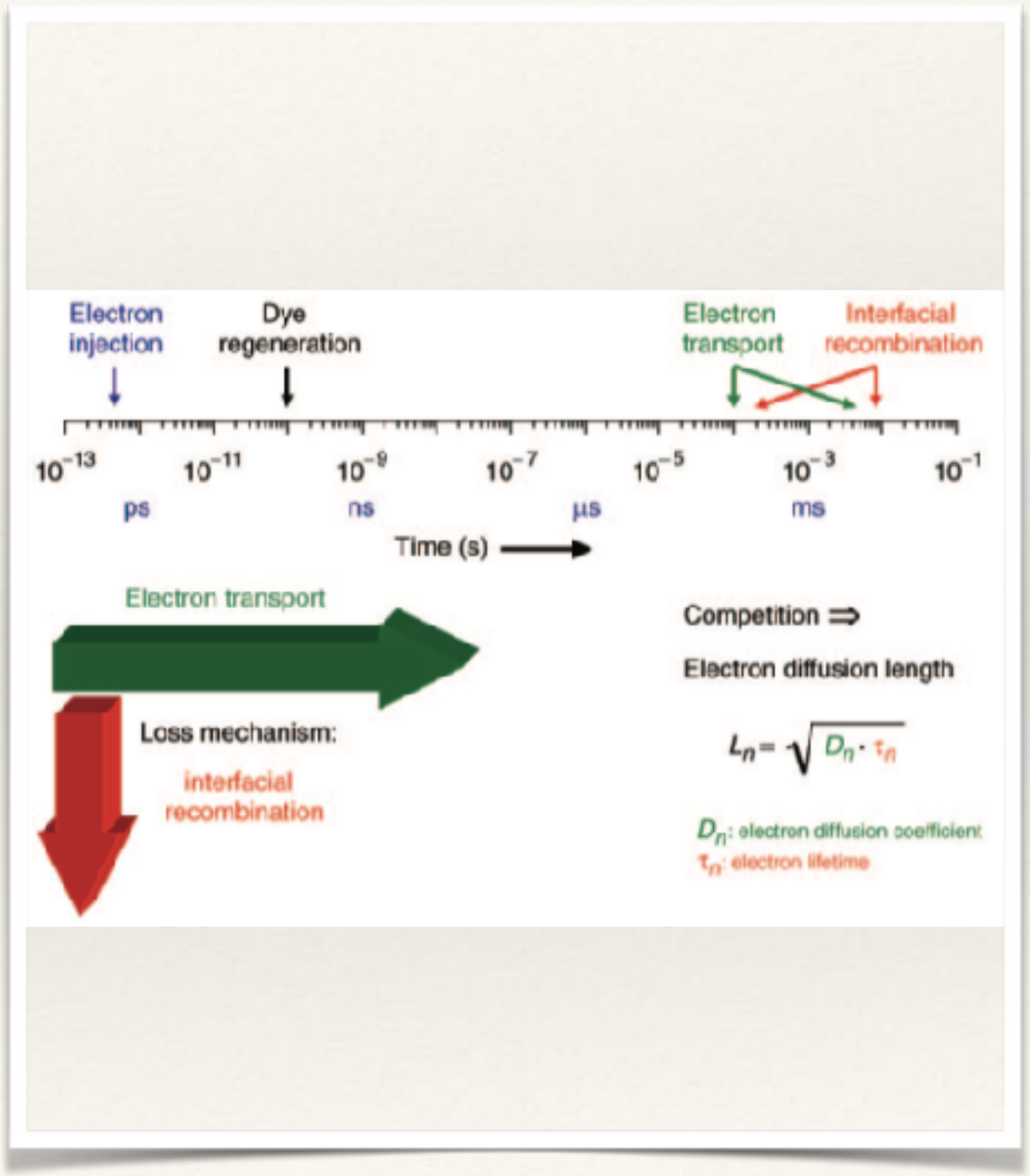

Applications

Michael Grantzel record!

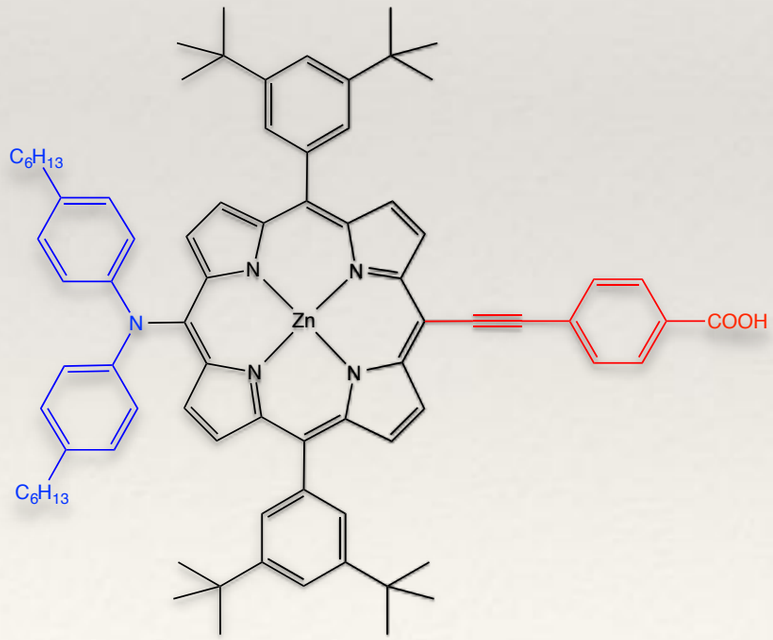

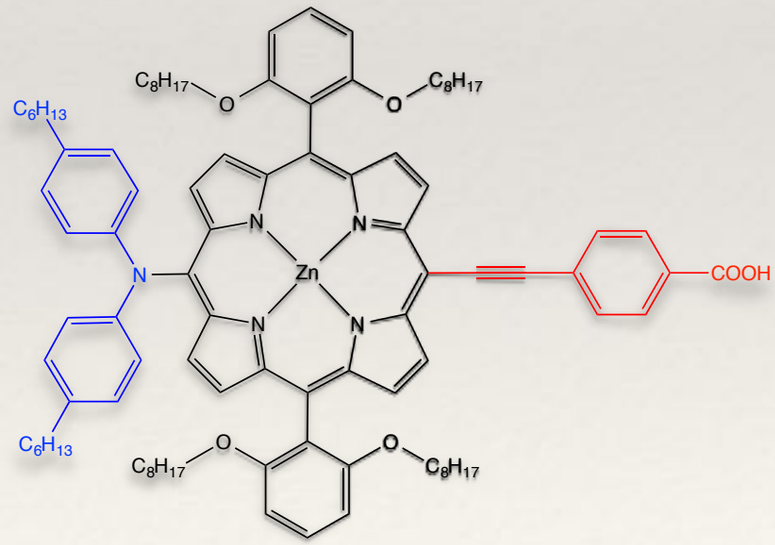

PCE 12.3%

Applications

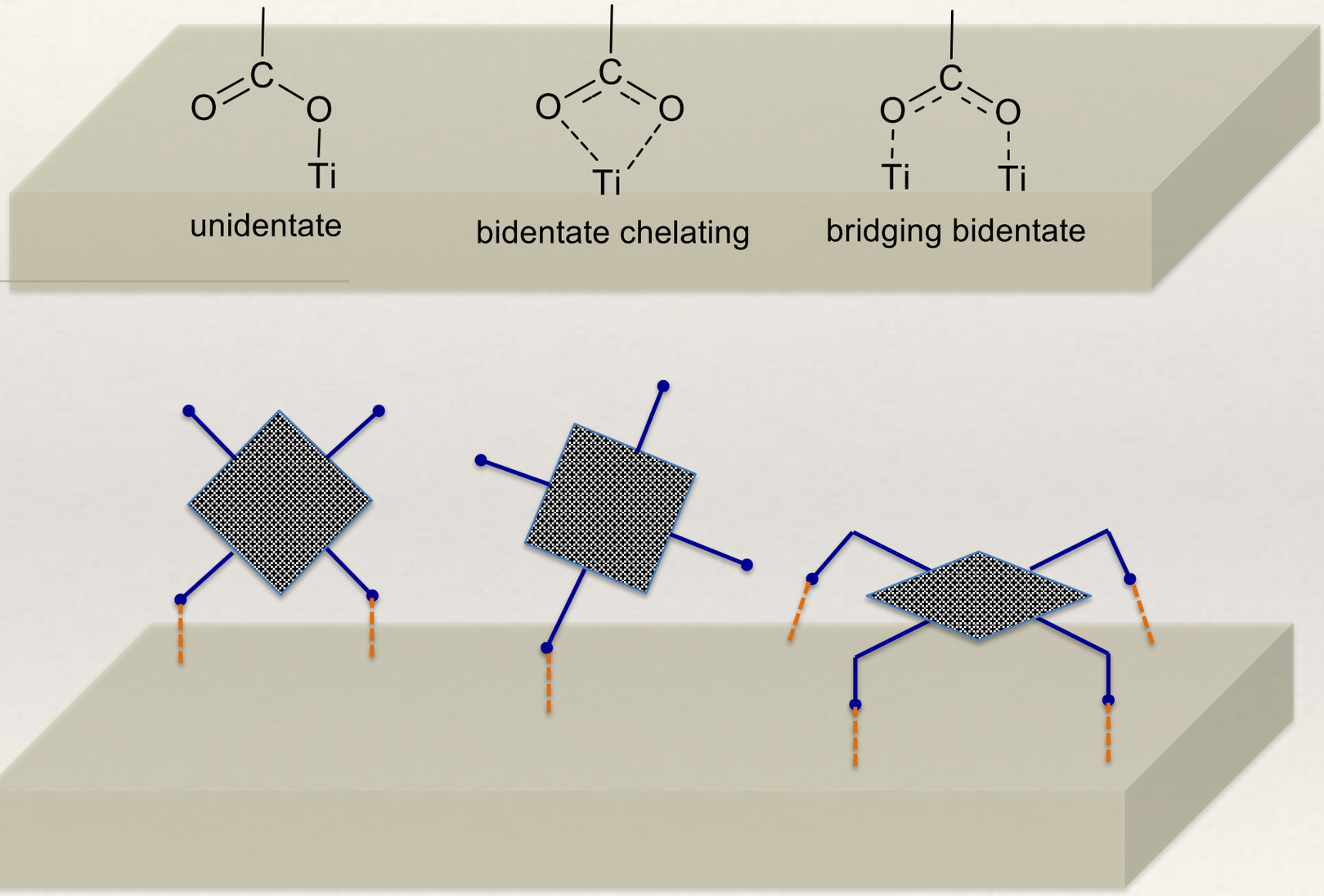

various modes for TiO_2

Solar cells

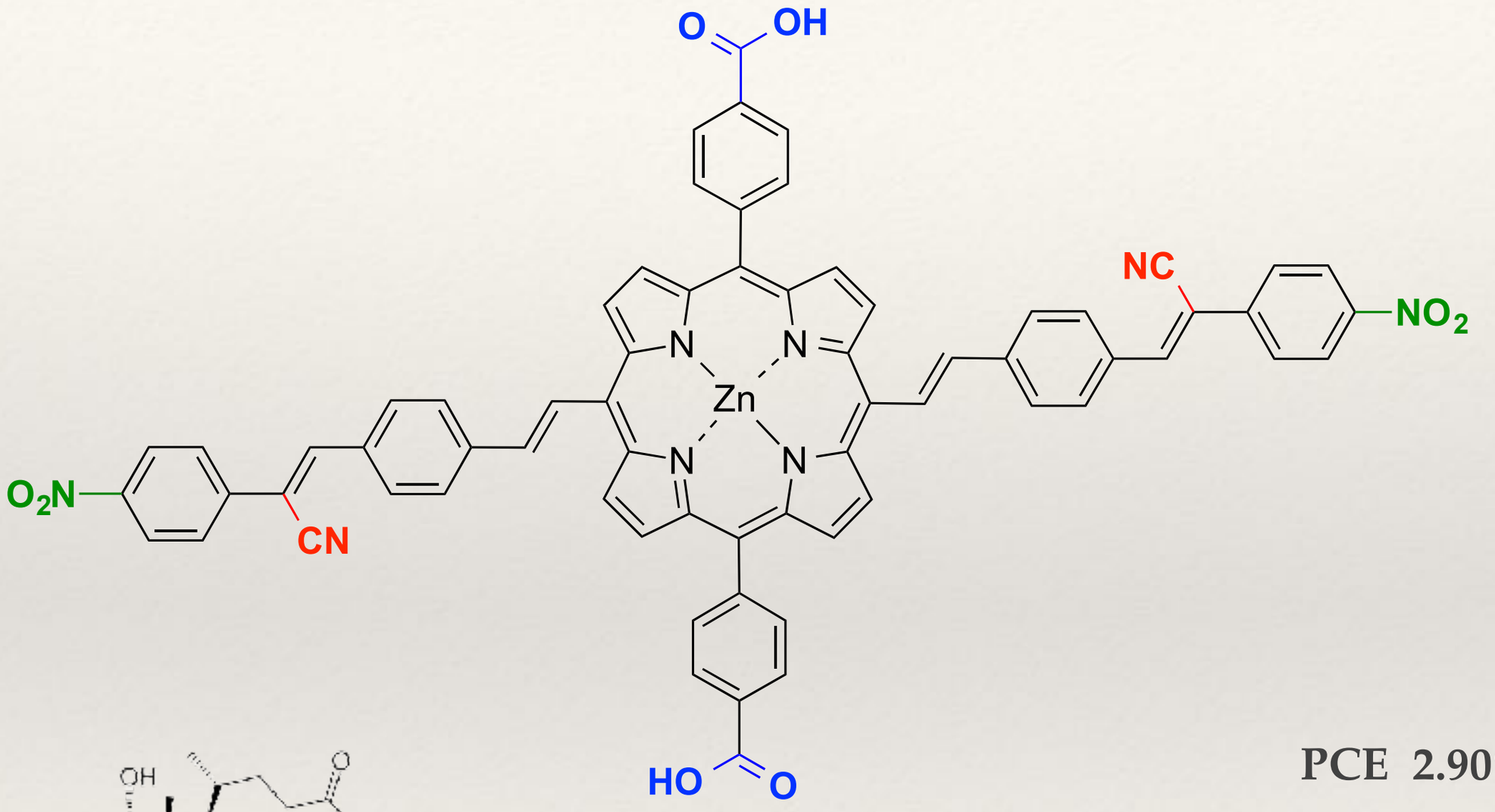

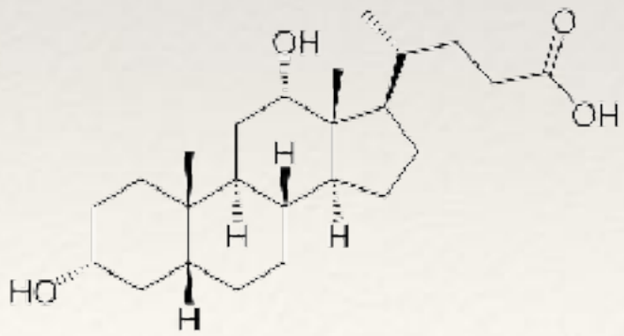

PCE 2.90%

+ Deoxycholic acid PCE 4.22%

J. Power Sources, 2011, 196, 6622-6628

Solar cells

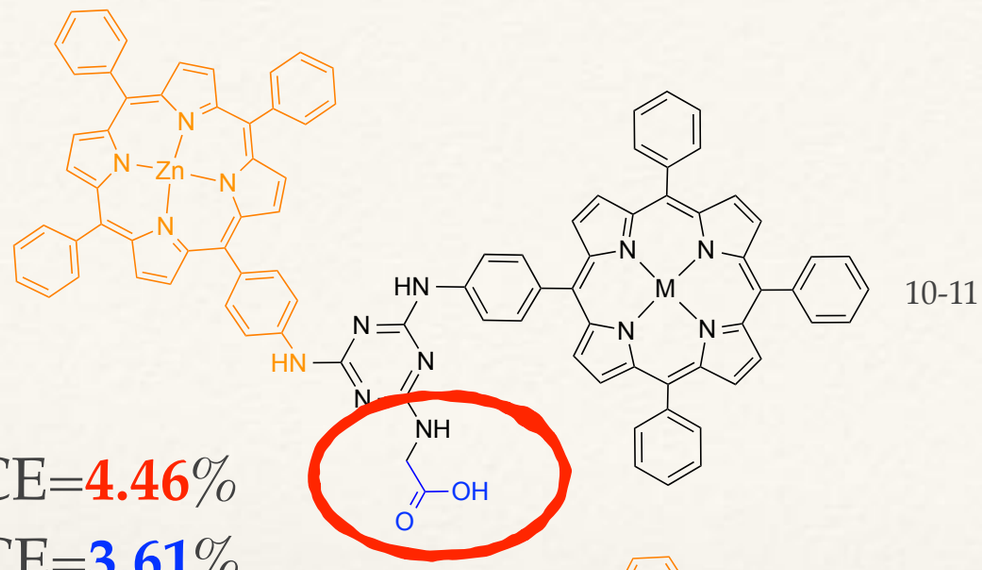

10-11

M=H_2 PCE=**4.46**%

M=Zn PCE=**3.61**%

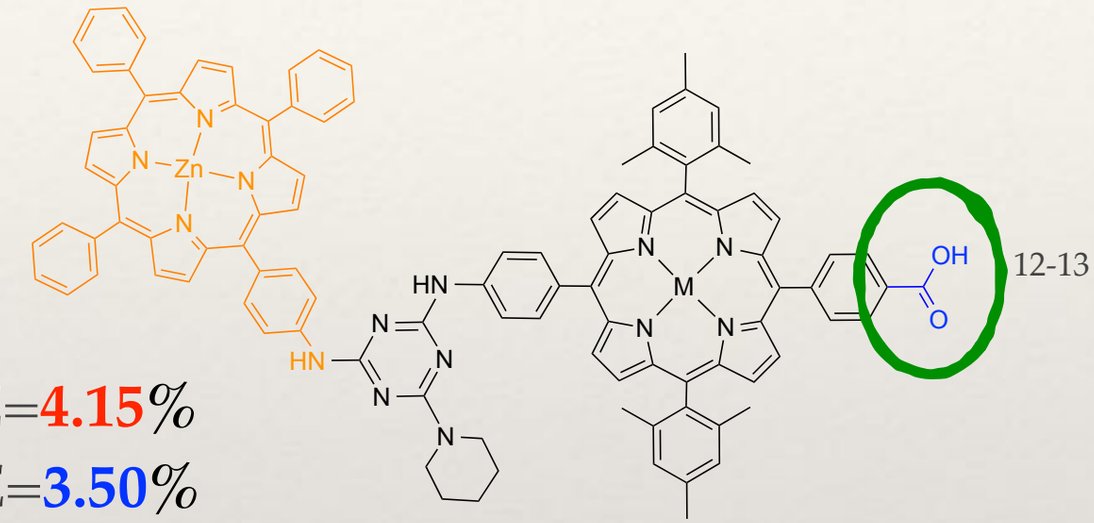

12-13

M=H_2 PCE=**4.15**%

M=Zn PCE=**3.50**%

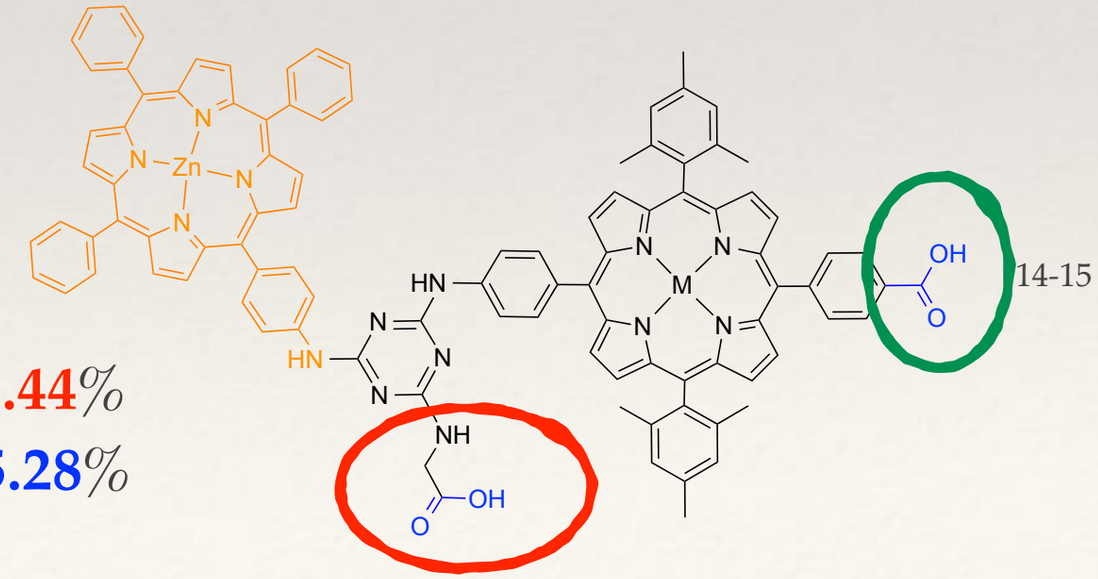

14-15

M=H_2 PCE=**5.44**%

M=Zn PCE=**5.28**%

Inorg. Chem., **2013**, 52, 9813-9825

J. Porphyrins Phthalocyanines, **2015**, **19**, 175-191

Inorg. Chem. Frontiers **2014**, 1, 256,

Solar cells

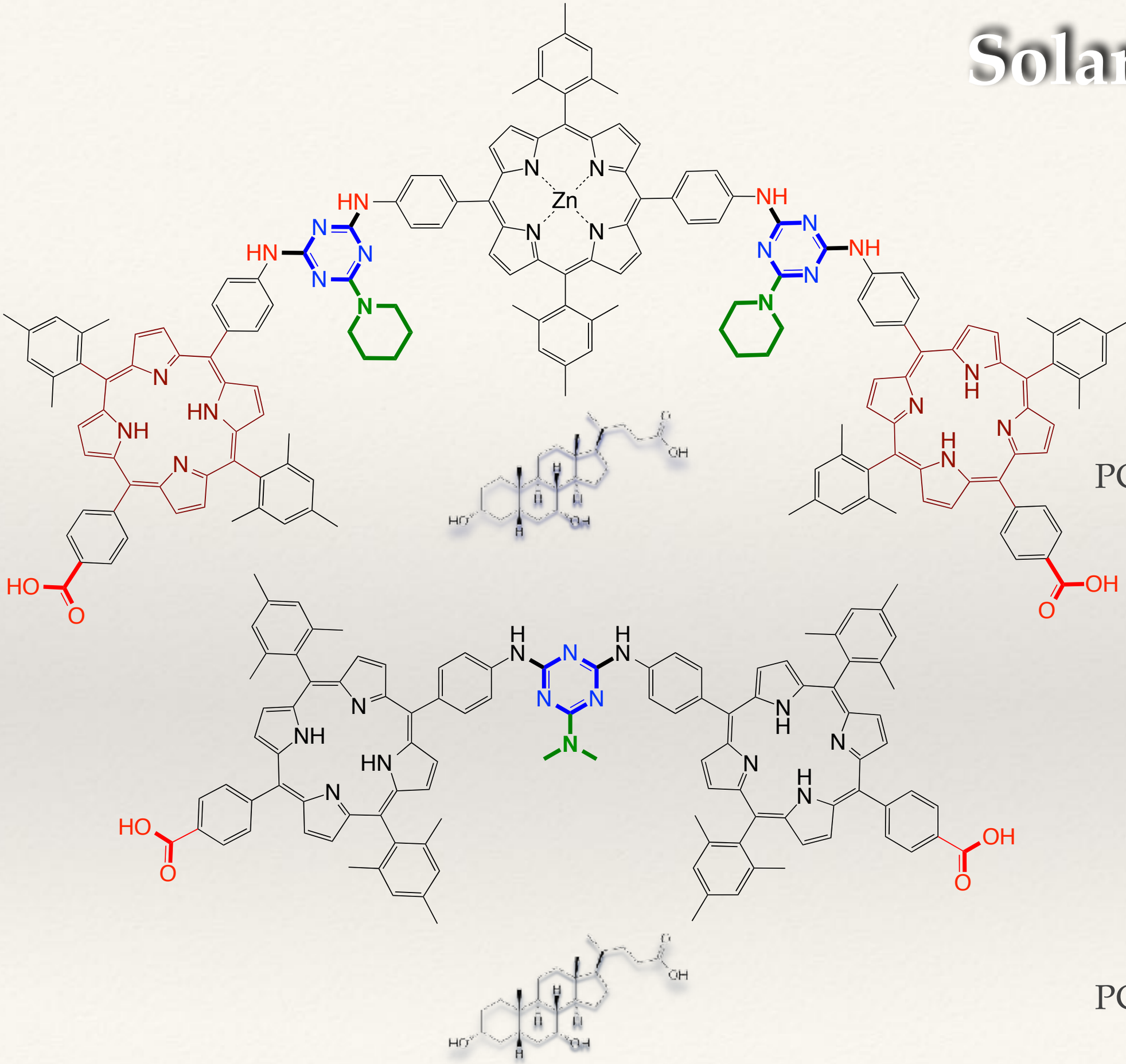

PCE=**5.88**%

PCE=**4.56**%

Dalton Trans., **2015**, **44**, 13550-13564

Solar cells

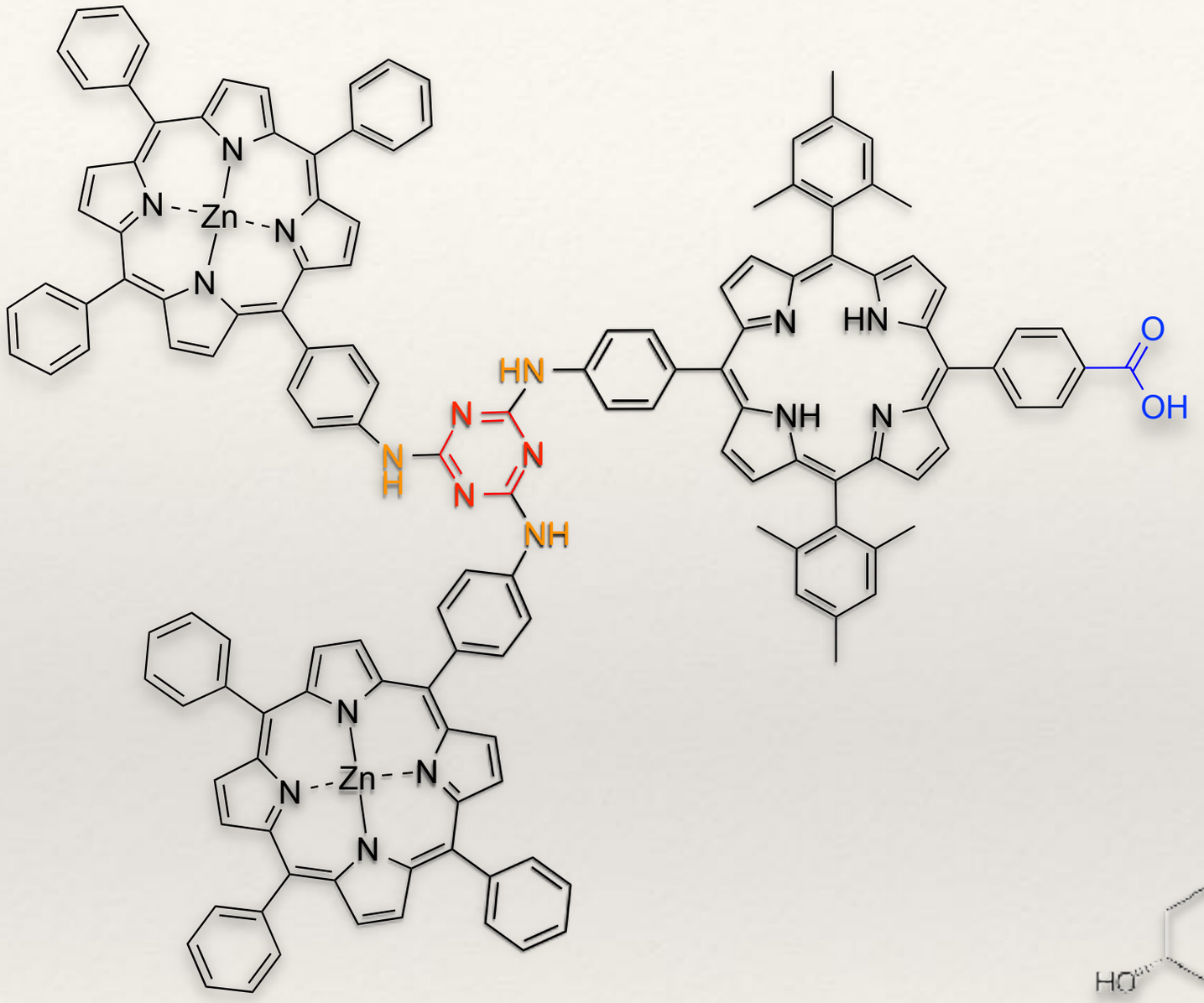

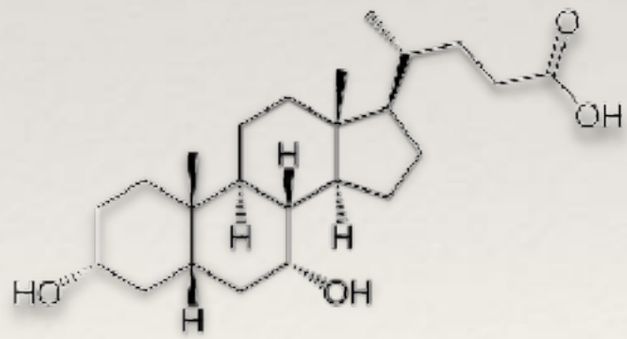

past coating PCE = **3.80%**

electrophoretic deposition PCE = **4.91%**

CDCA PCE = **5.56%**

Eur. J. Inorg. Chem. **2014**, 1020-1033

Applications

various modes for TiO_2

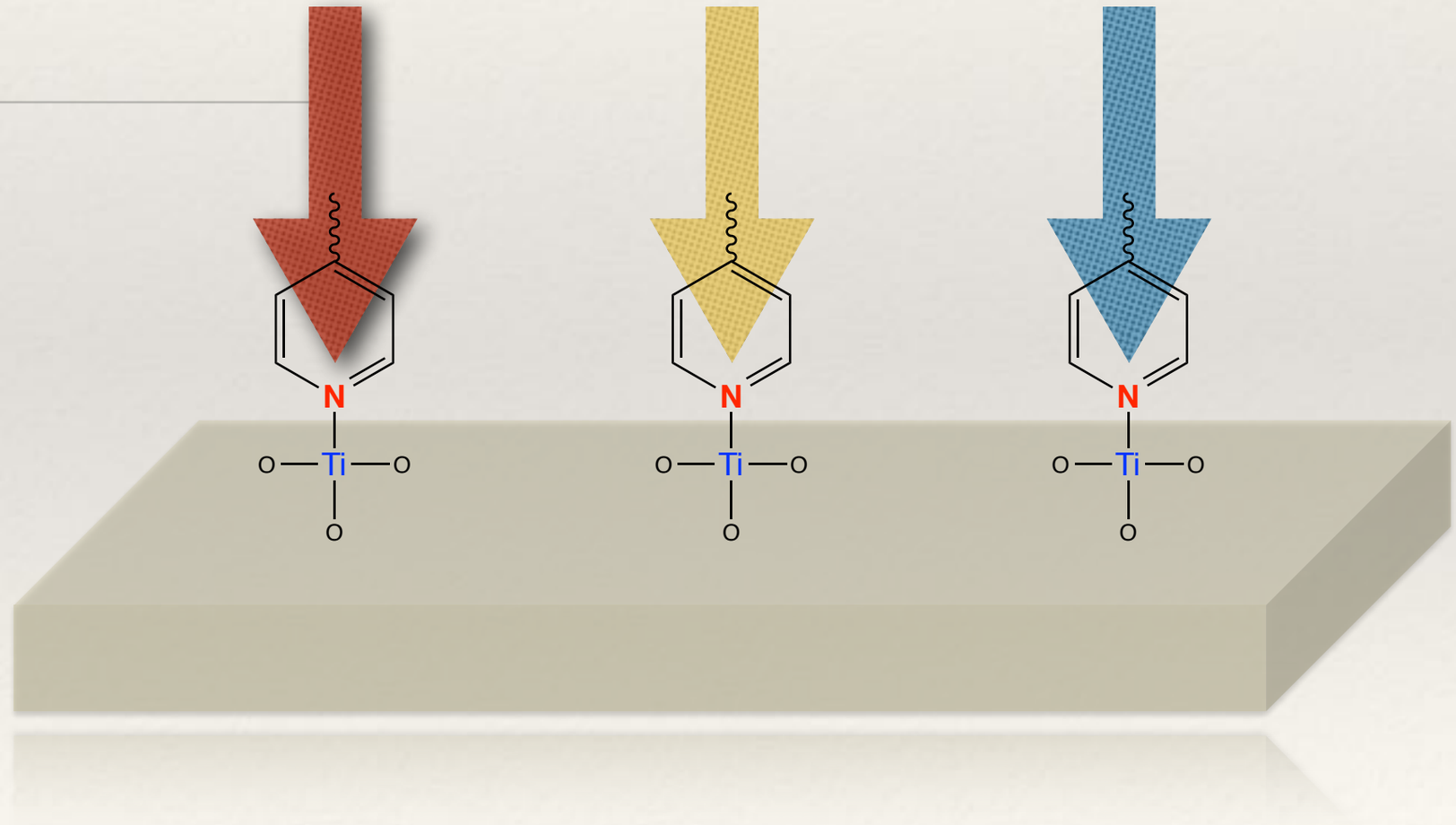

Solar cells

PCE=**3.10**%

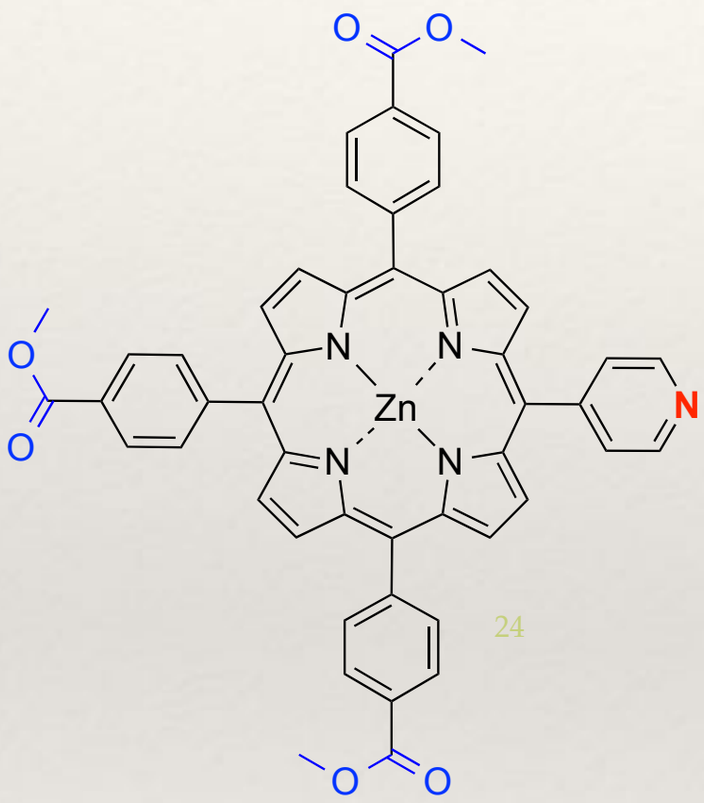

24

PCE=**3.90**%

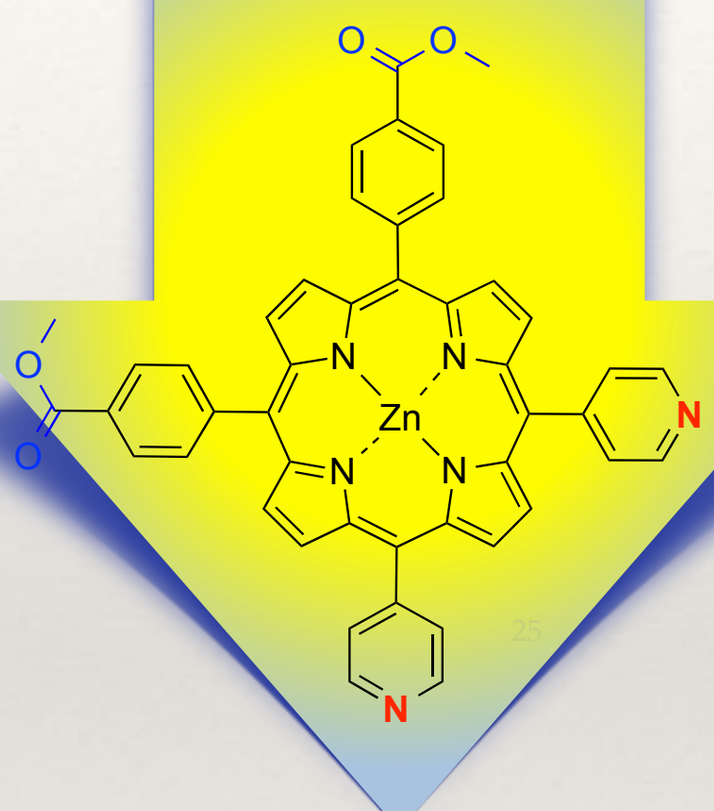

25

PCE=**2.46**%

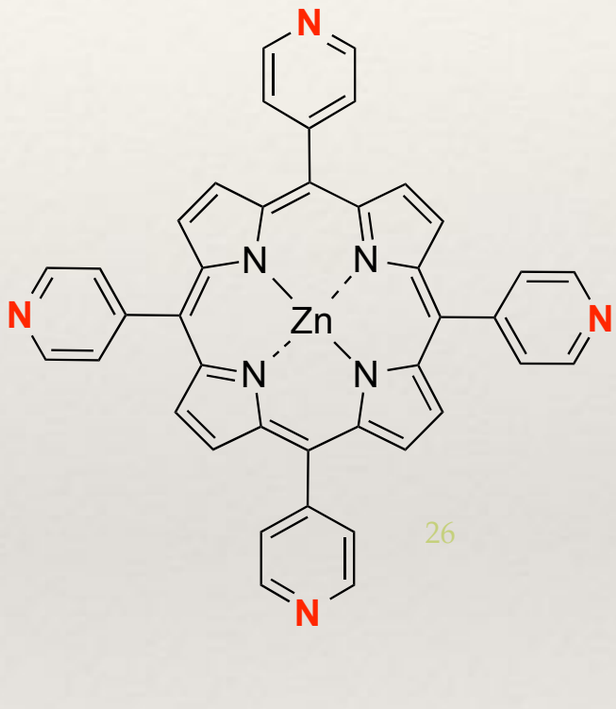

26

treatment of the photo anode with formic acid PCE=**5.24**%

DCA coadsorbant PCE=**6.12**%

PCE=**7.35**%

graphene modified TiO_2 photo anode PCE=**8.55**%

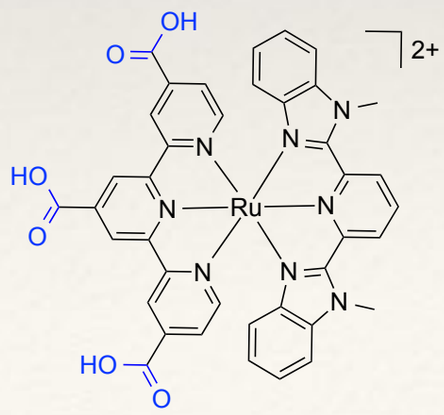

27

RSC Adv., **2013**, **3**, 22412-22420

RSC Adv., **2012**, **2**, 12899-12908

Solar cells

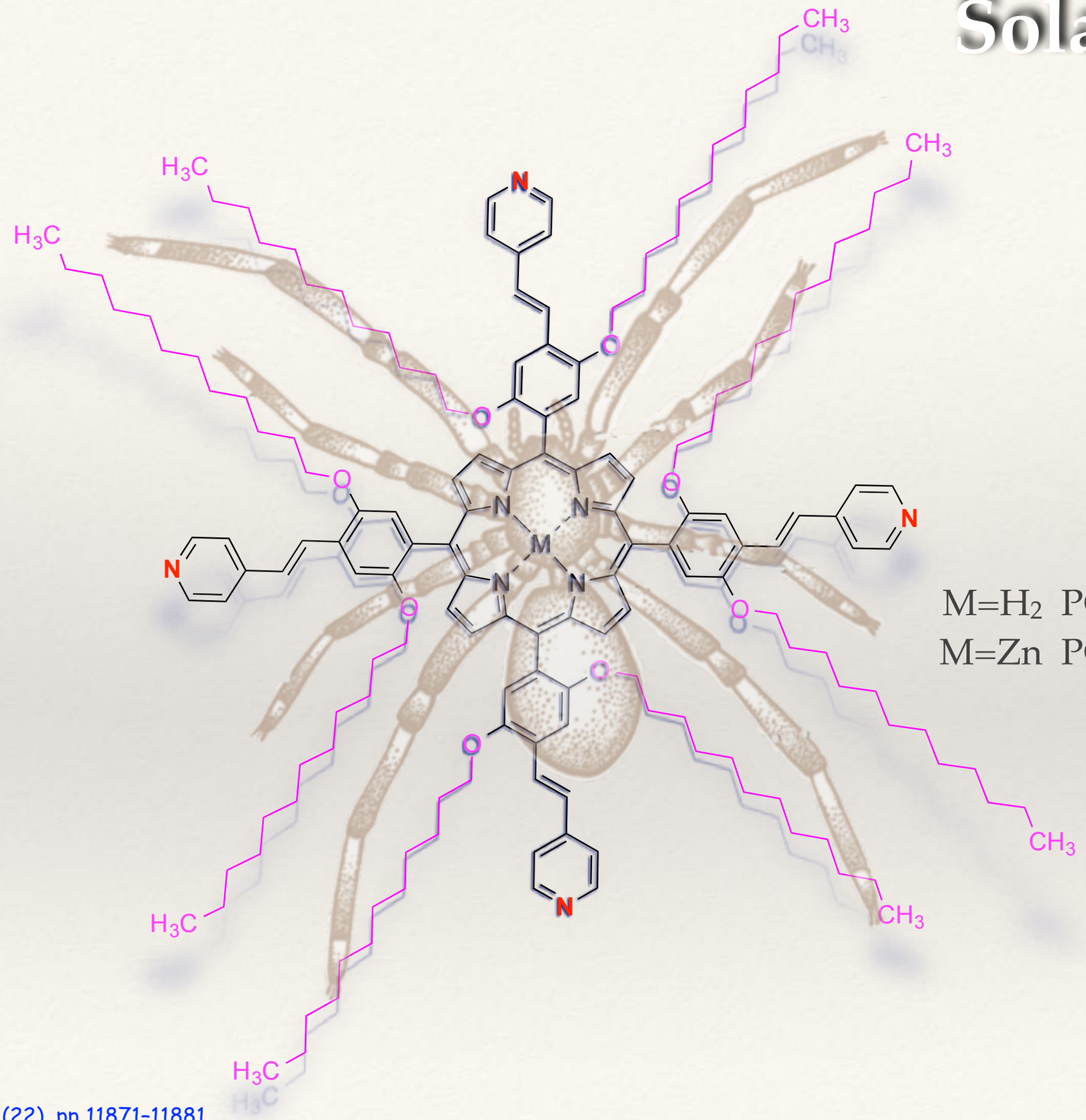

M=H_2 PCE=**3.28**%

M=Zn PCE=**5.12**%

Inorg. Chem., **2014**, 53 (22), pp 11871-11881

Applications

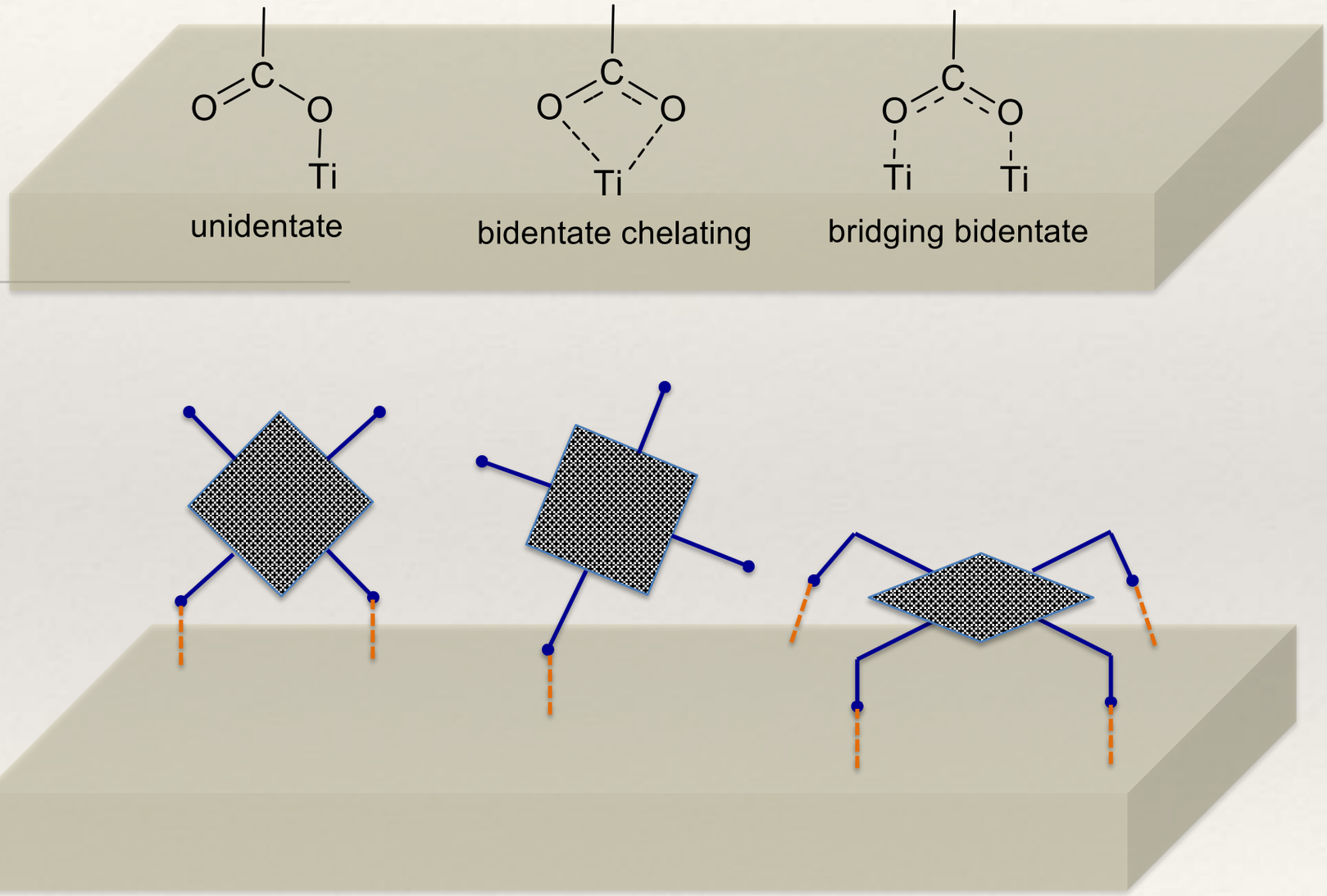

various modes for TiO_2

Artificial photosynth

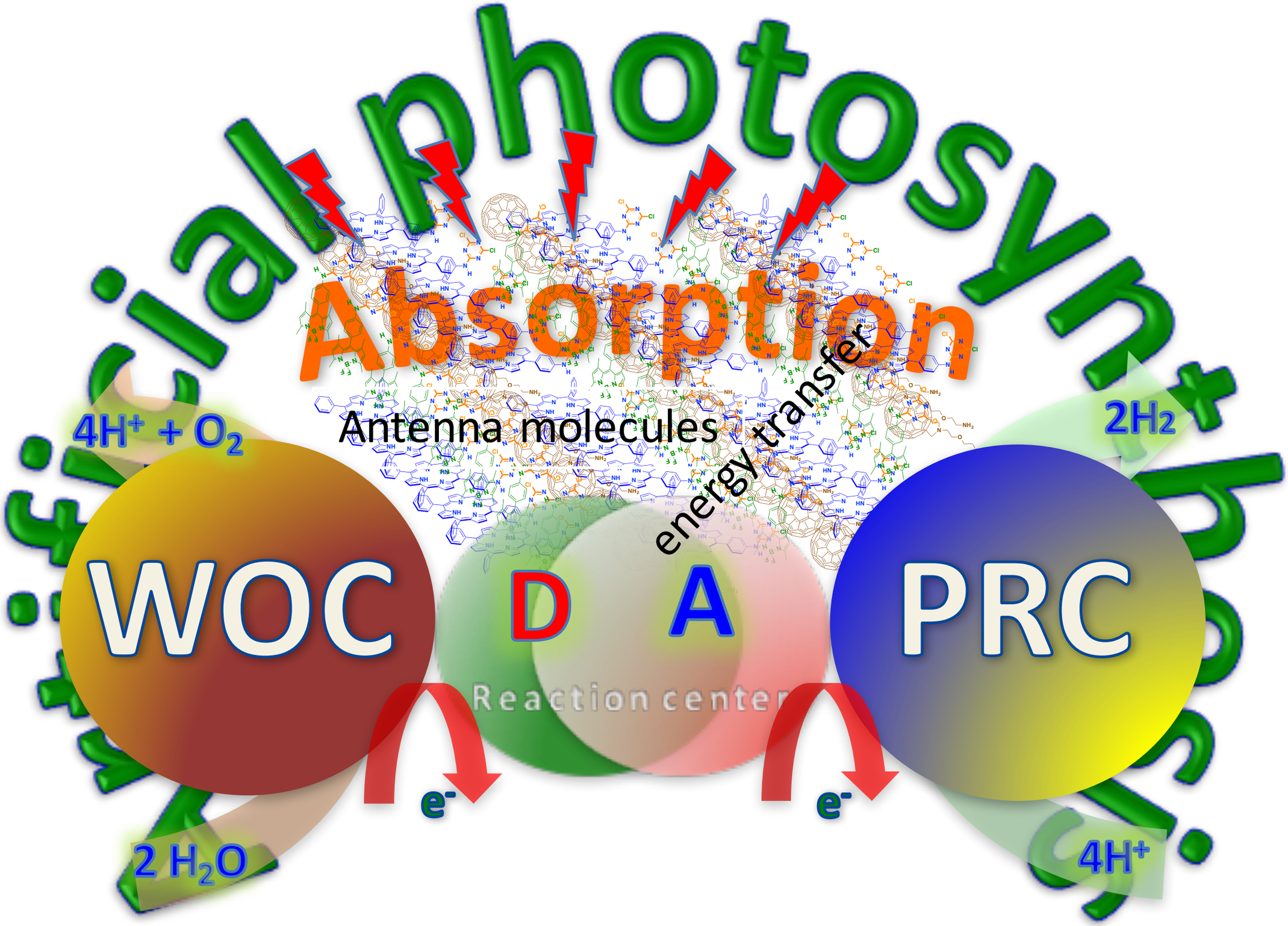

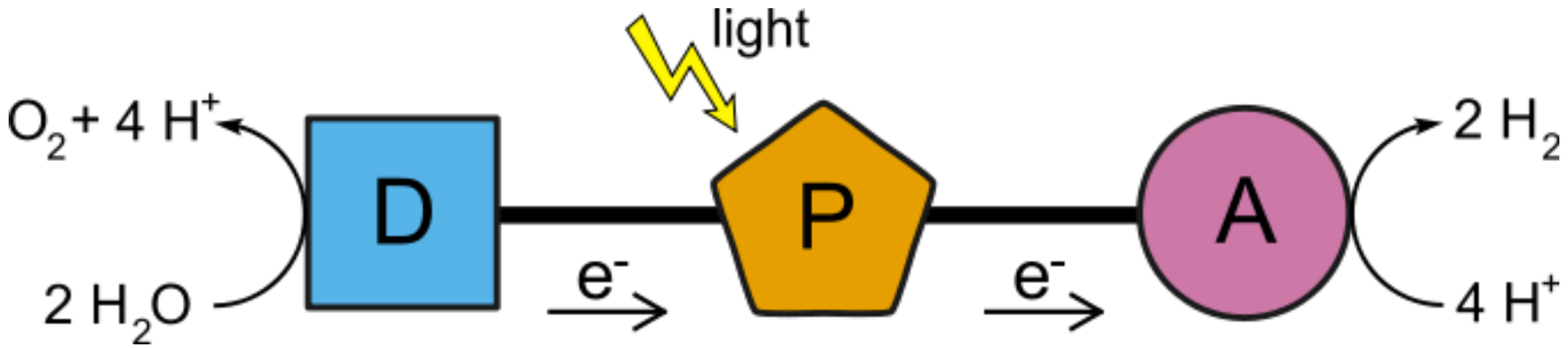
light
$O_2 + 4\ H^+$
$2\ H_2O$
D
P
A
e^-
e^-
$2\ H_2$
$4\ H^+$

covalently linked

Artificial photosynthesis

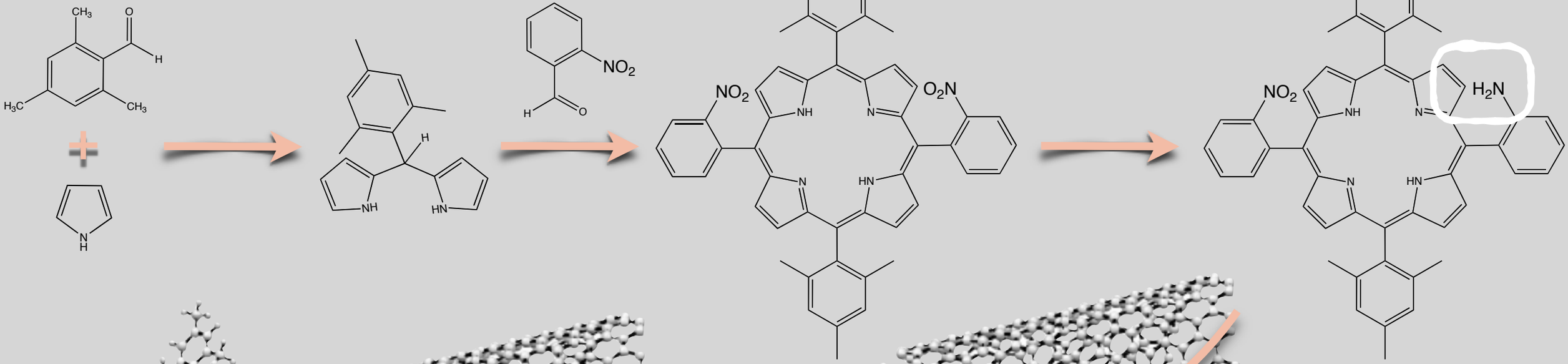

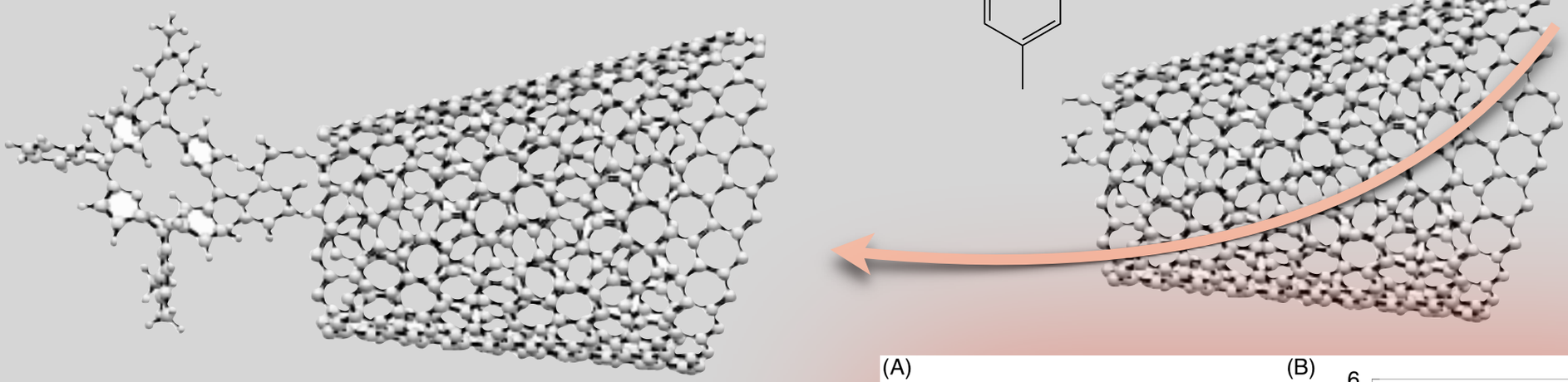

The charge-separated $CNH^{\cdot-}$–$H_2P^{\cdot+}$ states have been identified by transient absorption spectroscopy.

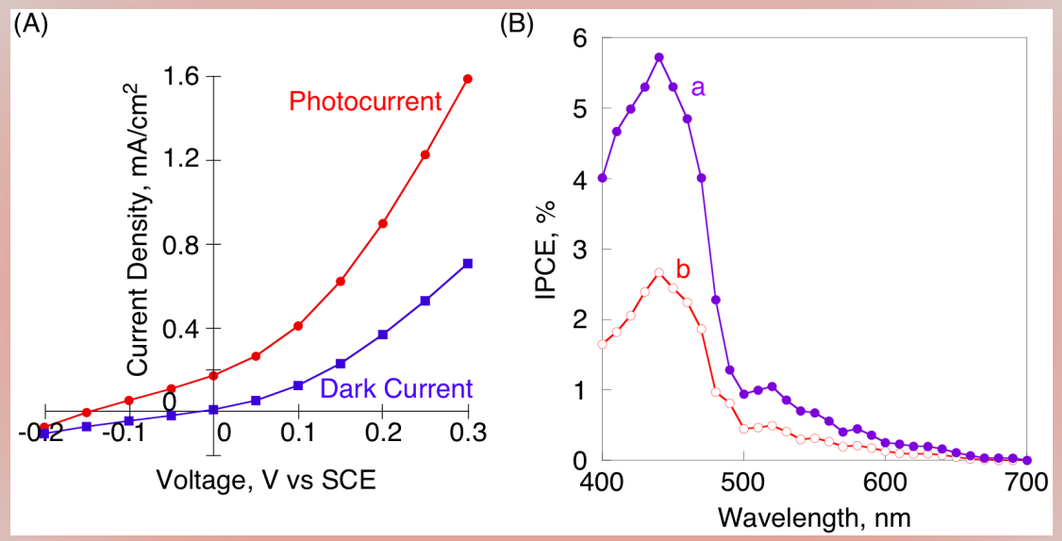

Adv. Funct. Mater. 2007, 17, 1705–1711

Artificial photosynthesis

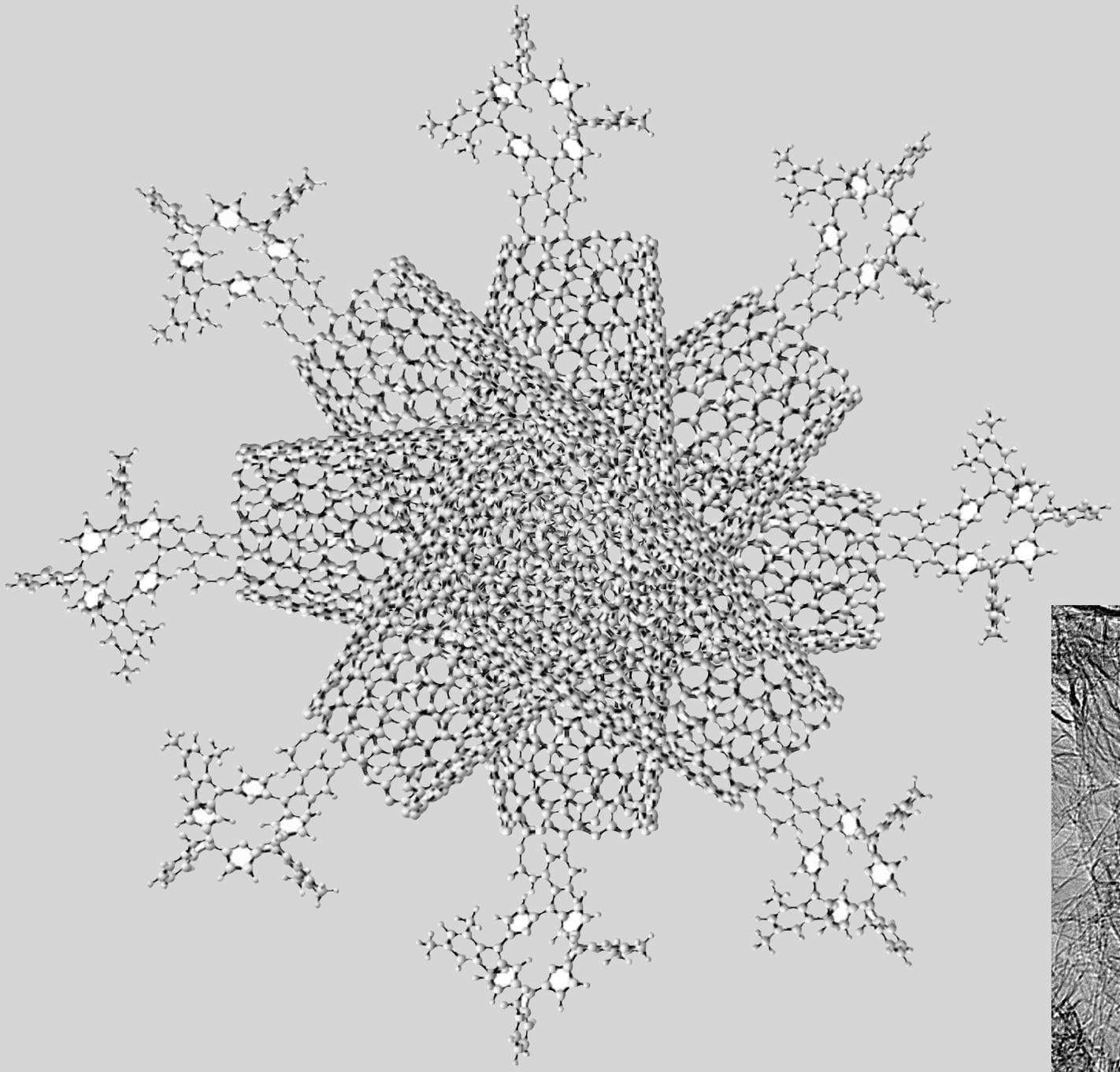

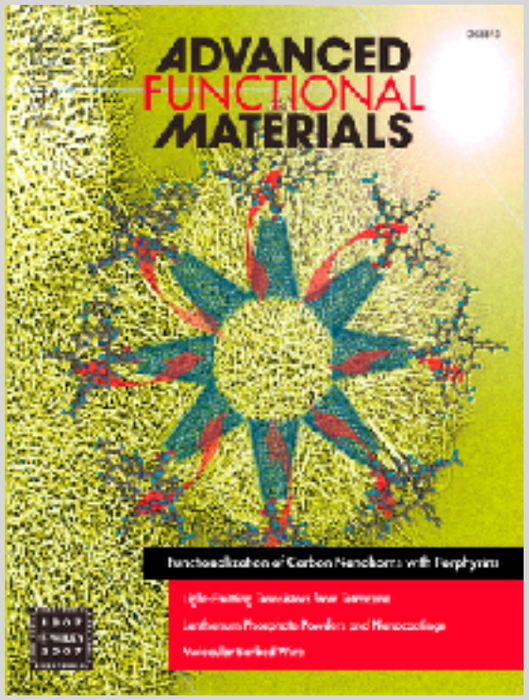

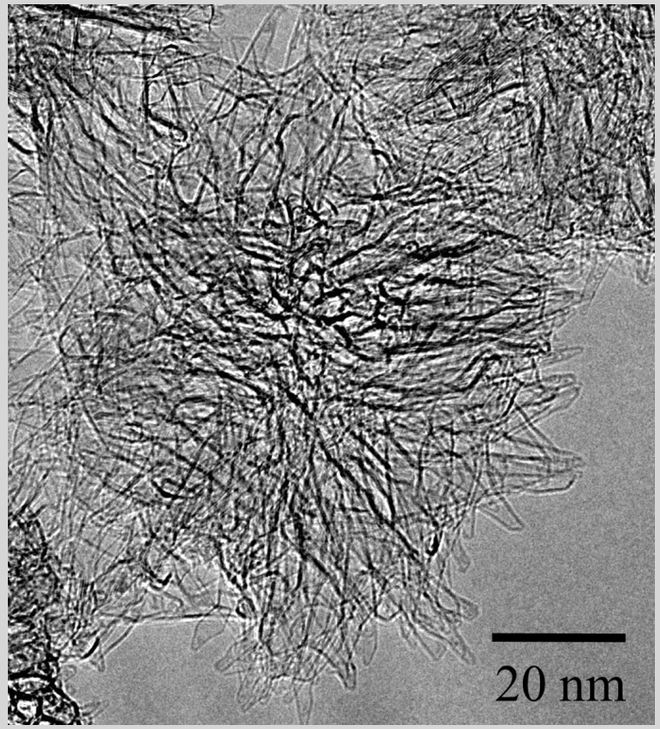

Adv. Funct. Mater. **2007**, 17, 1705–1711

Artificial photosynthesis

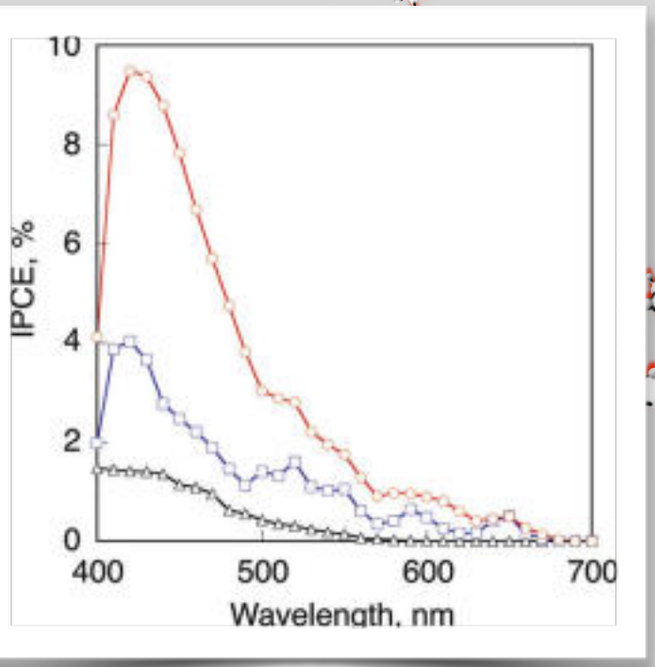

J. Phys. Chem. C, Vol. 112, No. 40, 2008

Artificial photosynthesis

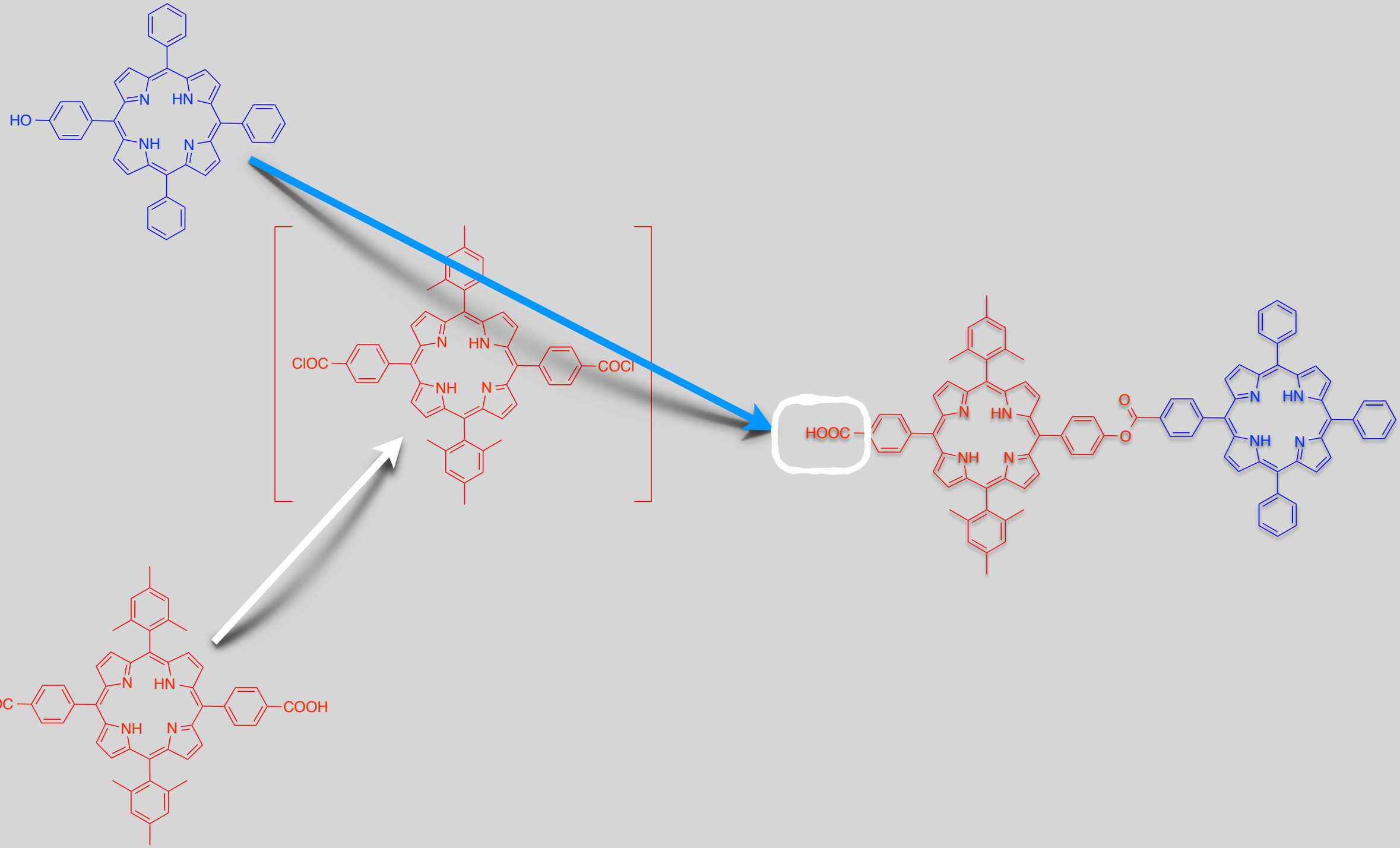

Adv. Funct. Mater. **2007**, 17, 1705–1711

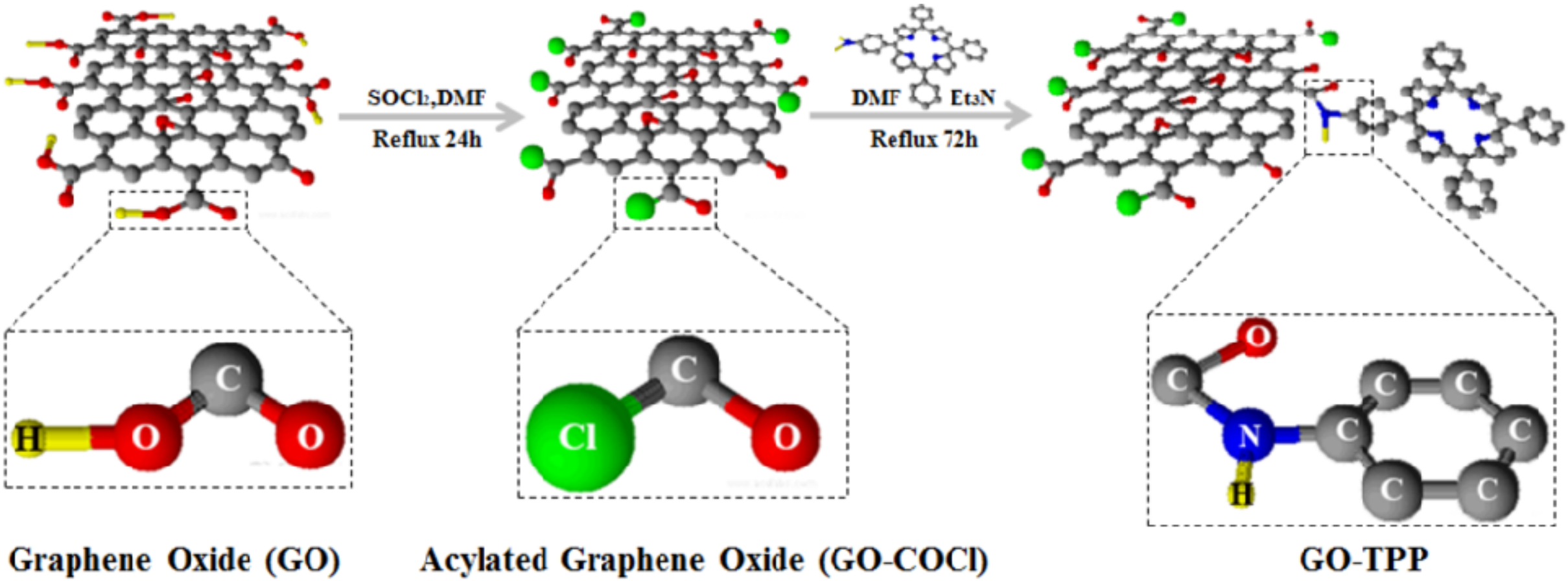

Graphene Oxide (GO) Acylated Graphene Oxide (GO-COCl) GO-TPP

M. Stylianakis, et al. Nanoscale, 2015, 7, 17827–17835

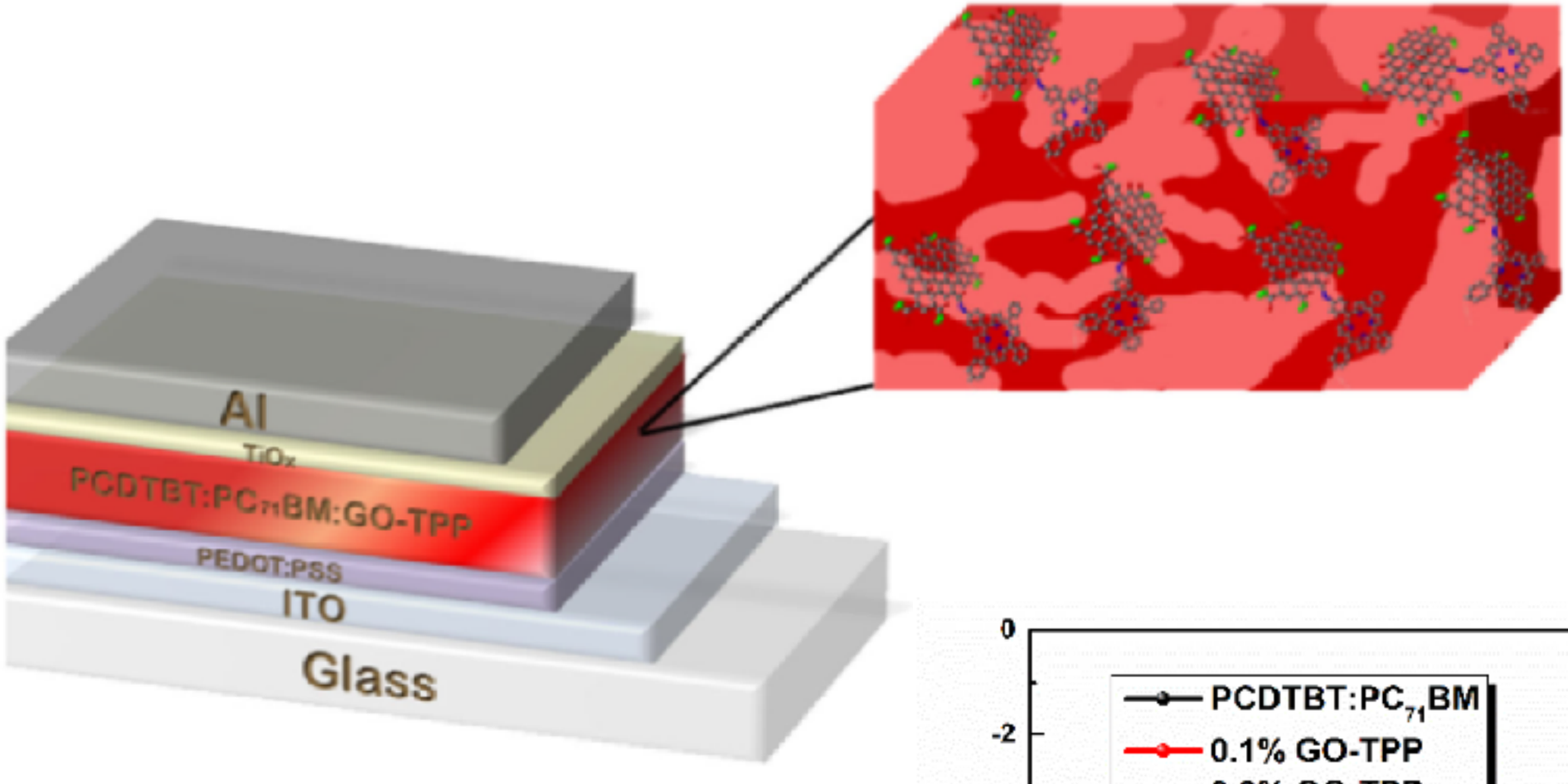

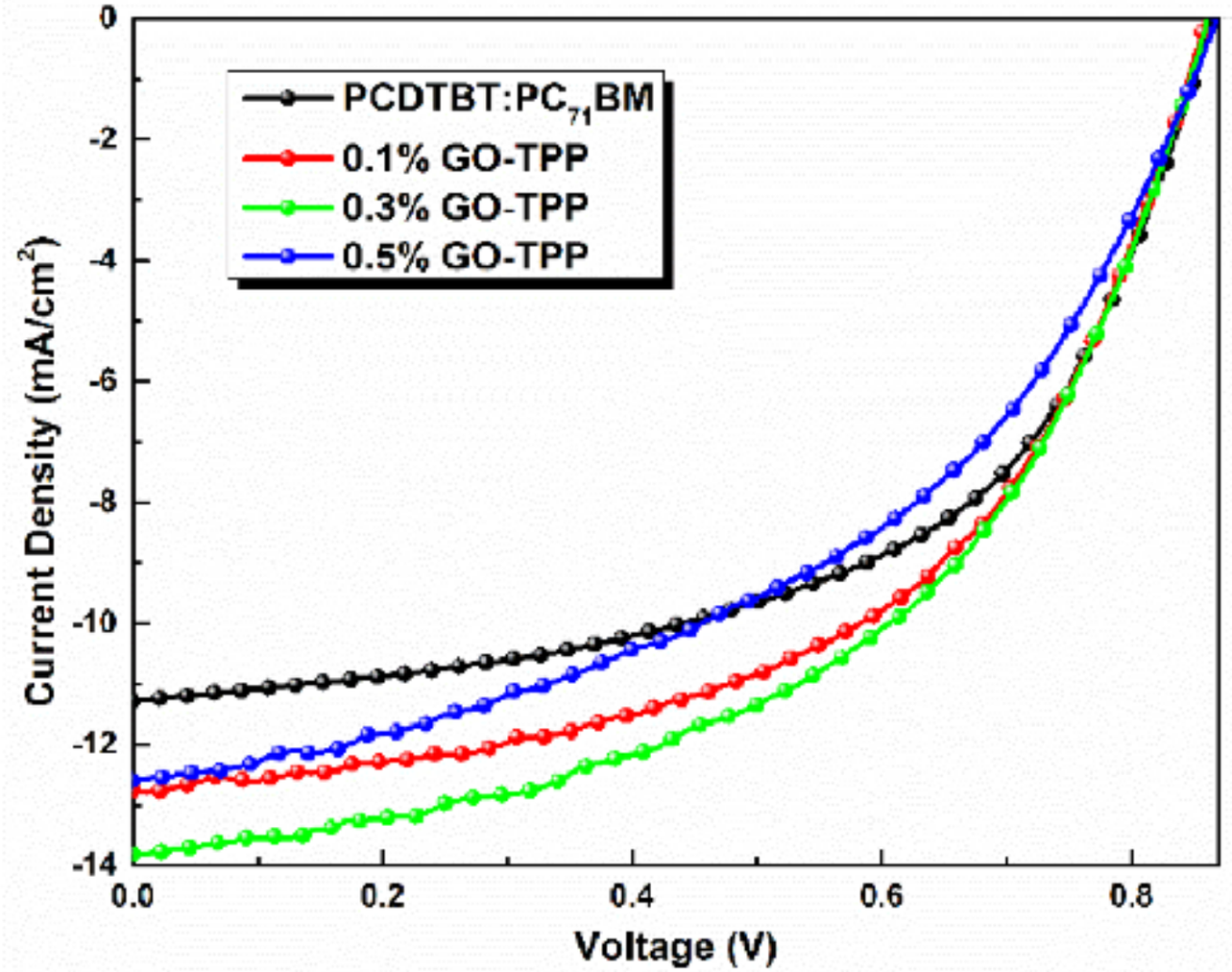

The ideal ternary blend devices based on the ITO/ PEDOT:PSS/ polymer: PC71BM:GO-TPP/interfacial layer/Al structure incorporating two different polymers (PCDTBT and PTB7) and containing 0.3% GO-TPP, resulted in a significant increase of Jsc

Photoinduced Energy Transfer

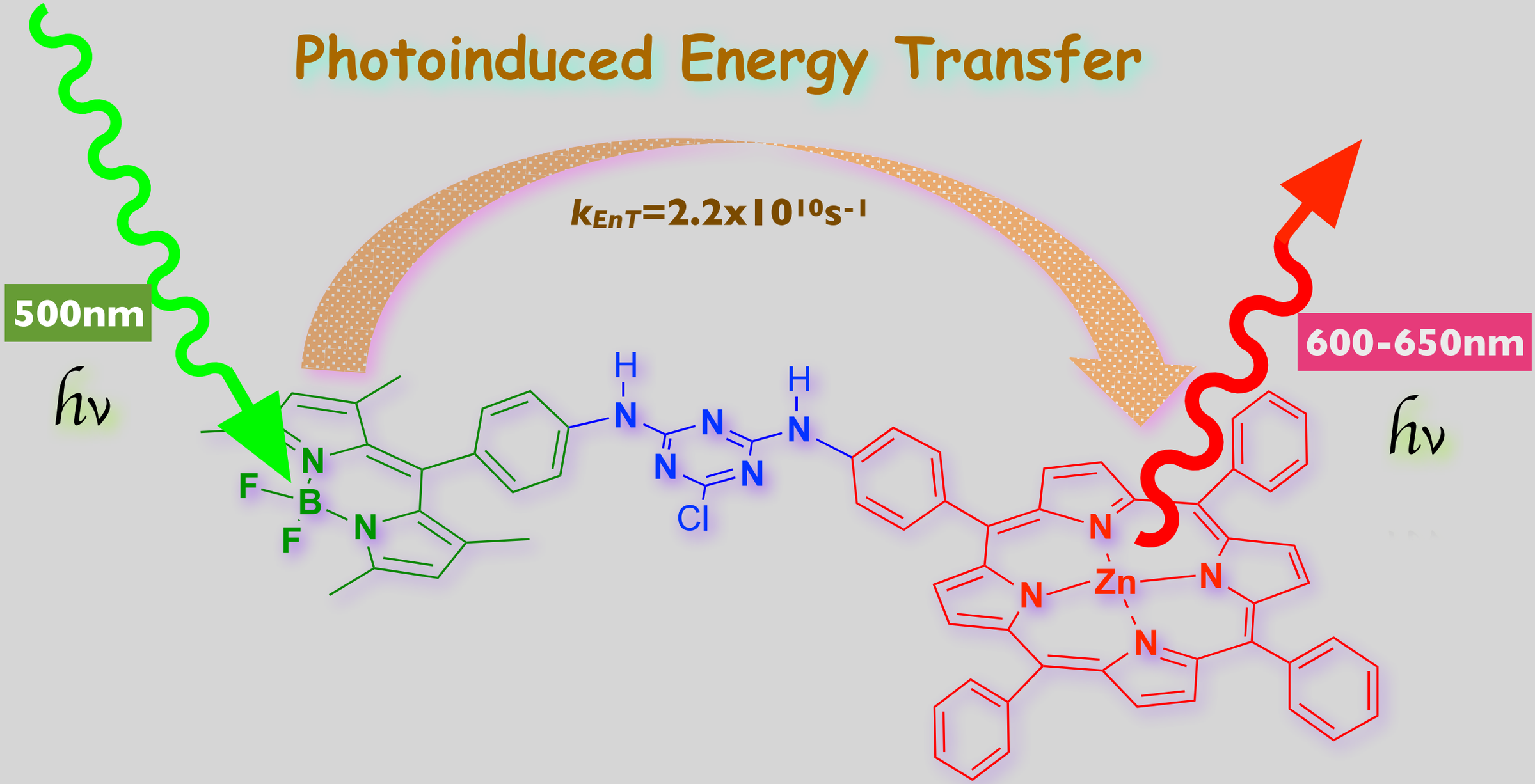

Inorg. Chem. 2011, 50, 8926-8936

Artificial photosynthesis

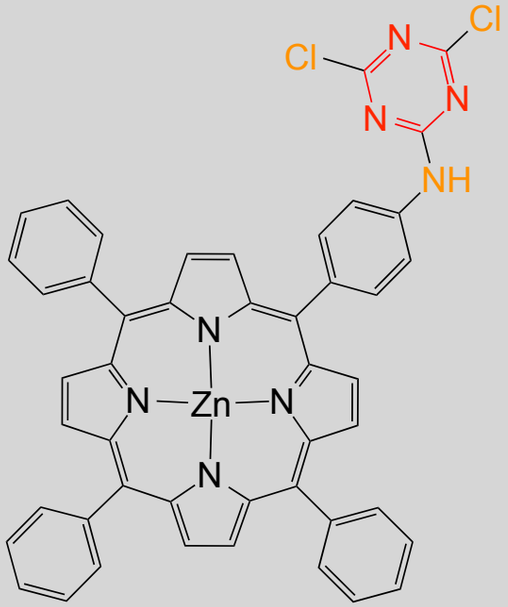

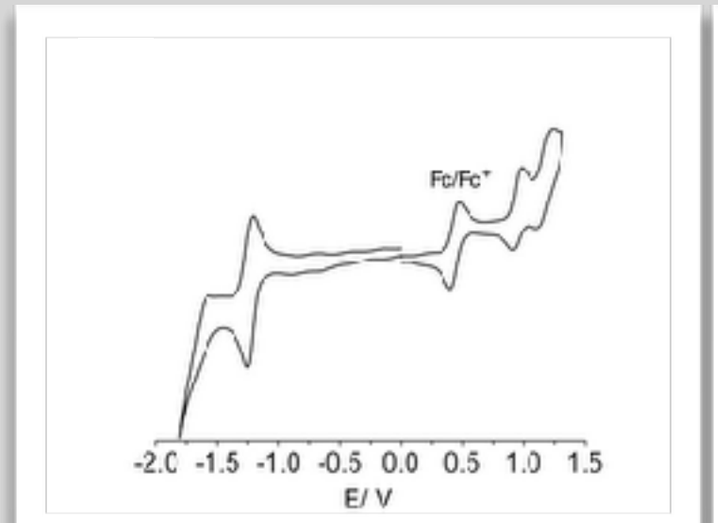

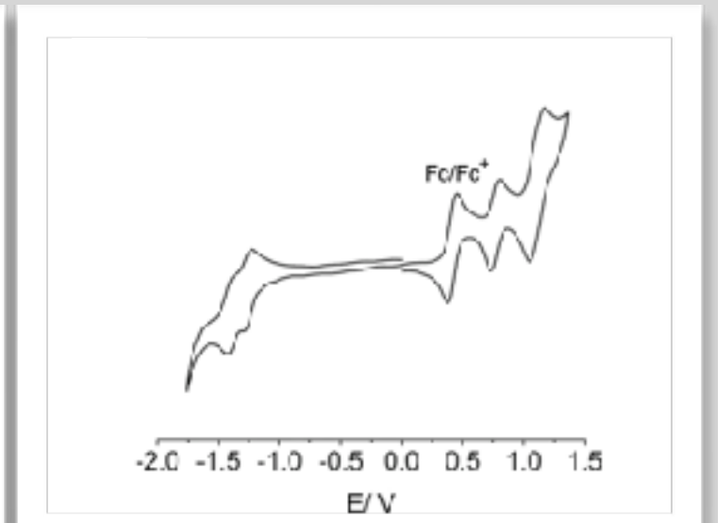

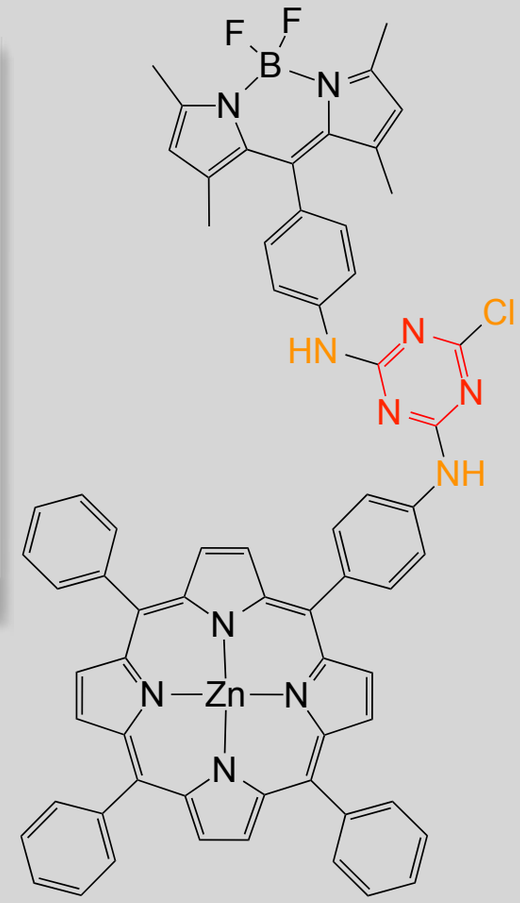

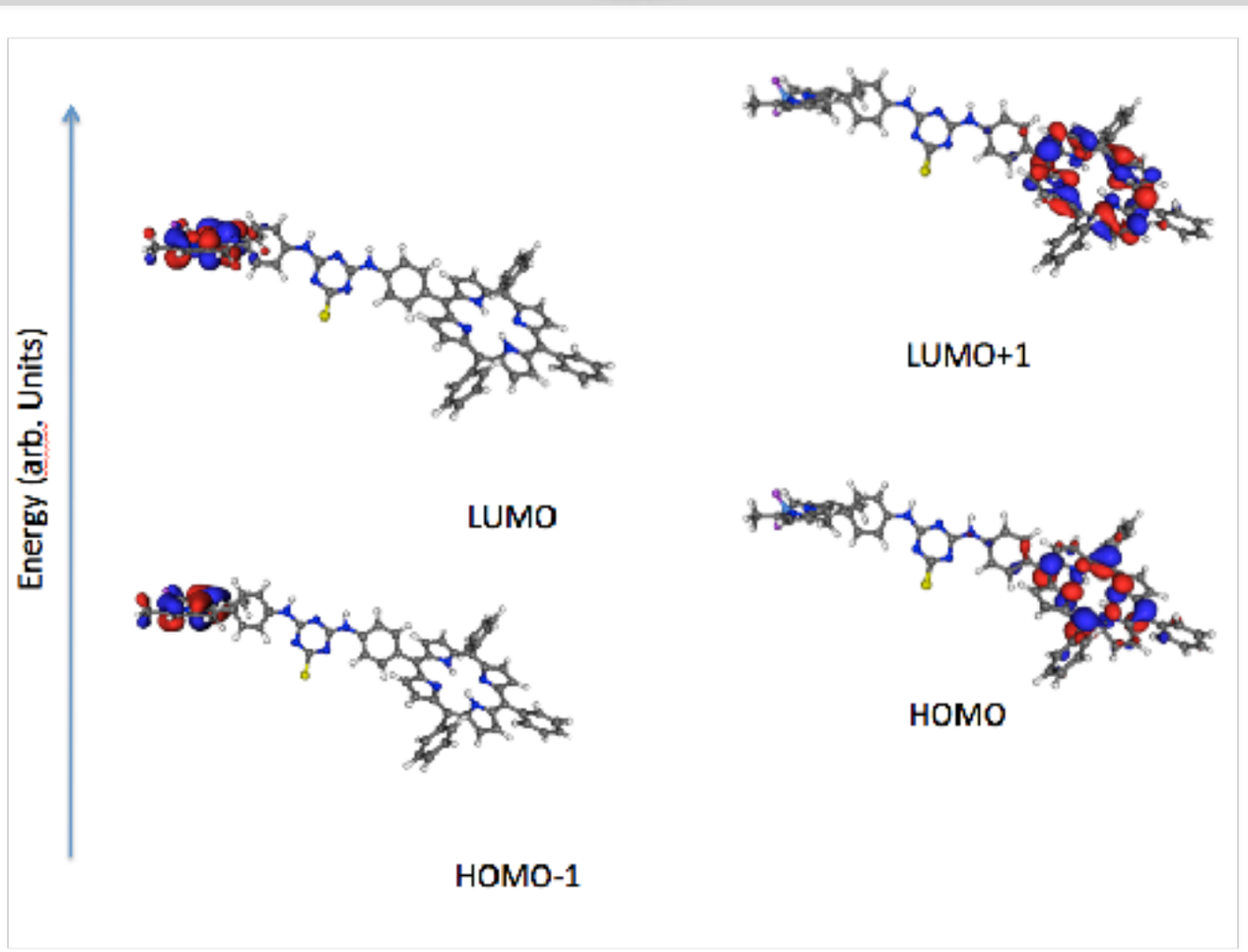

Inorg. Chem. 2011, 50, 8926-8936

Artificial photosynthesis

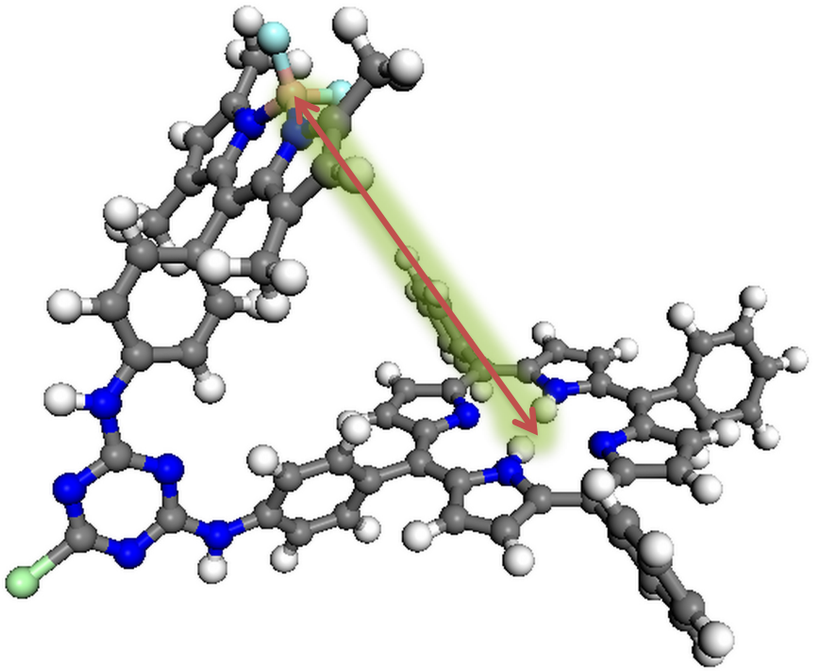

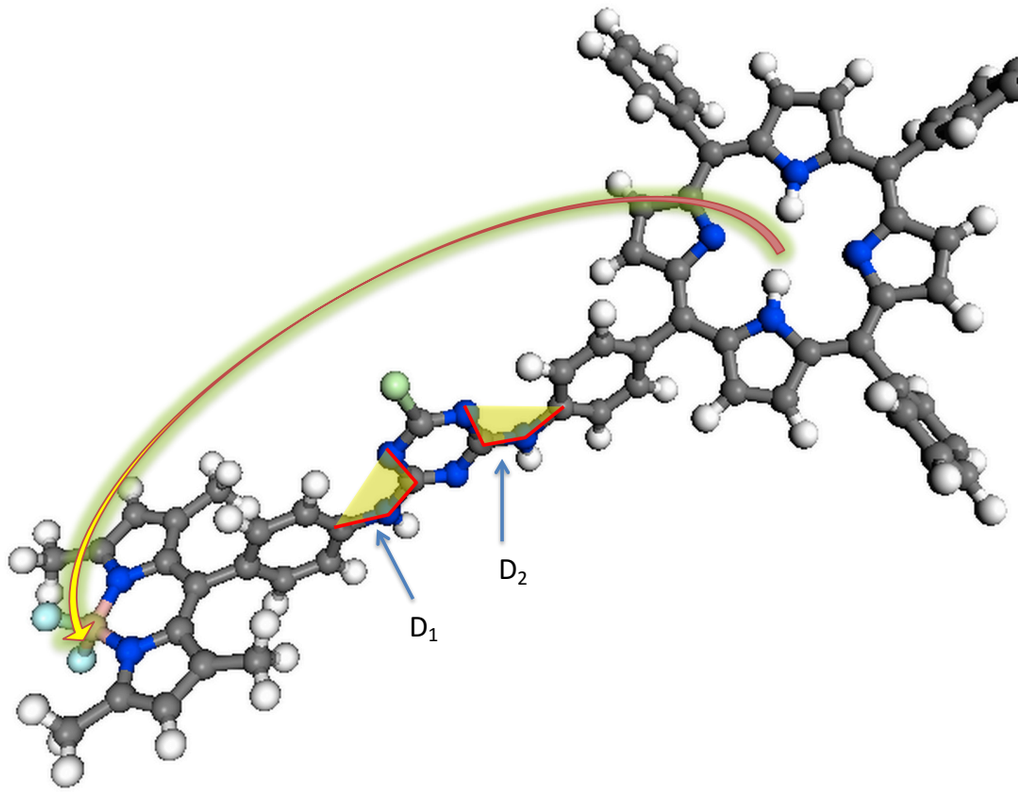

Dexter mechanism

versus

Forster mechanism

Inorg. Chem. 2011, 50, 8926–8936

Artificial photosynthesis

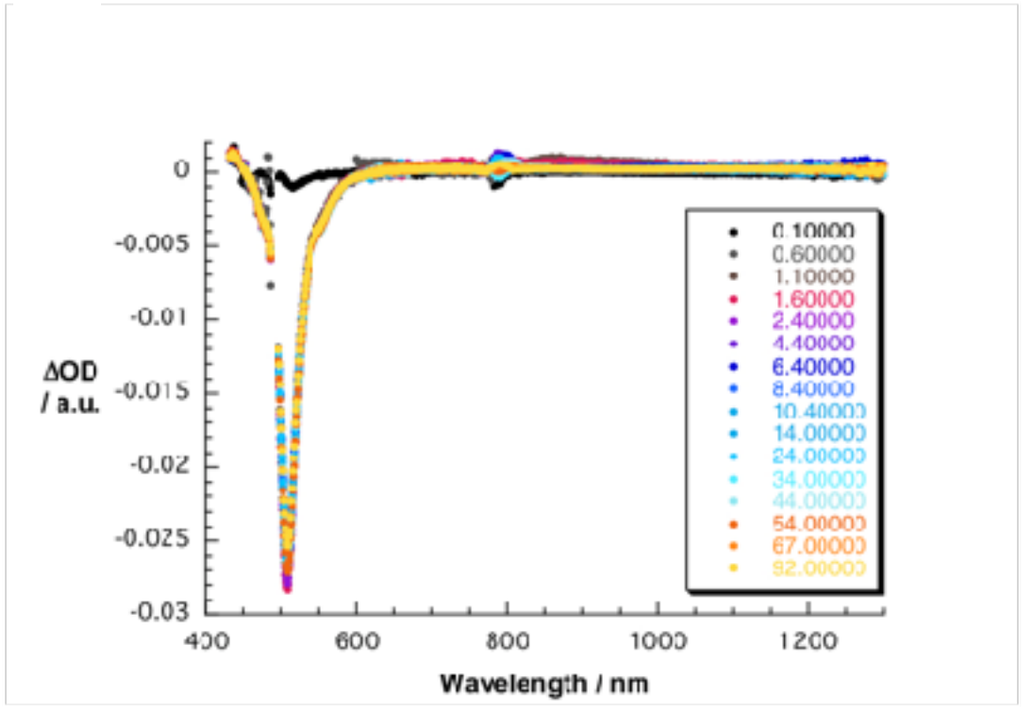

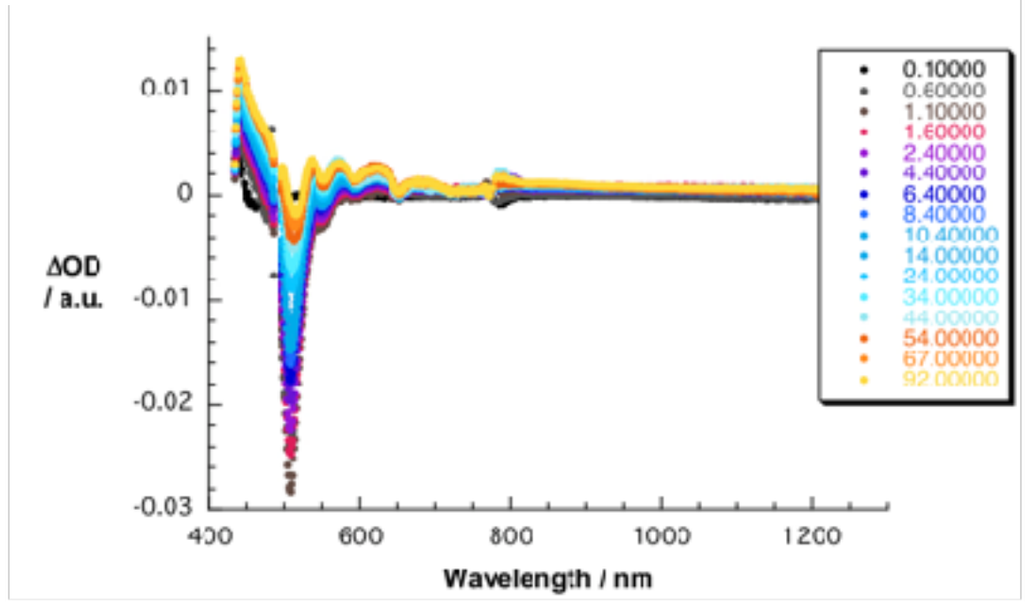

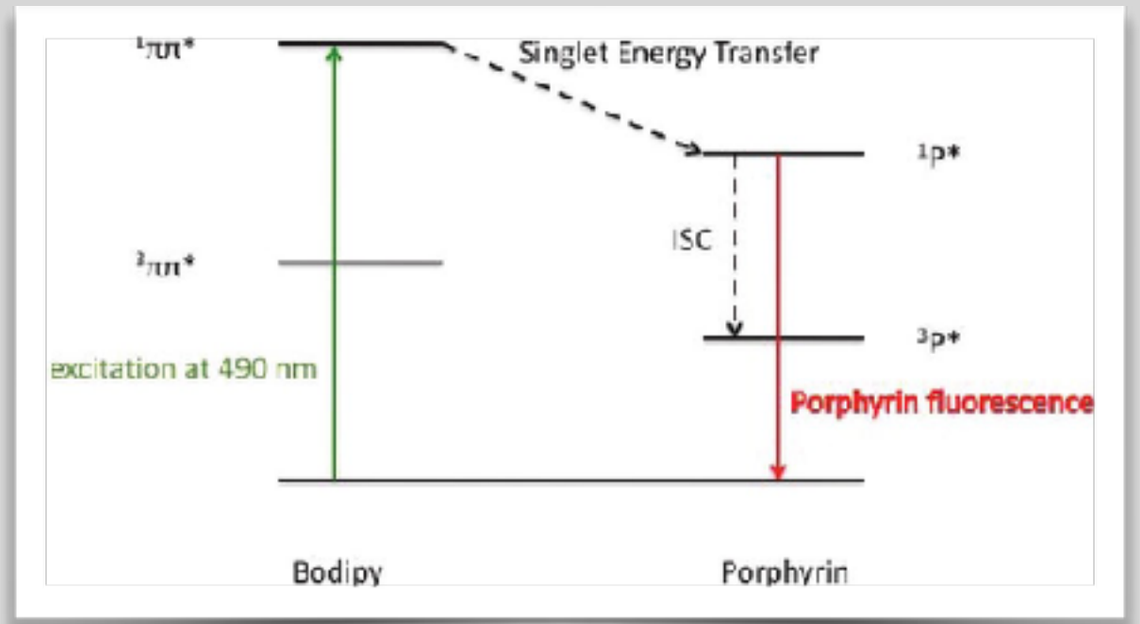

Inorg. Chem. 2011, 50, 8926-8936

Artificial photosynthesis

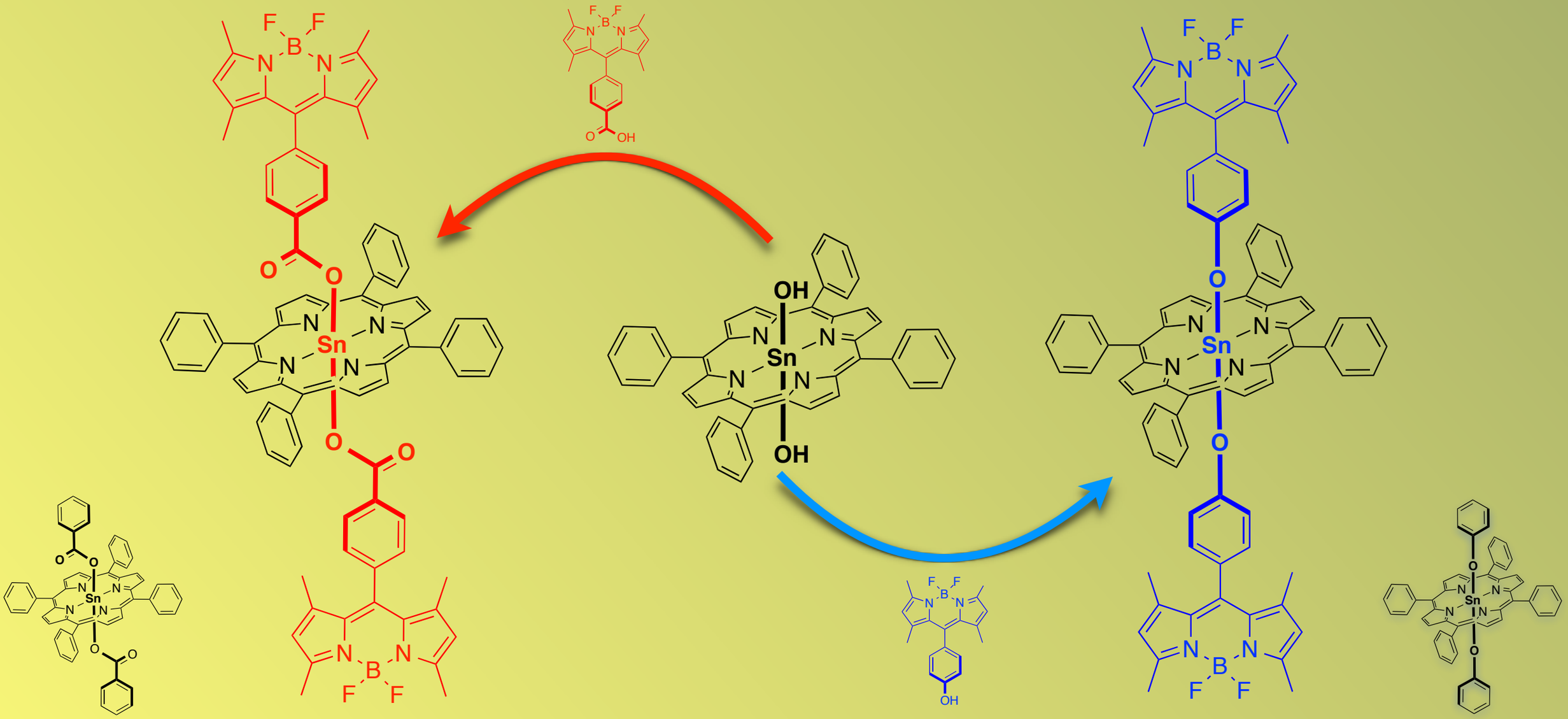

Inorg. Chem. 2011, 50, 8926-8936

Energy transfer versus electron transfer

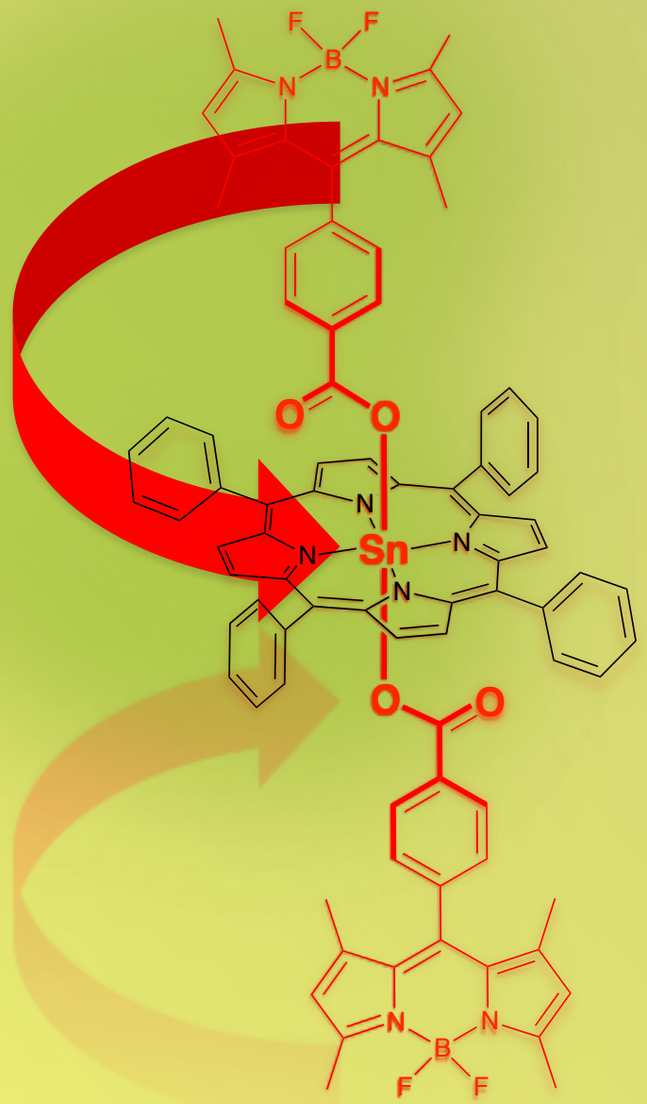

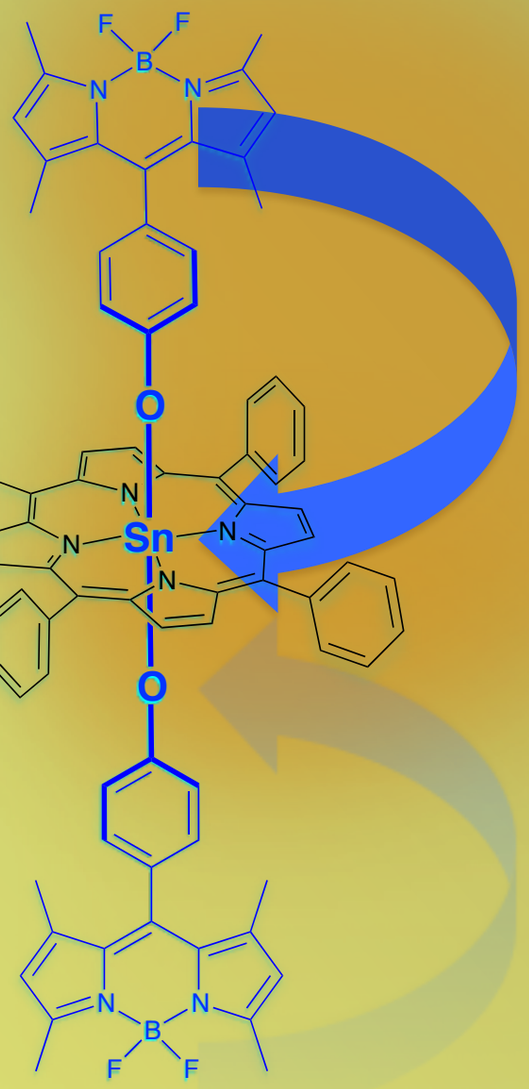

Inorg. Chem. 2012, 51, 4193-4204

Artificial photosynthesis

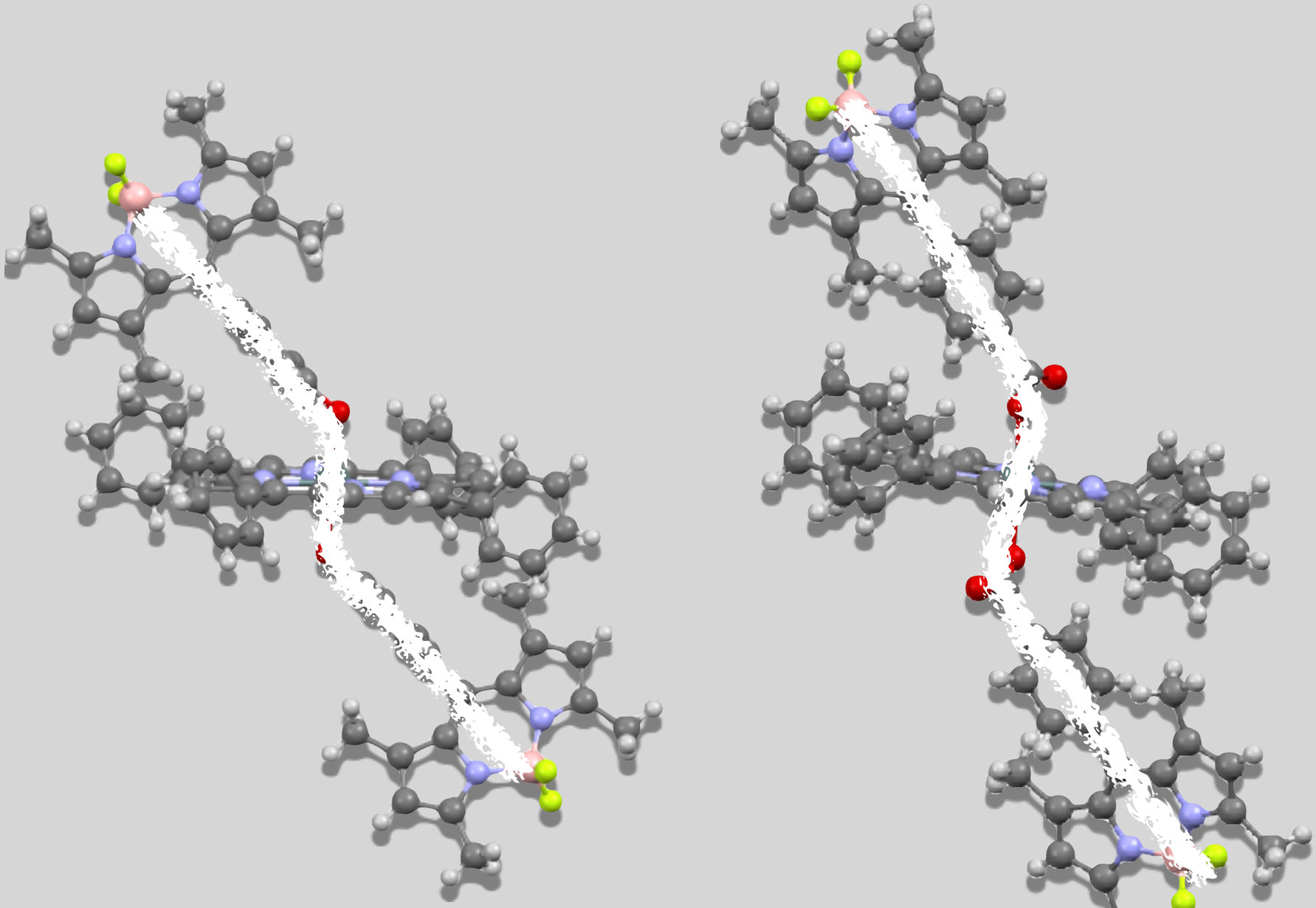

Inorg. Chem. 2011, 50, 8926-8936

Artificial photosynthesis

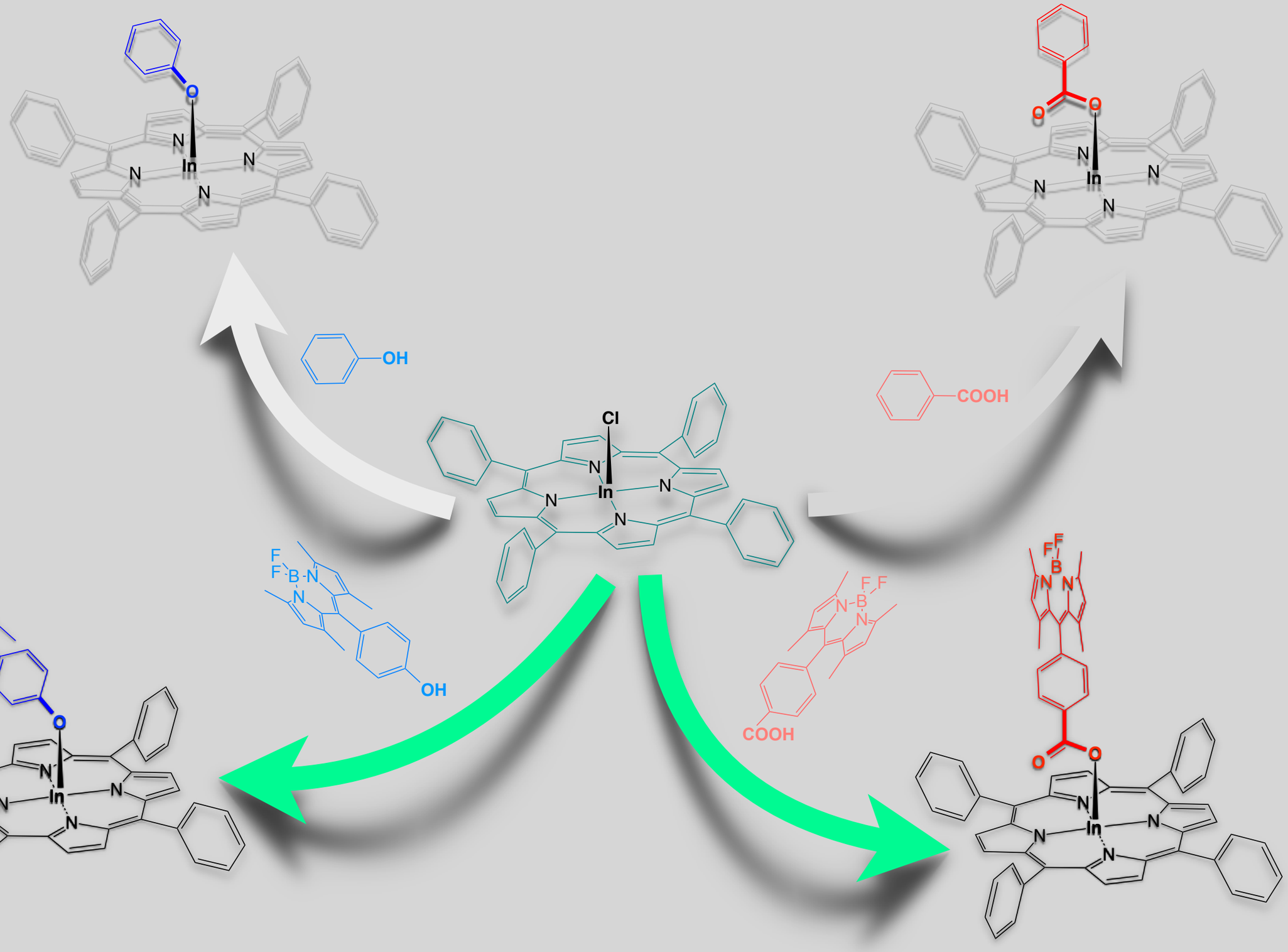

Eur. J. Inorg. Chem. **2015**, 468-477

Artificial photosynthesis

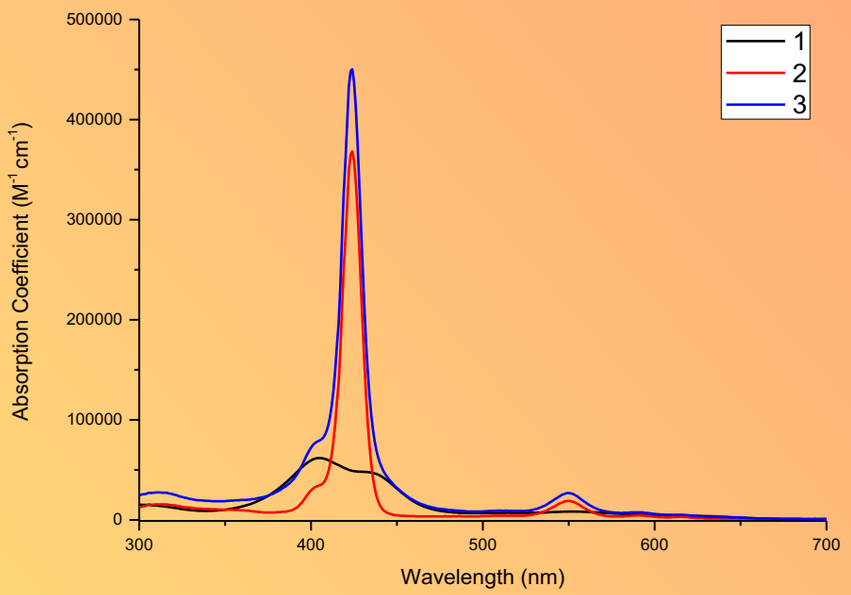

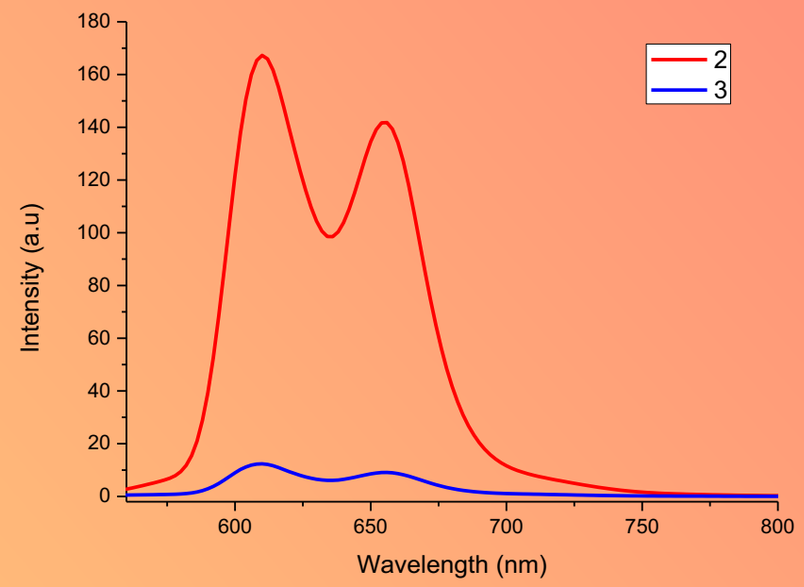

energy transfer

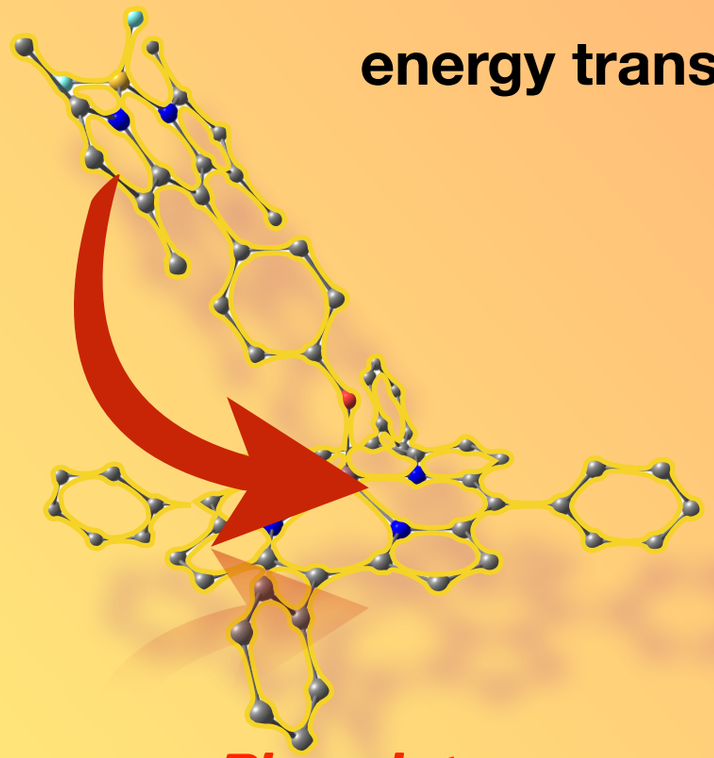

Phenolate

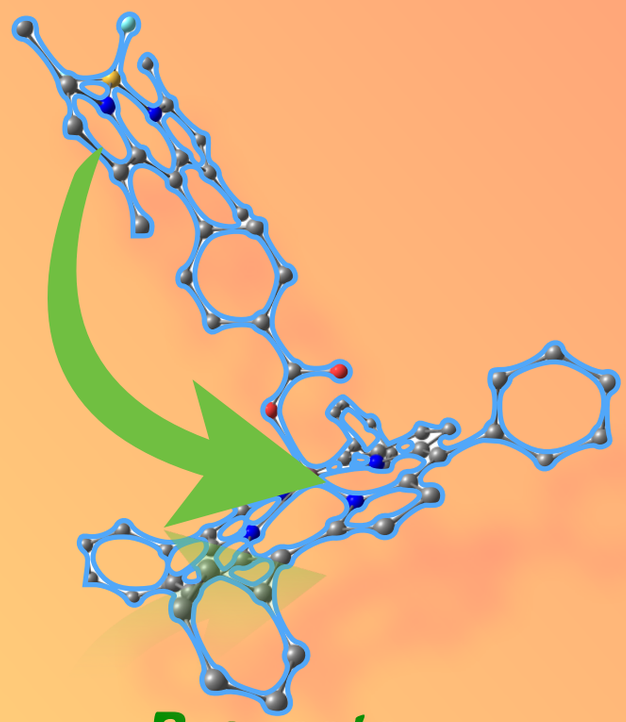

Benzoate

Eur. J. Inorg. Chem. 2015, 468–477

Artificial photosynthesis

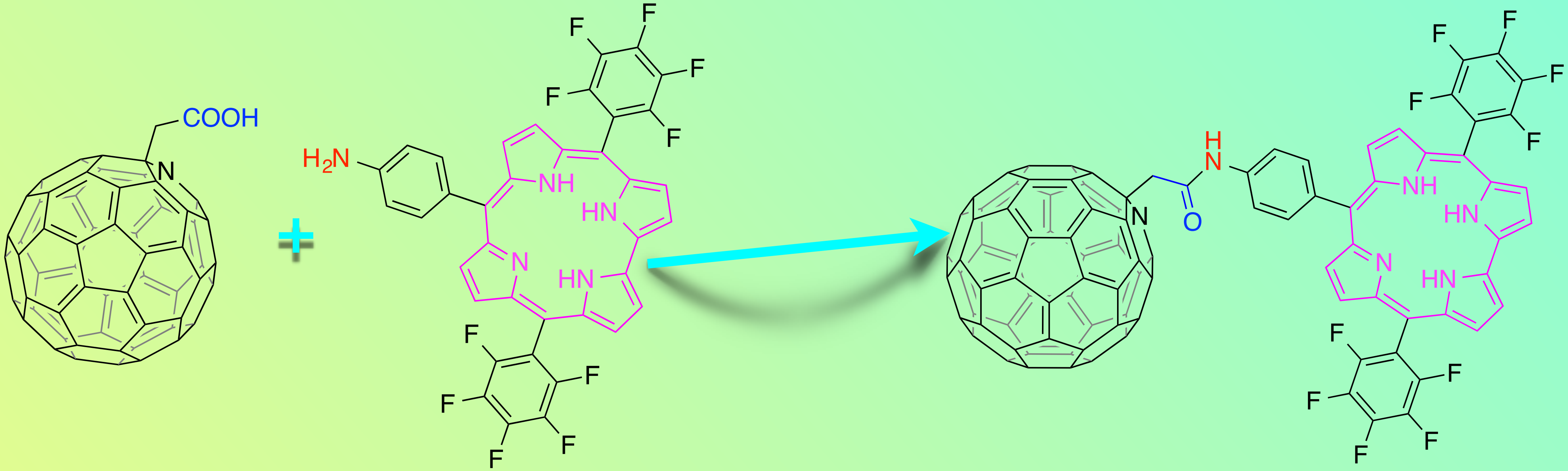

Chem. Commun., 2013, 49, 9128-9130

Artificial photosynthesis

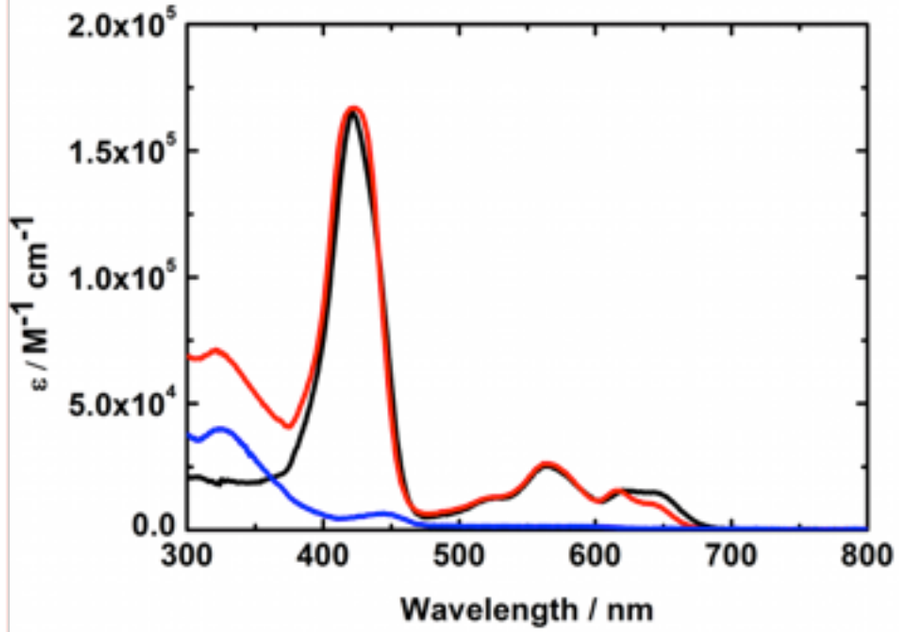

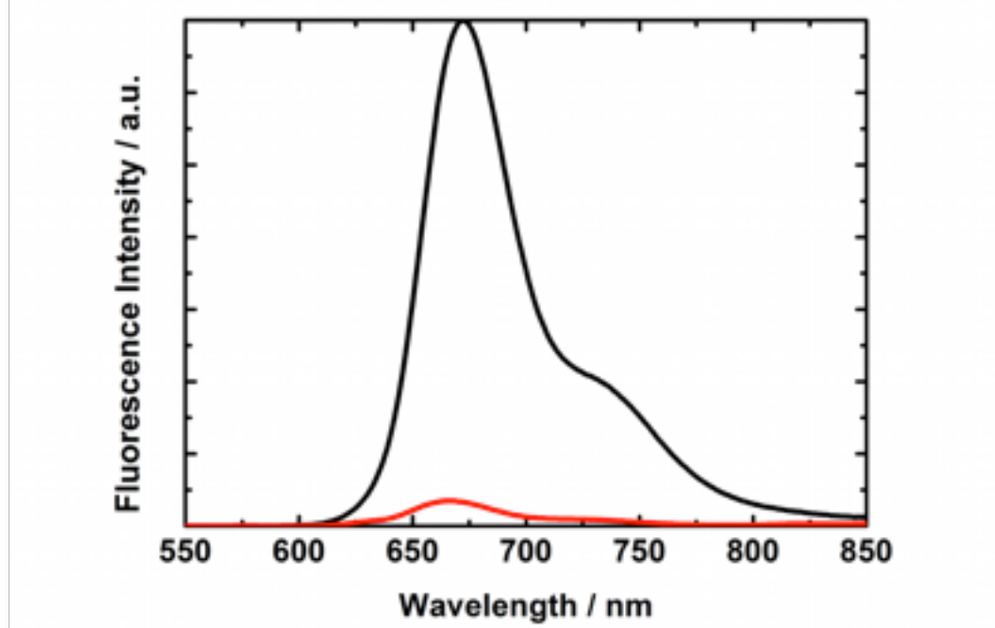

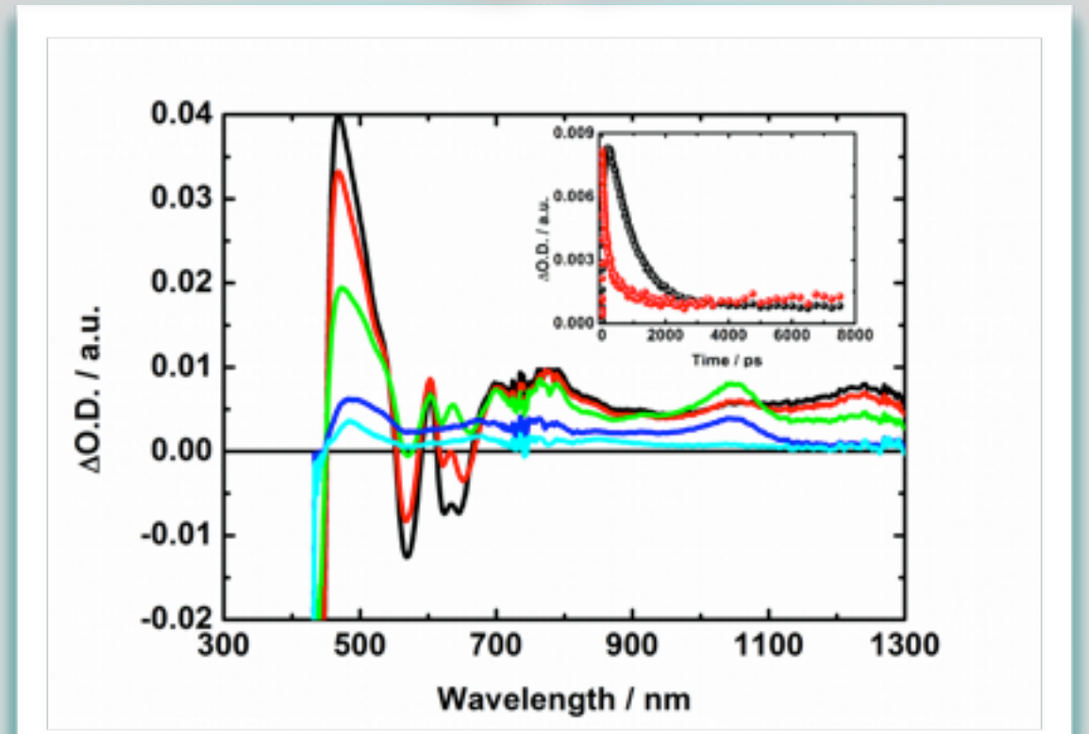

The (corrole) – (C59N)

charge separated state decays mainly to the singlet ground state.

Chem. Commun., **2013**, 49, 9128-9130

Artificial photosynthesis

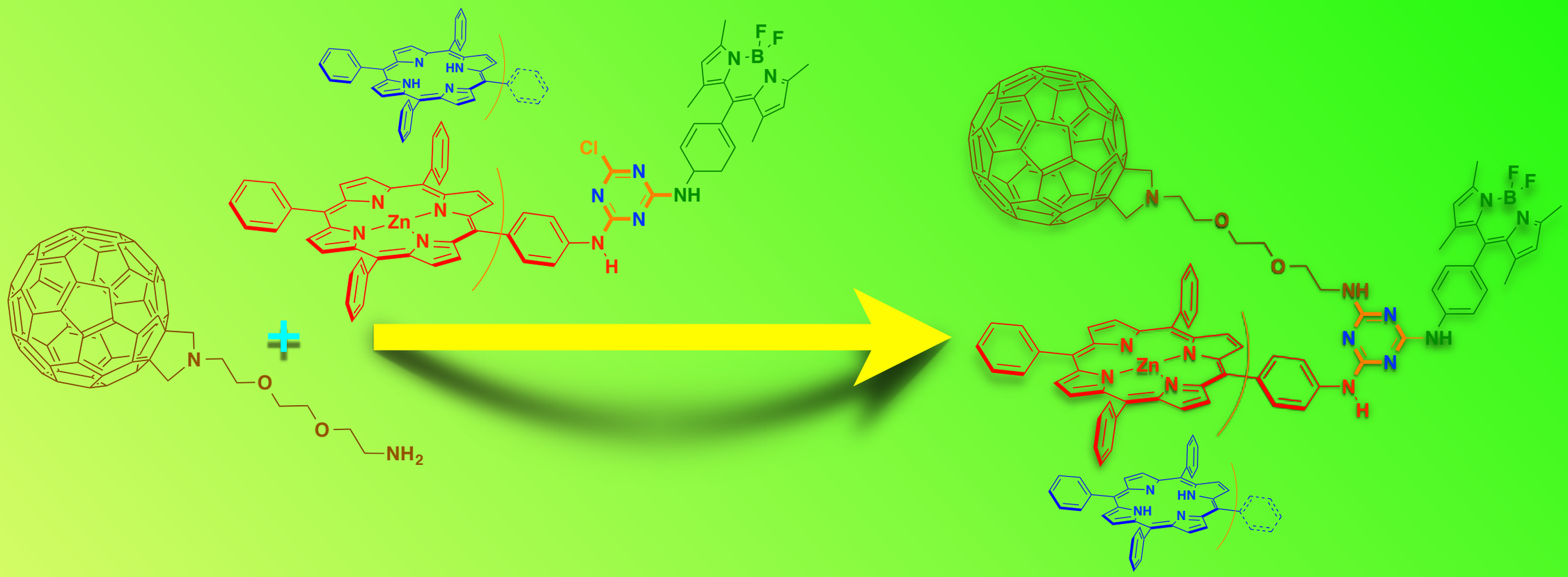

Chem. Eur. J. 2014, 20, 2049 – 2057

Artificial photosynthesis

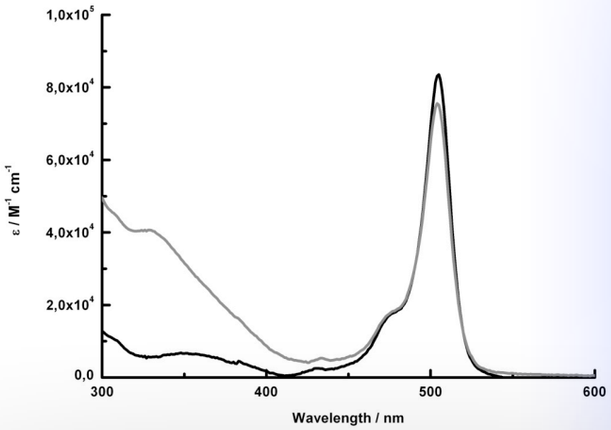

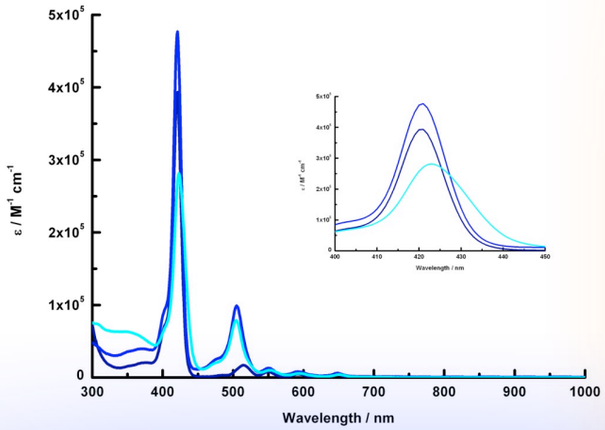

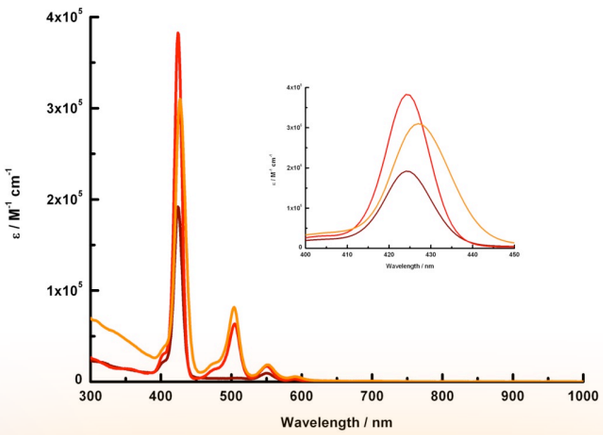

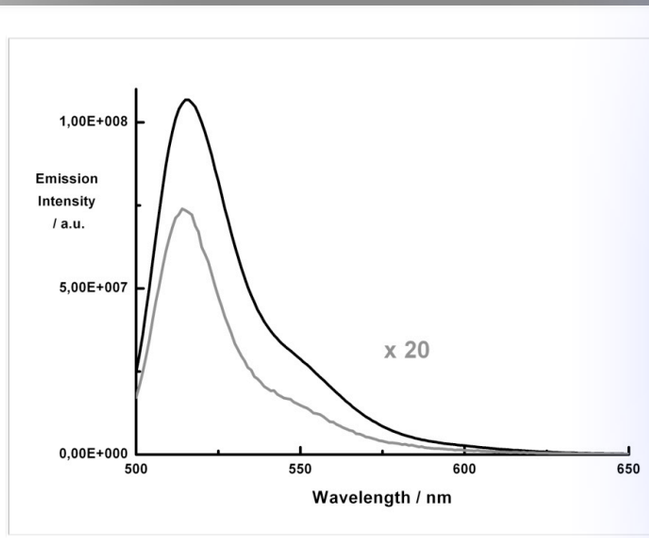

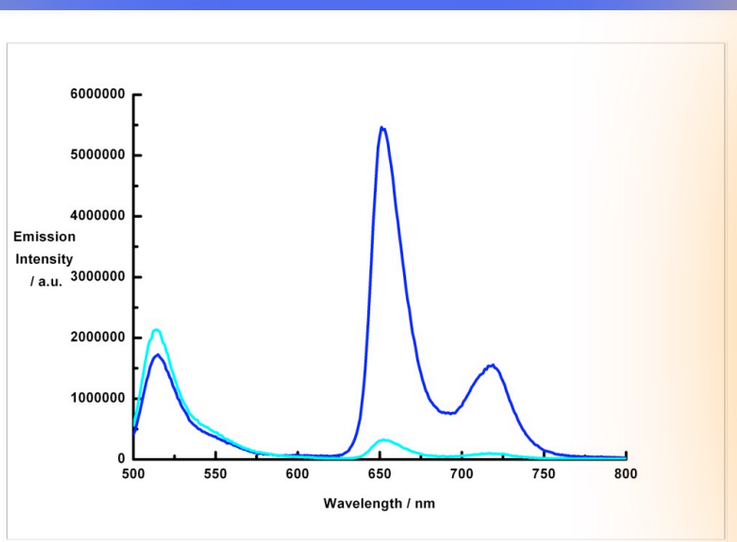

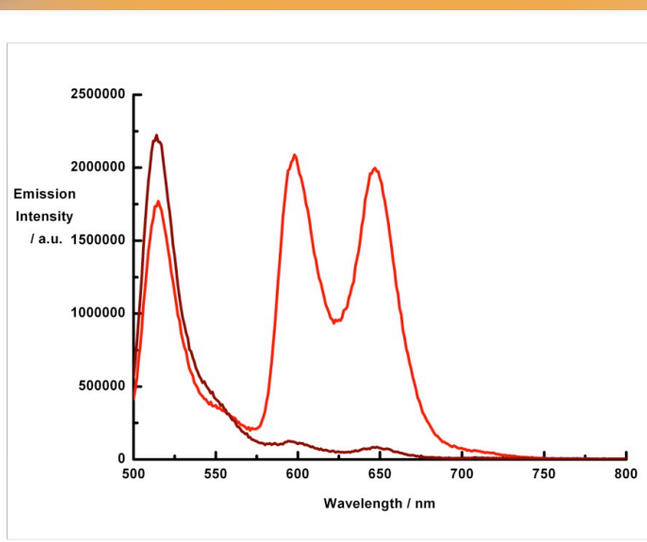

BDP-**NHCl** (**black**) and

BDP-C$_{60}$ (grey)

H$_2$P-NHCl (**dark blue**),

BDP-H$_2$P (**blue**), and

BDP-H$_2$P-C$_{60}$ (cyan)

ZnP-**NHCl** (**wine**),

BDP-ZnP (**red**), and

BDP-ZnP-C$_{60}$ (orange)

Chem. Eur. J. **2014**, 20, 2049 – 2057

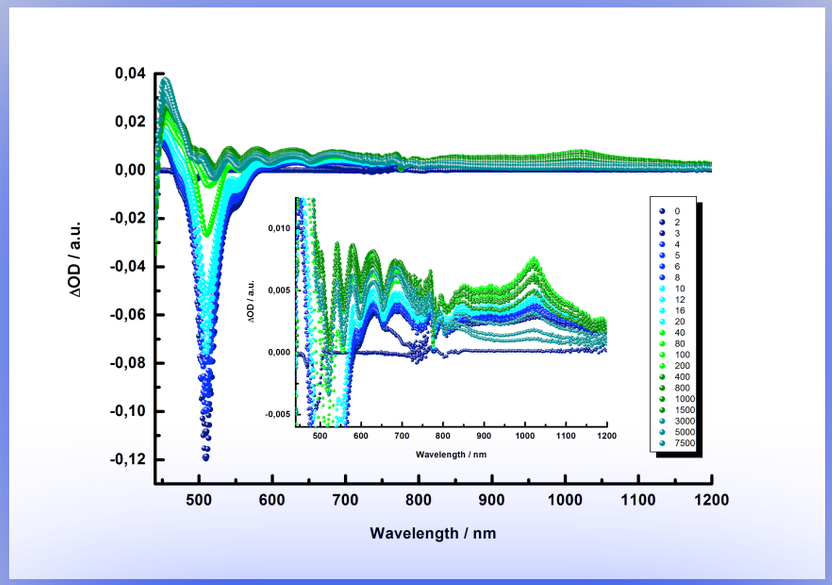

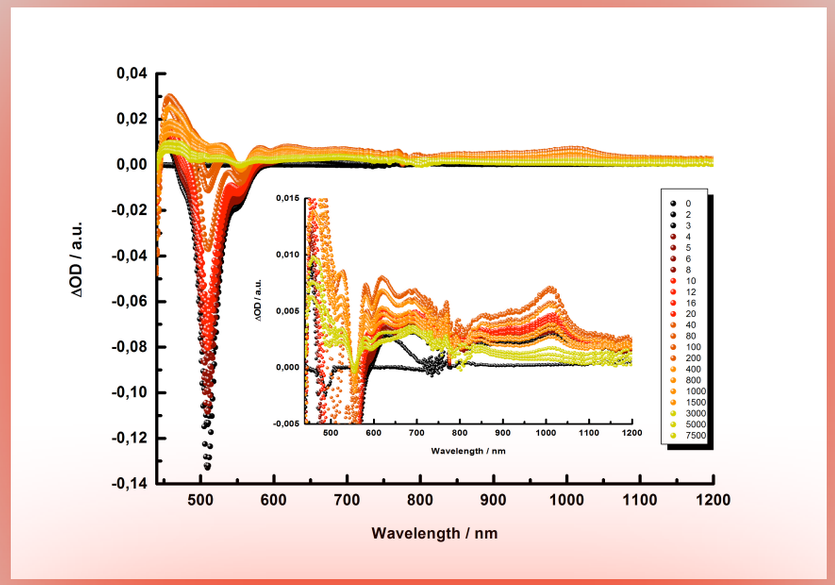

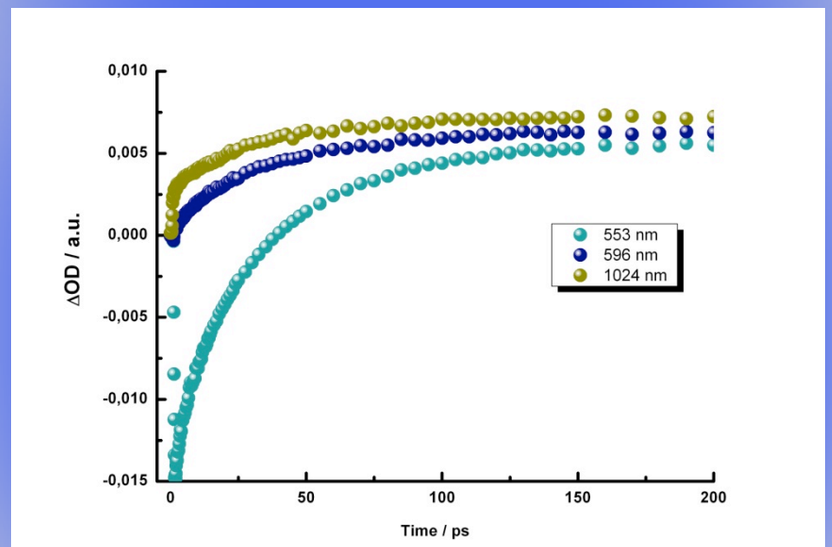

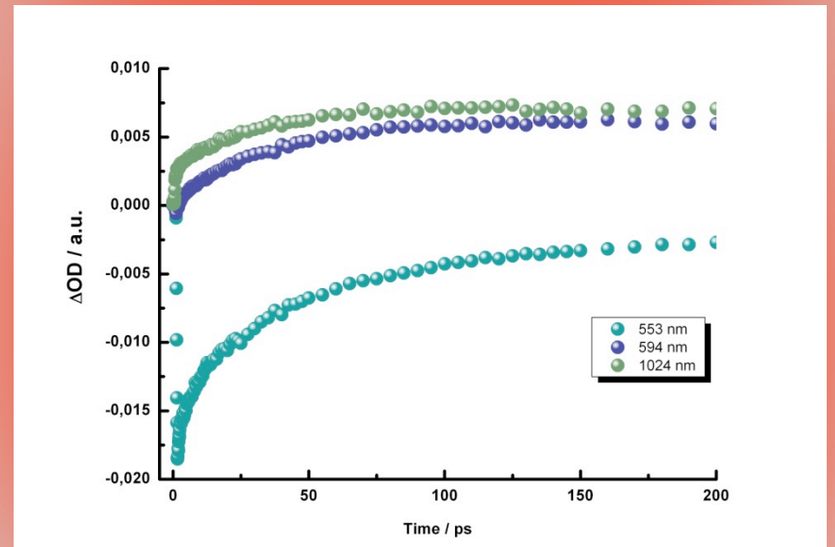

Top – differential absorption spectra (visible and near-infrared) obtained upon femtosecond flash photolysis (490 nm, 200 nJ) of **BDP-H_2P-C_{60}** in argon saturated toluene with several time delays between 0 and 8000 ps at room temperature, insert- zoom in to virtualize the relevant decays. Bottom – time-absorption profiles of the spectra at 553 and 596 nm, monitoring the **energy transfer (32 ps)** as well as at 1024 nm, monitoring the **charge separation (30 ps).**

Top – differential absorption spectra (visible and near-infrared) obtained upon femtosecond flash photolysis (490 nm, 200 nJ) of **BDP-ZnP-C_{60}** in argon saturated toluene with several time delays between 0 and 8000 ps at room temperature, insert- zoom in to virtualize the relevant decays. Bottom – time-absorption profiles of the spectra at 553 and 594 nm, monitoring the **energy transfer (32 ps)** as well as at 1024 nm, monitoring the **charge separation (26 ps)**.

Chem. Eur. J. **2014**, 20, 2049 – 2057

Artificial photosynthesis

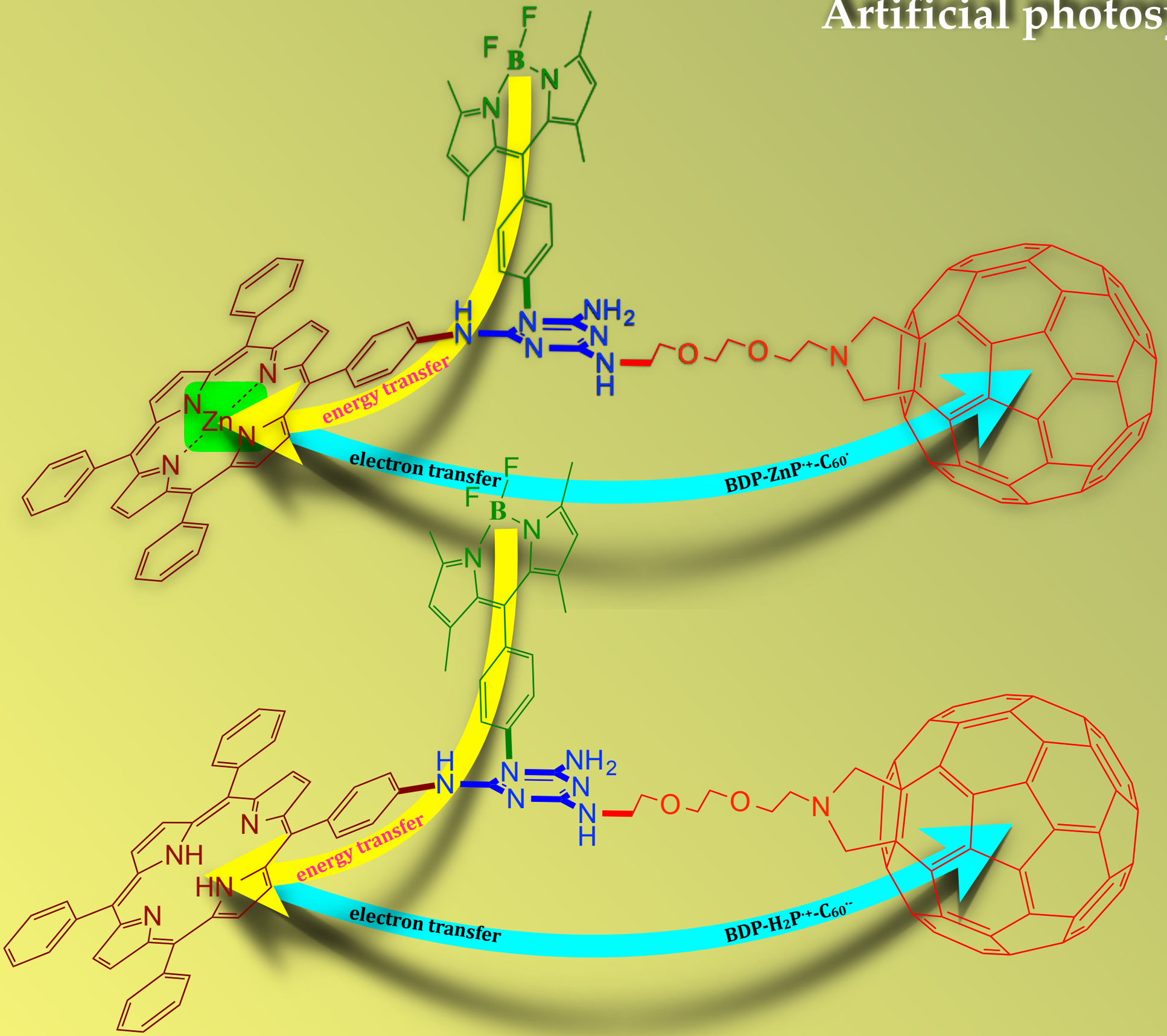

Chem. Eur. J. **2014**, 20, 2049 – 2057

non covalently linked

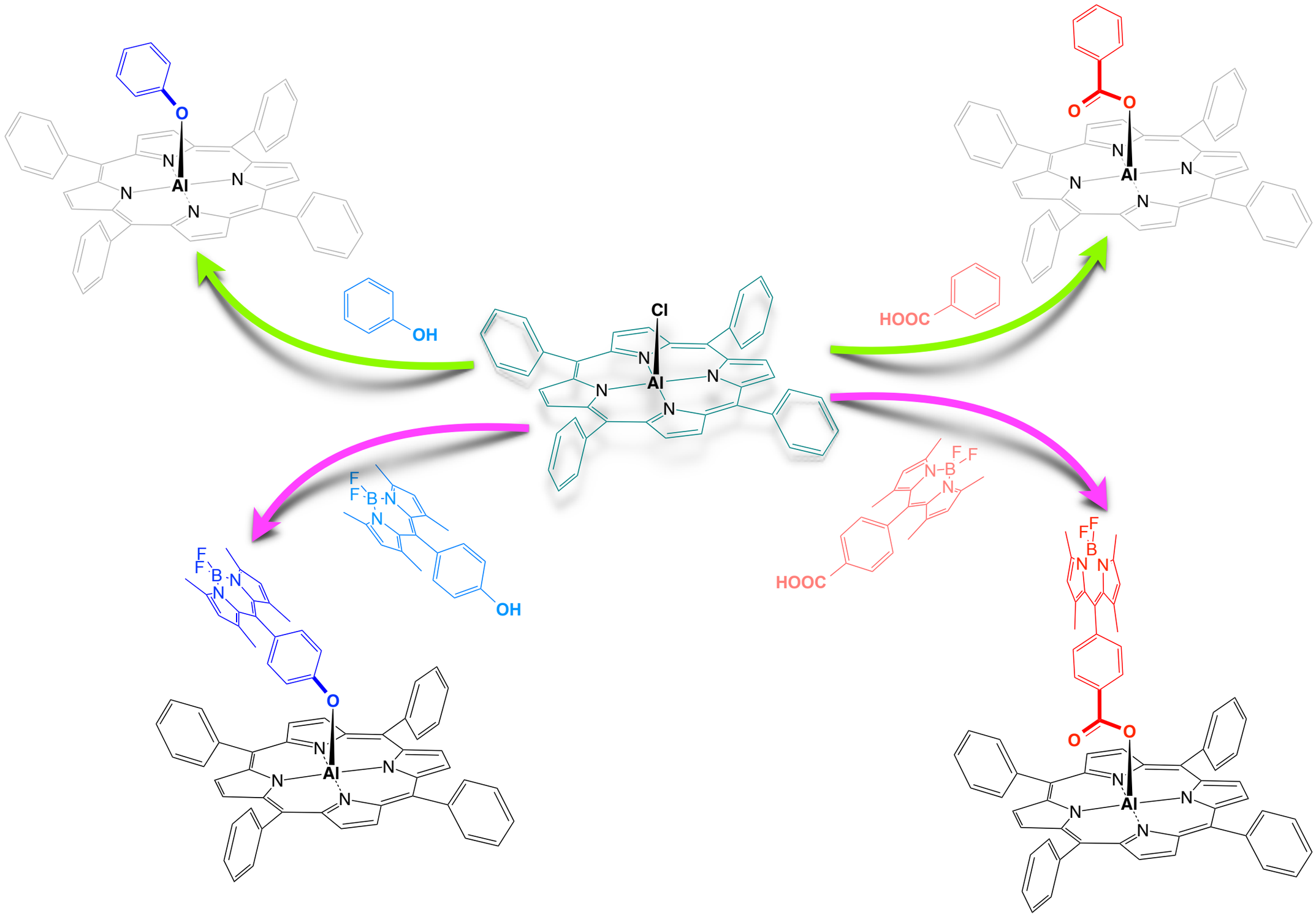

Inorg. Chem. 2017, 56, 10268−10280

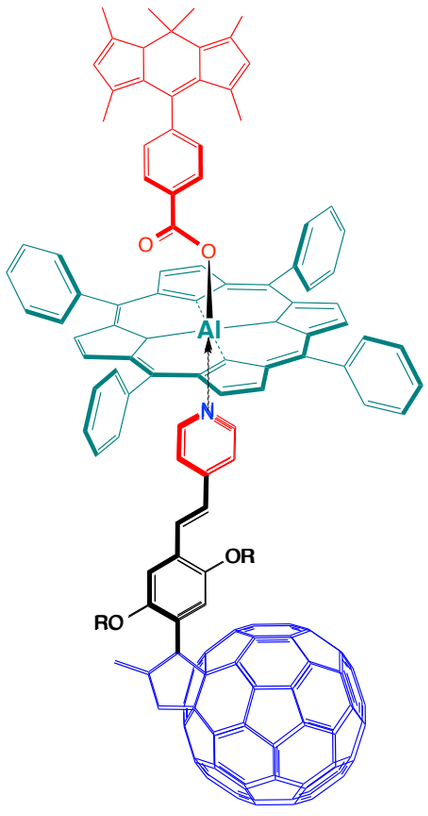

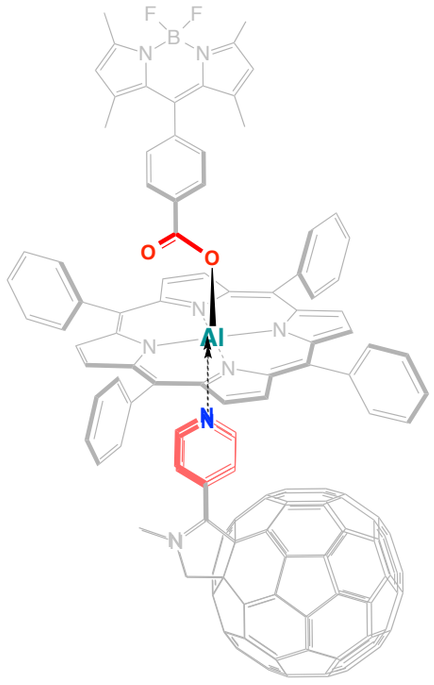

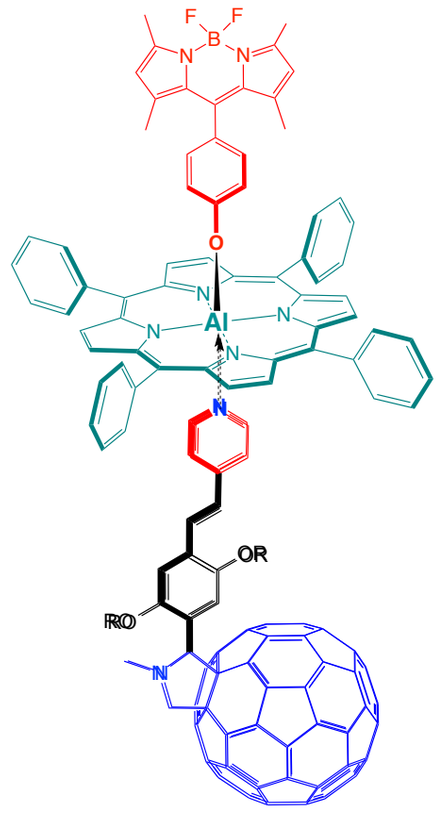

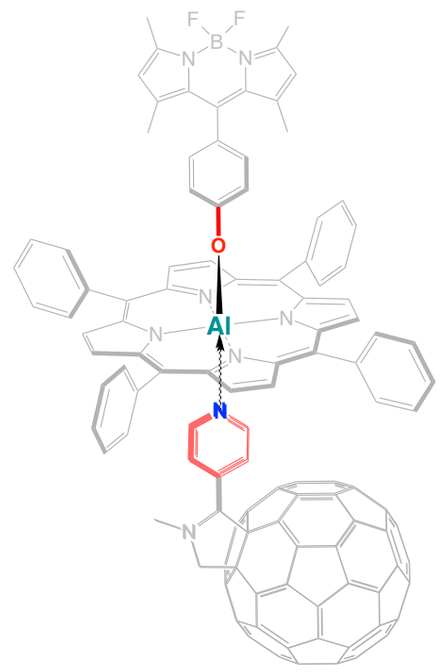

Inorg. Chem. 2017, 56, 10268−10280

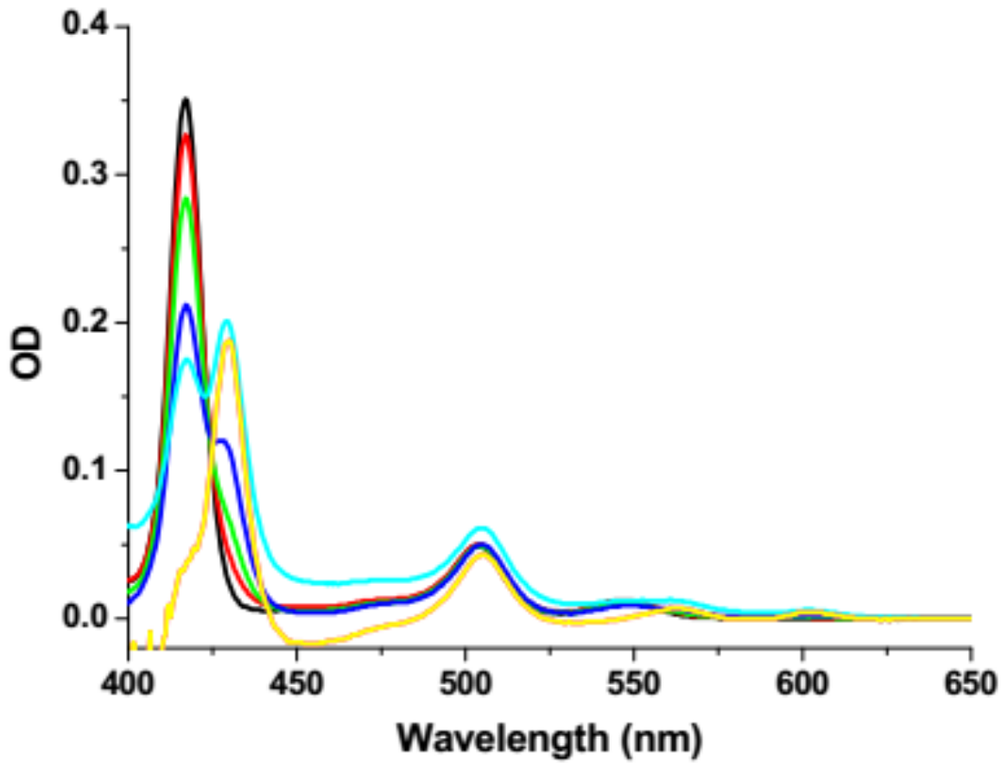

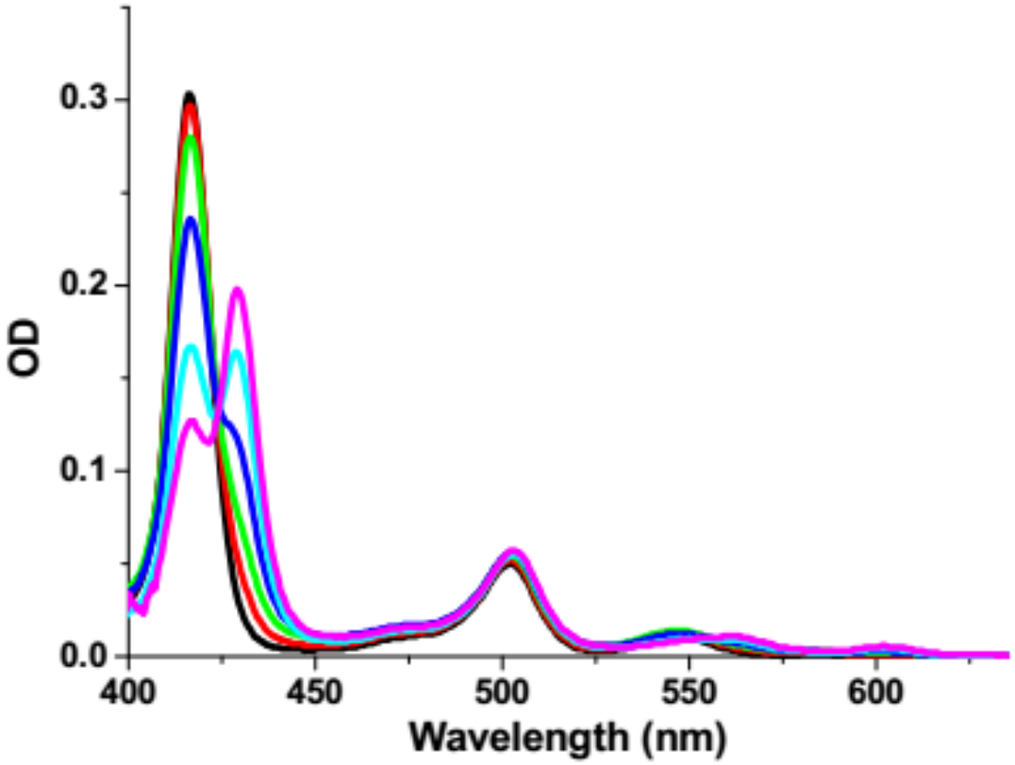

BDP-COO-AlTPP (1.0*10^-6 M) with C60-PPV-pyr (0 – 2.7*10^-4M) (left)
BDP-O-AlTPP (1.0*10^-6M) with C60-PPV-pyr (0 - 1.6*10^-4M) (right)

Inorg. Chem. 2017, 56, 10268−10280

Femtosencond Transient Absorption Spectra

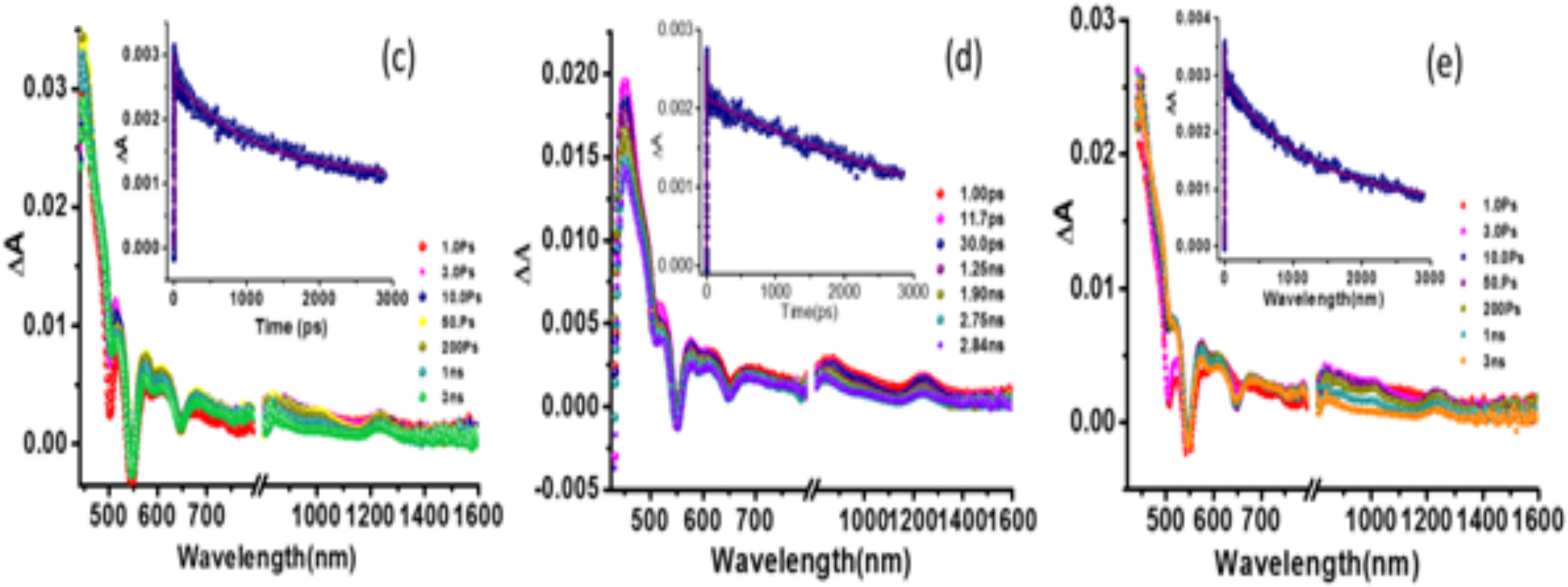

(c) BDP-O-AlTPP: C_{60}-pyr after selected irradiation of AlTPP
(d) BDP-O-AlTPP: C_{60}-PPV-pyr after selected irradiation of AlTPP
(e) BDP-COO-AlTPP: C_{60}-pyr after selected irradiation of AlTPP

Inorg. Chem. 2017, 56, 10268−10280

ENERGY TRANSFER

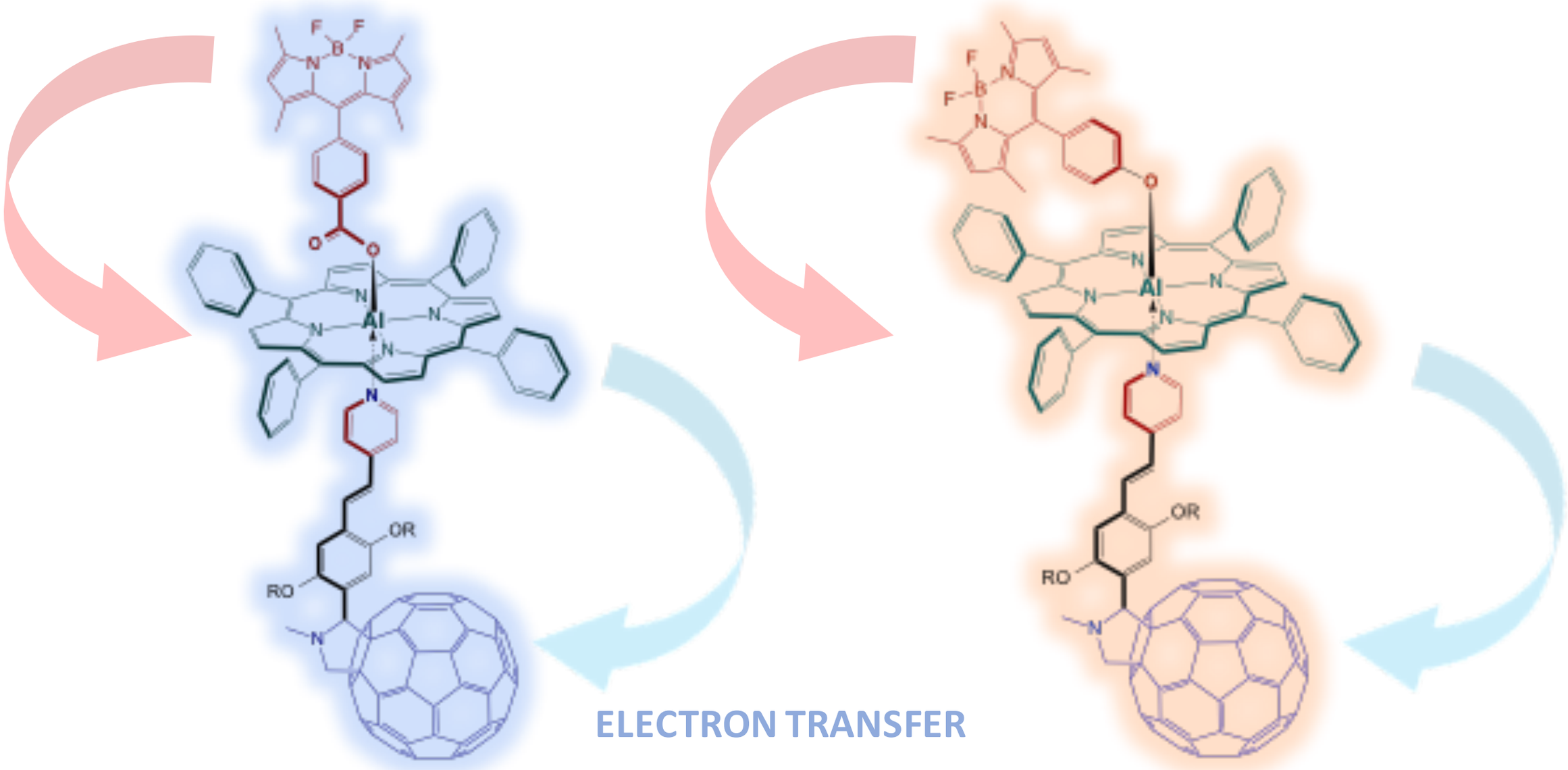

ELECTRON TRANSFER

Inorg. Chem. 2017, 56, 10268−10280

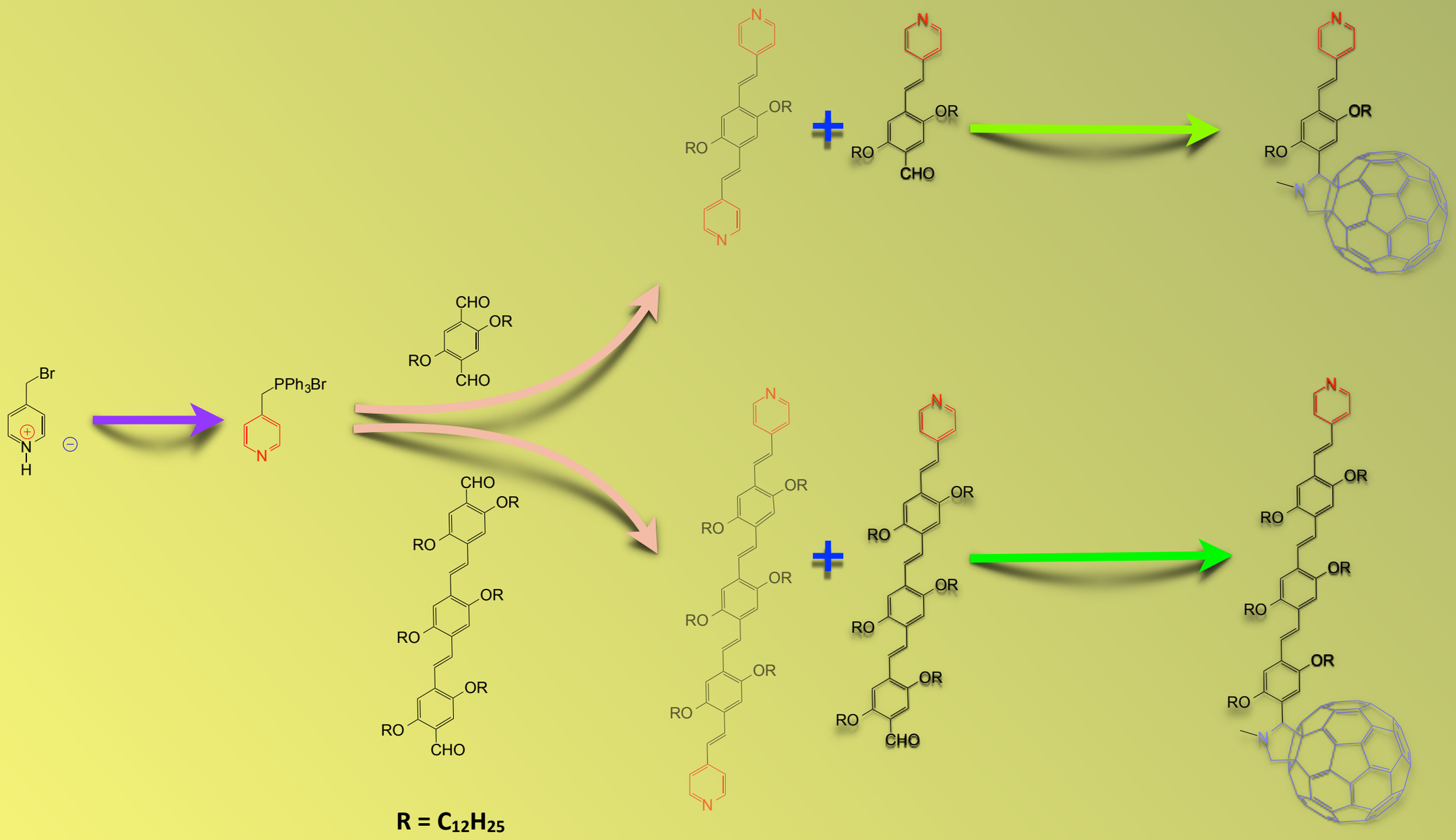

Nanoscale, 2015, 7, 2597-2608

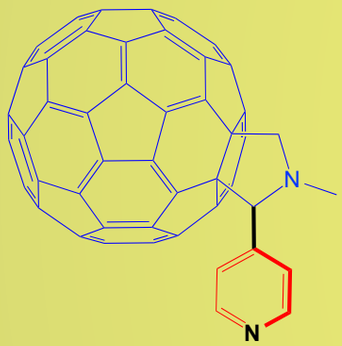
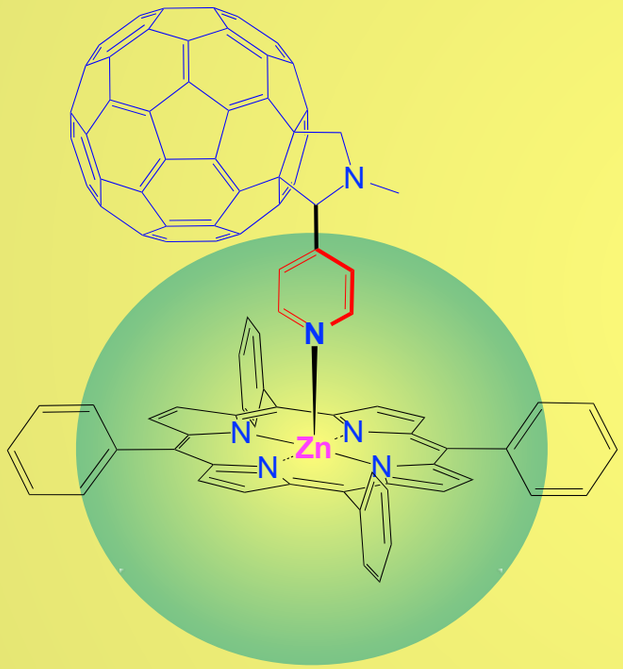
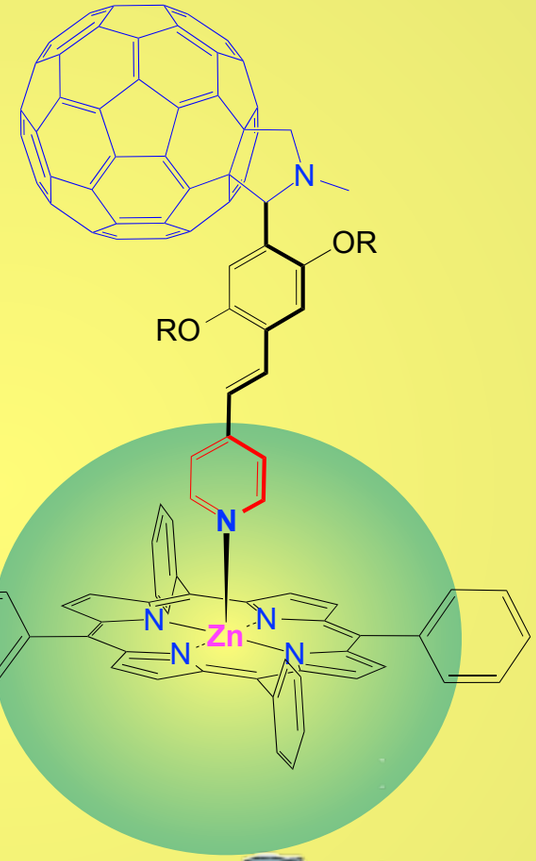
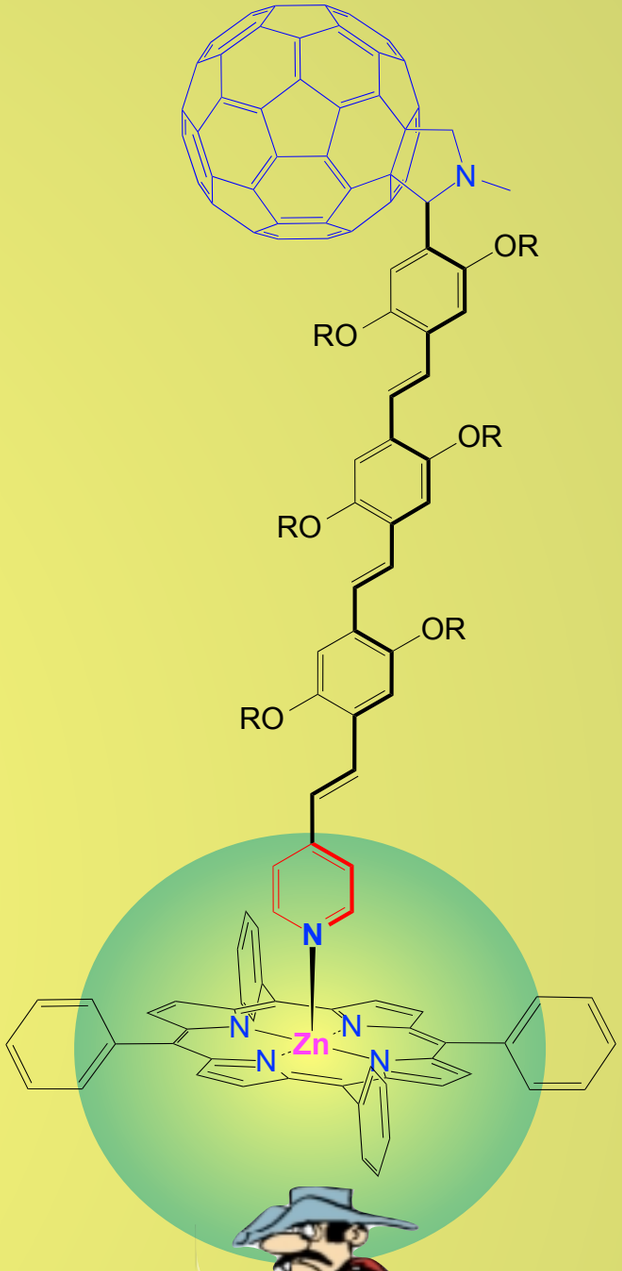



Nanoscale, 2015, 7, 2597-2608

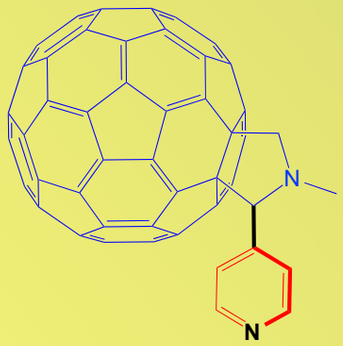

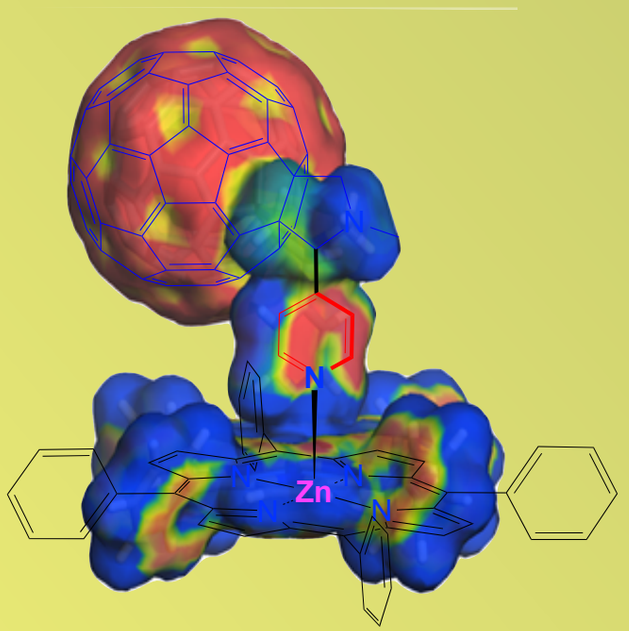

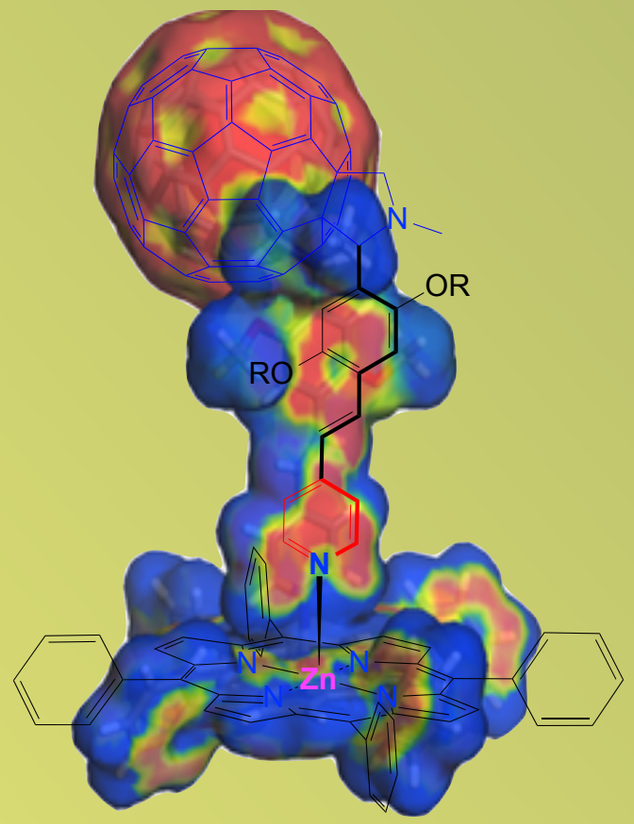

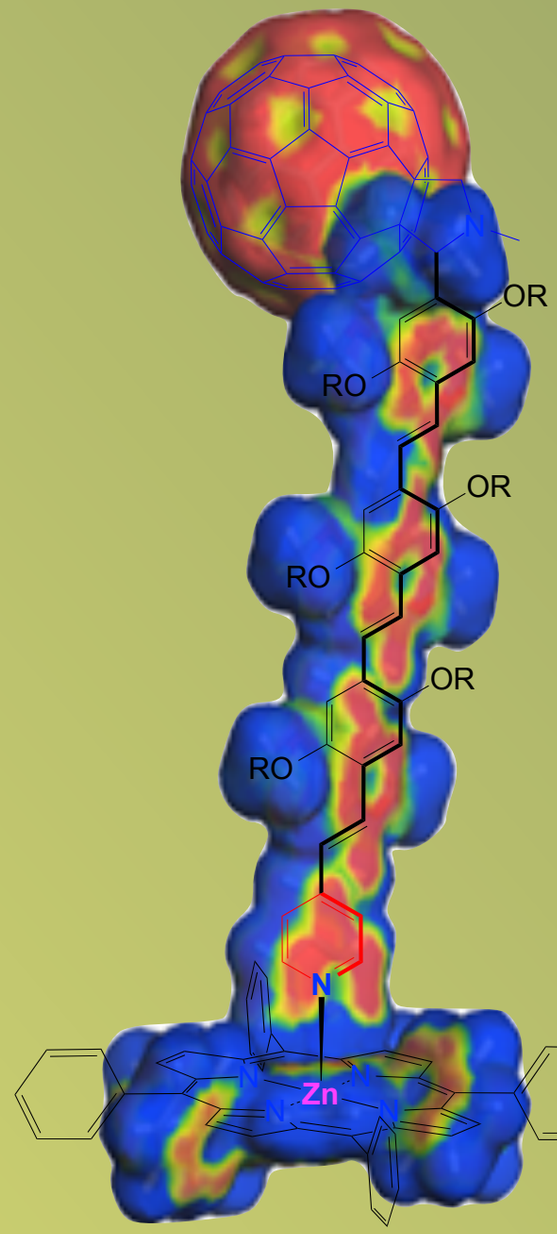

Nanoscale, 2015, 7, 2597-2608

Absorption and Emission Titrations

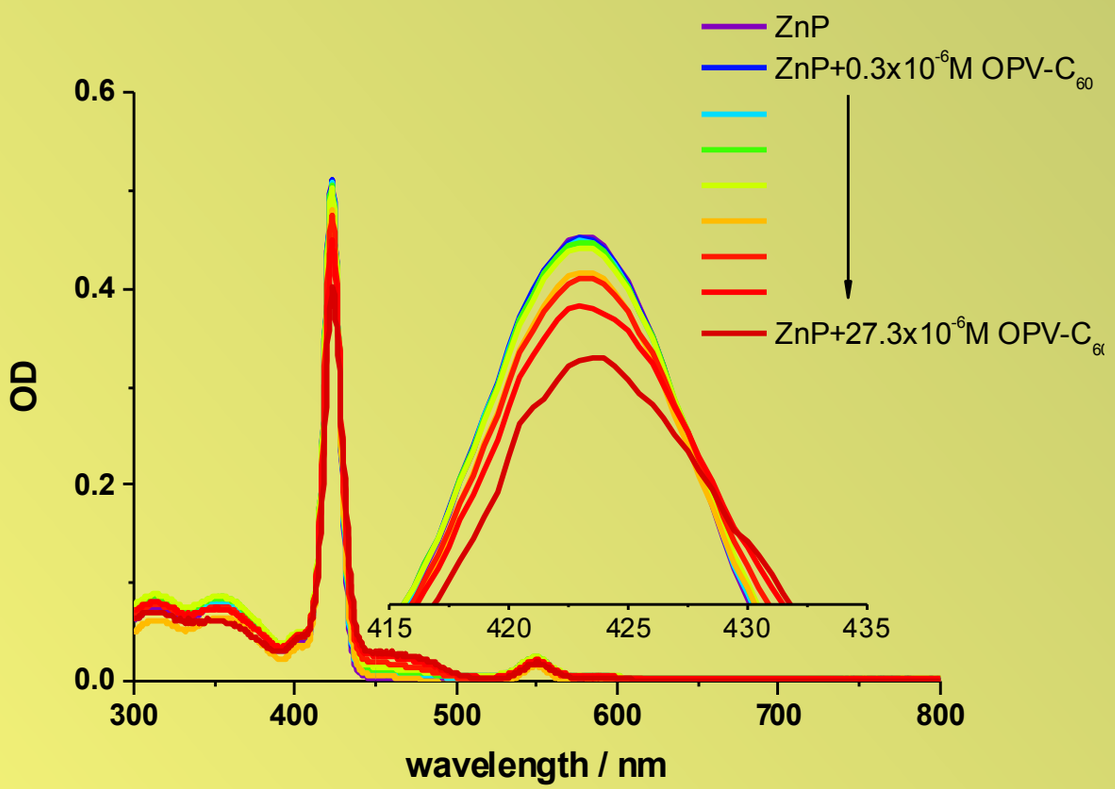

Absorption spectra in chlorobenzene of ZnTPP (1.0×10^{-6} M) with variable concentrations of C_{60}-PPV3-pyr (0 – 2.7×10^{-5} M).

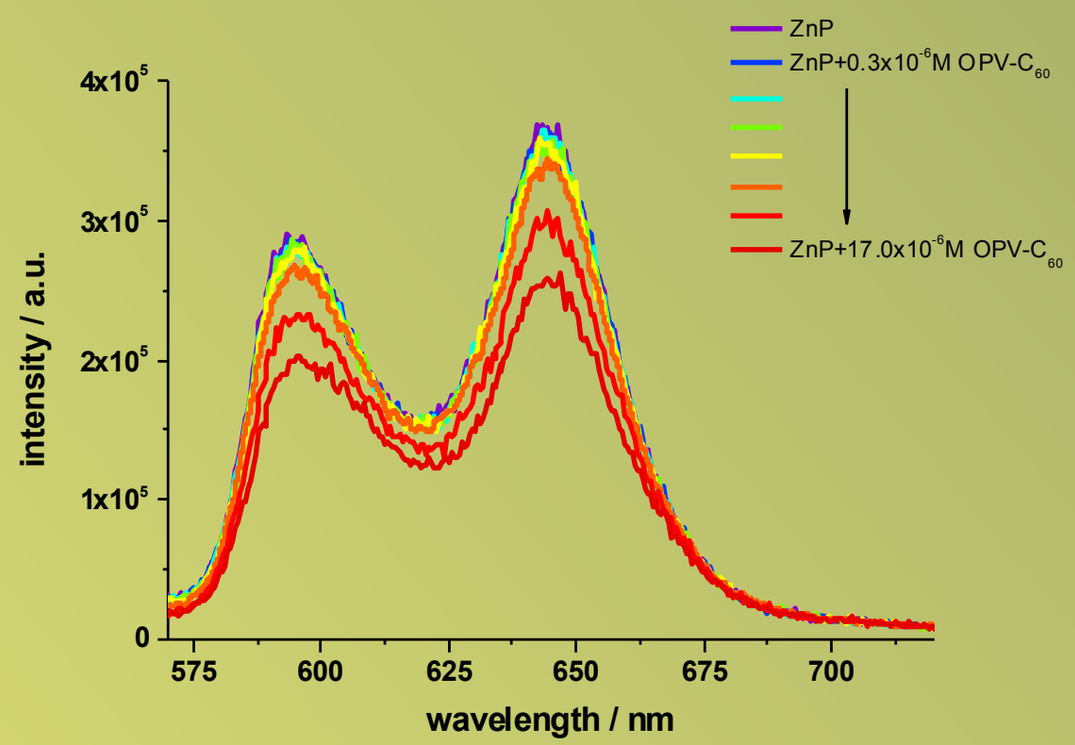

Fluorescence spectra of each titration excited at 556 nm.

$K_{ass} = 2.5 \times 10^{4}\ M^{-1}$

Nanoscale, **2015**, 7, 2597-2608

Femtosecond Transient Absorption Spectroscopy

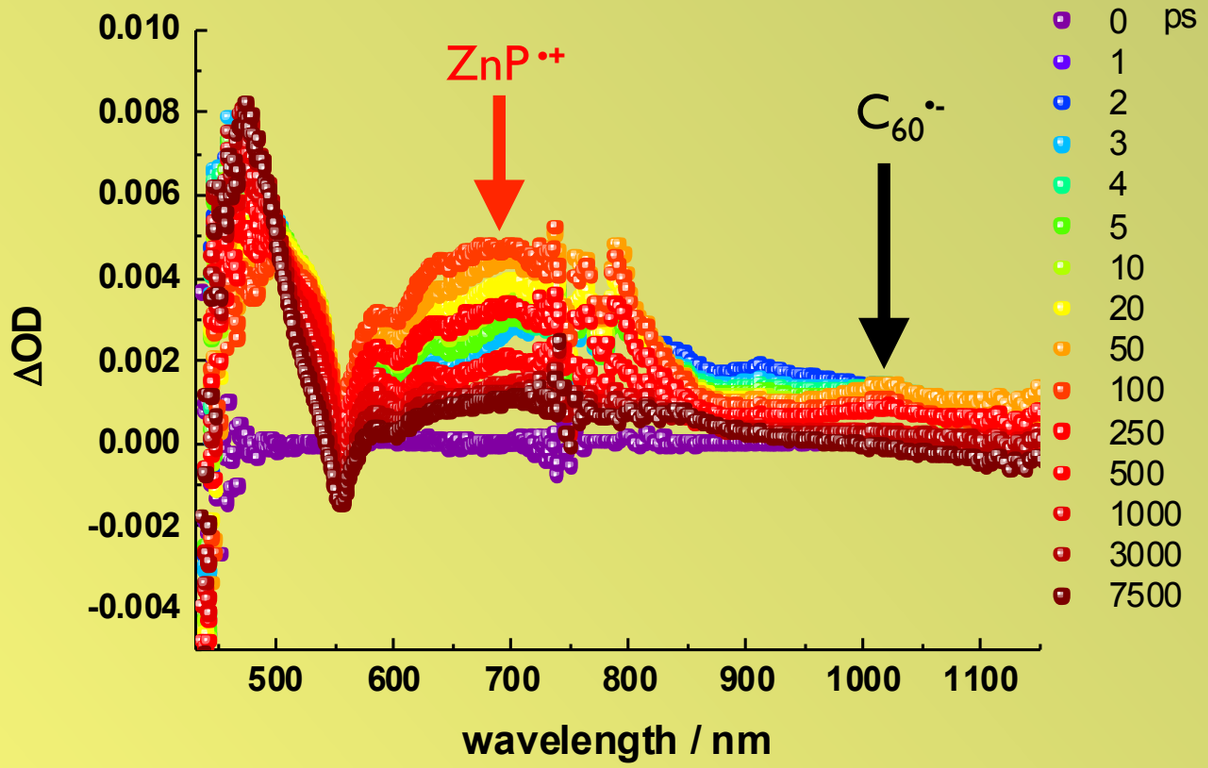

Differential absorption spectra (visible and near-infrared) obtained upon pump probe excitation (550 nm, 200 nJ) of C_{60}-PPV3-pyr•ZnP (in a 1 to 10 ratio) in chlorobenzene with several time delays between 1 and 7500 ps at room temperature

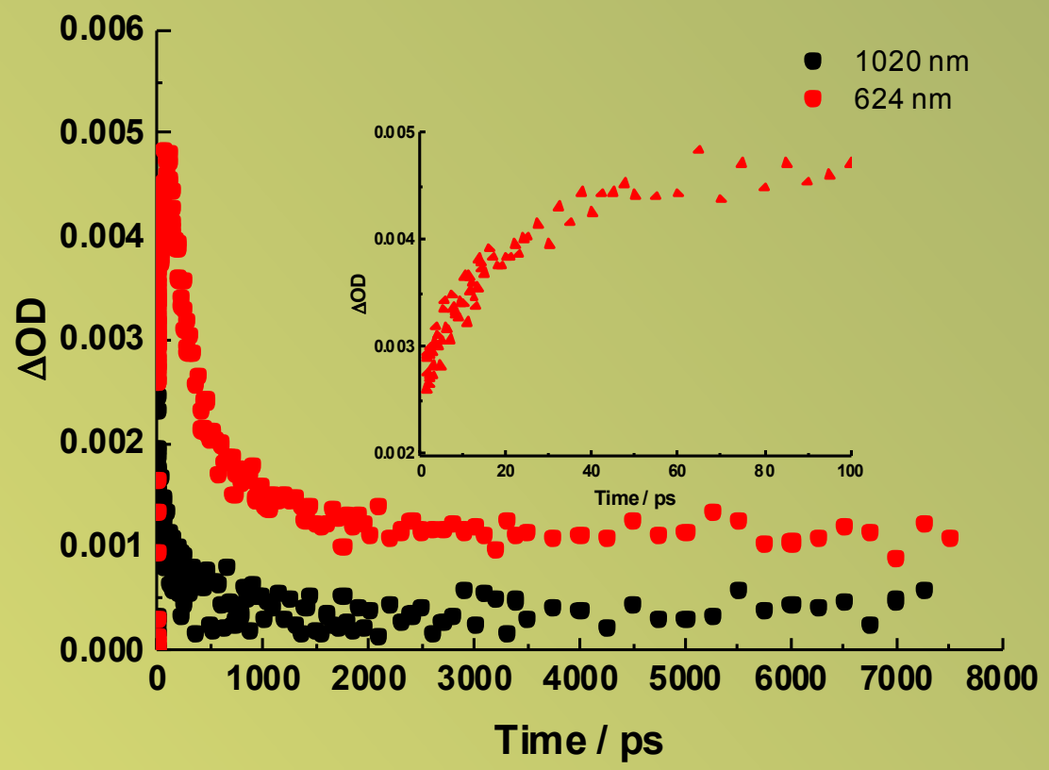

Absorption-time profiles of the spectra in chlorobenzene at 624 and 1020 nm monitoring the charge separation and charge recombination

Nanoscale, 2015, 7, 2597-2608

Compound	distances/Å	CS (ps)		CR (ps)	
		Anisole	Chlorobenzene	Anisole	Chlorobenzene
C_{60}-pyr·ZnP	10.6	25	37	1189	991
C_{60}-PPV_1pyr·ZnP	16.8	2	1	1585	**1076**
C_{60}-PPV_3-pyr·ZnP	30.0	23	15	320	**250**

The fact that **charge recombination** in C_{60}-PPV3-pyr·ZnP is **faster** than in C_{60}-pyr·ZnP and C_{60}-PPV1pyr·ZnP despite the larger electron donor–acceptor distance is **surprising**!

One possible **explanation**, **different total reorganizations energies (λ)** of **the hybrids** due to **larger** e^- donor – acceptor separations.

Nanoscale, **2015**, 7, 2597-2608

N. Martin and co-workers , Chem. Eur. J., **2005**, 11, 1267

Marcus Theory and Reorganization Energy

$$k_{ET} = \left(\frac{4\pi^3}{h^2 \lambda k_b T}\right)^{1/2} V^2 exp\left[-\frac{(\Delta G^0_{ET}+\lambda)^2}{4\lambda k_b T}\right]$$

ΔG^0_{ET}	standard free energy change
λ	reorganization energy
V	electronic coupling matrix element
k_b	BOLTZMANN constant
h	PLANCK constant
T	absolute temperature

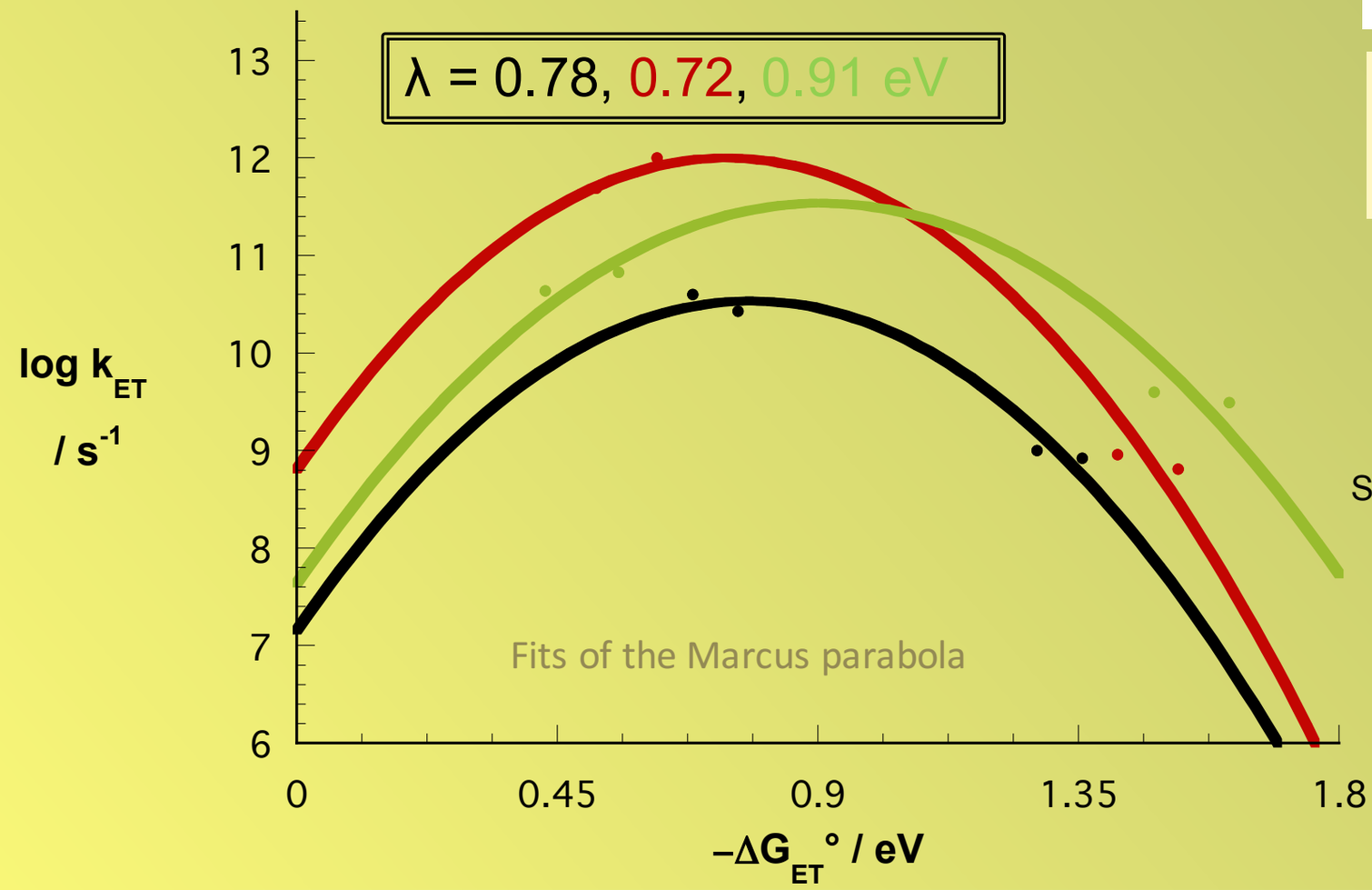

C_{60}-PPV3-pyr•ZnP
C_{60}-PPV1-pyr•ZnP
C_{60}-pyr•ZnP

Strong distance dependence of the total reorganization energy

Driving force ($-\Delta G^0_{ET}$) dependences of the rate constants for CS and CR for C_{60}-PPV3-pyr•ZnP ,C_{60}-PPV1-pyr•ZnP and C_{60}-pyr•ZnP

Nanoscale, **2015**, 7, 2597-2608

N. Martin and co-workers , Chem. Eur. J., **2005**, 11, 1267

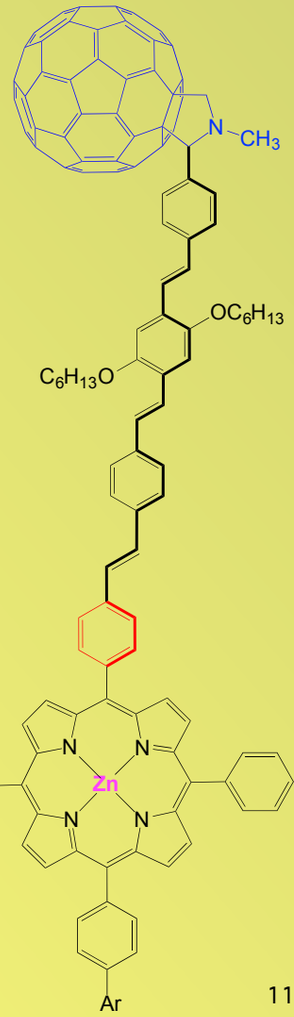

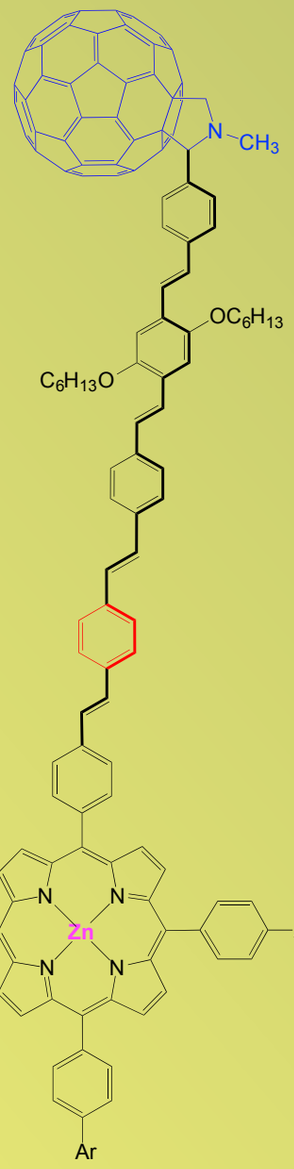

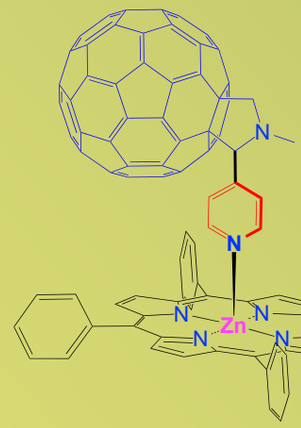

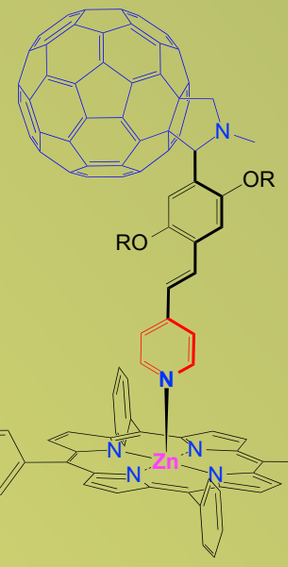

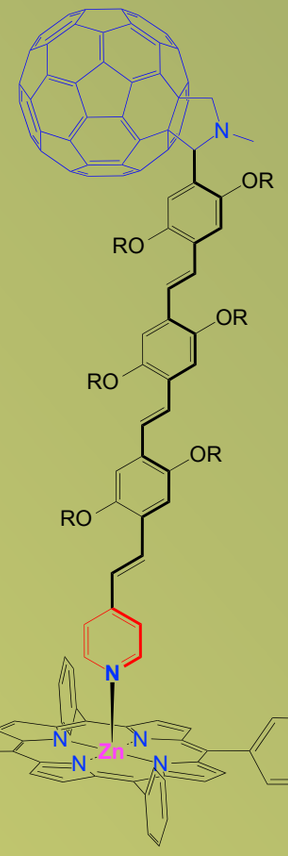

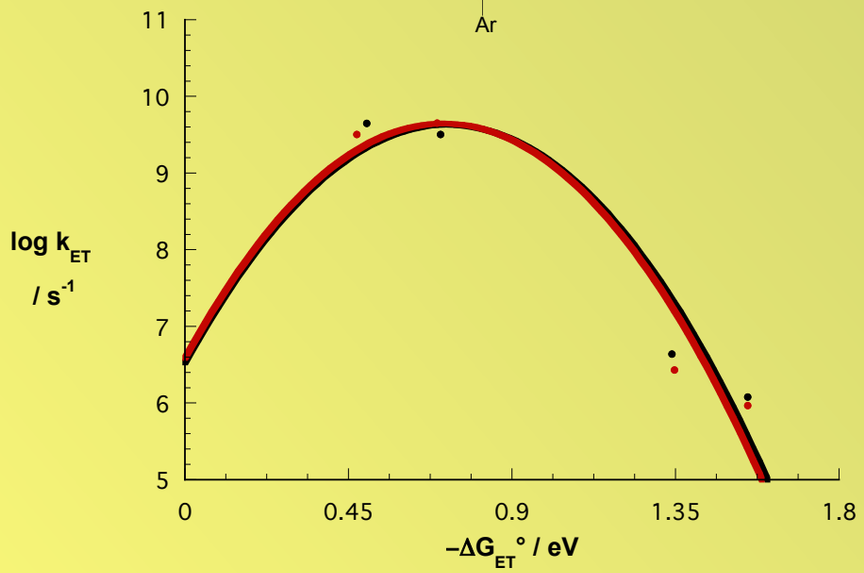

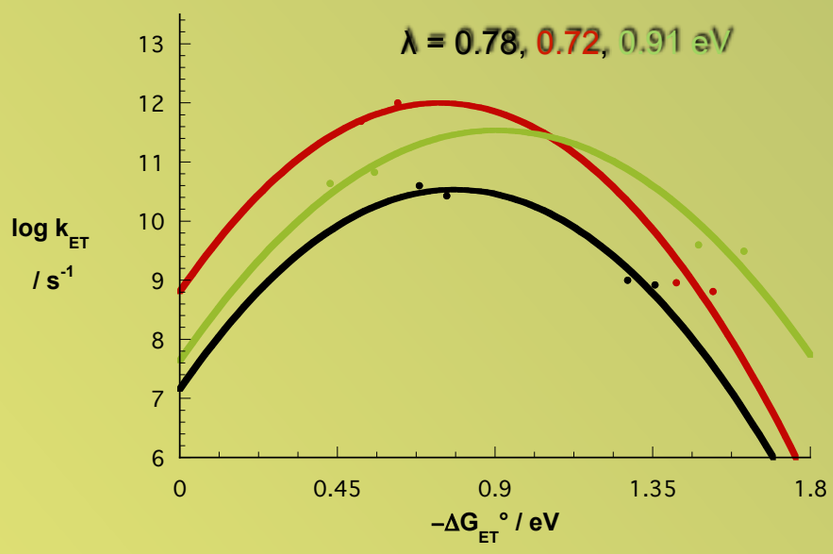

Nanoscale, **2015**, 7, 2597-2608

N. Martin and co-workers, Chem. Eur. J., **2005**, 11, 1267

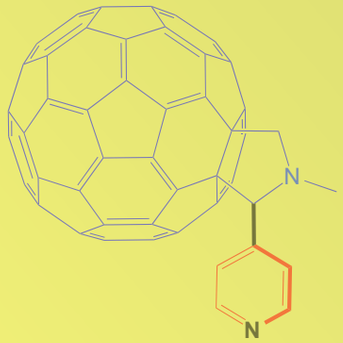

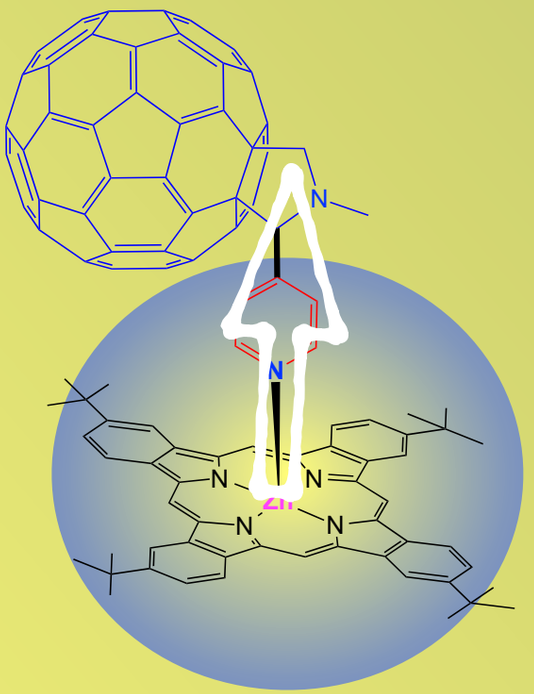

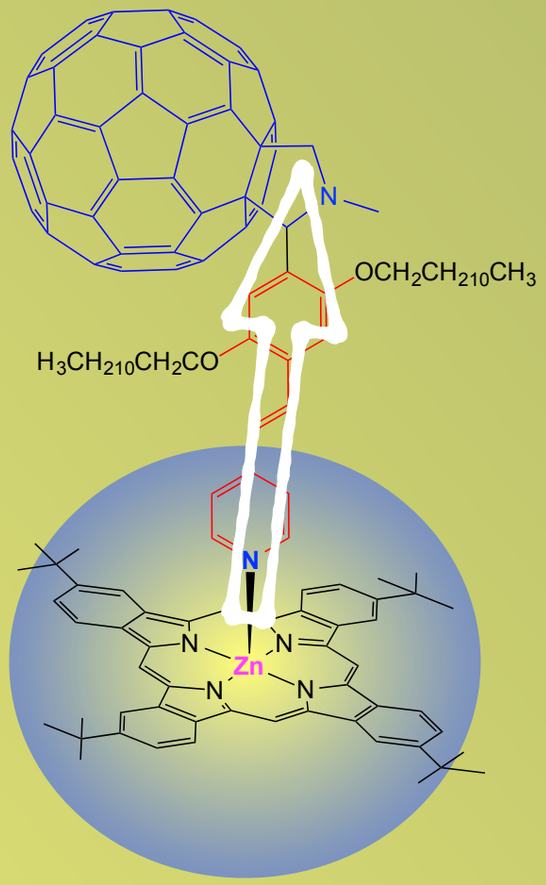

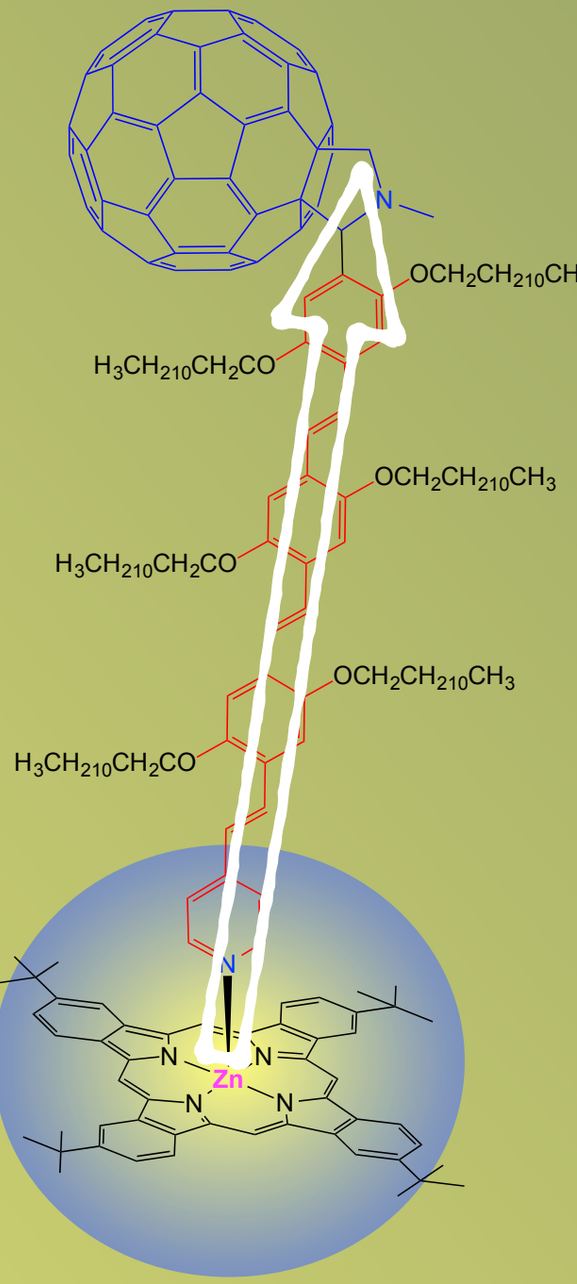

unpublished work

UV/Emission titrations

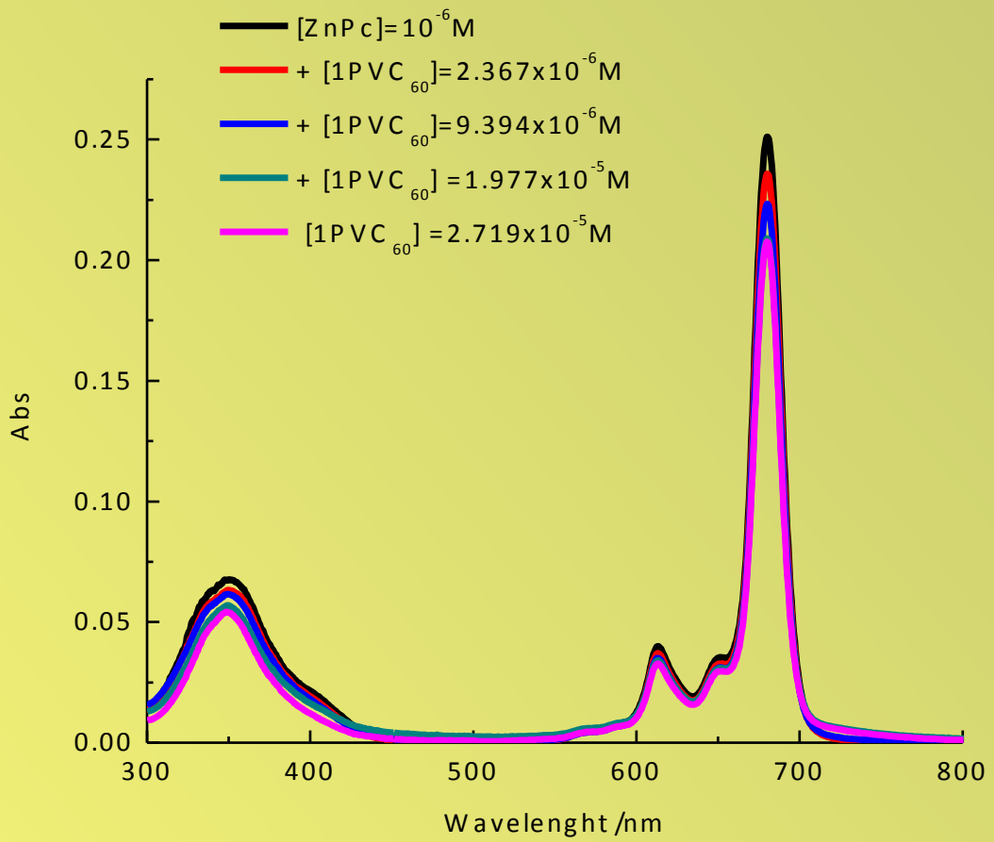

Absorption spectra in chlorobenzene of ZnPc (1.0×10^{-6} M) with variable concentrations of C_{60}-PPV1-pyr (0 – 2.7×10^{-5} M)

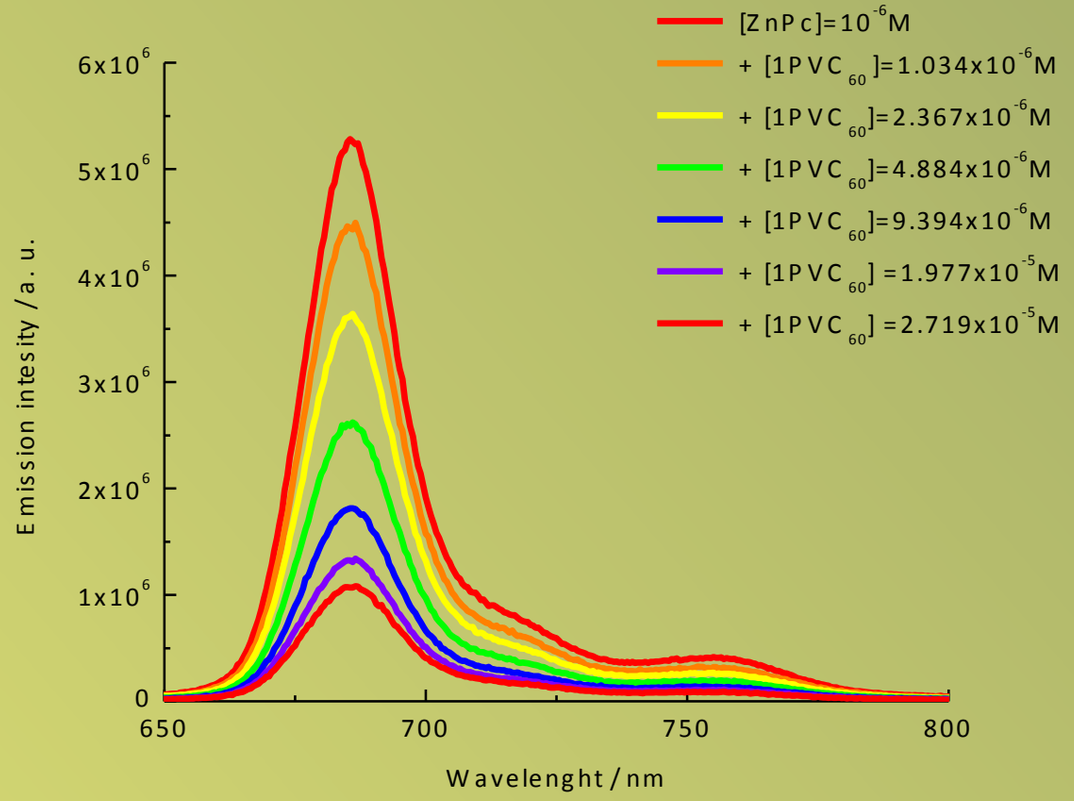

Fluorescence spectra of each titration excited at 615nm.

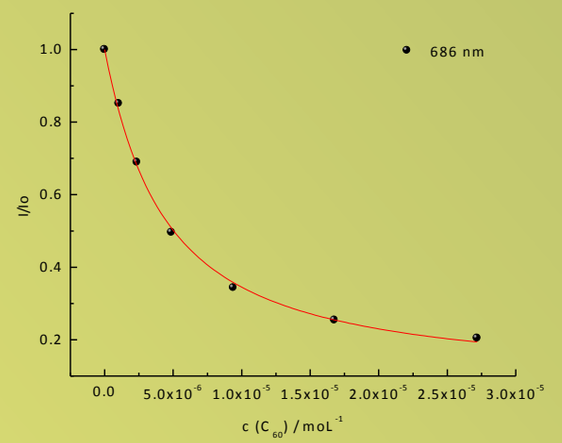

Kass =0.2 x 10^6 M^{-1}

unpublished work

Femtosecond Transient Absorption Spectroscopy

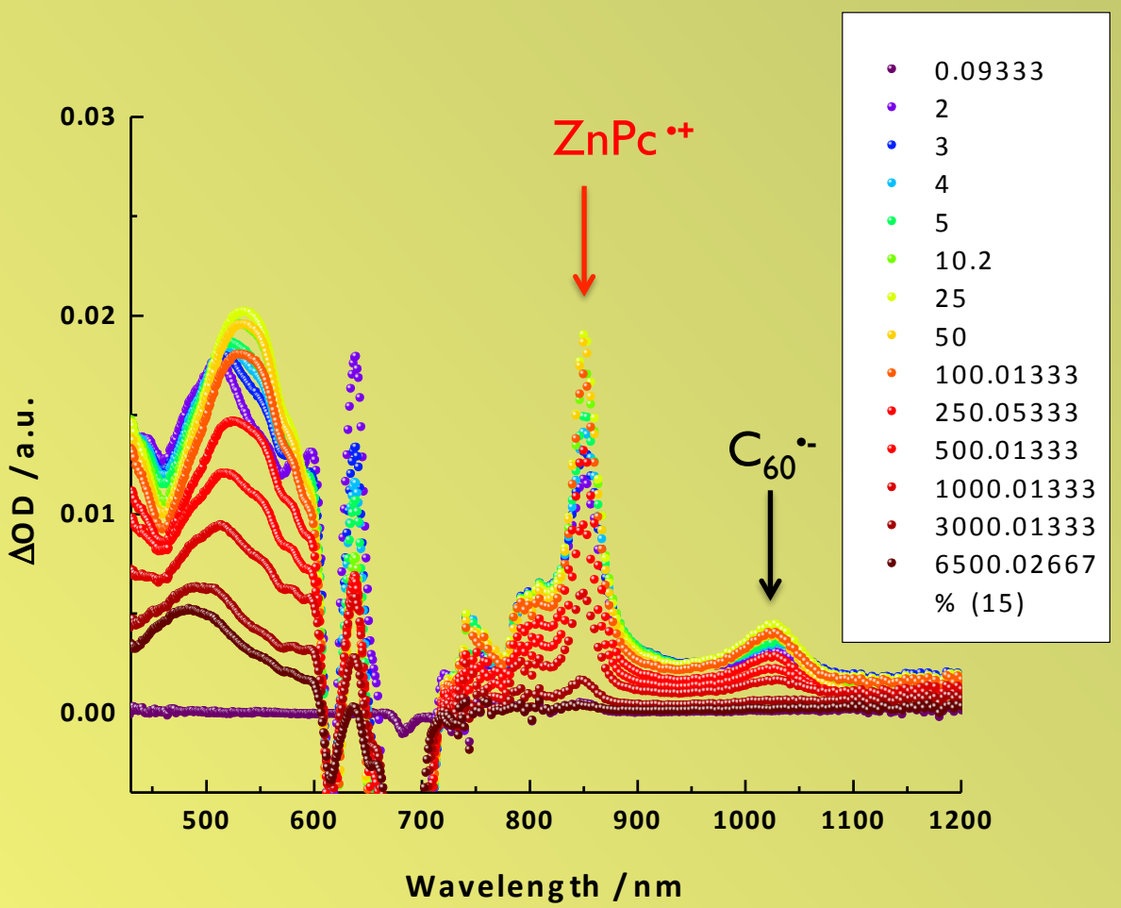

Differential absorption spectra (visible and near-infrared) obtained upon pump probe excitation (676 nm, 200 nJ) of C_{60}-PPV1-pyr•ZnPc (in a 1 to 10 ratio) in chlorobenzene with several time delays between 1 and 6500 ps at room temperature.

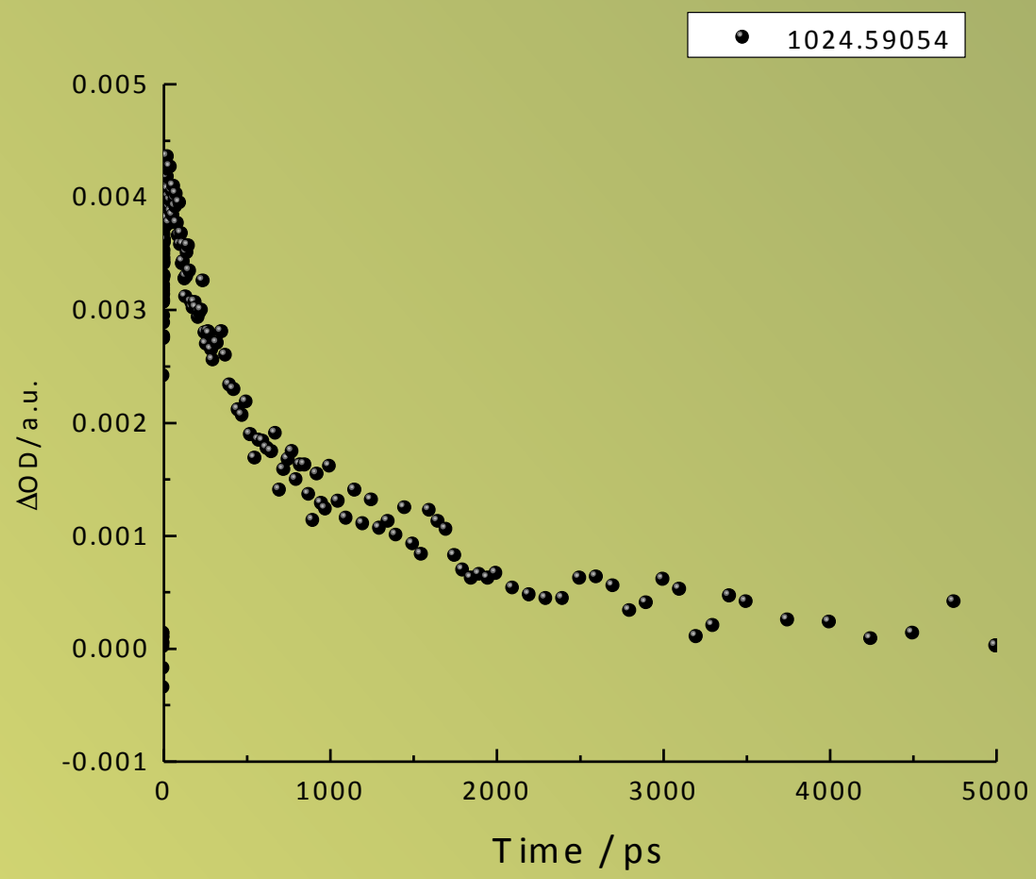

Absorption-time profiles of the spectra in chlorobenzene at 1024 nm monitoring the charge separation and charge recombination

unpublished work

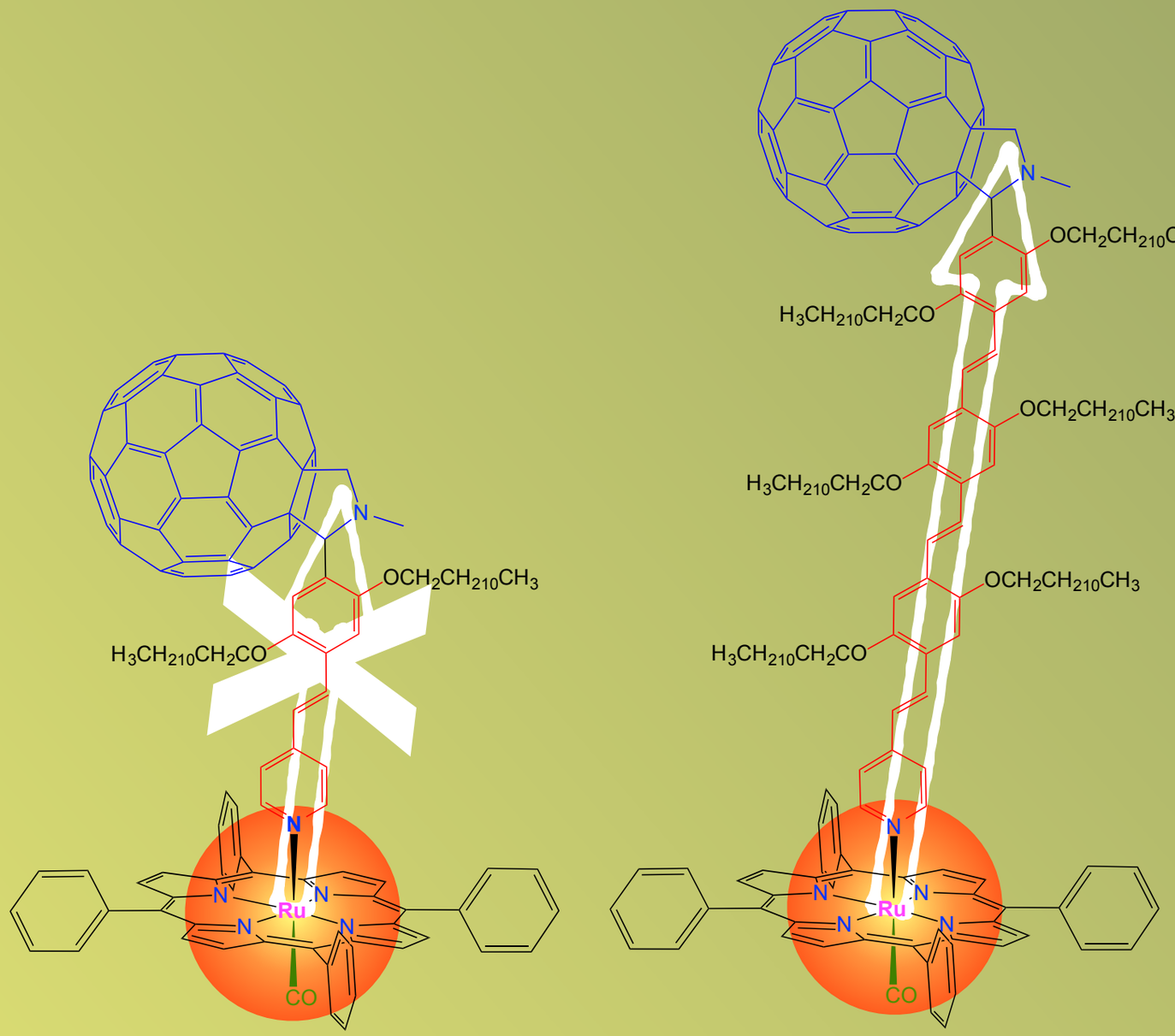

unpublished work

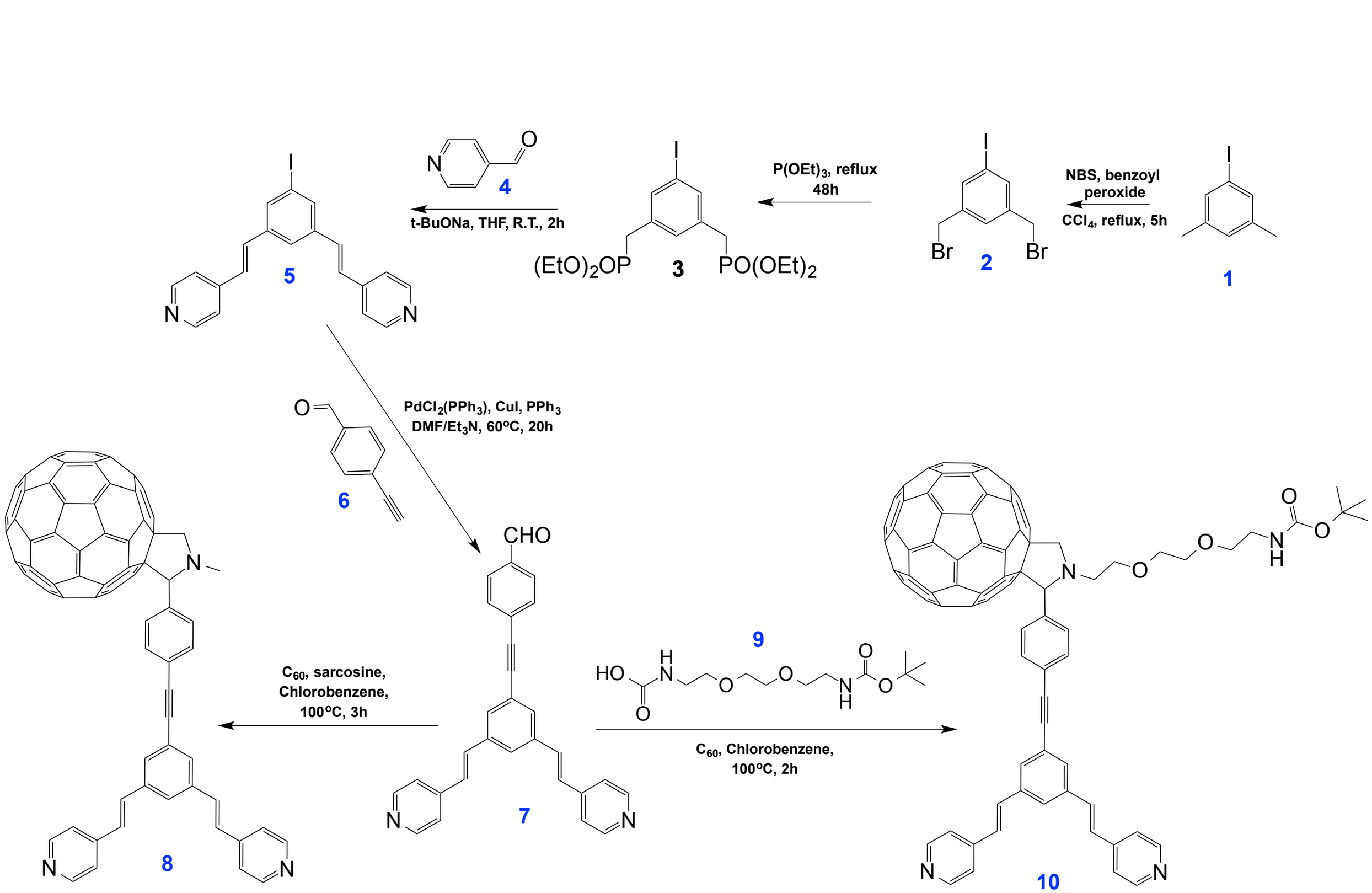

J. Phys. Chem. C 2017, 121, 4850−4858

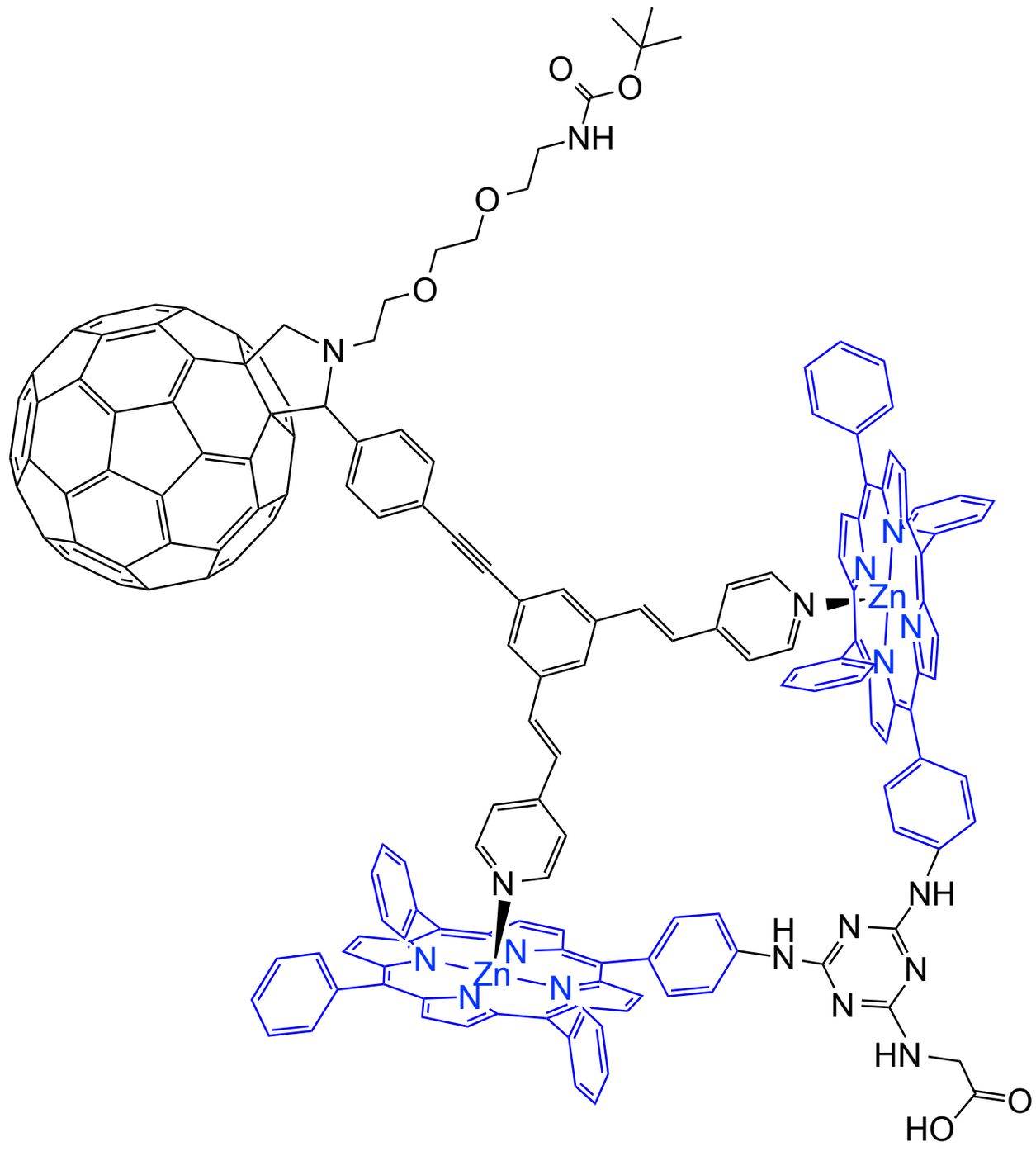

J. Phys. Chem. C 2017, 121, 4850−4858

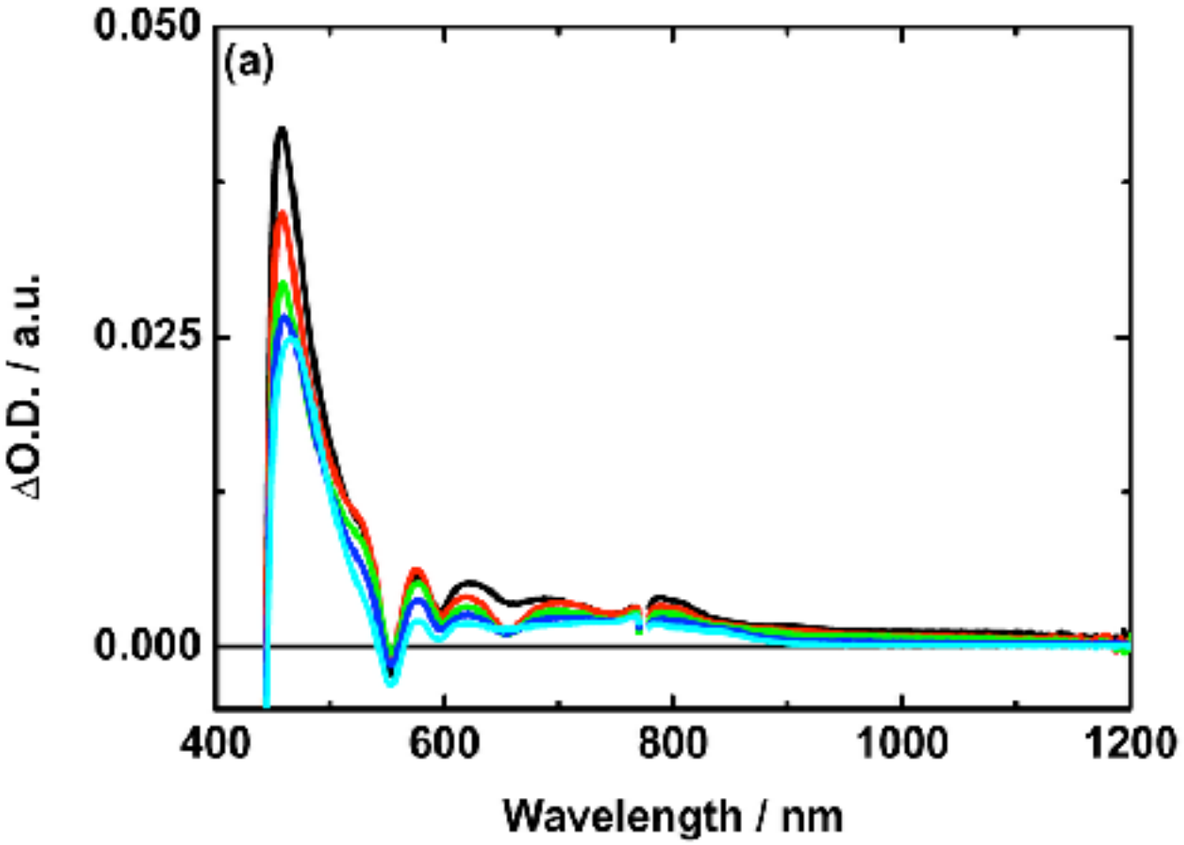

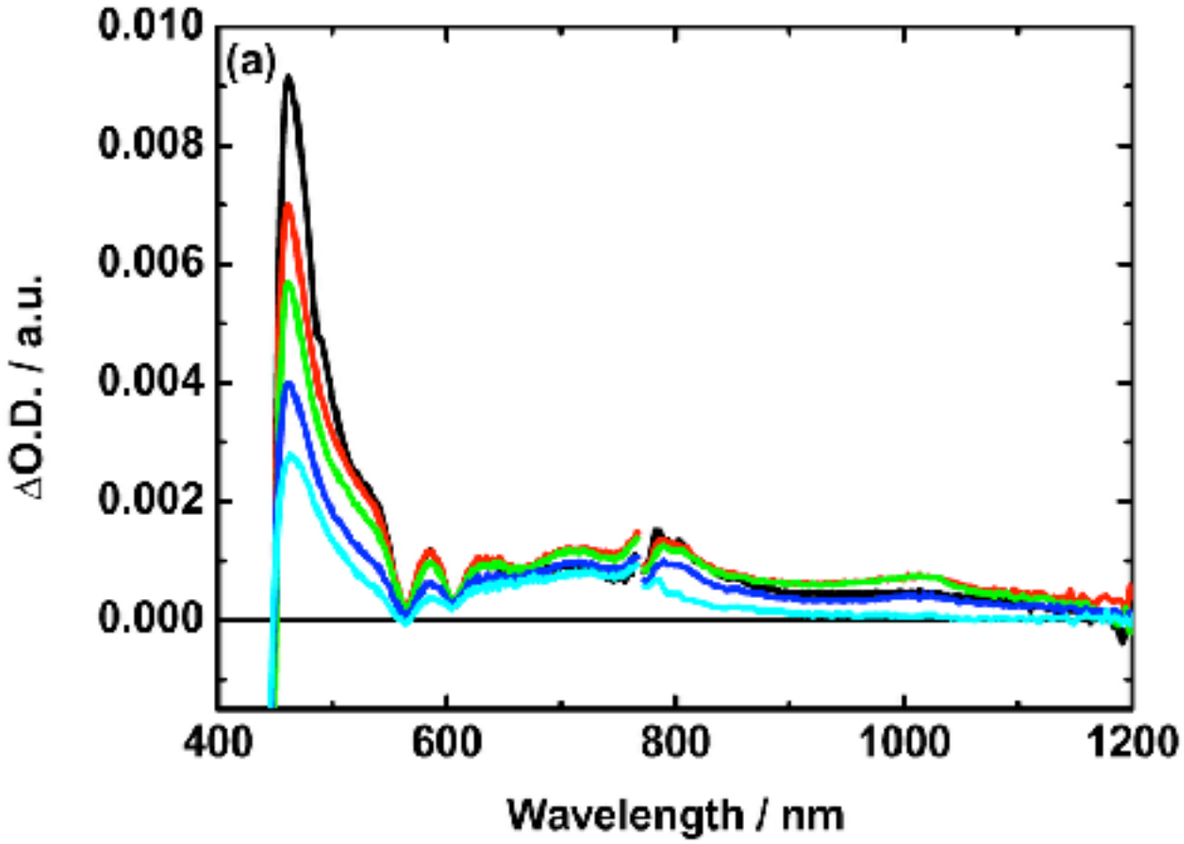

J. Phys. Chem. C 2017, 121, 4850−4858

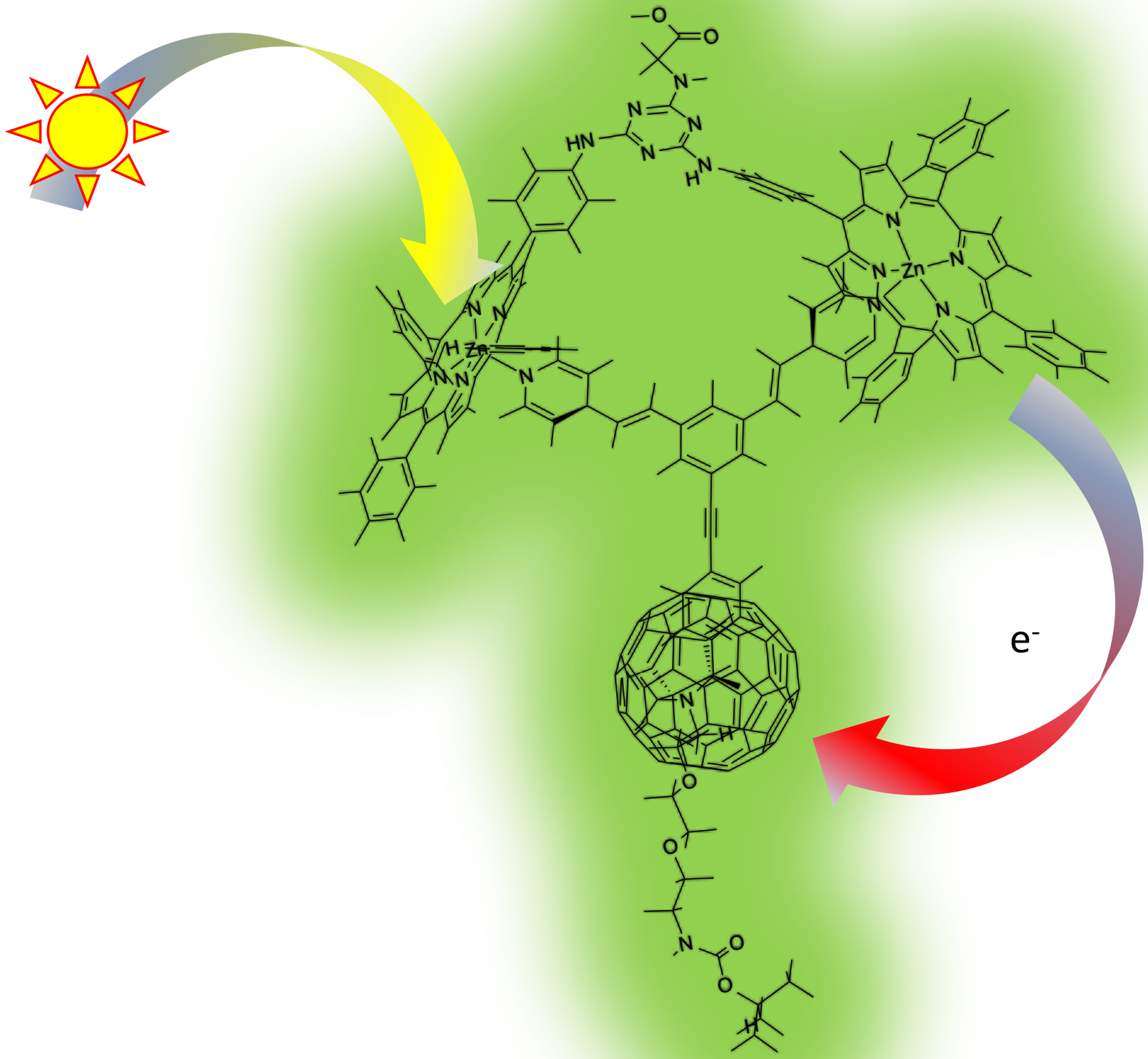
e-

future plans

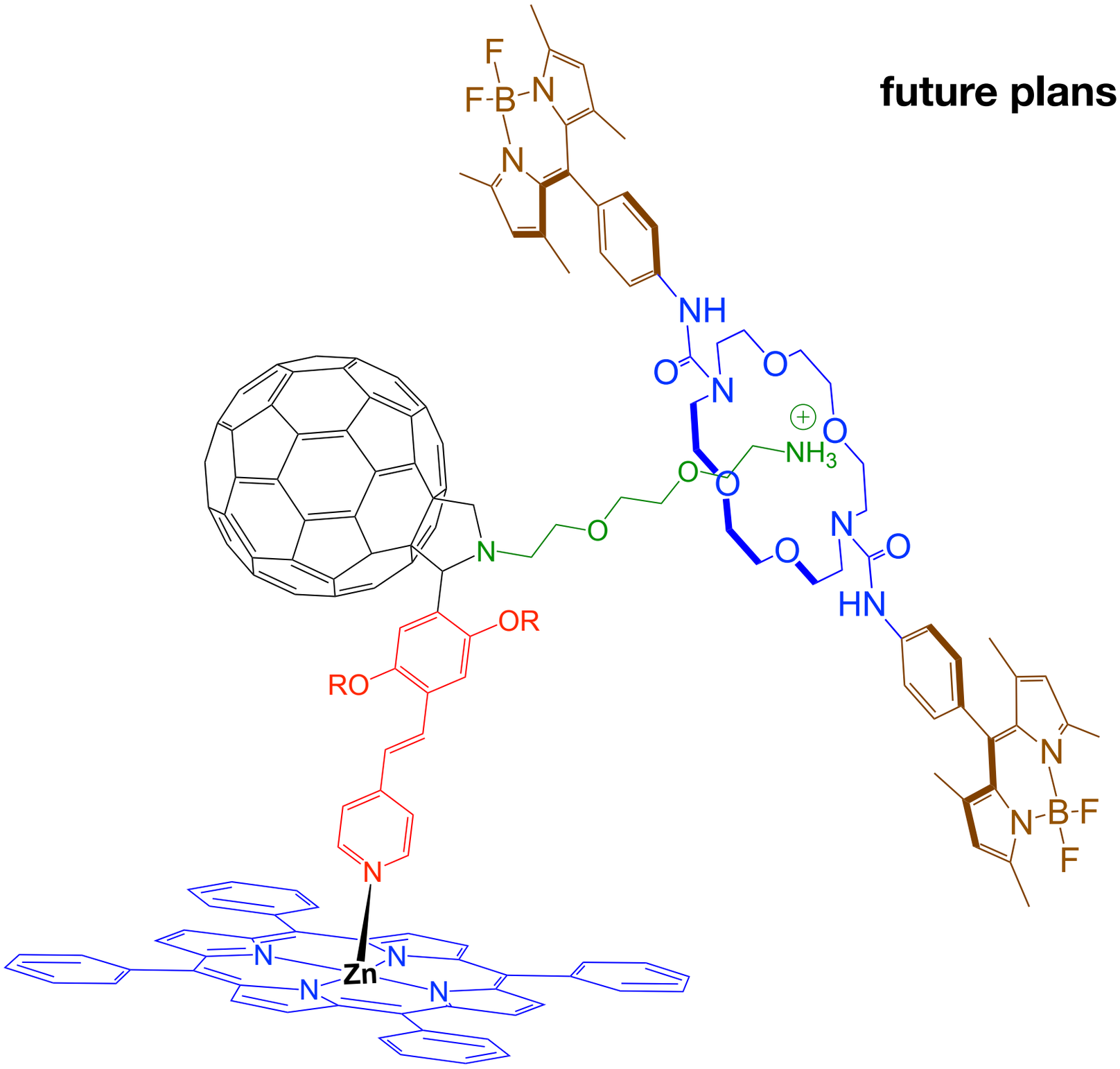

future plans

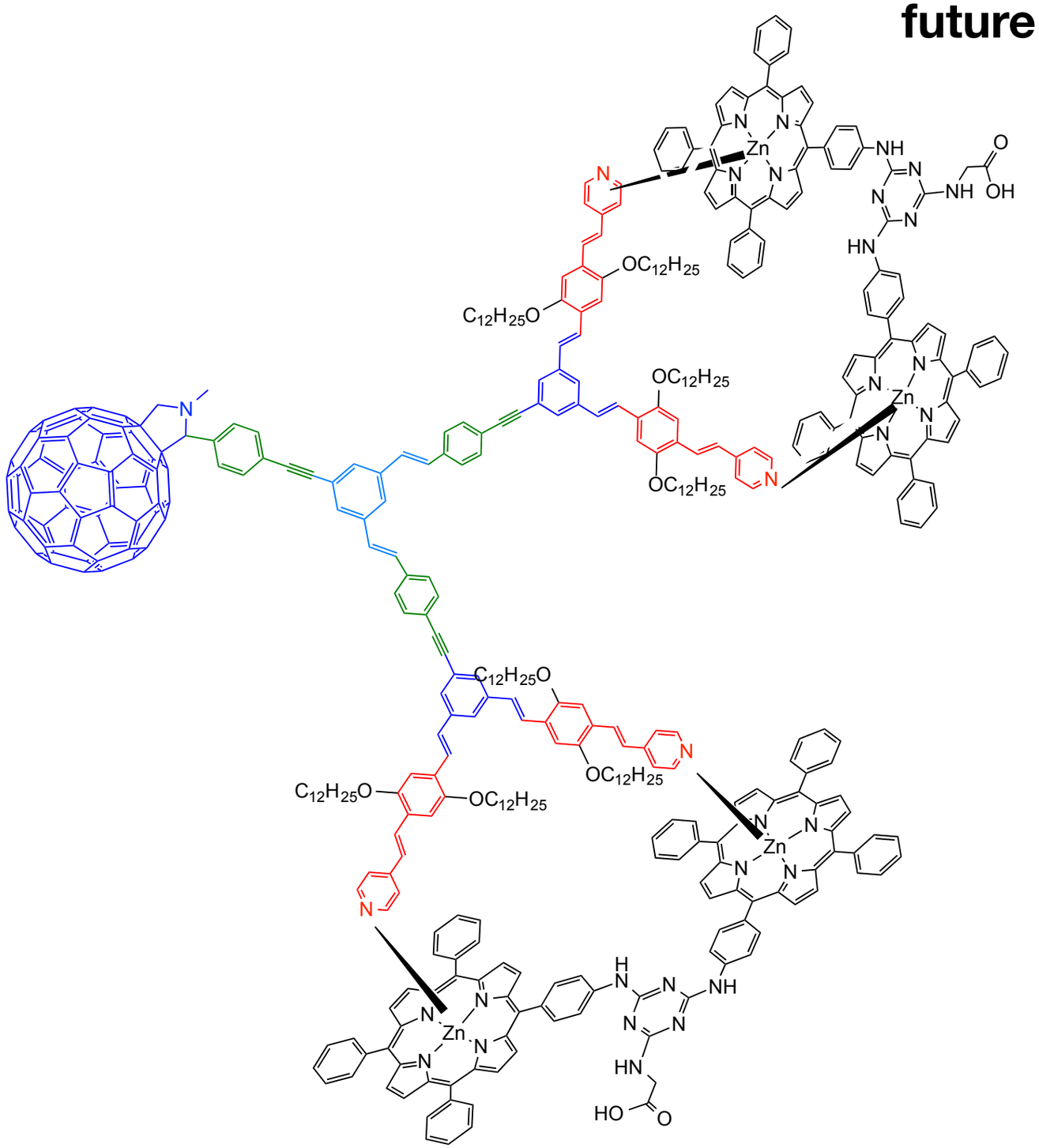

INPUT

VERTICAL POLARISATION

POWER ON

INTERLOCK HEALTHY

LASER READY

LASER ON

LASER ON/OFF

PULSE PERIOD

micro secs

EDINBURGH INSTRUMENTS

PICOSECOND PULSED DIODE LASER

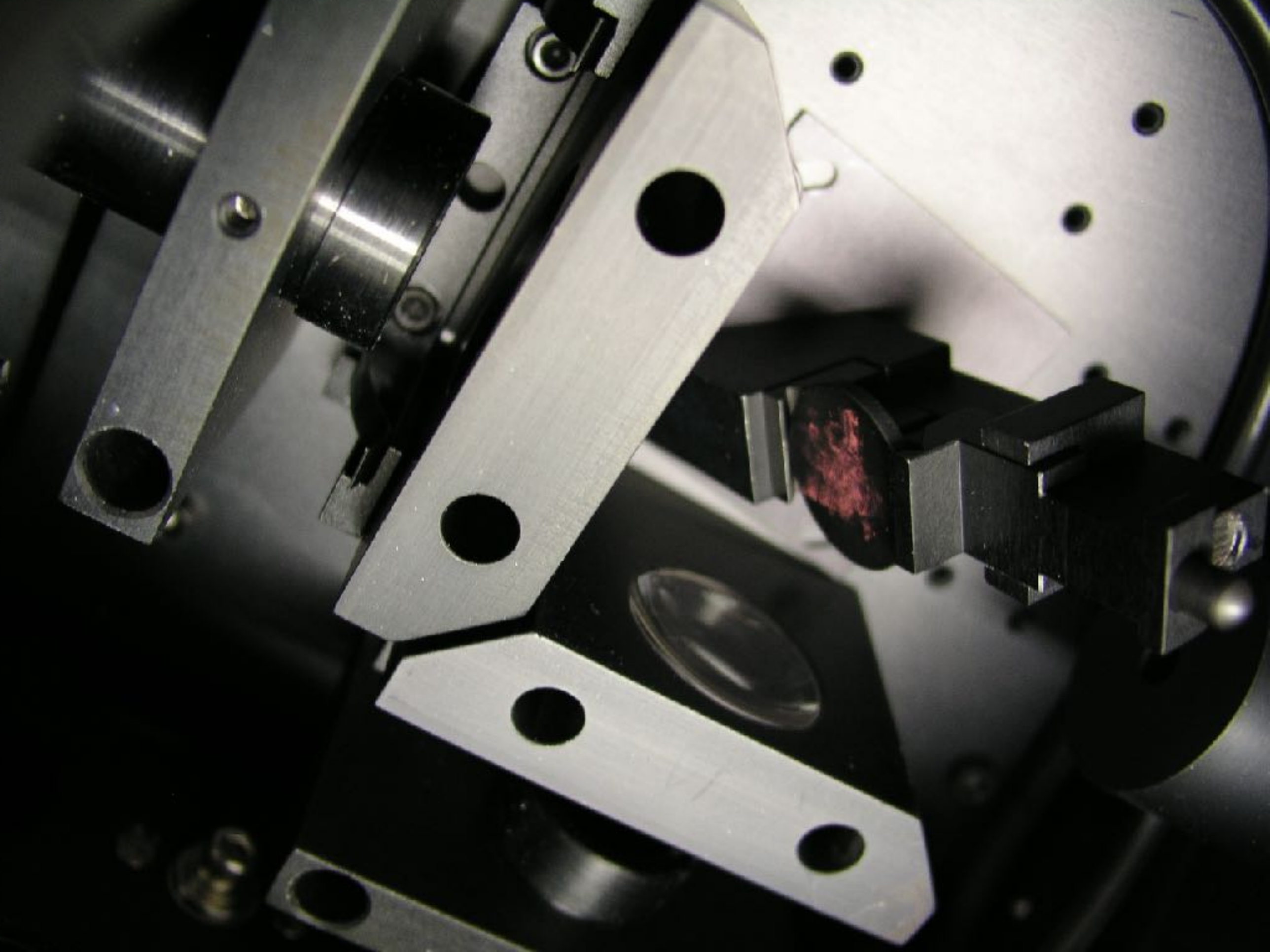


BRUKER - SPECTROSPIN
500


ORIEL
LAMP START
WATTS
VOLTS
AMPS
OUTPUT
OUTPUT PRE-ADJUST
ORIEL


TURBOX
ASUS

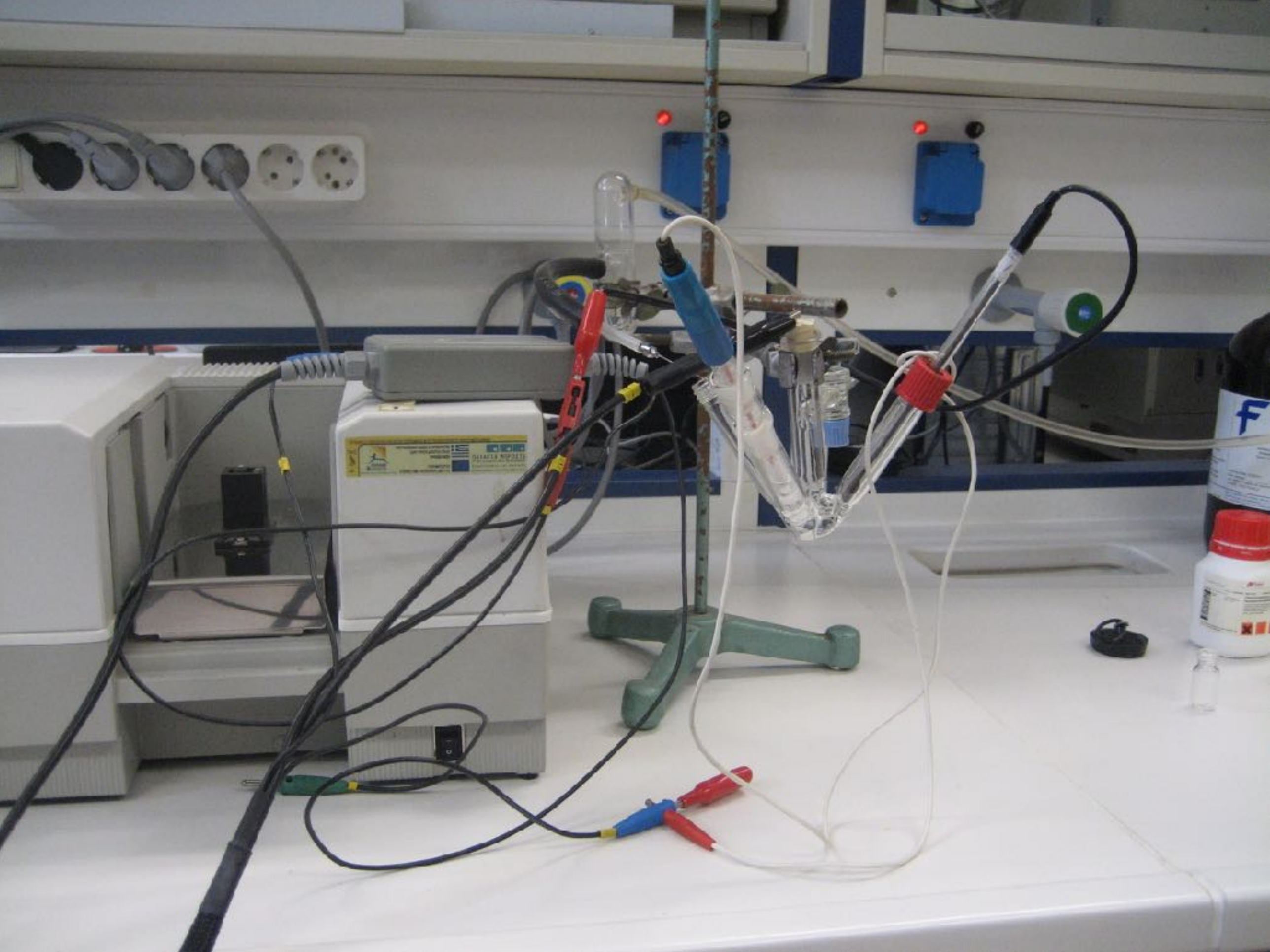


UV-visible cells


JASCO
FP-6500
Spectrofluorometer
Outlet
Inlet

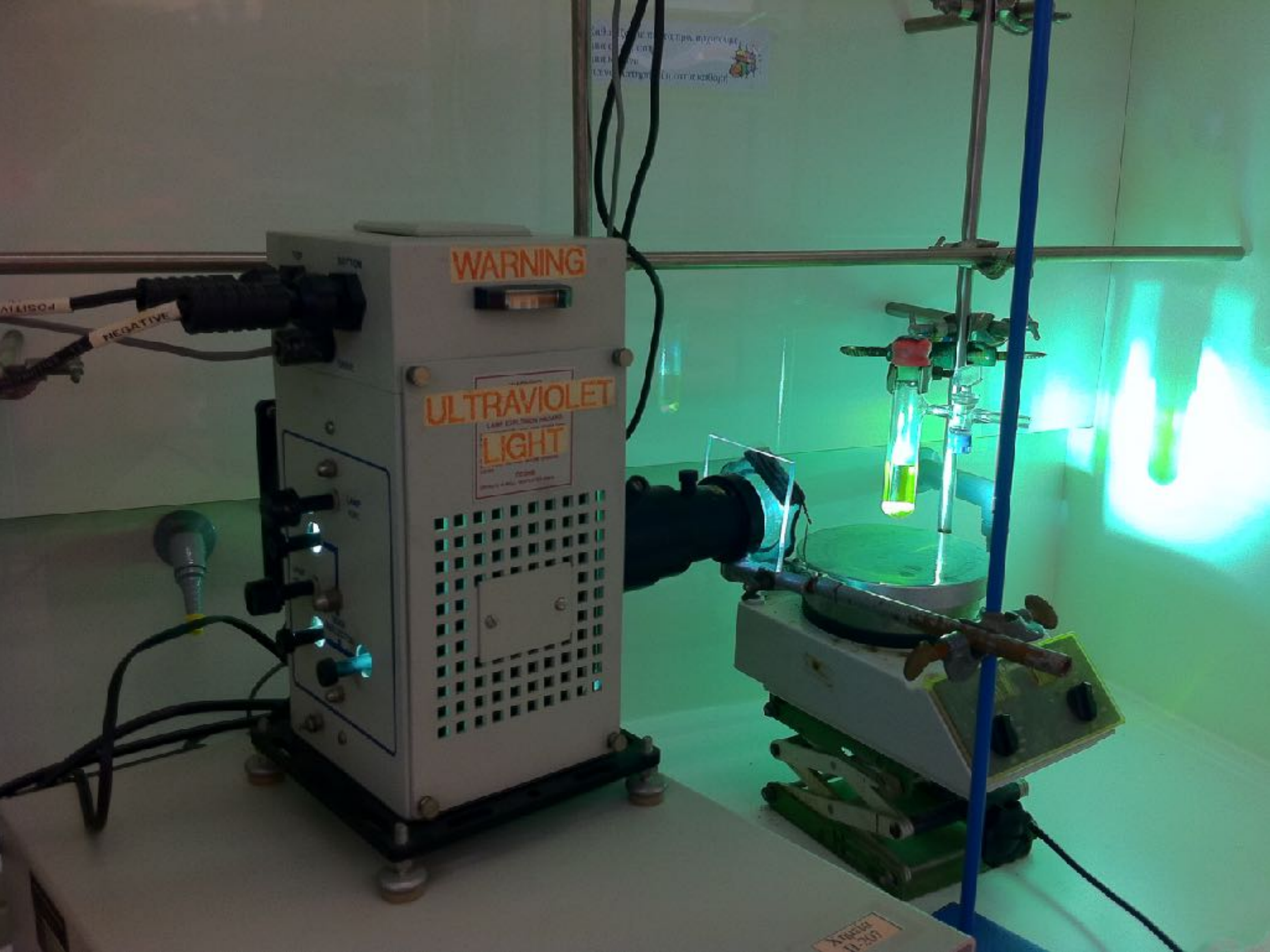
WARNING
ULTRAVIOLET
LIGHT
NEGATIVE


DELL
PowerEdge R310
DELL
PowerEdge R415
DELL PowerEdge 1850
DVD
SAS

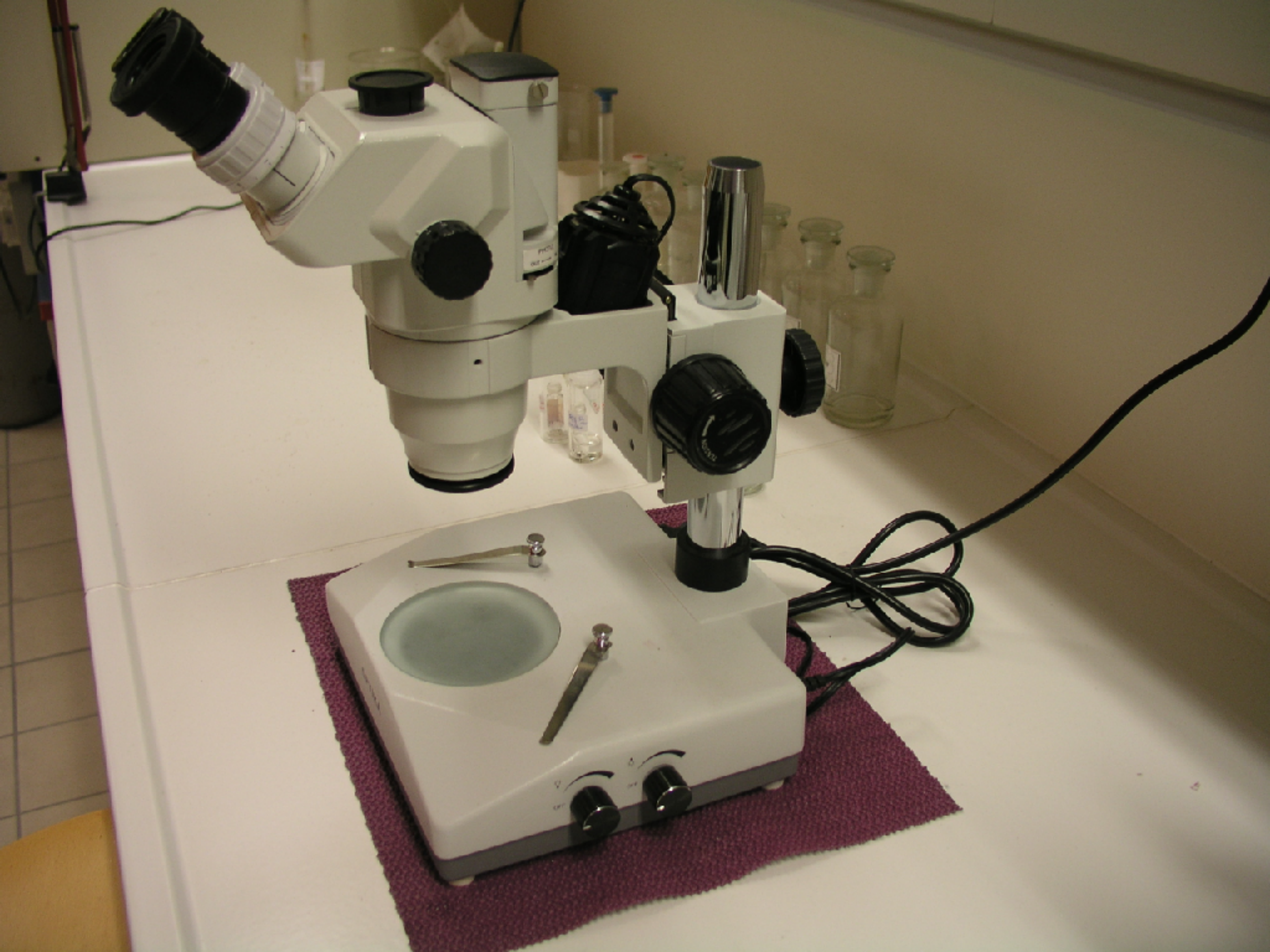

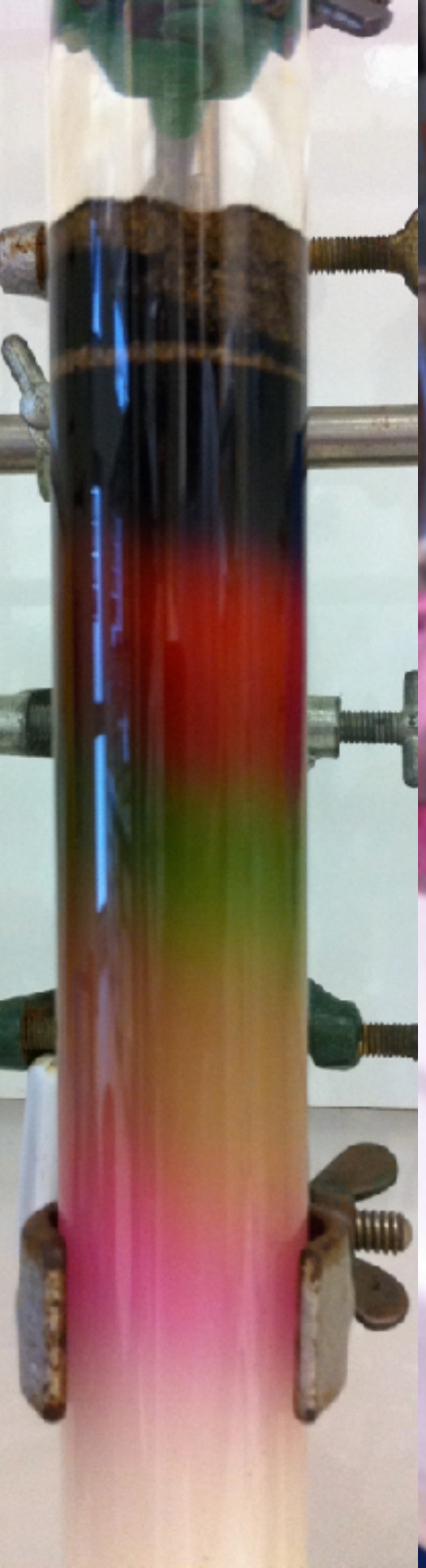

Lorem Ipsum Dolor